

AR TARGET SHEET

The following document was too large to scan as one unit, therefore, it has been broken down into sections.

EDMC#: 0000003

SECTION: 5 OF 11

DOCUMENT #: DOE/EIS-0113

TITLE: Final EIS Disposal of Hanford
Defense High-Level, Transuranic
and Tank Wastes

000003

3 of 5

DOE/EIS-0113
VOLUME 3 of 5

VOLUME 3
APPENDICES M-V

FINAL ENVIRONMENTAL IMPACT STATEMENT

DISPOSAL OF HANFORD DEFENSE HIGH-LEVEL, TRANSURANIC AND TANK WASTES

Hanford Site
Richland, Washington



DECEMBER 1987

U.S. DEPARTMENT OF ENERGY

PLEASE RETURN TO:
ENVIRONMENTAL DIVISION
RESOURCE CENTER

This report has been reproduced directly from the best available copy.

Available from the National Technical Information Service, U. S. Department of Commerce, Springfield, Virginia 22161.

Price: Printed Copy A17
Microfiche A01

Codes are used for pricing all publications. The code is determined by the number of pages in the publication. Information pertaining to the pricing codes can be found in the current issues of the following publications, which are generally available in most libraries: *Energy Research Abstracts*, (ERA); *Government Reports Announcements and Index* (GRA and I); *Scientific and Technical Abstract Reports* (STAR); and publication, NTIS-PR-360 available from (NTIS) at the above address.

COVER SHEET

RESPONSIBLE AGENCY: U.S. Department of Energy

TITLE: Final Environmental Impact Statement, Disposal of Hanford Defense High-Level, Transuranic and Tank Wastes, Hanford Site, Richland, Washington

CONTACTS: Additional copies or information concerning this statement can be obtained from: Mr. Tom Bauman, Communications Division, U.S. Department of Energy, Richland Operations Office, Richland, WA 99352. Telephone: (509) 376-7378.

For general information on DOE's EIS process contact: Office of the Assistant Secretary for Environment, Safety and Health, U.S. Department of Energy, ATTN: Carol M. Borgstrom, Forrestal Building, 1000 Independence Avenue, S.W., Washington, D.C. 20585. Telephone: (202) 586-4600.

ABSTRACT: The purpose of this Environmental Impact Statement (EIS) is to provide environmental input into the selection and implementation of final disposal actions for high-level, transuranic and tank wastes located at the Hanford Site, Richland, Washington, and into the construction, operation and decommissioning of waste treatment facilities that may be required in implementing waste disposal alternatives. Specifically evaluated are a Hanford Waste Vitrification Plant, Transportable Grout Facility, and a Waste Receiving and Packaging Facility. Also an evaluation is presented to assist in determining whether any additional action should be taken in terms of long-term environmental protection for waste that was disposed of at Hanford prior to 1970 as low-level waste (before the transuranic waste category was established by the Atomic Energy Commission but which might fall into that category if generated today).

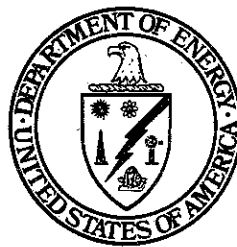
The following alternatives are considered in this EIS: 1) in-place stabilization and disposal, where waste is left in place but is isolated by protective and natural barriers; 2) geologic disposal, where most of the waste (by activity and to the extent practicable) is exhumed, treated, segregated, packaged and disposed of in a deep geologic repository; waste classified as high-level would be disposed of in a commercial repository developed pursuant to the Nuclear Waste Policy Act; transuranic waste would be disposed of in the Waste Isolation Pilot Plant near Carlsbad, New Mexico; 3) a reference alternative, where some classes of waste are disposed of in geologic repositories and other classes of waste are disposed of by in-place stabilization and disposal; 4) the preferred alternative, in which double-shell tank wastes, strontium and cesium capsules, and retrievably stored TRU wastes are disposed of according to the reference alternative, and in which decisions are deferred on disposal of single-shell tank wastes and on further remedial action for TRU-contaminated soil sites and pre-1970 buried suspect TRU-contaminated solid wastes (except the 618-11 site) until additional information is obtained on waste characterization, retrieval methods, and performance of near-surface disposal systems; and 5) a no disposal action alternative (continued storage).

**THIS PAGE INTENTIONALLY
LEFT BLANK**

FINAL ENVIRONMENTAL IMPACT STATEMENT

DISPOSAL OF HANFORD DEFENSE HIGH-LEVEL, TRANSURANIC AND TANK WASTES

**Hanford Site
Richland, Washington**



DECEMBER 1987

**U.S. DEPARTMENT OF ENERGY
ASSISTANT SECRETARY FOR DEFENSE PROGRAMS
WASHINGTON, D.C. 20545**

**THIS PAGE INTENTIONALLY
LEFT BLANK**

FOREWORD

This environmental impact statement (EIS) provides analyses of environmental impacts for the selection and implementation of final disposal strategies for the high-level (HLW), transuranic (TRU) and tank wastes generated during national defense activities and stored at the Hanford Site near Richland, Washington. Also an evaluation is presented to assist in determining whether any additional action should be taken in terms of long-term environmental protection for waste that was disposed of at Hanford prior to 1970 as low-level waste (before the transuranic waste category was established by the Atomic Energy Commission (AEC) but which might fall into that category if generated today). This document also addresses environmental impacts associated with the construction, operation and decommissioning of waste treatment facilities that may be required to implement the waste disposal alternatives.

Several previous documents have addressed environmental aspects of the management of defense waste at the Hanford Site. The first comprehensive one, The Final Environmental Statement for Hanford Waste Management Operations (ERDA-1538), was issued in 1975. In that statement, waste management practices at Hanford were shown to protect the public health and safety and the environment on an interim basis. Those practices, however, were not and are not intended as final solutions for long-term isolation and disposal of high-level, TRU and tank wastes.

In 1977, the Energy Research and Development Administration (ERDA) issued the report Alternatives for Long-Term Management of Defense High-Level Radioactive Waste (ERDA-77-44), which included preliminary cost estimates and analyses of near-term risks associated with alternatives considered. That document examined 27 variations on four options for the processing and disposal of Hanford HLW, encompassing numerous final waste forms and storage and disposal modes.

In 1978, the National Research Council of the National Academies of Science and Engineering issued a report entitled Radioactive Wastes at the Hanford Reservation: A Technical Review, concluding that there has not been in the past, and is not at the present, any significant radiation hazard to public health and safety from waste management operations at Hanford. The Council recommended that long-term isolation and disposal of Hanford high-level waste become the main focus of waste management research and development.

The need to include retrievably stored TRU waste within the scope of wastes to be disposed of, and concerns about potential environmental impacts of wastes disposed of before 1970 as low-level wastes (before the Atomic Energy Commission established the TRU waste category but which might be classed as TRU if generated today), led to enlarging the earlier plan that was to issue an EIS covering high-level waste only. Accordingly, on April 1, 1983, the Department of Energy (DOE) published in the Federal Register (48 FR 14029) a Notice of Intent (NOI) to prepare an EIS on Disposal of Radioactive Defense High-Level and Transuranic Wastes at Hanford.

Eighteen comment letters were received in response to the Notice of Intent to prepare this EIS. Ten of the letters only requested copies of the draft EIS when issued; eight

contained comments regarding its preparation. The draft EIS was published during March 1986, and its availability was published in the Federal Register on April 11 (51 FR 12547). During the 120-day agency and public comment period on the draft EIS, which began on April 11, 1986, 243 letters were received that provided about 2000 substantive comments on the draft EIS. In addition, oral testimony was heard on the draft EIS in public hearings held during July 1986, in Richland, Washington; Portland, Oregon; Seattle, Washington; and Spokane, Washington.

Excluded from consideration in this EIS are low-level radioactive wastes in liquid and solid disposal sites at Hanford (see ERDA 1538). These waste sites are presently being reviewed under hazardous-waste regulations. Also excluded are wastes generated by decontamination and decommissioning of surplus or retired facilities after the year 1983 (other than for those facilities directly associated with waste disposal). Those operations will be the subject of other National Environmental Policy Act (NEPA) reviews.

The Defense Waste Management Plan (DOE/DP 0015) states of the Hanford wastes: "Immobilization of new and readily retrievable high-level waste will begin about 1990 after sufficient experience is available from Savannah River's vitrification process. Other waste will be stabilized in place in the 1985-2015 time frame if, after the requisite environmental documentation, it is determined that the short-term risks and costs of retrieval and transportation outweigh the environmental benefits of disposal in a geologic mined repository."

It is necessary to understand the major differences between civilian and defense wastes and the programs to effect their disposal. Both types of waste include fission products and transuranic waste elements. On the other hand, the quantities of these elements, the physical and chemical forms of the wastes, and the technically sound alternatives for their disposal are markedly different. In all cases, for both civilian and defense, the final methods selected will have to meet the Environmental Protection Agency (EPA) standards (40 CFR 191) for the disposal of spent fuel and high-level and TRU wastes. The Nuclear Waste Policy Act of 1982 mandates a procedure to select the potential repository sites for detailed characterization.

A comparison of the Hanford waste inventory resulting from chemical processing of about 100,000 metric tons of nuclear reactor fuel with that of a commercial repository containing 70,000 metric tons of spent fuel elements is enlightening. In this comparison, the waste inventory from 100,000 metric tons of Hanford reactor fuel contains about 4% as much of the readily transportable (geohydrologically) isotopes ^{14}C , ^{99}Tc , and ^{129}I as is contained in 70,000 metric tons of commercial spent fuel. It contains only 1% as much ^{90}Sr and ^{137}Cs and about 0.1% as much of the primary transuranics ^{239}Pu , ^{240}Pu , and ^{241}Am . The volume of the Hanford wastes is markedly larger than the civilian wastes cited above--410,000 m³ of Hanford wastes as compared to 29,000 m³ of commercial spent fuel.

The physical and chemical characteristics of existing and potential waste forms considered in this EIS are highly diverse: liquid waste in double-shell tanks, vitrified/canistered wastes (from processed double-shell tank wastes); sludge and salts in the single-shell tanks; strontium and cesium capsules that are further protected with a

handling container; previously disposed of pre-1970 wastes in various forms and containers; and finally, low-level waste products, from the processing of double-shell-tank waste, in the form of grout.

In accordance with the requirements of NEPA, as amended, and implementing regulations of the Council on Environmental Quality (CEQ) published in the Code of Federal Regulations as 40 CFR 1500, this EIS was written early in the decision-making process to ensure that environmental values and alternatives are fully considered before any decisions are made that might lead to adverse environmental impacts or limit the choice of reasonable alternatives. This process will also help ensure that the public is fully informed and is involved in the decision-making process.

To comply with the NEPA's requirement for early preparation of environmental documentation, this EIS has been prepared early in the disposal decision process. As with any major action, it is expected that once a disposal decision is made, subsequent detailed engineering may enhance specific waste retrieval, treatment, handling, immobilization and/or disposal processes evaluated in the EIS. However, the processes evaluated in this document have been chosen such that, when finally implemented for any of the options, the processes would not be expected to result in environmental impacts that significantly exceed those described here. The DOE believes that bounding analyses performed in this EIS meet the requirements of CEQ regulations for analysis of all reasonably foreseeable significant adverse impacts.

Implementation of defense waste disposal under the alternatives described in this EIS will be done in compliance with the letter and spirit of applicable federal and state environmental statutes, regulations and standards. To ensure that impacts of specific processes used during disposal implementation do not differ significantly from the results of the analyses set forth in this document, DOE will conduct environmental reviews of the specific processes as finally proposed. On the basis of these reviews, DOE will determine in accord with agency guidelines what additional NEPA documentation is required. The DOE anticipates that a supplemental EIS will be prepared prior to a decision on a disposal option for single-shell tank waste.

This document is not intended to provide the environmental input necessary for siting or constructing a geologic repository. For analysis of environmental impacts of alternatives involving geologic disposal, generic designs for either an offsite or onsite repository were used. Detailed environmental documentation required by the Nuclear Waste Policy Act of 1982 will be prepared before a geologic repository is sited, constructed and operated. A future EIS to address site selection is expected to include a discussion of cumulative impacts of the repository program at all candidate sites, including Hanford.

Other NEPA documentation relevant to this EIS includes the supplement to ERDA-1538, Double-Shell Tanks for Defense High-Level Radioactive Waste Storage at the Hanford Site (DOE/EIS-0063), and the Final Environmental Impact Statement--Operation of PUREX and Uranium Oxide Plant Facilities (DOE/EIS-0089). (The draft PUREX EIS with an addendum constituted the final PUREX EIS.)

Environmental considerations regarding disposal of Hanford's retrievably stored TRU waste at the Waste Isolation Pilot Plant (WIPP) (except for retrieval, processing, packaging, certification and transportation of waste from Hanford to WIPP, which are discussed in this EIS) are based on the Final Environmental Impact Statement--Waste Isolation Pilot Plant (DOE/EIS-0026). Environmental considerations associated with waste disposal in geologic repositories are based on information from the Final Environmental Impact Statement--Management of Commercially Generated Radioactive Waste (DOE/EIS-0046F). Alternatives to disposal of high-level waste in geologic repositories were described in that document.

Environmental considerations associated with borosilicate glass as a waste form for repository disposal of waste and with the construction and operation of a plant to provide vitrified waste are based in part on information developed in three previous DOE documents: Final Environmental Impact Statement--Defense Waste Processing Facility Savannah River Plant, Aiken, South Carolina (DOE/EIS-0082); Environmental Assessment--Waste Form Selection for SRP High-Level Waste (DOE/EA-0179); and Analyses of the Terminal Waste Form Selection for the West Valley Demonstration Project (WVDP-100 DOE).

The EIS has been structured to conform as closely as possible to the format described in CEQ Regulation 40 CFR Parts 1502.1 through 1502.18. To provide more information for the reader than can be reported within the text of Volume 1, more detailed information is included in 22 appendices (Volumes 2 and 3). Figure 1 in the Introduction to the Appendices (Volume 2, p. xxiv) shows the purpose of each appendix and how appendices relate to each other and to the text of Volume 1. Lines in the margins of Volumes 1, 2 and 3 indicate the areas where revisions were made to the draft EIS. Volume 4 contains agency and public comments received and responses to them as well as the indication of location where revisions were made to the draft EIS. Volume 5 contains a reproduction of all of the comment letters received.

The final EIS is being transmitted to commenting agencies, made available to members of the public, and filed with the EPA. The EPA will publish a notice in the Federal Register indicating that the DOE has filed the final EIS. A DOE decision on proposed actions will not be made earlier than 30 days after the EPA has published the Federal Register notice for the final EIS. The DOE will record its decision in a publicly available Record of Decision (ROD) document published in the Federal Register.

VOLUME 3 CONTENTS--APPENDICES M-V

FOREWORD	v
APPENDIX M--PRELIMINARY ANALYSIS OF THE PERFORMANCE OF THE CONCEPTUAL PROTECTIVE BARRIER AND MARKER SYSTEM	M.1
M.1 INTRODUCTION	M.1
M.2 CONCEPTUAL DESIGN DESCRIPTION	M.6
M.3 DESIGN OBJECTIVES	M.9
M.4 REDUCTION IN RISK OF INADVERTENT INTRUSION THROUGH PASSIVE INSTITUTIONAL CONTROLS	M.12
M.5 MODEL SIMULATIONS OF WATER INFILTRATION CONTROL	M.17
M.6 COVER DISTURBANCE CONSIDERATIONS	M.26
M.7 PROTECTIVE BARRIER AND WARNING MARKER SYSTEM DEVELOPMENT PLAN	M.27
M.8 BARRIER FAILURE SCENARIOS	M.32
M.9 SUMMARY	M.33
M.10 REFERENCES	M.33
APPENDIX N--RADIOLOGICALLY RELATED HEALTH EFFECTS	N.1
N.1 LATE SOMATIC EFFECTS	N.2
N.2 GENETIC EFFECTS	N.7
N.3 CONCLUSIONS	N.9
N.4 REFERENCES	N.10
APPENDIX O--STATUS OF HYDROLOGIC AND GEOCHEMICAL MODELS USED TO SIMULATE CONTAMINANT MIGRATION FROM HANFORD DEFENSE WASTES	O.1
O.1 STRATIGRAPHY BENEATH THE HANFORD 200 AREAS	O.2
O.2 PHYSICS AND CHEMISTRY OF THE AQUIFER SYSTEM	0.5
O.3 THE CONCEPTUAL MODEL	0.8
O.4 MATHEMATICAL AND NUMERICAL MODELS	0.16
O.5 REFERENCES	0.40
APPENDIX P--RELEASE MODELS AND RADIONUCLIDE INVENTORIES FOR SUBSURFACE SOURCES	P.1
P.1 RELEASE MODELS	P.1
P.2 RELEASE MODELS FOR SPECIFIC WASTE FORMS	P.10
P.3 INVENTORIES AND LOCATIONS OF RADIONUCLIDES	P.21

P.4 SUMMARY OF SOURCE RELEASE-RATE DATA	P.23
P.5 REFERENCES	P.42
APPENDIX Q--APPLICATION OF GEOHYDROLOGIC MODELS TO POSTULATED RELEASE SCENARIOS FOR THE HANFORD SITE	Q.1
Q.1 INTRODUCTION	Q.1
Q.2 SCENARIOS AND ASSUMPTIONS	Q.1
Q.3 VADOSE-ZONE MODELING	Q.2
Q.4 AQUIFER MODELING	Q.4
Q.5 SOLUTE TRANSPORT ANALYSES	Q.10
Q.6 RESULTS OF FLOW AND SOLUTE TRANSPORT MODELING	Q.11
Q.7 300 AREA TRU BURIAL GROUNDS	Q.32
Q.8 WATER TABLE CHANGES RESULTING FROM POTENTIAL IRRIGATION SCENARIOS	Q.33
Q.9 CONCLUSIONS FROM IRRIGATION MODELING	Q.35
Q.10 REFERENCES	Q.38
APPENDIX R--ASSESSMENT OF LONG-TERM PERFORMANCE OF WASTE DISPOSAL SYSTEMS	R.1
R.1 WASTE MIGRATION THROUGH GROUNDWATER RECHARGE	R.3
R.2 FALLING OBJECTS	R.64
R.3 DRILLING	R.65
R.4 MAJOR EXCAVATION	R.67
R.5 RESETTLEMENT/FARMING/GARDENING	R.74
R.6 GLACIAL FLOODING	R.88
R.7 OTHER SURFACE FLOODING	R.91
R.8 WIND EROSION	R.93
R.9 MAGMATIC ACTIVITY	R.94
R.10 SEISMIC EVENTS	R.96
R.11 CRITICALITY	R.97
R.12 REFERENCES	R.98
APPENDIX S--PROBABILITY AND CONSEQUENCE ANALYSIS OF RADIONUCLIDE RELEASE AND TRANSPORT AFTER DISPOSAL	S.1
S.1 RELEASE-RATIO CONSEQUENCE	S.3
S.2 RADIONUCLIDE RELEASES TO ACCESSIBLE ENVIRONMENT	S.6
S.3 MATHEMATICAL MODEL OF NATURAL RELEASE CONSEQUENCES AND UNCERTAINTY	S.10
S.4 MATHEMATICAL MODEL OF CONSEQUENCES RELATED TO HUMAN INTRUSION	S.20

S.5 RESULTS	S.25
S.6 SENSITIVITY ANALYSIS	S.29
S.7 REFERENCES	S.36
APPENDIX T--METHOD FOR ESTIMATING NONRADIOLOGICAL AIR-QUALITY IMPACTS	T.1
T.1 AIR-QUALITY GUIDELINES AND AMBIENT AIR-QUALITY STANDARDS	T.1
T.2 AIR-QUALITY ANALYSIS PROCEDURES	T.2
T.3 METEOROLOGICAL INPUT	T.3
T.4 SOURCE-DATA INPUT	T.6
T.5 AIR-QUALITY IMPACT CALCULATIONS AND RESULTS	T.7
T.6 REFERENCES	T.8
APPENDIX U--PRELIMINARY ANALYSIS OF THE FUTURE GROUNDWATER TRANSPORT OF CHEMICALS RELEASED	U.1
U.1 INTRODUCTION	U.1
U.2 THE SOURCE TERM	U.1
U.3 ATTENUATION	U.4
U.4 RESULTS	U.5
U.5 CONSERVATISM	U.5
U.6 REFERENCES	U.10
APPENDIX V--SITE-MONITORING EXPERIENCE	V.1
V.1 INTRODUCTION	V.1
V.2 CRIBS	V.4
V.3 TRENCHES	V.17
V.4 FRENCH DRAINS	V.20
V.5 REVERSE WELLS	V.24
V.6 DISPOSAL PONDS	V.28
V.7 241-T-106 TANK LEAK	V.32
V.8 SUMMARY AND CONCLUSIONS	V.34
V.9 REFERENCES	V.37
INDEX	Ind-1

Volume 1 contains:

- EXECUTIVE SUMMARY
- 1.0 GENERAL SUMMARY
- 2.0 PURPOSE AND NEED
- 3.0 DESCRIPTION AND COMPARISON OF ALTERNATIVES
- 4.0 AFFECTED ENVIRONMENT
- 5.0 POSTULATED IMPACTS AND POTENTIAL ENVIRONMENTAL CONSEQUENCES
- 6.0 APPLICABLE REGULATIONS
- 7.0 PREPARERS AND REVIEWERS
- 8.0 GLOSSARY

Volume 2 contains:

- APPENDIX A--WASTE SITE DESCRIPTIONS AND INVENTORIES
- APPENDIX B--DESCRIPTION OF FACILITIES AND PROCESSES
- APPENDIX C--HANFORD WASTE VITRIFICATION PLANT
- APPENDIX D--TRANSPORTABLE GROUT FACILITY
- APPENDIX E--WASTE RECEIVING AND PROCESSING FACILITY
- APPENDIX F--METHOD FOR CALCULATING RADIATION DOSE
- APPENDIX G--METHOD FOR CALCULATING NONRADIOLOGICAL INJURIES AND ILLNESSES AND NONRADIOLOGICAL FATALITIES
- APPENDIX H--RADIATION DOSES TO THE PUBLIC FROM OPERATIONAL ACCIDENTS
- APPENDIX I--ANALYSIS OF IMPACTS FOR TRANSPORTATION OF HANFORD DEFENSE WASTE
- APPENDIX J--METHOD FOR CALCULATING REPOSITORY COSTS USED IN THE HANFORD DEFENSE WASTE ENVIRONMENTAL IMPACT STATEMENT
- APPENDIX K--SOCIOECONOMIC IMPACTS
- APPENDIX L--NONRADIOLOGICAL IMPACTS--CONSTRUCTION AND OPERATIONAL PERIOD

Volume 4 contains:

PUBLIC COMMENTS AND RESPONSES

- 1.0 INTRODUCTION
- 2.0 POLICY COMMENTS AND RESPONSES
- 3.0 TECHNICAL COMMENTS AND RESPONSES

4.0 ORGANIZATION AND PRESENTATION COMMENTS AND RESPONSES

APPENDIX A--INDEX FOR PUBLIC COMMENT LETTERS

APPENDIX B--INDEX FOR PUBLIC TESTIMONY

Volume 5 contains:

PUBLIC COMMENTS

FIGURES

M.1	Typical Multilayer Barrier Containing a Capillary Barrier	M.4
M.2	Water-Content Profiles for a Coarse-Textured and Fine-Textured Soil Contained in a Multilayer Soil Cover	M.5
M.3	Tank Farm Protective Barrier Concepts	M.8
M.4	Soil-Moisture Characteristics for the Materials Used in the Barrier Simulations	M.20
M.5	Logic Diagram for Barrier and Marker Development	M.29
0.1	Stratigraphic Units Present in the Pasco Basin	0.3
0.2	Depiction of Pathlines from Points Originating at Various Candidate Waste Source Locations	0.9
0.3	Depiction of the Streamtube Approach to Transport in the Vadose Zone and the Unconfined Aquifer	0.13
0.4	Diffusion- and Advection-Controlled Regions of the Simplified Model for Release of Waste with Barrier Emplaced	0.19
0.5	Streamtubes Conducting Contamination to the Water Table	0.20
0.6	Time Line of Release Through a Diffusion-Controlled Streamtube When Source Release Period Exceeds First Release Time	0.22
0.7	Time Line of Release Through a Diffusion-Controlled Streamtube When First Release Time Exceeds Source Release Period	0.22
0.8	Patterns of Hydraulic Conductivity on the Hanford Site	0.25
P.1	Conceptual Model for Release from Beneath a Barrier	P.6
Q.1	Groundwater Contours and Streamlines from the 200 Areas Waste Sites to the River, Assuming Steady-State Conditions, 0.5-cm/yr Recharge, and No Pond Disposals	Q.6
Q.2	Water-Table Contour Map of the Hanford Unconfined Aquifer with Streamlines Indicating Direction of Flow from the 200 Areas Plateau	Q.7
Q.3	Groundwater Contours and Streamlines Showing Flow from Waste Sites in 200 East and 200 West Areas with 5-cm/yr Annual Average Recharge Scenario	Q.8
Q.4	Generic Curves for Peak Concentration and Peak Flux at Accessible Environment	Q.12
Q.5	Location of Irrigated Hanford Site Regions for Simulations	Q.34
Q.6	Estimated Steady-State Water Table Contours at Hanford Site Resulting from 15.2-cm/yr Irrigation Infiltration on the North Slope of Rattlesnake Hills, to the West of the Cold Creek Drainage Boundary, and North of Gable Mountain	Q.36
Q.7	Estimated Steady-State Water Table at Hanford Site After Site Closure Resulting from 30.5-cm/yr Irrigation Infiltration on the North Slope of Rattlesnake Hills, to the West of the Cold Creek Drainage Boundary, and the Added Irrigated Area Between 200 West Area and Highway 240	Q.37

R.1	Concentration of Selected Radionuclides in Groundwater at a 5-km Well from 200 West Area Single-Shell Tanks, In-Place Stabilization and Disposal or Reference Alternatives, 5-cm/yr Recharge	R.27
R.2	Concentration of Selected Radionuclides in Groundwater at a 5-km Well from 200 West Area Single-Shell Tanks, No Disposal Action, 5-cm/yr Recharge	R.28
R.3	Concentration of Selected Radionuclides in Groundwater at a 5-km Well from 200 West Area Single-Shell Tanks, In-Place Stabilization and Disposal or Reference Alternative, Disruptive Barrier Failure at 500 Years	R.29
R.4	Concentration of Selected Radionuclides in Groundwater at a 5-km Well from the 200 West Area Single-Shell Tanks, In-Place Stabilization and Disposal or Reference Alternatives, Functional Barrier Failure	R.30
R.5	Individual Dose Rates from Drinking Water from the 5-km Well Down Gradient of the 200 West Area Single-Shell Tanks, In-Place Stabilization and Disposal or Reference Alternatives, 5-cm/yr Recharge	R.31
R.6	Individual Dose Rates from Drinking Water from the 5-km Well Down Gradient of the 200 West Area Single-Shell Tanks No Disposal Action, 5-cm/yr Recharge	R.32
R.7	Individual Dose Rates from Drinking Water for the 5-km Well Down Gradient of the 200 West Area Single-Shell Tanks, In-Place Stabilization and Disposal Alternatives, Disruptive Barrier Failure	R.33
R.8	Individual Dose Rates from Drinking Water from the 5-km Well Down Gradient of the 200 West Area Single-Shell Tanks, In-Place Stabilization and Disposal or Reference Alternatives, Functional Barrier Failure	R.34
R.9	Integrated Population Dose from Releases of Radionuclides from 200 West Area Single-Shell Tanks, With and Without Barriers	R.47
R.10	Water Concentration of Selected Radionuclides in Well from 200 West Area Single-Shell Tanks, No Disposal Action, 5-cm/yr Recharge	R.88
S.1	Assumed Probability Density Function of Annual Groundwater Recharge of Current Climate for the Next 10,000 Years	S.7
S.2	Assumed Probability Density Function of Annual Groundwater Recharge of Wetter Climate for the Next 10,000 Years	S.7
S.3	Probabilistic Scenario Tree	S.10
S.4	Flow Diagram of Natural Release Simulation Model for Calculating Probabilities and Consequences	S.11
S.5	Probability Density Function of K_d Values for Plutonium in Single-Shell and Double-Shell Tank Waste	S.18
S.6	Probability Density Function of K_d Values for Americium in Single-Shell and Double-Shell Tank Waste	S.18
S.7	Probability Density Function of K_d Values for Strontium and Nickel in Single-Shell and Double-Shell Tank Waste	S.19
S.8	Drywell Storage Facility Canister Area for Borehole Model	S.24

S.9	Release Curves for Alternatives for the Scenario of Current Climate, No Barrier Failure, and 400-Year Intrusion	S.25
S.10	Preliminary Composite CCDFs for All Alternatives Based on All Scenarios for Wastes Disposed of Near Surface	S.27
S.11	Preliminary Composite CCDFs With 90% Chance of Wetter Climate and 50% Chance of Barrier Failure	S.34
S.12	Preliminary Composite CCDFs with 90% Chance of Wetter Climate and 100% Chance of Barrier Failure	S.35
S.13	Preliminary Composite CCDFs with 90% Chance of Current Climate and 100% Chance of Barrier Failure	S.35
V.1	Locations of Sampling Wells CY 1984	V.3
V.2	Structural Details of the 216-A-24 Crib	V.6
V.3	216-Z-12 Crib Construction Details	V.7
V.4	Distribution of Plutonium Activity Beneath the 216-Z-12 Crib on Cross Section A-A'	V.8
V.5	Graphic Representation of Waste Plume Beneath the 216-Z-1A Crib	V.11
V.6	Total Transuranic Activity Distribution, North-South Cross Section	V.12
V.7	Total Transuranic Activity Distribution, East-West Cross Section	V.13
V.8	Results of the 1956 and 1966 216-S-1 and -2 Crib Field Evaluations	V.15
V.9	Cesium-137 Distribution Beneath the 216-S-1 and -2 Crib, B to B'	V.16
V.10	Construction and Geology of the 216-Z-9 Trench	V.19
V.11	The 216-Z-8 French Drain Facility	V.21
V.12	Plutonium-239 Concentrations Beneath the 216-Z-8 French Drain	V.22
V.13	Americium-241 Concentrations Beneath the 216-Z-8 French Drain	V.23
V.14	216-B-5 Reverse Well Disposal System	V.25
V.15	Radionuclide Distributions in the 216-B-5 Reverse Well	V.26
V.16	Cesium-137 Distribution	V.27
V.17	Plutonium-239-240 Distribution	V.29
V.18	Strontium-90 Distribution	V.30
V.19	Location of the U-Pond Disposal System and its Various Components	V.31
V.20	Structural Details of 241-T-106 Tank	V.33
V.21	Composite Drawing of Plan and Section Views of 0.1- μ Ci/L Concentrations of ^{144}Ce , ^{137}Cs and ^{106}Ru in 1973	V.34
V.22	Plan and Cross-Section View Through a Portion of 241-T Tank Farm with 1- μ Ci/L ^{106}Ru Isopleth Distribution Pattern	V.35
V.23	Plan and Cross-Section View Through a Portion of 241-T Tank Farm with 1- μ Ci/L ^{137}Cs Isopleth Distribution Pattern	V.36

TABLES

M.1	Water Storage in Uniformly Deep Soils Compared with Soils Underlain by Coarse Sand at 60 cm	M.6
M.2	Risk Reduction Factors for Intrusion into Near-Surface Waste Sites by Drilling	M.13
M.3	Risk Reduction Factors for Excavation in Near-Surface Waste Sites	M.14
M.4	Risk Reduction Factors for Major Excavation Through Near-Surface Waste Sites ..	M.15
M.5	Multilayer Simulation Cases	M.21
M.6	Summary of Multilayer Barrier Simulations	M.22
N.1	BEIR III Risk Projection Models	N.4
N.2	Comparison of Various Estimates of Cancer Deaths per Million per Rem	N.6
N.3	Estimates of Genetic Effects of Radiation Over All Generations	N.9
N.4	Health Effects Risk Factors Employed in this EIS	N.10
P.1	Summary of Release Models Applied to Waste Forms	P.11
P.2	Concentrations and Leach Periods for Radionuclides and Chemicals in Single-Shell Tanks	P.14
P.3	Single-Shell Tank Leach by Diffusion	P.15
P.4	Parameters for the Liquid-Release Model for Double-Shell Tanks	P.16
P.5	Volumes, Surface Areas, and Edges of the Grout Waste	P.19
P.6	Leach Parameters for Direct Infiltration and Contact of TRU Wastes Stored in the 618 Subareas	P.21
P.7	Radionuclide Inventories for Existing Single-Shell Tanks	P.22
P.8	Radionuclide Inventories for Grout from Existing Tank Wastes	P.23
P.9	Radionuclide Inventories for Existing Double-Shell Tank Wastes	P.24
P.10	Radionuclide Inventory of Future Double-Shell Tank Wastes	P.25
P.11	Radionuclide Inventories of Grout from Future Tank Waste	P.25
P.12	Radionuclide Inventories for Sr/Cs Capsules in the Drywell Storage Facility	P.26
P.13	Radionuclide Inventories for TRU	P.27
P.14	Inventory and Location Details for Wastes to be Disposed of Near Surface in the Geologic Disposal Alternative	P.28
P.15	Inventory and Location Details for the In-Place Stabilization and Disposal Alternative	P.29
P.16	Inventory and Location Details for the Reference Alternative	P.30
P.17	Inventory and Location Details for No Disposal Action	P.31

P.18	Inventory and Location of Selected Radionuclides	P.32
P.19	Inventory and Location of Selected Radionuclides for the Geologic Disposal Alternative	P.33
P.20	Inventory and Location of Selected Radionuclides for the In-Place Stabilization and Disposal Alternative	P.34
P.21	Inventory and Location of Selected Radionuclides for the Reference Disposal Alternative	P.35
P.22	Inventory and Location of Selected Radionuclides for the No Disposal Action Alternative	P.36
P.23	Summary of Release Model Data: Salt Cake and Sludge in Single-Shell Tanks	P.37
P.24	Summary of Release Model Data: Liquid	P.38
P.25	Summary of Release Model Data: Grout	P.39
P.26	Summary of Release Model Data of TRU Waste for No Disposal Action	P.40
P.27	Distribution Coefficients and Decay Half-Lives Used in the Leach and Transport Models	P.41
Q.1	Waste Forms for the Various Disposal Alternatives	Q.11
Q.2	Transport Assessment of the Geologic Repository Alternative for the 0.5-cm/yr Annual Average Recharge Scenario	Q.14
Q.3	Transport Assessment of the In-Place Stabilization and Disposal Alternative for the 0.5-cm/yr Annual Average Recharge Scenario	Q.16
Q.4	Transport Assessment of the Reference Alternative for the 0.5-cm/yr Annual Average Recharge Scenario	Q.17
Q.5	Transport Assessment for No Disposal Action for the 0.5-cm/yr Annual Average Recharge Scenario	Q.18
Q.6	Transport Assessment of the Geologic Repository Alternative for the 5-cm/yr Annual Average Recharge	Q.21
Q.7	Transport Assessment of the Geologic Repository Alternative for the 5-cm/yr Annual Average Recharge Scenario--Disruptive Barrier Failure	Q.22
Q.8	Transport Assessment of the Geologic Repository Alternative for the 5-cm/yr Annual Average Recharge Scenario--Functional Barrier Failure	Q.24
Q.9	Transport Assessment of the In-Place Stabilization and Disposal Alternative for the 5-cm/yr Annual Average Recharge	Q.25
Q.10	Transport Assessment of the In-Place Stabilization and Disposal Alternative for the 5-cm/yr Annual Average Recharge Scenario--Disruptive Barrier Failure	Q.25
Q.11	Transport Assessment of the In-Place Stabilization and Disposal Alternative for the 5-cm/yr Annual Average Recharge Scenario--Functional Barrier Failure	Q.27
Q.12	Transport Assessment of the Reference Alternative for the 5-cm/yr Annual Average Recharge	Q.28

Q.13	Transport Assessment of the Reference Alternative for the 5-cm/yr Annual Average Recharge Scenario--Disruptive Barrier Failure	Q.29
Q.14	Transport Assessment of the Reference Alternative for the 5-cm/yr Annual Average Recharge Scenario--Functional Barrier Failure	Q.30
Q.15	Transport Assessment for No Disposal Action for the 5-cm/yr Annual Average Recharge Scenario	Q.31
Q.16	Transport Assessment of the 618 Burial Ground Sites for 5-cm/yr Recharge	Q.33
Q.17	Unsaturated Zone Thickness Between the 200 Area Tank Farms and the Simulated Water Tables	Q.38
R.1	Events Investigated for Potential Impact on Waste Disposal Systems	R.2
R.2	Geologic Disposal Alternative--Individual Maximum Potential 1-Year Radiation Doses from Drinking Well Water	R.6
R.3	Geologic Disposal Alternative--Individual Maximum Potential 70-Year Radiation Doses from Drinking Well Water	R.7
R.4	Geologic Disposal Alternative--Individual Maximum Potential 1-Year Radiation Dose from Drinking Well Water--5-cm/yr Recharge with Disruptive Barrier Failure	R.8
R.5	Geologic Disposal Alternative--Individual Maximum Potential 70-Year Radiation Dose from Drinking Well Water--5-cm/yr Recharge with Disruptive Barrier Failure	R.9
R.6	Geologic Disposal Alternative--Individual Maximum Potential 1-Year Radiation Dose from Drinking Well Water--5-cm/yr Recharge with Functional Barrier Failure	R.10
R.7	Geologic Disposal Alternative--Individual Maximum Potential 70-Year Radiation Dose from Drinking Well Water--5-cm/yr Recharge with Functional Barrier Failure	R.11
R.8	In-Place Stabilization and Disposal Alternative--Individual Maximum Potential 1-Year Radiation Dose from Drinking Well Water	R.12
R.9	In-Place Stabilization and Disposal Alternative--Individual Maximum Potential 70-Year Radiation Dose from Drinking Well Water	R.13
R.10	In-Place Stabilization and Disposal Alternative--Individual Maximum Potential 1-Year Radiation Dose from Drinking Well Water--5-cm/yr Recharge with Disruptive Barrier Failure	R.14
R.11	In-Place Stabilization and Disposal Alternative--Individual Maximum Potential 70-Year Radiation Dose from Drinking Well Water--5-cm/yr Recharge with Disruptive Barrier Failure	R.15
R.12	In-Place Stabilization and Disposal Alternative--Individual Maximum Potential 1-Year Radiation Dose from Drinking Well Water--5-cm/yr Recharge with Functional Barrier Failure	R.16
R.13	In-Place Stabilization and Disposal Alternative--Individual Maximum Potential 70-Year Radiation Dose from Drinking Well Water--5-cm/yr Recharge with Functional Barrier Failure	R.17
R.14	Reference Alternative--Individual Maximum Potential 1-Year Radiation Dose from Drinking Well Water	R.18

R.15	Reference Alternative--Individual Maximum Potential 70-Year Radiation Dose from Drinking Well Water	R.19
R.16	Reference Alternative--Individual Maximum Potential 1-Year Radiation Dose from Drinking Well Water--5-cm/yr Recharge with Disruptive Barrier Failure	R.20
R.17	Reference Alternative--Individual Maximum Potential 70-Year Radiation Dose from Drinking Well Water--5-cm/yr Recharge with Disruptive Barrier Failure	R.21
R.18	Reference Alternative--Individual Maximum Potential 1-Year Radiation Dose from Drinking Well Water--5-cm/yr Recharge with Functional Barrier Failure	R.22
R.19	Reference Alternative--Individual Maximum Potential 7D-Year Radiation Dose from Drinking Well Water--5-cm/yr Recharge with Functional Barrier Failure	R.23
R.20	No Disposal Action Alternative--Individual Maximum Potential 1-Year Radiation Dose from Drinking Well Water	R.24
R.21	No Disposal Action Alternative--Individual Maximum Potential 70-Year Radiation Dose from Drinking Well Water	R.25
R.22	Ratio of Critical-Organ Dose to Total-Body Dose for Selected Radionuclides	R.26
R.23	Geologic Disposal Alternative--Individual Maximum Potential 7D-Year Radiation Doses from the Full-Garden Scenario	R.35
R.24	Geologic Disposal Alternative--Individual Maximum Potential 70-Year Radiation Doses from the Full-Garden Scenario--5-cm/yr Recharge with Disruptive Barrier Failure	R.36
R.25	Geologic Disposal Alternative--Individual Maximum Potential 7D-Year Radiation Dose from Full-Garden Scenario--5-cm/yr Recharge with Functional Barrier Failure	R.37
R.26	In-Place Stabilization and Disposal Alternative--Individual Maximum Potential 7D-Year Radiation Doses from the Full-Garden Scenario	R.38
R.27	In-Place Stabilization and Disposal Alternative--Individual Maximum Potential 70-Year Radiation Doses from the Full-Garden Scenario--5-cm/yr Recharge with Disruptive Barrier Failure	R.39
R.28	In-Place Stabilization and Disposal Alternative--Individual Maximum Potential 70-Year Radiation Dose from Full-Garden Scenario--5-cm/yr Recharge with Functional Barrier Failures	R.40
R.29	Reference Alternative--Individual Maximum Potential 70-Year Radiation Doses from the Full-Garden Scenario	R.41
R.30	Reference Alternative--Individual Maximum Potential 70-Year Radiation Dose from Full-Garden Scenario--5-cm/yr Recharge with Disruptive Barrier Failure	R.42
R.31	Reference Alternative--Individual Maximum Potential 70-Year Radiation Dose from Full-Garden Scenario--5-cm/yr Recharge with Functional Barrier Failure	R.43
R.32	No Disposal Action Alternative--Individual Maximum Potential 7D-Year Radiation Dose from the Full-Garden Scenario	R.44

R.33	Geologic Disposal Alternative--Public Doses from Contaminant Migration to the Columbia River for 0.5-cm/yr Recharge	R.48
R.34	Geologic Disposal Alternative--Public Doses from Contaminant Migration to the Columbia River for 5-cm/yr Recharge	R.49
R.35	Geologic Disposal Alternative--Public Doses from Contaminant Migration to the Columbia River for 5-cm/yr Recharge with Disruptive Barrier Failure	R.50
R.36	Geologic Disposal Alternative--Public Doses from Contaminant Migration to the Columbia River for 5-cm/yr Recharge with Functional Barrier Failure	R.51
R.37	In-Place Stabilization and Disposal Alternative--Public Doses from Contaminant Migration to the Columbia River for 0.5-cm/yr Recharge	R.52
R.38	In-Place Stabilization and Disposal Alternative--Public Doses from Contaminant Migration to the Columbia River for 5-cm/yr Recharge	R.53
R.39	In-Place Stabilization and Disposal Alternative--Public Doses from Contaminant Migration to the Columbia River for 5-cm/yr Recharge with Disruptive Barrier Failure	R.54
R.40	In-Place Stabilization and Disposal Alternative--Public Doses from Contaminant Migration to the Columbia River for 5-cm/yr Recharge with Functional Barrier Failure	R.55
R.41	Reference Alternative--Public Doses from Contaminant Migration to the Columbia River for 0.5-cm/yr Recharge	R.56
R.42	Reference Alternative--Public Doses from Contaminant Migration to the Columbia River for 5-cm/yr Recharge	R.57
R.43	Reference Alternative--Public Doses from Contaminant Migration to the Columbia River for 5-cm/yr Recharge with Disruptive Barrier Failure	R.58
R.44	Reference Alternative--Public Doses from Contaminant Migration to the Columbia River for 5-cm/yr Recharge with Functional Barrier Failure	R.59
R.45	No Disposal Action Alternative--Public Doses from Contaminant Migration to the Columbia River for 0.5-cm/yr Recharge	R.60
R.46	No Disposal Action Alternative--Public Doses from Contaminant Migration to the Columbia River for 5-cm/yr Recharge	R.61
R.47	Incremental Radiation Dose to the Maximum Average Individual in the Down-River Population, as a Fraction of Natural Background, and the Total Number of Postulated Health Effects Resulting from Each Waste Disposal Alternative for Assumed 5-cm/yr Groundwater Recharge	R.62
R.48	Cumulative Radionuclide Releases to the Columbia River from all Waste Forms	R.63
R.49	Potential Total-Body Radiation Doses Resulting from Impact Crater Scenario	R.65
R.50	Source of Inventory for Drilling Scenario	R.66
R.51	Potential Doses Resulting from the Well-Drilling Scenario for the Geologic Disposal Alternative	R.68

R.52	Potential Doses Resulting from the Well-Drilling Scenario for the In-Place Stabilization and Disposal Alternative	R.69
R.53	Potential Doses Resulting from the Well-Drilling Scenario for the Reference Alternative	R.70
R.54	Potential Doses Resulting from the Well-Drilling Scenario for the No Disposal Action	R.71
R.55	Source of Inventory Used for Excavation Scenario	R.72
R.56	Potential Doses Resulting from the Excavation Scenario for the No Disposal Action Alternative	R.73
R.57	Fraction of Roots in Deeply Buried Waste as a Function of Time	R.75
R.58	Source of Inventory Used for Farmer Scenario	R.76
R.59	Potential Doses Resulting from the Residential/Home Garden Scenario for the No Disposal Action Alternative	R.77
R.60	Burrowing Habits of Potential Animal Intruders at an Unprotected Waste Burial Site	R.79
R.61	Plant Community Composition for the Waste Burial Site	R.80
R.62	Potential Doses Resulting from the Biotic Transport Scenario for the No Action Alternative	R.81
R.63	Potential Doses Resulting from the Postdrilling Scenario for the Geologic Disposal Alternative	R.82
R.64	Potential Doses Resulting from the Postdrilling/Excavation Scenario for the In-Place Stabilization and Disposal Alternative	R.83
R.65	Potential Doses Resulting from the Postdrilling Scenario for the Reference Alternative	R.84
R.66	Potential Doses Resulting from the Postdrilling Scenario for the No Disposal Action Alternative	R.85
R.67	Potential Integrated Population Doses from the Multiple-Small-Farm Scenario for the Waste Disposal Alternatives	R.87
R.68	No Disposal Action Alternative--Individual Maximum Potential Lifetime Dose for the Multiple-Small-Farm Scenario	R.89
R.69	Potential Radiological Health Effects from the Multiple-Small-Farm Scenario for No Disposal Action Followed by Loss of Institutional Control of the Site	R.90
R.70	Summary of Peak Flow Rates for Various Types of Floods at the Hanford Area	R.91
S.1	Fractions of Existing and Future Radionuclide Inventories Disposed of Near Surface for Geologic Disposal and Reference Alternatives	S.5
S.2	40 CFR 191 Table 1 Values and Partitioned Release Limits for Each Radionuclide Disposed of Near Surface for Each Alternative	S.6
S.3	Annual Recharge and Water Travel Times	S.12
S.4	Summary of Probability Density Functions and Corresponding Parameters	S.19

S.5	Annual Probabilities of Boreholes in Waste Classes and Waste-Class Surface Areas	S.21
S.6	Percentile Values of the Number of Boreholes in Each Waste Class	S.22
S.7	Numerical Comparison of Calculated Consequences with EPA Standard	S.27
S.8	Accumulated Radionuclide Releases to the Accessible Environment Over 10,000 Years for Scenarios with No Barrier Failure	S.29
S.9	Accumulated Radionuclide Releases to the Accessible Environment Over 10,000 Years for Scenarios with Current Climate and Barrier Failure	S.30
S.10	Accumulated Radionuclide Releases to the Accessible Environment Over 10,000 Years for Scenarios with Wetter Climate and Barrier Failure	S.31
S.11	Radionuclide Releases to the Accessible Environment for 100-Year Intrusion Scenario	S.32
T.1	Ambient Air-Quality Standards and Maximum Measured Background Concentrations for Hanford	T.2
T.2	ISC Receptors Outlining the Hanford Site	T.4
T.3	ISC Receptors at Selected Locations of Interest	T.5
T.4	Lapse-Rate Stability Classes	T.6
T.5	Maximum Annual Emissions and Emission Rates for Pertinent Time Periods	T.7
T.6	Maximum Ambient Air-Quality Impacts for Each Alternative	T.8
U.1	Estimated Mass of Chemical Components of Existing Single-Shell Tank Wastes After Completion of Jet Pumping	U.2
U.2	Parameters and Data for the Source Model of Selected Chemicals in Single-Shell Tanks	U.3
U.3	Chemical Transport from Salt and Sludge in Single-Shell Tanks-- With Protective Barrier--5-cm/yr Average Annual Recharge	U.6
U.4	Chemical Transport from Salt and Sludge in Single-Shell Tanks-- No Barrier--5-cm/yr Average Annual Recharge	U.7
U.5	Chemical Transport from Salt and Sludge in Single-Shell Tanks-- With Protective Barrier--0.5-cm/yr Average Annual Recharge	U.8
U.6	Chemical Transport from Salt and Sludge in Single-Shell Tanks-- No Barrier--0.5-cm/yr Average Annual Recharge	U.9
V.1	Radioactivity Remaining in the 216-A-24 Crib as of December 31, 1974	V.5
V.2	Radionuclide Inventory of Waste Discharged to the 216-S-1 and -2 Crib	V.14
V.3	Actinide Concentrations at Selected Depths Below the 216-Z-9 Trenches	V.20
V.4	Estimated Waste Inventory Released to the 241-B-361 Settling Tank and 216-B-5 Reverse Well	V.24

**THIS PAGE INTENTIONALLY
LEFT BLANK**

APPENDIX M

**PRELIMINARY ANALYSIS OF THE PERFORMANCE OF THE CONCEPTUAL PROTECTIVE
BARRIER AND MARKER SYSTEM**

**THIS PAGE INTENTIONALLY
LEFT BLANK**

APPENDIX M

PRELIMINARY ANALYSIS OF THE PERFORMANCE OF THE CONCEPTUAL PROTECTIVE BARRIER AND MARKER SYSTEM

M.1 INTRODUCTION

One aspect of certain disposal options analyzed in this EIS is the application of an engineered cover system over waste sites. This integrated system, consisting of a protective barrier and markers, would be applied to prevent or reduce the likelihood of wind erosion, water infiltration, and plant, animal, and human intrusion. There are several candidate cover concepts that could provide long-term environmental safety. Those concepts include soil mounding, revegetated covers, synthetic and natural impermeable layers (for example concrete and asphalt pavements), chemically treated soils, and multilayer earthen covers. After assessing the ability of these candidate concepts to perform as desired over long periods of time, a multilayer earthen cover concept was chosen for analysis in this EIS. The earthen cover concept was chosen largely because there is onsite evidence that layered soil systems have durability and, if designed properly, can minimize water infiltration (Adams and Wing 1987) and hence reduce movement of nuclides to groundwater, the expected environmental pathway of major interest. The multilayer system is referred to throughout this EIS as the protective barrier and marker system; or, for the sake of brevity, the term "protective barrier" is used to denote the complete system.

The conceptual protective barrier described here is designed to minimize (reduce to acceptable level) natural perturbations, water infiltration, animal and plant intrusion, and disruptive activities by humans. Use of multilayer earthen barriers to prevent biointrusion as well as infiltration of moisture is not a new concept. Two examples from the Far East provide evidence that ancient tombs have been effectively isolated from plant and animal intrusion as well as water infiltration for thousands of years under climate conditions with substantially more precipitation than at Hanford. The Silla tombs in Korea (Hoefer, Leuras and Chung 1983) and the Hunan Province tombs in China (Lee, Oscarson and Cheung 1986) both indicate that items buried several thousand years ago have been preserved extremely well under conditions of high rainfall. As an example, in China buried objects remained dry for over 2100 years under annual rainfalls of 139 cm (about 10 times that at Hanford) when isolated by compacted sands and clays. While these archeological data cannot be construed as proof of the performance to be expected of the protective barrier design under Hanford conditions, they do suggest that multilayer barriers have successfully operated for many hundreds of years under conditions more severe than those at Hanford. Engineered multilayered systems therefore appear to have promise for long-term isolation of materials from infiltrating water in unsaturated soil systems, particularly in semiarid regions such as at the Hanford Site.

In recent times, properly layered soil materials have been shown to be efficient at limiting vertical moisture movement (Miller 1973; Winograd 1981). Consequently, recent research in controlling unsaturated flow at near-surface waste sites in the United States has

been focused on evaluating multilayer-soil systems which confine the water movement (infiltration, redistribution, evapotranspiration) and biologic activity to the overlying fine soil zone (Herzog et al. 1982; Perkins and Cokal 1986; Hakonson 1986; Nyhan et al. 1986).

Winograd (1981) has suggested that multilayer barriers may be effective for disposal of high-level radioactive waste at arid sites. Multilayer covers of various designs and configurations have been proposed for use at low-level waste sites. As an example, a multilayer cover has been constructed at Canonsburg, Pennsylvania, and is used to control water infiltration and gas exhalation from uranium tailings waste (Bone and Schruben 1984). Several multilayer earthen-barrier designs have been proposed for isolating radioactive wastes at Weldon Springs, Missouri (DOE 1987). Studies by PNL (Cline, Gano and Rogers 1980; Gee et al. 1981; Hartley and Gee 1981) have evaluated several multilayer systems in the field for controlling plant and animal intrusion and for restricting gas exhalation from waste materials.

In a recent field study using a "soil/rock intrusion barrier" similar in concept to the protective barrier described in this appendix, Hakonson (1986) concludes that "experience gained through field studies and modeling is encouraging with respect to performance of this design for semiarid and arid sites." A multilayer-cover system for Hanford defense wastes which utilizes fine soil over coarse rock has been selected because for this arid site it appears to have potential for long-term protection against water infiltration and simultaneously to minimize intrusion of animals or plant roots into the waste.

Manmade markers complement the geophysical properties of the multilayer cover system to warn against human intrusion, which might occur if active institutional control were absent. While there is no intention of the DOE to ever leave the site, the EPA standard (40 CFR 191) for protection of the environment from disposal of high-level and transuranic waste states that active institutional control cannot be relied upon for more than 100 years after disposal.

As stated in the Foreword, in order to comply with the NEPA's requirement for early preparation of environmental documentation, this EIS has been prepared before final designs have been developed for all processes (including the protective barrier) necessary to complete the disposal options. It is expected that once a disposal decision is made, detailed engineering and testing will confirm performance expectations of specific waste retrieval, treatment, handling, immobilization and/or disposal processes evaluated in the EIS. This testing and evaluation will include both anticipated performance as designed and performance under perturbed (natural or human-caused) conditions. Furthermore, this review will be based on actual laboratory and field data collected under the Hanford Waste Management Technology Program. The details of the Protective Barrier/Marker Technology Development Program (Barrier Development Program) have been outlined in the Protective Barrier and Warning Marker System Development Plan (Adams and Wing 1987). A summary of this development plan is provided later in Section M.7.

This appendix presents a preliminary evaluation of the ability of the protective barrier concept to prevent water infiltration and discusses the qualitative features of this barrier in preventing or reducing the likelihood of plant, animal, and human intrusion.

M.1.1 Multilayer Concepts

Soil water is always moving. It can move rapidly (e.g., more than 1 cm/sec) during natural precipitation or irrigation events, or very slowly (less than 1 mm/yr) during water redistribution in dry soil. Water moves in response to total head differences. The pressure heads are positive in saturated soils because of hydrostatic forces and negative in unsaturated soils because of capillary forces. Steady water flow in either saturated or unsaturated soils can be expressed in terms of Darcy's Law:

$$J = -K(\theta) \nabla H$$

where J = the water flux

$K(\theta)$ = the hydraulic conductivity (a function of water content, θ , for unsaturated soils)

∇H = the total head gradient (combined hydrostatic, capillary, and gravity head).

In unsaturated soil, water movement is influenced both by capillary forces and by gravity. For relatively salt-free soils, the combination of capillary and gravitational heads determines the total hydraulic head, usually expressed in terms of length (centimeters or meters) of an equivalent water column. Infiltration and movement into either uniform or layered soils can be predicted by properly characterizing the hydraulic conductivity and the total head gradient.

M.1.1.1 Multilayer System with Capillary Barrier

The multilayer cover-system is a composite of layered rock (riprap) and soil materials. An integral part of the layering sequence is a coarse-textured layer, sometimes called a capillary barrier. The capillary barrier consists of a layer of coarse material (e.g., sand, gravel, or rock) placed directly below finer-textured soil and some significant distance above the water table. The coarse layer acts as a one-way check-valve system. Figure M.1 shows schematically a typical multilayer system with a capillary barrier. In an unsaturated system, water from below cannot be carried to the surface through the capillary barrier (except at an extremely low rate either by capillary rise or vapor transport) because of the very large pores in the gravel or rock. The capillary forces in the large rock pores are far too weak to overcome the downward gravitational forces. More importantly, for water from above to move into a coarse layer of riprap (capillary barrier) which is at atmospheric pressure, the outflow law (Richards 1950) for soil water requires that the soil at or near the interface with the capillary barrier must approach saturation (i.e., the soil water at the interface approaches atmospheric pressure, which implies that the capillary head approaches zero). This does not mean the total soil profile must be saturated. Water storage in the soil above the capillary barrier will be determined by the unsaturated

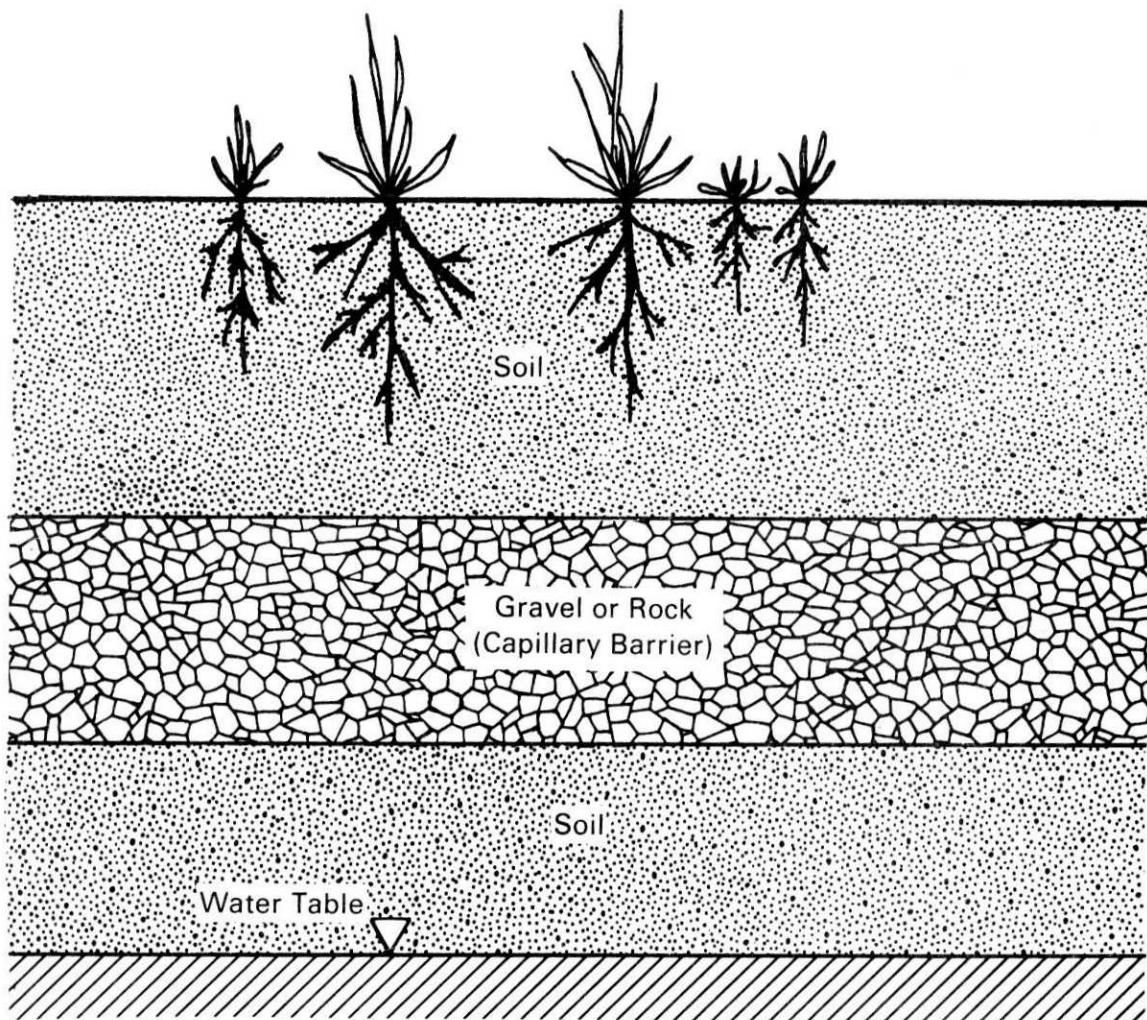


FIGURE M.1. Typical Multilayer Barrier Containing a Capillary Barrier
(not to scale)

conductivity of the coarse layer and by the characteristics of the overlying soil (Miller 1969). In other words, the overlying soil will vary in moisture content according to its specific drainage characteristics (Figure M.2), and the net water balance will be determined by the net balance or cycling of precipitation input and evapotranspiration (i.e., surface evaporation and plant water uptake). Layered soil effects on water storage are described in detail in numerous soil physics references (e.g., Miller and Bunker 1963; Miller 1969; Miller 1973; Hillel 1977).

The capillary barrier acts as a barrier to downward flow until the soil water at the soil-barrier interface approaches saturation. However, if saturation is achieved at the layer interface, water will drain into the capillary barrier at a rate controlled largely by the hydraulic conductivity of the overlying soil. In other words, if the storage capacity of the soil above the capillary barrier is exceeded, the capillary barrier will no longer be

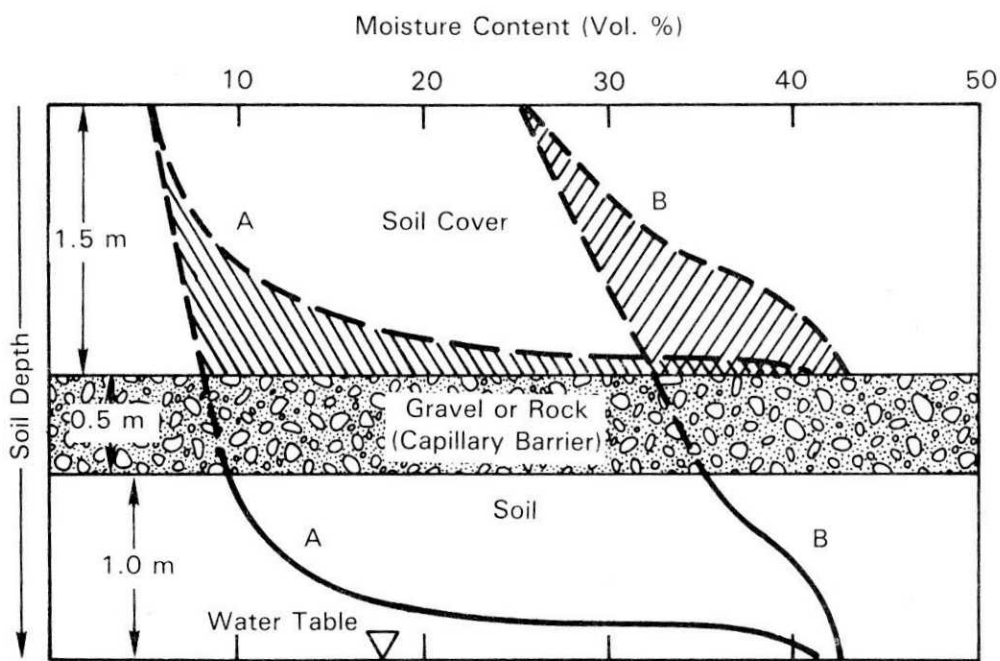


FIGURE M.2. Water-Content Profiles for a Coarse-Textured (A) and Fine-Textured (B) Soil Contained in a Multilayer Soil Cover. Dashed lines and hatched areas for curves A and B represent moisture contents and amounts of increased water stored in profile due to capillary barrier. Solid lines represent expected moisture content profiles if no gravel or rock layer were present.

effective, and moisture could reach the waste disposal system. For arid site conditions, where rainfall is limited and sporadic, this is assumed to be a temporary condition whose frequency depends upon both rainfall intensity and distribution as well as soil texture and plant cover characteristics. The use of a multilayer cover system, containing a capillary barrier, is contingent on its being able to store and subsequently lose water, via evapotranspiration, so that the layer above the barrier remains unsaturated.

M.1.2 Increased Water Storage

Field observations of layered soil systems indicate that significant increases in soil water storage can be attained when soils are underlain by coarse-textured materials (Miller 1969; Miller 1973). This is particularly true when the soil is moderately fine-textured. Figure M.2 and Table M.1 show the effect of layering on storage in finer textured soils overlying coarser textured soils.

The greater water retention in the overlying soil layer is attributed to the textural differences between the upper soil and the capillary barrier. Though this is counterintuitive (when considered in terms of saturated flow concepts), water does not move into coarse-textured materials at significant rates when flow is unsaturated. In other words, the coarser materials will not suck water out of the finer materials, but the finer materials will drain water downward if and only if the water potential gradients are in the downward

TABLE M.1. Water Storage in Uniformly Deep Soils Compared with Soils Underlain by Coarse Sand at 60 cm (Miller 1973)

Soil Material	Stored Water in 60 cm of Soil, cm H ₂ O		
	Loamy Sand	Loam	Silt Loam
Soil Underlain by Sand Layer (at 60 cm depth)	16.4	17.4	20.0
Uniform, Deep Soil with No Layer	<u>6.7</u>	<u>11.7</u>	<u>16.7</u>
Ratio Layered/Uniform	2.5	1.5	1.2

direction and the conductivity at the soil/rock interface is significantly above zero. Miller (1969, 1973) has shown that measurable flow rates into the capillary barrier occur only if the soil becomes nearly saturated at the interface. The coarser the capillary barrier material, the less flow is expected until near-saturated conditions prevail at the barrier-soil layer interface.

A coarse surface soil, because it provides little storage capacity for water, would not be recommended as a surface layer in a capillary barrier system. In addition to texture, the depth of cover material is an important consideration and will be evaluated along with the water retention and hydrologic properties of the soil materials. Cover material type and thickness is considered in Section M.5, in the discussion of model simulations.

M.1.3 Enhanced Water Removal

Results from laboratory and field studies (Miller 1969, 1973) indicate that more water is available for removal by plants when a subsurface coarse soil layer is present than when it is absent. The specific amount of water removed depends on plant and climatic factors as well as the water storage characteristics of the layered soil system. This suggests that a properly designed multilayer system utilizing a capillary barrier could effectively recycle water and hence reduce drainage more than a cover system without a capillary barrier. Field tests of capillary barriers underlying a soil cap at Los Alamos (Hakonson 1986) have demonstrated enhanced water removal by plants. Hakonson (1986) suggests that designing the cover with proper soil thickness, so that the "cap soil depth would be sufficiently large to store all (at a specified probability level) precipitation infiltrating into the cap....", the infiltrating water could be available for complete loss by evaporation. The cyclic removal of precipitation water by soil evaporation and plant water uptake is a key concern for infiltration control by the barrier.

M.2 CONCEPTUAL DESIGN DESCRIPTION

The multilayer earthen cover concept selected as the protective barrier system for this EIS comprises a 5.4-m thick mound containing a 1.5-m deep layer of revegetated soil as the upper surface underlain by 3.6 m of basalt riprap. The basalt riprap consists of 12- to 25-cm diameter rock material. A 0.3-m thick graded sand/gravel filter-layer separates the

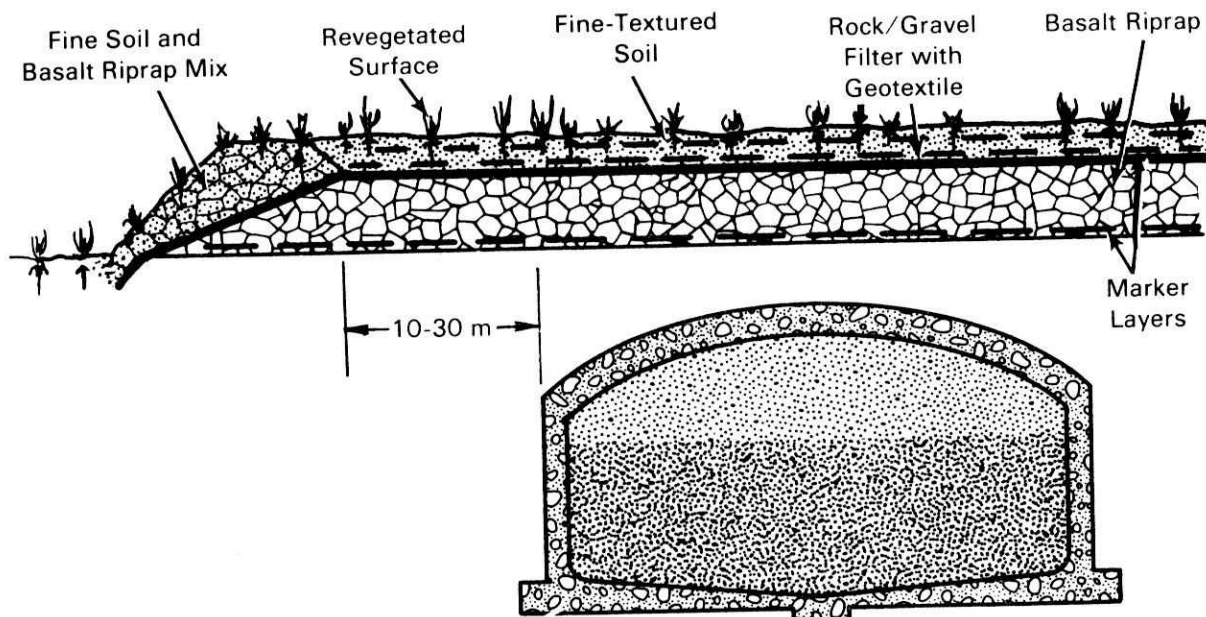
fine soil from the riprap and aids in minimizing the sifting of fines into riprap interstices. A 5-m wide edge (or berm) of riprap is provided for slope protection. The sides of the barrier are constructed on a 1-to-1 slope, and a riprap-filled trench is provided at the toe of the barrier to prevent or reduce the likelihood of animal intrusion. The berm consists of both riprap and fine soil mixed with riprap material separated by a gravel filter-layer.

Figure M.3 shows the barrier covering a waste tank. These or similar barriers may also be used for other waste sites. In the case of grouted wastes, where disposal vaults are located below grade in noncontaminated soil, the protective barrier system could be constructed so that the barrier surface is at ground level (i.e., not mounded); hence, the armored perimeter would not be required.

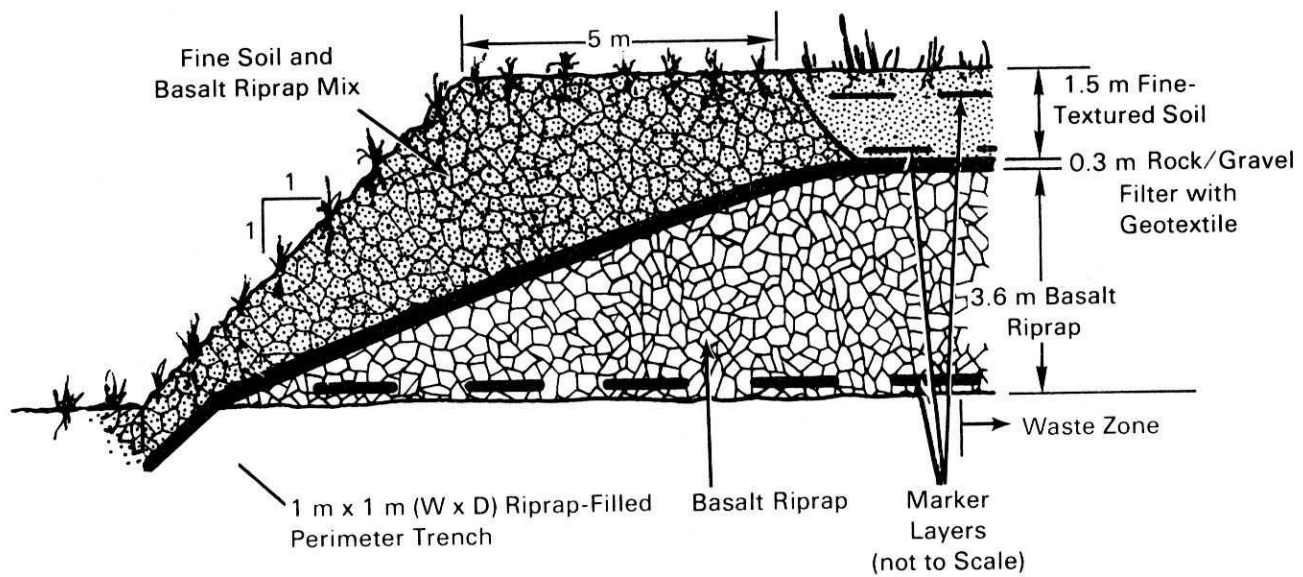
The natural materials (fine soil, gravel, basalt) for the multilayer cover are available on the Hanford Site. A geotextile mat, placed directly under the soil material, is being considered as an optional aid in layer construction; however, no credit is taken for the geotextile layer's enhancing the lifetime of the barrier. The thin, porous geotextile layer, composed of either woven silica glass or inert plastic, is not expected to compromise the drainage control characteristics of the protective barrier. Tests which include selected geotextile layers are planned in the barrier development program (Adams and Wing 1987).

The marker system is described conceptually as follows: Granite monoliths that protrude above grade would provide surface markers for the completed barrier. The marker base would be 1.5 m below grade while the apex would extend 3.8 m above grade. A series of repetitive messages would be engraved into each face of the monolith. The surface face near the message would be polished. The message would be inscribed to a depth of at least 2.5 cm, based on extrapolations from data on weathering of tombstones. The actual message content has not been determined but would consist of simple wording such as "Caution: Buried Hazardous Waste" as well as a radiation symbol or simple pictograph.

Three layers of subsurface markers would be distributed at various levels within the barrier above the waste site. These layers would be approximately 0.6, 1.5, and 5 m from the top of the selected barrier. Markers in each layer would be spaced on 6-m centers. The two top layers would overlap to give an effective 3-m distribution so that any excavation would probably uncover at least one of the warning markers. The markers would consist of 12.7-cm diameter porcelain or stoneware discs. The markers would warn the intruder about the potential hazard underlying the barrier, as well as protecting the barrier from further disruption. Additional detail as to how the protective barrier and marker system would be applied to different waste sites is reflected in Appendix B, Description of Facilities and Processes.



Cross-Section of Barrier System Overlying Waste Tanks



Detail of Barrier Perimeter

FIGURE M.3. Tank Farm Protective Barrier Concepts

M.3 DESIGN OBJECTIVES

The objectives of the protective barrier and marker system are to minimize water infiltration, biointrusion, erosion and human intrusion. The performance of the multilayer cover systems will be discussed in terms of these objectives. Field experiments, including plot and lysimeter tests, climate change reconstruction and forecasting, and natural analog studies, will be conducted as independent tests of barrier performance to provide assurance that the objectives are met.

M.3.1 Water Infiltration Control

Water infiltrates into surface soils and, if not removed by evaporation and plant transpiration processes, may contact and potentially leach waste materials into groundwater. Hence water infiltration is a transport mechanism that must be addressed for present and future conditions on the Hanford Site. Environmental safety associated with buried radioactive wastes at Hanford depends heavily upon the hydrologic and hydrogeochemical isolation of radionuclides from the relatively deep groundwater table at Hanford (Galley 1966; NAS-NRC 1978).

The majority of soils and sediments in the vadose zone at Hanford consist of coarse-textured materials which tend to drain readily (LaSala and Doty 1975; Routson and Fecht 1979). Under conditions where excess water is applied at the surface either as a result of irrigation, liquid waste disposal, process water disposal or above-normal precipitation, these sediments can readily transmit water downward below the root zone. Such additions of water may be a source for deep drainage to the water table.

Data from field and lysimeter studies (e.g., Enfield, Hsieh and Warrick 1973; Brownell et al. 1975) have been used to infer that little or no meteoric water infiltrates or drains below the root zone on the 200 Area Plateau at Hanford (Isaacson and Brown 1978; NAS-NRC 1978). However, studies near the Hanford 300 Area indicate that measurable amounts of water can move below the root zone of coarse-textured soils, particularly under conditions where plants are shallow rooted or absent (Kirkham and Gee 1984; Gee and Kirkham 1984). Drainage is further enhanced in coarse soils when the soil surface is kept bare (Jones and Gee 1984). (a) Modifying the soil profile by incorporating fine soil at the surface and revegetating could reduce drainage to the water table by retarding water percolation below the root zone. A multilayer cover consisting of fine soil overlying coarse materials, as described in Figure M.3, would optimize infiltration control, by keeping water near the surface so that evaporation and plant water uptake could recycle the water and limit water transmission below the root zone.

-
- (a) Recent evidence (Appendix B of Fayer, Gee and Jones 1986) suggests that coarse soil that is vegetated with deep-rooted plants can be effective in eliminating drainage (recharge) under present climate (past 14-year) conditions. Clearly variation in soil type and plant cover combined with climate (e.g., precipitation) variability will determine the quantity of recharge at any location at the Hanford Site (see M.5.2.4 for further discussion in this subject).

M.3.2 Upward Water Migration

The potential for long-term accumulation of salts in the protective barrier and the negative impact on plants has been considered. The net balance of salt transport is not envisioned to be a problem, since salt accumulation in the root zone or at shallow depth typically occurs only at arid sites where shallow water tables persist for long time periods. The barrier, on the other hand, is designed to optimize water accumulation and the rapid recycle of precipitation without excess salt accumulation. It is far more likely that in time, salts, such as carbonates, may accumulate (at the bottom of or below the root zone) creating a carbonate rich "caliche" layer, typical of well-developed soil profiles in arid climates. Study of these caliche formations at "natural analog" sites at Hanford is part of the Barrier Development Program (Adams and Wing 1987).

M.3.3 Biointrusion Control

Plant and animal activity at unprotected near-surface (shallow-land) waste burial sites can affect the performance of the containment system. Biological factors other than those resulting from human activity could lead to radiation dose to humans in the long term although they can also create a nuisance in the short-term. Plant and animal activity is a long-term consideration because the establishment of a species in an area is relatively slow and the transport of contaminants could occur slowly.

M.3.3.1 General Features of Biotic Intrusion

Investigations of radionuclide transport by biotic vectors has shown that the dose to humans resulting from biotic transport can be significant over long time periods (McKenzie et al. 1982). Biota can increase the probability of contaminant escape by altering the structure of the cover system. Burrowing animals and plant roots penetrating the soil cover result in a series of tunnels and chambers. As an indication of how extensive burrowing can be, about two miles of pocket gopher tunnels were estimated over one low-level waste site (at Los Alamos National Laboratory) that was only a few acres in extent (Hakonson, Martinez, and White 1982). At Hanford, tunnel volumes for harvester ant colonies averaged about 1.8 L per colony on low-level waste burial grounds, with tunnel depth ranging from 2 to 3 m in depth while colonies per burial ground ranged from 0 to 358 (Fitzner et al. 1979). Channels created by animals and plants may also promote the infiltration of surface water into the waste. Burrowing animals can increase erosion of cover materials by bringing soil to the surface (Winsor and Whicker 1980).

Active biological transport is a process considered to be significant in contaminant transport from unprotected waste buried near surface. Plant roots can penetrate into waste and translocate toxic elements through roots and stems to the above-ground plant parts. Burrowing animals may actively transport waste by physically moving contaminated material, by contaminating their bodies externally and redistributing contaminants in their day-to-day movements, and by ingesting contaminants and spreading the material in feces or, ultimately, in their carcasses. Once the contaminated material has escaped the containment system, secondary transport mechanisms can move it further. Leached material that returns to the

surface can enter the food chain through biotic transport. Contaminated plant material may be transported by wind or by ingestion by animals. It is important therefore that cover designs include considerations for biotic control.

M.3.3.2 Design Features for Biotic Control

Layers of coarse rock (graded filter) placed beneath fine soil have been used as a cover system for biotic control under semiarid and arid site conditions (Hakanson 1986). Dry cobblestones (i.e., clean coarse gravel), placed at depth, have been shown to be effective in preventing plant and animal intrusion (Cline, Gano and Rogers 1980). Cobble or rock barriers are most effective when fine soil particles are prevented from filtering into the spaces between the stones or rocks. Cline, Gano and Rogers (1980) suggest the following to ensure the effectiveness of biobarriers: 1) the zone beneath the barrier should be kept as dry as possible; 2) enough soil or other earthen material should be above the barrier to store annual precipitation; and 3) plants should be established, or other means provided, to remove excess soil water. Water control is necessary because plants and some animals (such as ants) tend to seek soil water, especially in arid areas. Thus a zone of relatively high soil moisture in a cover or in the waste is likely to attract plants and animals. The chances of exclusion are increased by efforts to ensure that soil moisture does not accumulate below the biotic barrier. The cycling of water in fine soil above the rock (riprap) layer as a result of soil evaporation and plant water uptake will minimize the chance for water accumulation below the biobarrier.

The cover system concept shown in Figure M.3 should be an effective biotic barrier. The layer of basalt riprap immediately over the waste is designed to discourage burrowing mammals from tunneling into the waste. Typical small mammals that burrow on the Hanford Site, such as pocket mice and ground squirrels, have not been observed to dig through riprap materials. Plant roots have been observed to grow horizontally above rock or gravel layers (Cline, Gano and Rogers 1980). The fine soil above the rock layer is designed to store several times the annual precipitation and, as indicated above, release it back to the atmosphere annually via evapotranspiration processes. Since arid site conditions dictate that the soil is primarily unsaturated, the burrows may act as water exclusion zones except for short intervals when thunderstorms or rapid snow melt may partially wet the burrows. The effects of plant and animal activity on infiltration control of the barrier will be the subject of study during the next several years (Adams and Wing 1987).

M.3.4 Human Intrusion Control

When determining potential consequences of the candidate disposal actions, the possibility of human intrusion and preventive measures must be considered. Several methods have been identified for reducing the likelihood of human interference at high-level waste repositories (ONWI 1984). These include site-selection factors that consider dedicated federal government ownership and possible future resource value; land use that reflects consideration of impeding future access to the site; and institutional controls that essentially provide for retaining site-specific information for extremely long periods. Institutional control must consider both active measures, site operation and surveillance,

and passive measures, control effected by related or ancillary activities. These same methods are appropriate considerations also in disposal of waste by other than deep geologic means.

All of these methods are incorporated to varying degrees when considering the application of the protective barrier and marker system. The federal government has no intention of vacating the Hanford Site; as previously implied, the possibility must be addressed for regulatory compliance. Given continued federal control, human intrusion is highly improbable. Passive controls include public records, maps, and markers. As described earlier, markers include peripheral granite monoliths plus several layers of discs emplaced in the multilayer barrier above the waste zone. The markers are combined to provide redundant levels of warning to potential intruders. The efficacy of the barrier and marker system in inhibiting human intrusion is addressed in the following discussion.

M.4 REDUCTION IN RISK OF INADVERTENT INTRUSION THROUGH PASSIVE INSTITUTIONAL CONTROLS(a)

Intrusion into waste sites is analyzed in a probabilistic sense in Appendix S. Briefly, in that analysis a drilling frequency of 0.01 boreholes per year per square kilometer is used. Based on the area of contaminated waste sites, the probability of encountering a waste site from randomly selected drilling sites is determined and the statistically expected number of boreholes penetrating waste sites over the 10,000-year period is estimated. At that point in the calculation, no credit was taken for the existence of barriers, markers, and other passive control measures in reducing the likelihood of encountering a waste site. This subsection presents a system of risk reduction factors that provides some measure (albeit judgmental) of the efficacy of passive institutional control systems for reducing the likelihood of intrusion into a waste site. A risk reduction factor is a value assigned to an element of passive institutional control that would reduce the likelihood of an event occurring. The risk reduction factors and the consequences of intrusion events are used to estimate overall long-term risk for the waste disposal alternatives and the no disposal action alternative. Since risk reduction factors are speculative, consequences of intrusion events are also presented in Section 3.4.2 without use of risk reduction factors.

The risk reduction factors presented here are based on subjective judgment; at present there are neither empirical nor theoretical models upon which these risk reduction factors can be based. Risk reduction factors typically range from 0 to 1.0 but in this system can also exceed 1.0. Low risk reduction factors indicate small likelihood of occurrence, while a factor of 1.0 indicates that no credit is given for a particular control. Factors greater than 1.0 indicate conditions where intrusion might be enhanced by a particular feature that acts as an attraction. Ranges of risk reduction factors for drilling into a waste site are given in Table M.2. Choices are explained in the text.

(a) DOE has no intention of vacating the Site. However, the EPA in its standard 40 CFR 191 states that active institutional controls may not be relied upon for more than 100 years after disposal. Consequently, only passive institutional controls are assumed to exist on the Site after the year 2150.

TABLE M.2. Risk Reduction Factors for Intrusion into Near-Surface Waste Sites by Drilling

	Unprotected Site	Sites with Protective Barrier and Marker System
Land Use Records	0.2	0.1 - 0.3
Boundary Marker	NA(a)	0.1 - 0.3
Monuments	NA	0.05 - 0.15
Protective Barrier	NA	0.1 - 0.3
Basalt Riprap		1.0
Vegetated Soil Layer		1.0
Internal Markers		0.1 - 1.5
Massive Presence	0.2(b)	$4 \times 10^{-4}(b)$

(a) NA = not applicable.

(b) Total risk reduction factor used in calculations (midpoint values of each of the ranges of factors).

Land use records, were they to survive loss of active institutional control, were thought to convince from seven to nine out of ten potential intruders (a) that drilling on a waste site would be unwise and should be avoided. This evaluation addresses the inadvertent intruder; the determined intruder who believes there is something of value buried beneath waste sites would probably not be deterred. In a scenario where the Hanford Site is abandoned because of a natural or manmade (war) catastrophe, it may be appropriate to conclude that land use records are lost; in which case no risk reduction would be assigned for land use records. In most other scenarios it is assumed that land use records will be preserved in some form; hence, credit is given for them (Table M.2).

The second line of defense against inadvertent intrusion is the Hanford Waste Disposal Site boundary markers that are employed in all but the no disposal action alternative. These markers, made of highly durable material, would contain warning messages, e.g., "Danger Radioactive Waste Disposal Sites Ahead ~ Do Not Disturb." It was judged that these warning markers would also or by themselves be heeded by seven to nine out of ten individuals.

The monuments proposed for marking near-surface waste sites themselves are expected to clearly communicate the hazards within the waste sites. It was concluded that 85 to 95 out of 100 individuals would heed the warnings and not drill through the barrier into a waste site.

The massive presence of the barrier itself was thought to suggest to half of the intentional intruders that something dangerous rather than valuable lay beneath and that therefore drilling might be unwise. On the other hand, the massive presence of the protective barrier

(a) Defined here as persons who make unauthorized entrance onto a waste site.

might be seen as an attraction particularly to someone manually exploring for something of value, hence an enhancement factor of 1.5 was also suggested.

The basalt riprap barrier itself would be expected to provide varying degrees of deterrence to drilling. Diamond-core drilling or similar apparatus would probably move through the barrier and wastes with little resistance. Other types of drilling might be found too impractical and thus preclude intrusion by those means. For example, in the loosely consolidated angular basalt riprap there may be nothing onto which the drills could "bite." In any case, those not drilling for "suspected valuables" beneath the barrier would in all likelihood move a few meters to one side and avoid drilling through the additional 5.5 m. It was judged that seven to nine of ten drillers would be deterred by physical features of the barrier and choose to drill elsewhere.

The vegetated soil layer, while preventing infiltration of water into the barrier and into the waste, was not judged to reduce the risk of drilling into waste sites. Similarly, the markers placed inside the barrier were not seen as reducing the risk of intrusion because, if markers are drilled through or are missed by the drilling, no warning of the underlying hazard would be given.

For purposes of risk calculation, the following factors taken from the ranges given in Table M.2 were used: where land use records are presumed to exist, 2×10^{-1} for unprotected waste sites and 4×10^{-4} for near-surface disposal with protective barrier. If it were assumed that land use records did not exist, the risk reduction factors used were 1.0 (no reduction) and 2×10^{-3} , respectively.

Ranges of risk reduction factors that might be associated with excavation activities (basement sized) are given in Table M.3. Table entries are explained in text.

TABLE M.3. Risk Reduction Factors for Excavation (basement sized) in Near-Surface Waste Sites^(a)

	Unprotected Site	Sites with Protective Barrier and Marker System
Land Use Records	0.1	0.05 - 0.15
Boundary Markers	NA ^(b)	0.05 - 0.15
Monuments	NA	0.025 - 0.075
Protective Barrier	NA	
Basalt Riprap		1.0
Vegetated Soil Layer		1.0
Internal Markers		0.05 - 0.15
Massive Presence		0.05 - 0.15
	0.1 ^(c)	5×10^{-6} ^(c)

(a) Excludes grout sites since basement excavation is about 3 m deep and grout is 5 m deep.

(b) NA = not applicable.

(c) Total risk reduction factor where midpoint values of each of the ranges of factors are used in calculations.

Since excavation would be expected to involve more planning, equipment, and expenditures than in the case of drilling, it was concluded that it would be more likely for land use records to be consulted before beginning operations. As a consequence, the risk reduction factors were nominally reduced from a range of 0.1 to 0.3 to a range of 0.05 to 0.15.

By similar argument, the efficacy of the boundary markers and monuments was concluded to be greater where more was at stake if the activity would be abandoned because of intrusion into a waste site. Consequently, the risk reduction factors were reduced further by a factor of 0.5.

The massive presence of the barrier was judged to deter 85 to 95 out of 100 individuals from excavation activities (such as performed by backhoe or small bulldozer) since it would be substantially easier to excavate in the nearby sandy to gravelly soils rather than in the basalt riprap.

Neither the basalt riprap nor the vegetated soil cover was given credit for deterrence to excavation. On the other hand, it would be expected that the markers inside the barrier would be uncovered at some point in the excavation. It was assumed that 85 to 95 individuals in 100 would stop excavation following discovery of one or more of the warning markers.

For purposes of risk calculation, the risk reduction factors employed for small excavations were 0.1 for unprotected sites and 5×10^{-6} for those disposed near surface with protective barrier. Where land use records were assumed to be lost, the factors used were 1.0 and 5×10^{-5} , respectively.

Ranges of risk reduction factors that might apply for a large excavation scenario (large earth-moving equipment) such as that supporting development of canals or subways are given in Table M.4. Table entries are explained in the text.

TABLE M.4. Risk Reduction Factors for Major Excavation Through Near-Surface Waste Sites (canals/subways).

	<u>Unprotected Site</u>	<u>Sites with Protective Barrier and Marker System</u>
Land Use Records	0.01	0.005 - 0.015
Boundary Markers	NA(a)	0.005 - 0.015
Monuments	NA	0.005 - 0.015
Protective Barrier	NA	
Basalt Riprap		1.0
Vegetated Soil Layer		1.0
Internal Markers		0.005 - 0.015
Massive Presence		0.005 - 0.015
	0.01(b)	$1 \times 10^{-10}(b)$

(a) NA = not applicable.

(b) Total risk reduction factor where midpoint values of each of the ranges of factors are used in calculations.

Again because of the additional planning, capital, and expense involved, land use records would probably be consulted before operators began major excavations. It was assumed that from 98 to 99 individuals out of 100 would seek out and heed land use records and would heed boundary markers or monuments before undertaking a major excavation.

The massive presence of the barrier would be assumed to deter 98 to 99 out of 100 from a major excavation into a waste site. For conditions where those deterrents all fail, it was assumed that 1 to 2 in 100 might proceed with major excavation if one or more warning markers were unearthed in the process of excavation.

For purposes of risk calculation, the risk reduction factors used for a major excavation scenario were 1×10^{-2} for an unprotected site and 1×10^{-10} for a near-surface site covered with protective barrier and marker system. Where land use records were assumed to be lost, the reduction factors used were 1.0 and 1×10^{-8} , respectively.

An additional scenario was envisioned in which after (perhaps long after) a drilling event someone inhabits a site that had been contaminated by the earlier drilling event. The risk reduction factors associated with such an event, assuming that land use records do not exist, were taken to be the same as for the drilling scenario (Table M.2) except that the vegetated soil layer on top of the barrier is given a value of 10; that is, when compared to surrounding soil, the vegetated soil is taken to be an attractive place for habitation. Thus the risk reduction factors (central values) for habitation over a waste site were taken to be (in absence of land use records) 1.0 for unprotected sites and 1×10^{-1} for near-surface disposal with barrier. The combined risk reduction factors would then be 1.0 for unprotected sites and 4×10^{-5} for sites with the protective barrier and marker system.

To illustrate the use of risk reduction factors, an estimate of the number of intrusions into a single-shell waste tank is developed below. The total area of these tanks is about $60,000 \text{ m}^2$ or about 0.06 km^2 . Then applying the probability of borehole drilling of 0.01 boreholes per square kilometer per year, the probability of intercepting a single-shell waste tank would be $(0.06 \text{ km}^2)(0.01 \text{ km}^{-2} \text{ yr}^{-1})$, or 6×10^{-4} per year. Then if the tanks were left unprotected, as would result in the long-term no disposal action scenario, the probability of intrusion (assuming land use records are also absent) would be $6 \times 10^{-4} \text{ yr}^{-1}$. In the case of near-surface disposal with the barrier and marker system, the risk reduction was 2×10^{-3} (central value from Table M.3 except no credit for land use records), and the combined probability of intrusion would be $1 \times 10^{-6} \text{ yr}^{-1}$.

Over the 10,000-year period, the average number of intrusions into unprotected sites would amount to about $(6 \times 10^{-4} \text{ yr}^{-1})(1 \times 10^4 \text{ yr})$, or 6 intrusions. Applying Poisson distribution statistics to the average number of statistically expected intrusions of 6, there would be less than one chance in 10,000 of the number of such boreholes exceeding 17.

On the other hand, the average expectation of intrusions into a barrier-covered single-shell tank would be $(1 \times 10^{-6} \text{ yr}^{-1})(1 \times 10^4 \text{ yr})$, or 1×10^{-2} , or on the average less than one intrusion over 10,000 years. Again applying Poisson statistics, there would be less than one chance in 10,000 of the number of such boreholes exceeding one. (The probability that the

number of intrusions would be zero was 0.999.) Thus risk of adverse impacts in terms of intrusion into a single-shell-tank waste site is at least 17 times smaller (safer) where the protective barrier and marker system has been applied over the waste site than where no barrier or marker system is in place.

These factors are used for some of the intruder scenario impacts reported in Section 3.4 of Volume 1. Also presented are impacts where all records, markers, and monuments are assumed to be removed, destroyed, or ignored.

M.5 MODEL SIMULATIONS OF WATER INFILTRATION CONTROL

To assess the protective barrier performance systems in minimizing infiltration, calculations were performed using climatic and soils data incorporated in a simulation model for evaluating water infiltration. In the model analysis, the variables considered were:

- the amount and seasonal distribution of rainfall for a given year
- the soil texture (whether coarse or fine) and soil thickness
- the presence of plants.

The unsaturated flow-code UNSAT1D (Gupta et al. 1978; Bond, Freshley, and Gee 1982) was used because it can handle these variables and can evaluate drainage through the barrier. Ongoing field testing (Adams and Wing 1987) will provide data to calibrate and validate the model. A brief description of the model follows.

M.5.1 Unsaturated Flow Code

The model used to simulate water movement in the multilayer barrier was developed from the one-dimensional unsaturated groundwater flow code UNSAT1D. The code is a finite-difference numerical code that has been tested against other numerical codes for adequacy in describing typical soil-flow processes such as infiltration, drainage, redistribution, and evaporation (Simmons and Cole 1985). The computer code was originally developed to describe water movement under typical agricultural conditions (Gupta et al. 1978). The modeling system can be applied to any unsaturated flow problem in one dimension. This model was applied to the multilayer test cases.

The model can be used to estimate surface infiltration, water removal by evaporation and plant root extraction (evapotranspiration), vertical seepage (redistribution), and drainage to the saturated zone. The model is designed for use under varied field conditions. Application of water can be in the form of rain (or snow), sprinkler irrigation, or flooding. Actual evapotranspiration as related to available soil moisture, can be simulated using on-off, linear decrease, logarithmic decrease, or combination methods (Gupta et al. 1978). The soil profile can be homogeneous or layered, and hydraulic properties can be defined analytically by polynomials or by simplified exponential relationships. The root uptake submodel incorporates root suction and root distribution, or the user can define his own mathematical model. The lower boundary can be described by a fixed water table, a flux boundary, or a no-flow boundary condition. The model has been used to model water flow at low-level nuclear

waste sites, uranium mill tailings sites, and oil shale waste disposal sites under arid climate conditions (Gee and Simmons 1979; Simmons and Gee 1981; Bond, Freshley, and Gee 1982).

M.5.1.1 Input Data Requirements

The following input information is necessary to define a model simulation of a specific site using the model:

- depth of the soil profile and location of each soil layer; the lower boundary is set to the maximum depth of the simulated profile
- type of lower boundary condition specified as a water table, no flow, or free drainage situation (free drainage conditions are applicable if the water table is well below the simulated profile)
- the soil hydraulic properties defined by a soil-water characteristic curve (water retention relationship) and hydraulic conductivity/suction head relationship for each soil type present in the profile
- the rainfall and potential evapotranspiration for each day of the simulation period, including the pattern of diurnal variation (rainfall should be by hour, and diurnal variation should be expressed as a fraction of daily amounts for each hour)
- the initial suction head distribution over the soil profile as established by a water movement history
- plant growth and water extraction behavior, including root-density distribution as a function of the growth period and actual transpiration as some factor of the potential transpiration when water is not limiting.

The above list represents a considerable amount of data. The difficulty of unsaturated flow modeling is that many of these data are seldom available from direct measurements and so must be estimated by various theoretical methods. Auxiliary programs to the model have been developed that use various theoretical methods to provide the data (such as unsaturated hydraulic conductivity and specific water capacity) required by the model. A list of these programs and a brief description of their function is given elsewhere (Bond, Freshley, and Gee 1982).

M.5.1.2 Specific Input for Test Cases

Precipitation and Climate Variables. A total annual precipitation of 30.1 cm was used in all simulation runs. This value was selected after review of meteorological data obtained at the Hanford Meteorology Station, located in the 200 Area at the Hanford Site (Stone et al. 1983). While this amount of annual precipitation has never been observed at Hanford, the 30.1 cm represents the maximum amount of annual precipitation that on the average will occur once every 100 years. This value was determined by use of extreme-value statistics (Kinnison 1983) applied to 63 years of record dating by the meteorology station, from 1913 through 1980 (years 1943-1946 had incomplete records and were not used). It should be noted that the

100-year maximum precipitation (30.1 cm) is considered to be a reasonable estimate for the mean value of precipitation in a future climate scenario at Hanford (see, for example, the work of Kukla 1979), but may not be the upper limit of annual precipitation under extreme conditions. For this reason, additional climate change studies are warranted (Adams and Wing 1987). Two rainfall-distribution patterns were examined--one with most of the rain in the fall (1947) and the other with most of the rain in the spring (1948). The rainfall for those years was 23.6 cm and 24.7 cm for 1947 and 1948, respectively, or about 50% higher than the average annual precipitation. The annual rainfall amount for both years was normalized to 30.1 cm. Daily rainfall was used in the model and partitioned into hourly values (Bond, Freshley and Gee 1982). Values of daily maximum and minimum air temperatures combined with solar radiation, wind speed and humidity measured at the Hanford Meteorology Station were used in computing potential evapotranspiration (PET). Daily values of PET were calculated using the Penman equation (Doorenbos and Pruitt 1977) and entered into the code. For no plants, the profile was allowed to evaporate the potential amount until the surface dried to a maximum suction head (10^5 cm). At that point, the surface head was held constant and the evaporation rate equaled that which the soil could supply from below (see Nimah and Hanks 1973 for a discussion of this methodology). When plants were present, water was extracted from the root zone until the suction head reached 1.5×10^4 cm (the wilting point), after which water flow was controlled by the surface boundary condition at maximum suction head as described previously.

Soil Texture. Two soils, one coarse-textured and the other fine-textured, representative of soils of the 200 East Area at Hanford were considered for simulation of the top layer of the barrier. The soil-moisture characteristics (water-retention curves) for the two soils are displayed in Figure M.4. Also displayed is the characteristic for a "clean-rock" gravel material obtained from the literature (Simmons and Gee 1981). This information was used to estimate the water retention characteristics of the gravel filter material overlying the basalt riprap. The thickness of the soil layer was selected at 1.5 m. In addition, a soil thickness of 3.0 m was simulated to indicate the relative value of added soil. For modeling purposes, the thickness of the gravel underlayer was set equal to the difference between the total barrier thickness (5.4 m) and the soil thickness. The hydraulic properties of riprap have not been measured directly and would be difficult to model because the extremely coarse texture results in very nonlinear hydraulic properties. Using measured clean-rock gravel characteristics (Simmons and Gee 1981) instead of riprap provided a conservative estimate of the capillary barrier performance of the cover system.

Plant Cover. Although plants will initially be present on the barriers, they may not be active at certain times during the life of the barrier because of fires or drought. This, however, is likely to be a transient situation of short duration. Therefore the intent of the simulations with plants was to provide an example of the relative importance of a plant cover by simulating a barrier with and without plants. The plant cover selected was cheatgrass with a growing (transpiration) cycle of 152 days. Details of the transpiration

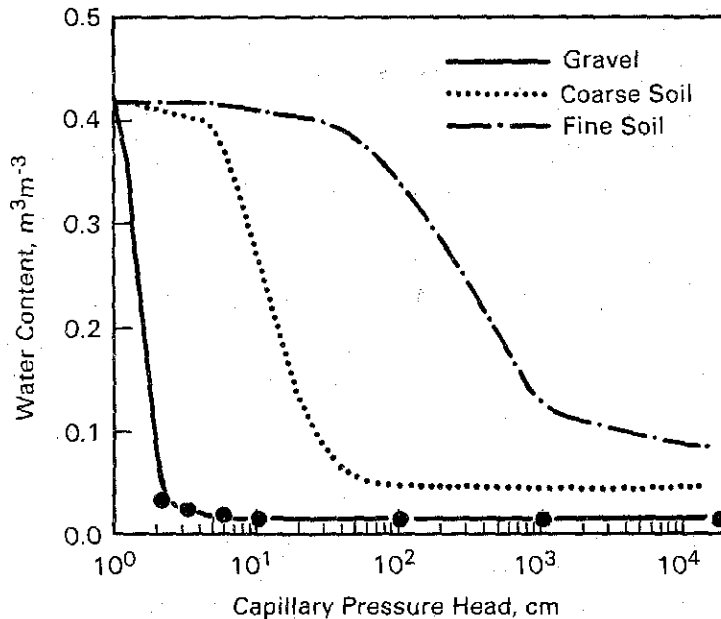


FIGURE M.4. Soil-Moisture Characteristics for the Materials Used in the Barrier Simulations

algorithm are given by Fayer, Gee and Jones (1986). Plant transpiration is computed as a fraction of PET using cheatgrass data from Hinds (1975). Modifications of this algorithm are also described in Fayer et al. (1985).

The cases tested are shown in Table M.5 and their results are given in the following section.

M.5.2 Simulation Results

In any modeling effort, the results are only as good as the conceptual model, the computer code, and the input data. The barrier simulation results that follow are no exception. Questions concerning the specific soil properties used, the methods used to model evaporation and transpiration, and even the way the initial conditions were set up, are all legitimate and must be ultimately resolved through a multiyear research and demonstration project focused on the performance of the protective barrier. The intent of the modeling effort was to use the best simulation techniques available to gauge the effectiveness of the multilayer cover in stopping infiltration of water into the waste. Although the results (see Table M.6) should be viewed as preliminary, they do reflect the performance of a multilayer cover system under the constraints imposed by the assumed climate and soils used in the simulations; hence, they provide some assurance as to the overall effectiveness of a cover system for infiltration control under Hanford Site conditions. As previously stated, the successful model prediction of field data provided from the Barrier Development Program (Adams and Wing 1987) will resolve these specific uncertainties. The test cases reported here reflected a

TABLE M.5. Multilayer Simulation Cases

Case Number	Precipitation Distribution (a)	Plant Presence	Soil Texture	Soil Thickness, m
1	Fall	No	Coarse	1.5
2	Spring	Yes	Fine	1.5
3	Fall	Yes	Fine	1.5
4	Fall	No	Fine	1.5
5	Fall	Yes	Fine	3.0
6	Spring	No	Fine	1.5
7	Fall	Yes	Coarse	1.5
8	Fall	No	Fine/No Gravel Layer	5.4

(a) Normalized to the 100-year maximum (30.1 cm).

range of soil, plant and climate conditions simulated by the UNSAT1D model. The impact of selected parameters for drainage is reflected in the test cases described in the following sections.

M.5.2.1 Test Cases

The first task was to simulate the cover system with the combination of factors most and least likely to contribute to drainage. The most likely barrier leakage was expected to occur with the fall rainfall distribution, the coarse soil, and no plants (case 1). After the first simulation year, 2.3 cm of water had drained through the barrier (Table M.6). During the second year, 20.3 cm of water, or two-thirds of the yearly precipitation, had drained through. Quite clearly, the cover constructed with a coarse soil failed for this scenario. Not shown in Table M.6 is the mass balance error associated with the numerical simulation. For the coarse soil, the mass balance error for the first-year simulation was 1.2 cm, but this was reduced to 0.1 cm for the second-year simulation. Depending on the type of simulation (coarse soil, plants), the mass balance generally ranged from less than 0.1 to 1.5 cm and accounts for the difference in water balances for each year's simulation.

The next step was to simulate the cover under conditions for which drainage was least likely to occur--spring rainfall distribution, fine soil, and plants (case 2). For each of eight consecutive simulation years, the computed drainage through the barrier was less than 0.1 cm, even though storage of water in the fine soil had increased by about 17 cm of water. As the soil profile became wetter, evaporation increased because the hydraulic conductivity of the wetter soil was higher. A near-equilibrium was eventually reached where the yearly evapotranspiration approached the yearly rainfall. In this scenario, the barrier constructed with a fine soil effectively prevented drainage of water. The value (<0.1 cm/yr) for drainage indicates that the computed drainage was less than 0.1 cm/yr. Since these model simulations were run, additional soils and plant cover situations have been simulated

TABLE M.6. Summary of Multilayer Barrier Simulations

<u>Case</u>	<u>Initial Storage, cm</u>	<u>Final Storage, cm</u>	<u>Total Drainage at Base, cm</u>	<u>Evaporation/Transpiration, cm</u>	<u>Sequence Number of Year</u>	<u>Case Description</u>
1	26.8	44.5	2.3	8.9/0.0	1	Fall rain, no plants, coarse soil, 1.5 m
		45.3	20.3	9.0/0.0	2	
2	47.6	52.9	<0.1	17.0/7.0	1	Spring rain, plants, fine soil, 1.5 m
		56.8	<0.1	18.5/7.0	2	
		59.8	<0.1	19.4/7.0	3	
		64.1	<0.1	22.2/7.0	7	
		64.2	<0.1	22.2/7.0	8	
3	47.6	50.2	<0.1	16.9/9.5	1	Fall rain, plants, fine soil, 1.5 m
		52.9	<0.1	17.0/9.5	2	
		55.2	<0.1	17.3/9.5	3	
		61.2	<0.1	18.8/9.5	7	
		62.0	<0.1	19.0/9.5	8	
4	47.6	58.3	<0.1	19.5/0.0	1	Fall rain, no plants, fine soil, 1.5 m
		65.1	<0.1	23.4/0.0	2	
		68.7	<0.1	26.7/0.0	3	
		70.2	<0.1	28.7/0.0	4	
		71.3	<0.1	30.2/0.0	14	
		71.4	<0.1	30.2/0.0	15	
		71.4	<0.1	30.2/0.0	16	
5	74.7	80.1	<0.1	17.1/7.1	1	Fall rain, plants, fine soil, 3.0 m
		84.0	<0.1	18.5/7.0	2	
		87.4	<0.1	19.0/7.0	3	
		90.7	<0.1	19.2/7.0	4	
		111.5	<0.1	20.9/7.0	14	
		112.3	0.4	21.0/7.0	15	
		112.3	1.1	21.0/7.0	16	
6	47.6	56.6	<0.1	21.1/0.0	1	Spring rain, no plants, fine soil, 1.5 m
		62.2	<0.1	24.7/0.0	2	
		65.3	<0.1	27.1/0.0	3	
		66.5	<0.1	29.1/0.0	4	
		66.9	<0.1	29.8/0.0	5	
7	26.9	43.2	0.1	7.3/5.2	1	Fall rain, plants, coarse soil, 1.5 m
		45.0	14.7	7.4/6.0	2	
8	165.5	176.2	<0.1	19.5/0.0	1	Fall rain, no plants, fine soil, 5.4 m, no underlying gravel layer
		183.5	<0.1	22.8/0.0	2	
		189.1	1.1	23.4/0.0	3	
		191.7	3.8	23.6/0.0	4	
		192.5	5.7	23.7/0.0	5	

(Fayer et al. 1985). The new simulations had mass balance errors of less than 0.1 cm and indicated that fine soils and plants can control drainage to levels less than 0.1 cm/yr for the climate conditions specified here.

M.5.2.2 Precipitation

It was expected that, with cool-season plants (cheatgrass), the fall rain (case 3) would be more conducive to drainage than the spring rain (case 2) because the simulated plants transpired only in the spring. In both cases no drainage (<0.1 cm) was observed during any of the eight years of simulation. In contrast to the original expectation, however, more water was stored at the end of each year under spring rain conditions. Although the precipitation (30.1 cm) was normalized for the fall and spring rain years, the potential evapotranspiration was not normalized; hence the spring rain years always had 11% lower potential evapotranspiration than the fall rain years. The computed evaporation for the first simulation year was similar for fall and spring rain conditions, but the transpiration was more for the fall rain conditions (9.5 cm) than for spring rain conditions (7.0 cm). Hence annual water loss was less for spring rain simulations. These differences account for the higher stored water under spring rain conditions. By the eighth simulation year, however, evaporation during the spring rain year was 3.2 cm greater than for the fall rain year, thus tending to offset the greater transpiration of the fall rain year.

In contrast, when there were no plants, more storage occurred in the fall rain year (case 4) because evaporation was about 2.0 cm less than in the spring rain year (case 6). In some way, distribution of the spring rain was more conducive to its removal from the profile by evaporation. Thus, with or without plants, it is not just the rainfall distribution but the combination of rainfall and evapotranspiration distributions and amounts that are important in determining drainage rates at a given site. A variety of rainfall distributions including extreme events (1000-year storms, etc), will be modeled in the Barrier Development Program (Adams and Wing 1987).

M.5.2.3 Soil Texture

The coarse soil used in this study has a low storage, or water-holding, capacity. For the fall rain year, with no plants, the coarse soil (case 1) stored 17.7 cm of the rain water, and 2.3 cm of water drained through the barrier by the end of the first simulation year. In contrast, for the same conditions (fall rain year, no plants), the fine soil (case 4) stored more than 23 cm of water over 16 consecutive years and still did not drain. This finding points out dramatically the effect of soil texture on the performance of the barrier.

A simulation was conducted with a fine soil layer 3.0 m thick (case 5), instead of 1.5 m, to judge the added value of a thicker design. Although no drainage occurred during 14 consecutive years of flow simulation, a significant amount of water (1.4 cm/yr) was still moving below the 1.5-m depth and being stored between 1.5 and 3.0 m. Water at these depths is less likely to be withdrawn by plants and/or evaporation than is water near the surface. It is therefore more susceptible to drainage, especially if the storage capacity of the deeper layer is eventually exceeded. In fact, during the fifteenth simulation year, 0.4 cm

of water drained through the bottom of the barrier, even as the fine soil stored an additional 0.8 cm of water. During the sixteenth year, 1.1 cm of water drained through. The thicker soil layer actually decreases the effectiveness of the barrier because it routes water down and away from the upper soil layer where it would otherwise be lost to evapotranspiration. The simulation represents a conservative estimate of drainage since deeper-rooted plants (>0.8 m rooting depths) would be more effective in removal of water at depth than those simulated here.

A final simulation was conducted in which the barrier was made up entirely of the fine soil (case 8) with no underlying gravel layer. With the fall rain year and no plants, drainage was 1.1, 3.8, and 5.7 cm in the third, fourth, and fifth years, respectively. In addition, storage in the profile increased during all five years. In contrast, recall that with the gravel layer (case 4), no drainage occurred for sixteen consecutive years and storage essentially remained constant after only the fourth year. The gravel layer is indeed necessary for the barrier to perform effectively.

Although not simulated, the addition of a clay or an asphalt layer placed directly below the fine soil has been considered in addition to the rock sublayer as a redundant protective layer to minimize drainage. Based on simulation cases 4 and 6 and considering present climate conditions, these redundant layers would not be needed. Only in extremely wet conditions (>30 cm/yr) would there appear to be any advantage to a redundant layer; hence, it was not included in the analysis. The clay or asphalt layer would tend to limit drainage (because of low conductivity) to less than a fraction of a centimeter per year, even under extremely wet conditions. Tests to evaluate redundant barriers are currently being considered (Adams and Wing 1987).

M.5.2.4 Plant Cover

Simulation work with plants indicates that vegetated barriers are more effective in preventing drainage of water than nonvegetated barriers. For example, for the fall rain year and the fine soil, the total evaporation without plants (case 4) was 19.5 cm versus the total evapotranspiration of 26.4 cm with plants (case 3). For the coarse soil (case 7), barrier performance improved somewhat, but drainage still occurred (0.1 cm the first year, 14.7 cm the second year). Thus it does not appear that a barrier constructed with coarse soil would work under the imposed conditions. Note that a less conservative estimate of cheatgrass transpiration would account for increased biomass production and increased transpiration with increased rainfall. Also, increased precipitation could induce deeper-rooted plants (e.g., perennial grasses and shrubs) to invade the soil cover, thus enhancing root water extraction and transpiration. Because the response function (transpiration versus biomass increase) is not known quantitatively for our native vegetation, we can only qualitatively state that increased transpiration, with above-normal precipitation, would tend to reduce estimated drainage in both the coarse- and fine-textured soil cases.

Although no details are provided here, simulations were also performed assuming irrigated corn was growing on the barrier. In those simulations, the corn roots penetrated the entire soil depth (150 cm) and had a transpiration rate that approached the potential

evapotranspiration rate for the growing season. More than 82 cm of water was removed from the soil profile in one year when 52 cm of irrigation water was applied, in addition to an annual rain input of 30 cm. Clearly, plant cover, rooting depth, and soil texture all have major effects on the simulated water balance and thus barrier performance.

The presence or absence of plants, as well as other factors, can determine whether recharge is low or high. Evidence that net recharge can be near zero for a specific site at Hanford is given by Fayer, Gee and Jones (1986). Soil water contents and water storage in a lysimeter^(a) located just south of the 200 East Area were measured by gravimetric sampling in October 1985. Plant cover had been observed on the lysimeters since 1974 (Gee and Heller 1985). The measured water contents and storage values were compared with those obtained during installation of the lysimeter in December 1970 (Hsieh, Brownell and Reisenauer 1973). A net loss in water storage was observed, indicating that for over 14 years there had been an apparent decrease of water in the soil profile. Water flow simulations utilizing daily values for climate obtained at the nearby Hanford Meteorology Station and measured soil characteristics (Hsieh, Brownell and Reisenauer 1973), were conducted with and without plant water uptake (Fayer, Gee and Jones 1986). The simulations clearly indicate that plant water uptake could account for the observed storage changes. These data, when compared with bare soil lysimeter measurements, in the 300 Area during the same time period, which show storage increases and drainage (Jones and Gee 1984), further emphasize the importance of plants in controlling drainage.

M.5.3 Model Simulation Summary

Key results from the model simulation can be summarized as follows:

1. Coarse soil layers (with or without plants) will not prevent drainage when subjected to elevated rainfall (30.1 cm/yr).
2. Fine-textured soil overlying coarse layers will store and transmit water so that evapotranspiration processes can effectively recycle the precipitation, thus preventing drainage even under elevated rainfall conditions.
3. Soil thickness must be properly designed. The fine soil tested had sufficient conductivity that for bare soil under elevated rainfall conditions, drainage was possible, when the soil thickness exceeded 1.5 m. The presence of plants combined with fine soil can significantly reduce the potential for drainage.
4. Annual rainfall distribution and potential evapotranspiration, as determined by climatic variables, are important factors in determining annual evaporation and transpiration but appear to be less important than soil thickness and texture in determining drainage.

(a) The lysimeter on which these measurements were made is a 3-m-dia, soil-filled container with a sealed bottom. The lysimeter is buried upright in the ground with the top flush with the soil surface. Its purpose has been to detect deep drainage at Hanford. The reader is referred to Hsieh, Brownell and Reisenauer (1973) and Gee and Jones (1985) for additional details regarding this lysimeter.

5. A proper cover design is possible using onsite materials, layered so as to maximize evapotranspiration and minimize drainage.

M.6 COVER DISTURBANCE CONSIDERATIONS

With respect to water infiltration, the uppermost soil layer on the protective barrier is of critical importance. Therefore, it is important to consider potential disturbances to this barrier. Such disturbances might include improper placement, earthquakes, erosion, and subsidence. These disturbances are being analyzed as part of a multiyear research and demonstration program at Hanford.

Earthquake activity may be important from a geotechnical viewpoint since the disruptions of the barrier by vibration and earth shaking may cause a mixing of the fine soil with the basalt riprap. Although mechanisms like this and even possibly liquefaction seem highly unlikely, some additional data are probably needed. There is no direct evidence to support long-term protection of the barrier from earthquakes. However, indirect evidence from observation of the glaciofluvial deposits at Hanford shows that clean rock and gravel have persisted below fine soil layers without disruption for at least 10,000 years. Studies are under way to further evaluate these natural conditions (Adams and Wing 1987).

Wind erosion (by particle suspension and dispersion by wind) has been qualitatively considered as a mechanism for transport of contaminants and soil materials from existing waste sites at Hanford, especially those undergoing some type of construction (Sehmel 1976, 1979, 1981). Loss or gain of material from the proposed protective barrier by wind erosion should be considered in long-term predictions of barrier integrity. Sehmel (1979), however, indicates that, at present, data are insufficient to predict wind erosion and resuspension rates at Hanford because the effects of particle diameter and vegetative cover have not been sufficiently quantified. Furthermore, conditions on top of an engineered barrier are likely to be different from those encountered at existing ground-level waste burial grounds at Hanford. Therefore, extrapolation would not be wise.

Bander (1982) suggests methods to estimate soil erosion and deposition from wind stresses using agriculturally based wind erosion models (e.g., Chepil and Woodruff 1963; Skidmore 1974), but these have not been tested on nonagricultural sites, and additional research is required to evaluate their effectiveness for long-term erosion predictions for the protective barrier. At best, there are only qualitative estimates of erosion and deposition rates at Hanford. Based on long-term accumulation records and recurrences of volcanic ash deposits (e.g., from Mount St. Helens) and other wind-blown materials from off site over the last several thousand years, it appears that there would tend to be a net accumulation of soil material at Hanford with time, as opposed to net erosion. Localized erosion might still take place, however, on elevated mounds (cover systems) if adequate rock armoring or vegetative cover were not present.

No quantitative estimates of localized surface soil erosion exist. It is anticipated, however, that both rock armoring (incorporation of surface amendments of gravel or rock into the fine texture soil) and vegetative cover can be adequately engineered into the cover

design. Vegetation and rock armoring would both minimize wind erosion and enhance deposition of wind-blown material onto the cover. Some consideration should be made for the potential for and impact of sand dune formation and migration on top of the protective barrier. In addition, water erosion should be considered. The barrier design (Figure M.3) should preclude mechanisms for rill or sheet erosion since the surface is flat and the sides are armored. There are plans currently in progress by Hanford Site contractors to scientifically evaluate the potential for both wind and water erosion for various cover designs (Adams and Wing 1987).

Other mechanisms that may contribute to cover performance perturbations include surface removal by humans (human intrusion) and subsidence effects caused by collapse of underlying waste containers, improper barrier emplacement, or natural compaction. Possible subsidence, resulting from tank collapse, is a long-term consideration that is to be addressed in engineering studies on dome-filling methods and tank stability within the next several years at Hanford. Subsidence in general will be analyzed as part of the multiyear research and demonstration program for barriers. Such information will then be used to guide the final design and construction, if necessary. Various improvements in design to address subsidence are presently being considered. One of these improvements is to fill the tanks with gravel.

M.7 PROTECTIVE BARRIER AND WARNING MARKER SYSTEM DEVELOPMENT PLAN

The protective barrier and marker system described in this appendix is conceptual only. No full-scale barrier system has yet been built or tested; however, there have been several demonstration-scale barrier systems constructed at Hanford during the past several years (Phillips et al. 1985). These reflect the essence of the multilayer earthen cover system described in this appendix. However, only limited testing of these barriers has been completed to date. The ability of the protective barrier to minimize infiltration and biologic and human intrusion must be demonstrated before a definitive design is selected. A comprehensive plan to evaluate protective barriers for use at Hanford has been developed under the Barrier Development Program (Adams and Wing 1987). A brief outline of this plan follows.

The protective barrier and warning marker system is designed to isolate radioactive wastes from the accessible environment by minimizing the following influences:

- biointrusion--the penetration of deep-rooting plants and burrowing animals into the waste zone
- water infiltration--the percolation of water into the waste zone and subsequent transport of radionuclides to the water table
- wind and water erosion--the deterioration of the surface of the protective barrier due to erosive forces
- human interference--the inadvertent or intentional intrusion of humans into the waste sites.

M.7.1 Scope

The Protective Barrier and Warning Marker System Development Plan has the following objectives: identify unresolved questions about the design and performance of barriers and markers that require experiments, tests, or demonstrations to be performed in order to answer those questions; support and elaborate on barrier and marker development plans specified by the Department of Energy for the Hanford Site (DOE 1986); provide a logically related basis for proceeding with barrier and marker development activities; provide manpower, materials, cost and capital equipment estimates that can be used in budget preparation; and provide a schedule for barrier and marker development activities.

The emphasis of the Barrier Development Plan is on the development of barriers and markers for above-grade (mounded barrier) applications to existing waste sites. Many of the barrier development tasks described in the plan are also relevant and applicable to various components of at-grade or below-grade barriers at new waste disposal sites.

The current focus of design efforts is to provide a protective barrier and warning marker system that will remain functional and maintenance free for up to 10,000 years despite the occurrence of natural hazards (i.e., earthquakes, volcanic ashfall events, high winds, maximum probable precipitation events, and subsidence) or any other phenomena that could reasonably be expected to occur during the design life of the barrier.

M.7.2 Methodology

Conceptual designs for protective barrier and warning marker systems have been developed to isolate radioactive wastes from the accessible environment and to provide protection against water infiltration, biointrusion, wind and water erosion, and human interference. Prior to implementation, the performance of these designs will be tested and verified to ensure adequate functioning. Figure M.5 illustrates the process, which is presented in the following paragraphs. A set of preliminary quantitative performance objectives and specifications is being developed for these potential pathways against which testing results can be compared and the adequacy of various designs can be evaluated.

Eleven groups of tasks have also been identified to resolve technical concerns and complete the development of barriers and markers:

1. development of biointrusion control methods
2. development of water infiltration control methods
3. development of erosion control methods
4. physical stability testing
5. development of human interference control methods
6. evaluation of barrier construction materials
7. field monitoring and model validation
8. natural analog study
9. evaluation of long-term climate change effects
10. design
11. documentation.

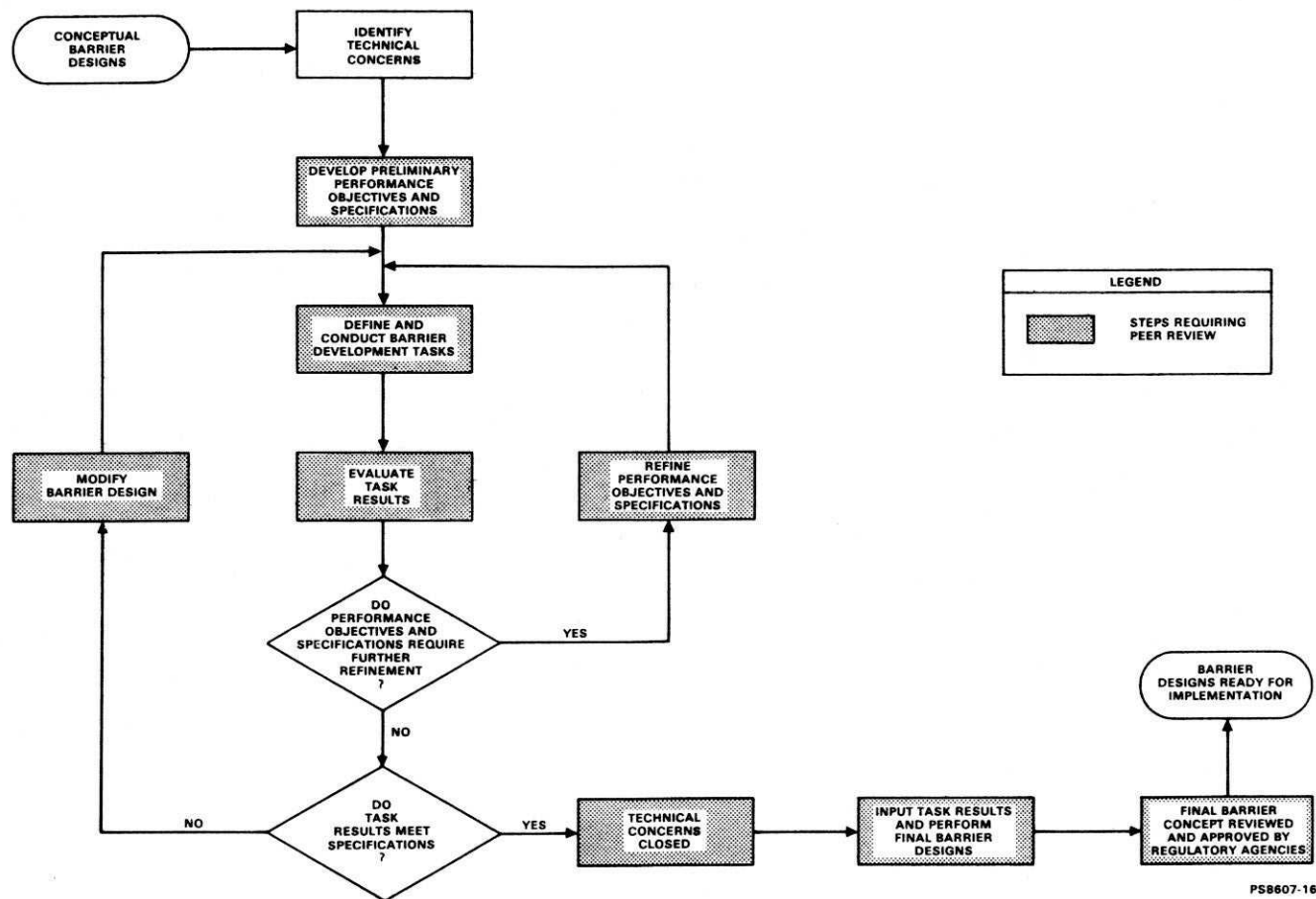


FIGURE M.5. Logic Diagram for Barrier and Marker Development (Adams & Wing 1987)

Each of the tasks and activities within these task groups will be performed according to specific test plans and other detailed planning documents written to direct the work. The results will be evaluated and compared to the applicable performance objectives and specifications. If the results of a particular task meet the performance criteria, the task is completed and the technical concern is considered closed. If the task results do not meet the performance criteria, any necessary barrier or marker design modifications will be made and the affected tasks will be repeated (see Figure M.5).

The data and results obtained from completed tasks will be used to enhance barrier and marker designs and serve as input to other tasks whose activities are dependent upon the results. At the completion of the barrier and marker development tasks, a final design of a barrier/marker system will be performed. After this final design has been reviewed and approved by the appropriate regulatory agencies, the barrier and marker system will be ready for implementation.

The major barrier development activities completed or in progress to date are presented below.

1. Engineering studies have been completed in which more than a dozen barrier concepts were evaluated, including rigid, impermeable barrier types and barriers utilizing manmade materials.
2. Five configurations of protective barriers have been constructed and monitored (Phillips et al. 1985) at the Protective Barrier Test Facility (PBTF) located in the 200 West Area.
3. Natural geologic deposits, analogous to multilayer barrier designs, have been identified and examined, and several selected sites have been characterized. The objective of the barrier analog studies is to project the long-term performance of protective barriers by analyzing analogous geologic deposits and ecological settings.
4. The computer simulation modeling of unsaturated flow for various multilayer barrier configurations is under way (see Fayer et al. 1985).
5. An engineering study (Myers 1986) and additional characterization activities have been completed, which identify quarry and borrow pit locations capable of supplying projected quantities (and quality) of rock and soil to construct protective barriers over applicable waste sites. The studies have also evaluated the most efficient means of transporting and placing the materials on the sites.
6. The design of the Field Lysimeter Test Facility (FLTF), located near the Hanford Meteorology Station in the 200 Area, has been completed and construction has begun.
7. Work statements have been prepared to enlist the services of outside contractors, consultants, and universities to perform the following tasks:

- determine the effects of geomorphic and other natural hazards on the performance of multilayer barriers.
 - analyze the distribution of carbonates in layered Hanford formation sediments as a means of determining long-term water balance.
8. Test plans have been or are being written to direct testing activities in the following areas:
- Biointrusion control development tasks
 - Animal intrusion field tests will be performed to determine the degree to which animal burrow systems affect the infiltration of water through a protective barrier. These tests will also determine the effectiveness of various barrier construction materials in deterring intrusion by animals expected to live on the barrier.
 - Evapotranspiration/water balance studies will be performed to obtain field data on the transpiration of perennial plants. These data will be used to support the modeling effort for predicting water infiltration throughout the barrier.
 - Water infiltration control development tasks
 - The FLTF tests will be performed to obtain quantitative measurements of water movement through various barrier configurations. The results from the tests at the FLTF will be used to validate water infiltration simulation models.
 - Erosion control development tasks
 - Admix gravel field tests are designed to determine the effects that gravel mulches have on the soil's ability to retain water, support vegetation growth, and provide erosion resistance to the barrier surface.
 - Wind tunnel tests will be conducted to assess the effectiveness of gravel mulches and vegetative covers in preventing the erosion of barrier surfaces as a function of wind velocity. Results from other companion erosion studies will be tested in a wind tunnel so that an optimal erosion-resistant barrier surface can be designed. Wind tunnel data will then be input into erosion models that will be developed to predict the performance of optimal barrier surfaces over a 10,000-year period.
 - Bergmounds are naturally occurring geologic deposits (~13,000 years old) of fine soils with gravel armoring on the surface. The bergmounds provide a good natural analog for certain features of the protective

- barrier concept, and tests of the bergmounds may provide valuable insights into the expected performance of protective barriers over thousands of years.
- Blowouts are circular or semicircular depressions that are caused by the removal of sandy soils by wind erosion. A field investigation will be performed to determine what conditions cause blowouts to occur and how blowouts can be prevented from occurring on the barrier surface.
- Physical stability testing task
 - A number of subsidence tasks are planned for subsequent fiscal years to determine how a protective barrier will perform following a subsidence event. These tests will require that simulated subsidence events be performed. As a result, a subsidence trigger test plan is being prepared to identify methods of simulating a subsidence event and observing the effects of the subsidence on the barrier. These developmental efforts will be used in subsequent subsidence tests.
9. A plan has been written for obtaining long-term projections of variability in climate and vegetation.
- Additional detail related to the protective barrier and marker test plan can be found in Adams and Wing (1987). In response to public comment, DOE has committed to testing the barrier under simulated irrigation conditions and will also test the barrier to failure under extreme wetting conditions. The test plan will be revised to reflect this commitment.

M.8 BARRIER FAILURE SCENARIOS

The preliminary analysis described earlier in this appendix leads to the conclusion that an undisturbed barrier would protect the underlying waste from water infiltration under present climate conditions. For analysis in this EIS, though, two barrier failure scenarios have been hypothesized.

M.8.1 Disruptive Failure Scenario

A scenario has been created that simulates a massive disruption of part of the barrier system. The most plausible mechanism for such a failure is that someone blades off the barrier topsoil for use elsewhere.

The net effect of this disruptive failure is that enough soil is removed over 10% of the barrier area that it acts as a catchment rather than a barrier. With high precipitation (30 cm/yr) it is assumed that this waste area is exposed to direct leaching. For analysis it is assumed that 15 cm/yr infiltrates through this disrupted area. This is in contrast to the 5 cm/yr estimated to infiltrate through 200 Areas plateau soil (with no barrier) under similar meteorological conditions.

M.8.2 Functional Failure Scenario

In a second barrier failure scenario, an attempt has been made to test a failure of a large barrier area. Certain phenomena might cause such a degraded performance. One could be wind erosion in such a way that some cover soil is removed. Another phenomenon, blowing sand, could affect optimal barrier thickness. Seismic events could conceivably disturb the interface between the fines and the riprap such that some fines would percolate into the coarse material, thus degrading the barrier performance. Subsidence of underlying wastes is another mechanism that could reduce a barrier's effectiveness. Lastly, the use of construction materials, particularly topsoils, that are out of specifications could cause barriers to perform below standard.

The functional barrier failure is defined such that 50% of the barrier area allows 0.1 cm/yr to infiltrate the underlying wastes with precipitation conditions of 30 cm/yr.

M.9 SUMMARY

In summary, the protective barrier and marker system consisting of fine soil material with admixed ceramic tile markers, overlying coarse gravel or rock holds promise as a method for providing enhanced isolation of wastes disposed near surface at the Hanford Site. A soil with adequate water-holding and water-transmission characteristics is desirable for the surface soil. The underlying coarse gravel or riprap provides a sharp textural break which, in effect, hydrologically isolates the surface soil from the underlying waste materials. The available soil water is held near the surface, where it is accessible for plant uptake and evaporation. The cover system materials are durable so that a protective barrier system is expected not only to limit water infiltration but also to reduce the likelihood of plant, animal, and human intrusion into the wastes. The barrier presented in this appendix is conceptual only. A development program has been initiated to evaluate barrier performance under Hanford Site conditions using onsite materials and configurations similar to those analyzed in the model-simulation test cases. Failure mechanisms such as erosion, subsidence and intrusion will be addressed experimentally in tests conducted at Hanford. Redundant barrier systems containing subsurface layers of clay and/or asphalt that may be called for to provide additional long-term protection are also included in the test program. Climate change is an uncertainty that can affect barrier performance and will also be addressed in the development program.

M.10 REFERENCES

- Adams, M. R., and N. R. Wing. 1987. Protective Barrier and Warning Marker System Development Plan. RHO-RE-PL-35 P, Rockwell Hanford Operations, Richland, Washington.
- Bander, T. J. 1982. Literature Review of Models for Estimating Soil Erosion and Deposition from Wind Stresses on Uranium Mill Tailings Covers. NUREG/CR-2768 (PNL-4302), Nuclear Regulatory Commission, Washington, D.C.
- Bond, F. W., M. D. Freshley and G. W. Gee. 1982. Unsaturated Flow Modeling of a Retorted Oil Shale Pile. PNL-4284, Pacific Northwest Laboratory, Richland, Washington.

Bone, M. J., and T. J. Schruben. 1984. "Long-Term Stability--Canonsburg, Pennsylvania UMTRA Site." In Proceedings of the Sixth Symposium on Uranium Mill Tailings Management, pp. 453-461. Civil Engineering Department, Colorado State University, Fort Collins, Colorado.

Brownell, L. E., J. G. Backer, R. E. Isaacson and D. J. Brown. 1975. Soil Moisture Transport in Arid Site Vadose Zones. ARH-ST-123, Atlantic Richfield Hanford Company, Richland, Washington.

Chepil, W. S., and N. P. Woodruff. 1963. "The Physics of Wind Erosion and Its Control." Advances in Agronomy 15:211-302.

Cline, J. F., K. A. Gano and L. E. Rogers. 1980. "Loose Rock as Biobarriers in Shallow Land Burial." Health Physics 39:497-504.

Department of Energy (DOE). 1986. Interim Hanford Waste Management Technology Plan. DOE/RL/01030-T4, Operations Office, Richland, Washington.

Department of Energy (DOE). 1987. Remedial Action at the Weldon Spring Site: Draft Environmental Impact Statement. DOE/EIS-0117D, Washington D.C.

Doorenbos, J., and W. O. Pruitt. 1977. Guidelines for Predicting Crop Water Requirements. Irrigation and Drainage Paper 24 (2nd Ed.) Food and Agriculture Organization of the United Nations, Rome.

Enfield, C. G., J. J. C. Hsieh and A. W. Warrick. 1973. "Evaluation of Water Flux Above a Deep Water Table Using Thermocouple Psychrometers." Soil Sci. Soc. Am. Proc. 37:968-970.

Fayer, M. J., G. W. Gee and T. L. Jones. 1986. UNSAT-H Version 1.0: Unsaturated Flow Code Documentation and Applications for the Hanford Site. PNL-5899, Pacific Northwest Laboratory, Richland, Washington.

Fayer, M. J., W. Conbere, P. R. Heller, and G. W. Gee. 1985. Model Assessment of Protective Barrier Designs. PNL-5604, Pacific Northwest Laboratory, Richland, Washington.

Fitzner, R. E., K. A. Gano, W. H. Rickard and L. E. Rogers. 1979. Characterization of the Hanford 300 Area Burial Grounds Task IV--Biological Transport. PNL-2774, Pacific Northwest Laboratory, Richland, Washington.

Galley, J. E. 1966. Report of the Committee on Geologic Aspects of Radioactive Waste Disposal. National Academy of Sciences--National Research Council, Washington, D.C.

Gee, G. W., and P. R. Heller. 1985. Unsaturated Water Flow at the Hanford Site: A Review of Literature and Annotated Bibliography. PNL-5428, Pacific Northwest Laboratory, Richland, Washington.

Gee, G. W., and T. L. Jones. 1986. Lysimeters at the Hanford Site: Present Use and Future Needs. PNL-5578, Pacific Northwest Laboratory, Richland, Washington.

Gee, G. W., and R. R. Kirkham. 1984. Arid Site Water Balance: Evapotranspiration Modeling and Measurements. PNL-5177, Pacific Northwest Laboratory, Richland, Washington.

Gee, G. W., and C. S. Simmons. 1979. Characterization of the Hanford 300 Area Burial Grounds. Task III--Fluid Transport and Modeling. PNL-2921, Pacific Northwest Laboratory, Richland, Washington.

Gee, G. W., J. T. Zellmer, M. E. Dodson, R. R. Kirkham, B. E. Opitz, D. R. Sherwood and J. Tingey. 1981. "Radon Control by Multilayer Earth Barriers; 2. Field Tests." In Proceedings of the Fourth Symposium on Uranium Mill Tailings Management, pp. 289-308. Civil Engineering Dept., Colorado State University, Fort Collins, Colorado.

Gupta, S. K., K. K. Tanji, D. R. Nielson, J. W. Bigger, C. S. Simmons and J. McIntyre. 1978. "Field Simulation of Soil Water Movement with Crop Water Extraction." Water Science and Engineering, Paper No. 4013, University of California Davis, Davis, California.

- Hakonson, T. E., J. L. Martinez and G. C. White. 1982. "Disturbance of a Low-Level Waste Burial Site Cover by Pocket Gophers." Health Physics 42:868-871.
- Hakonson, T. E. 1986. Evaluation of Geologic Materials to Limit Biological Intrusion into Low-Level Radioactive Waste Disposal Sites. LA-10286-MS, Los Alamos National Laboratory, Los Alamos, New Mexico.
- Hartley, J. N., and G. W. Gee. 1981. "Uranium Mill Tailings Remedial Action (UMTRA) Joint Field Test." In Proceedings of the Fourth Symposium of Uranium Mill Tailings Management, pp. 115-134. Civil Engineering Dept., Colorado State University, Fort Collins, Colorado.
- Herzog, D. L., K. Cartwright, T. M. Johnson and H. J. H. Harris. 1982. A Study of Trench Covers to Minimize Infiltration at Waste Disposal Sites. NUREG/CR-2478 (Vol. 1), Nuclear Regulatory Commission, Washington, D.C.
- Hillel, D. 1977. Computer Simulation of Soil-Water Dynamics. International Development Research Centre, Ottawa, Canada.
- Hillel, D., and H. Talpaz. 1977. "Simulation of Soil Water Dynamics in Layered Soils." Soil Sci. 123:54-62.
- Hillel, D., and C. H. M. Van Bavel. 1976. "Dependence of Profile Water Storage on Soil Hydraulic Properties: A Simulation Model." Soil Sci. Soc. Amer. J. 40:807-815.
- Hinds, W. T. 1975. "Energy and Carbon Balances in Cheatgrass: An Essay in Autoecology." Ecological Monographs 45:367-388.
- Hoefer, H. J., L. Leuras and N. Chung. 1983. Korea. 2nd ed., APA Productions, Hong Kong.
- Hsieh, J. J. C., L. E. Brownell and A. E. Reisenauer. 1973. Lysimeter Experiment, Description and Progress Report on Neutron Measurements. BNWL-1711, Pacific Northwest Laboratory, Richland, Washington.
- Isaacson, R. E., L. E. Brownell and J. C. Hanson. 1974. Soil Moisture Transport in Arid Site Vadose Zones. ARH-2983, Atlantic Richfield Hanford Company, Richland, Washington.
- Isaacson, R. E., and D. J. Brown. 1978. "Environmental Assessment Related to Hanford Radioactive Waste Burial." RHO-SA-36, Rockwell Hanford Operations, Richland, Washington.
- Johnson, T. M., T. H. Larson, B. L. Herzog, K. Cartwright, C. J. Stohr and S. J. Klein. 1983. A Study of Trench Covers to Minimize Infiltration at Waste Disposal Sites. NUREG/CR-2478 (Vol. 2), Nuclear Regulatory Commission, Washington, D.C.
- Jones, T. L., and G. W. Gee. 1984. Assessment of Unsaturated Zone Transport for Shallow Land Burial of Radioactive Waste: Summary Report of Technology Needs, Model Verification, and Measurement Efforts (FY78-FY83). PNL-4747, Pacific Northwest Laboratory, Richland, Washington.
- Kinnison, R. R. 1983. Applied Extreme Value Statistics. PNL-4690, Pacific Northwest Laboratory, Richland, Washington.
- Kirkham, R. R., and G. W. Gee. 1984. "Measurements of Unsaturated Flow Below the Root-Zone at an Arid Site." In Proceedings of the National Water Well Association Conference on Characterization and Monitoring of the Vadose Zone. National Water Well Association, Las Vegas, Nevada (PNL-SA-11629).
- Kukla, G. K. 1979. "Probability of Expected Climate Stresses in North America in the Next One Million Years." In Summary of FY-1978 Consultant Input for Scenario Methodology Development, ed. B. L. Scott et al. PNL-2851, Pacific Northwest Laboratory, Richland, Washington.
- La Sala, A. M., Jr., and G. C. Doty. 1975. Geology and Hydrology of Radioactive Solid Waste Burial Grounds at the Hanford Reservation, Wash. Open File Report 75-625, United States Department of the Interior, Geological Survey, Reston, Virginia.

- McKenzie, D. H., L. L. Cadwell, C. E. Cushing, Jr., R. Harty, W. E. Kennedy, Jr., M. A. Simmons, J. K. Soldat and B. Swartzman. 1982. Relevance of Biotic Pathways to the Long-Term Regulation of Nuclear Waste Disposal. A Report on Tasks 1 and 2 of Phase 1. NUREG/CR-2675 (PNL-4241), Vol. I, Nuclear Regulatory Commission, Washington, D.C.
- Miller, D. E. 1969. Flow and Retention of Water in Layered Soils. USDA Conservation Research Report No. 13, 28 pp. Department of Agriculture, Washington, D.C.
- Miller, D. E. 1973. "Water Retention and Flow in Layered Soil Profiles." In Field Soil Water Regime, ed. R. R. Bruce, pp. 107-117. Soil Science Am. Special Publ. Series #5, Madison, Wisconsin.
- Miller, D. E. and W. C. Bunker. 1963. "Moisture Retention by Soil With Coarse Layers in the Profile." Soil Sci. Soc. Amer. Proc. 27:586-589.
- Myers, D. R. 1986. Disposal Material Study. RHO-WM-EV-12P, Rockwell Hanford Operations, Richland, Washington.
- National Academy of Sciences-National Research Council (NAS-NRC). 1978. Radioactive Wastes at the Hanford Reservation, A Technical Review. Washington, D.C.
- Nimah, M. N., and R. J. Hanks. 1973. "Model for Estimating Soil Water, Plant and Atmospheric Interrelations: I. Description and Sensitivity." Soil Sci. Soc. Amer. Proc. 37:522-527.
- Nyhan, J. W., W. Abeele, T. Hakonson and E. A. Lopez. 1986. Technology Development for the Design of Waste Repositories at Arid Sites: Field Studies of Biointrusion and Capillary Barriers. LA-10574-MS, Los Alamos National Laboratory, Los Alamos, New Mexico.
- Office of Nuclear Waste Isolation (ONWI). 1984. Reducing the Likelihood of Future Human Activities That Could Affect Geologic High-Level Waste Repositories. BMI/ONWI-537, Battelle Memorial Institute, Columbus, Ohio.
- Perkins, B. A., and E. J. Cokal. 1986. Subsurface Moisture Regimes and Trace Movement Under Two Types of Trench-Cap Designs for Shallow Land Burial Sites. LA-10449-MS, Los Alamos National Laboratory, Los Alamos, New Mexico.
- Phillips, S. J., M. R. Adams, T. W. Gilbert, C. C. Meinhardt, R. M. Mitchell and W. J. Waugh. 1985. Engineered Barrier Test Facility Status Report: 1984. RHO-WM-SR-3P, Rockwell Hanford Operations, Richland, Washington.
- Reisenauer, A. E. 1963. "Methods of Solving Problems of Multi-dimensional Partially Saturated Steady Flow in Soils." J. Geophys. Res. 68(20):5725-5733.
- Richards, L. A. 1950. "Laws of Soil Moisture." Trans. Amer. Geophys. Union 31(5):750-756.
- Routson, R. C., and K. R. Fecht. 1979. Soil (Sediment) Properties of Twelve Hanford Wells with Geologic Interpretation. RHO-LD-82, Rockwell Hanford Operations, Richland, Washington.
- Sehmel, G. A. 1976. "Initial Observations of Airborne Concentrations of Small Particle Size Ranges During Two Dust Storms." In Pacific Northwest Laboratory Annual Report for 1975 to USEDA Division of Biomedical and Environmental Research Part 3, Atmospheric Sciences. BNWL-2000, Pacific Northwest Laboratory, Richland, Washington.
- Sehmel, G. A. 1979. Deposition and Resuspension Processes. DE84-00517, National Technical Information Service, Springfield, Virginia.
- Sehmel, G. A. 1981. "Volcanic Ash and Ambient Airborne Soils Concentration at Hanford, Washington Sampling Sites Subsequent to the Mt. St. Helens' Eruption." In Pacific Northwest Laboratory Annual Report for 1980 to the DOE Assistant Secretary for Environment. Pacific Northwest Laboratory, Richland, Washington.

Simmons, C. S., and C. R. Cole. 1985. Guidelines for Selecting Codes for Ground-Water Transport Modeling of Low-Level Waste Burial Sites, Vol. 2: Special Test Cases. PNL-4980, Pacific Northwest Laboratory, Richland, Washington.

Simmons, C. S., and G. W. Gee. 1981. Simulation of Water Flow and Retention in Earthen Cover Material Overlying Uranium Mill Tailings. UMT-0203/PNL-3877, Pacific Northwest Laboratory, Richland, Washington.

Skidmore, E. L. 1974. "A Wind Erosion Equation: Development, Application, and Limitations." In Atmosphere-Surface Exchange of Particulate and Gaseous Pollutants. ERDA Symposium Series 38, National Technical Information Service, Springfield, Virginia.

Stone, W. A., J. M. Thorp, O. P. Gifford and D. J. Hoitink. 1983. Climatological Summary for the Hanford Area. PNL-4622, Pacific Northwest Laboratory, Richland, Washington.

Winograd, I. J. 1981. "Radioactive Waste Disposal in Thick Unsaturated Zones." Science 212(4502):1457-1464.

Winsor, T. E., and F. W. Whicker. 1980. "Pocket Gophers and Redistribution of Plutonium in Soil." Health Physics 39:257-262.

**THIS PAGE INTENTIONALLY
LEFT BLANK**

APPENDIX N

RADIOLOGICALLY RELATED HEALTH EFFECTS

**THIS PAGE INTENTIONALLY
LEFT BLANK**

APPENDIX N

RADIOLOGICALLY RELATED HEALTH EFFECTS

The radiation dose to humans from ingestion, inhalation, or external exposure to specified quantities of radionuclides can be calculated with reasonable confidence. Estimates can be made of the amounts of radioactive materials that may be released from operations associated with waste management and disposal; however, the fractions reaching humans via various environmental pathways are not as well defined. The relationship of dose to so-called "health effects" is even less well defined. Thus estimates of "health effects" that may result from radiation exposure consequent to such activities can be derived only from a chain of estimates of varying uncertainty. The usual practice in making these estimates is that if an error is to be made, it will be made in a way intended to overprotect the individual. As a result, if the chain of estimates is long, there may be considerable conservatism in the final value.

Because expected releases of radioactive materials are small and the radiation dose to any individual is small, the effects considered are long-delayed somatic and genetic effects; these will occur, if at all, in a very small fraction of the persons exposed. Except as a consequence of the unusually severe accident involving larger doses, no possibility exists for an acute radiation effect. The effects that must be considered are 1) cancers that may result from whole-body exposures and, more specifically, from radioactive materials deposited in lung, bone, and thyroid and 2) genetic effects that are reflected in future generations because of exposure of the germ cells.

Knowledge of these delayed effects of low doses of radiation is necessarily indirect. This is because their incidence is too low to be observed against the much higher background incidence of similar effects from other causes. Thus, for example, it is not possible to attribute any specific number of human lung cancers to the plutonium present in everyone's lungs from weapons-test fallout because lung cancers are known to be caused by other materials present in much more hazardous concentrations and because lung cancers occurred before there was any plutonium. Even in controlled studies with experimental animals, because of limited numbers, one reaches a low incidence of effect that is statistically indistinguishable from the level of effect in unexposed animals, at exposure levels far higher than those predicted to result from waste management and disposal activities. Hence only a relationship between health effect and radiation dose can be estimated, basing this estimate on observations made at very much higher exposure levels, where effects have been observed in humans, and on carefully conducted animal experiments. Passages from the United Nations Scientific Committee on Atomic Radiation (UNSCEAR 1982) and the International Commission on Radiation Protection (ICRP 1977) suggest some level of confidence in the realism of the simulated hazards. In this context, however, the National Council on Radiation Protection and Measurements (NCRP) has said: "The NCRP wishes to caution governmental policy-making agencies of the unreasonableness of interpreting or assuming 'upper limit' estimates of

carcinogenic risks at low radiation levels derived by linear extrapolation from data obtained at high doses and dose rates, as actual risks, and of basing unduly restrictive policies on such interpretation or assumption" (NCRP 1975).

An alternative approach involves direct comparison of the estimated radiation doses from waste management and disposal activities with the more accurately known radiation doses from other sources. This avoids the most uncertain step in estimating health effects (the dose-effect relationship) and provides a comparison with firmly established data on human exposure (i.e., the exposure to naturally occurring radiation and radioactive materials). Some people prefer to judge a risk's acceptability on knowledge that the risk is some certain fraction of an unquantifiable, but unavoidable, natural risk, rather than to base this judgment on an absolute estimate of future deaths that might be too high or too low by a large factor. Because of these judgmental problems, it is the practice in this Statement to compare estimated radiation exposure from waste management and disposal activities with naturally occurring radiation exposure as well as to indicate estimates of cancer deaths and genetic effects.

N.1 LATE SOMATIC EFFECTS

Recently much literature has dealt with the prediction of late somatic effects of very low-level irradiation. This literature is not reviewed in detail here because it is recent and readily available. Instead, the various dose-effect relationships and the models for projecting risks forward in time that have been proposed are briefly considered and justification is given for the range of values employed in this appendix.

Several publications include efforts to quantify risks of late somatic effects of irradiation. The most extensive of these are the Biological Effects of Ionizing Radiations (BEIR) III Report, issued in 1980 by the National Academy of Sciences as a report of its Advisory Committee (NAS/NRC 1980), and the UNSCEAR Report, a report to the General Assembly by the United Nations Scientific Committee on the Effects of Atomic Radiation published in 1977 (UNSCEAR 1977). (A more recent UNSCEAR report was published in 1982 but does not focus on late somatic effects.) The most recent attempt to quantify risks of late somatic effects is the Health Effects Model for Nuclear Power Plant Accident Consequence Analysis (NRC 1985), provided to replace the health effects model used in the Reactor Safety Study of the Nuclear Regulatory Commission (1975), and referred to here as NRC 1985. In the discussion below, the BEIR III and NRC 1985 reports are emphasized because they provide the most up-to-date information on radiation risks.

The various reports noted above draw their conclusions from human effects data derived from medical, occupational, accidental, or wartime exposures to a variety of radiation sources: external x-irradiation, atomic bomb gamma and neutron radiation, radium, radon and radon decay products, etc. These observations on humans were, of course, the result of exposures to relatively large total doses of radiation at relatively high dose rates.

Many problems are encountered in attempting to use these data for estimation of lifetime risks due to low-level radiation exposure. These problems are briefly summarized in the following excerpt from BEIR III (page 142-3; transcript edition page 190):

The quantitative estimation of the carcinogenic risk of low-dose, low-LET [linear energy transfer] radiation is subject to numerous uncertainties. The greatest of these concerns the shape of the dose-response curve. Others pertain to the length of the latent period, the RBE [relative biological effectiveness] for fast neutrons and alpha radiation relative to gamma and x radiation, the period during which the radiation risk is expressed, the model used in projecting risk beyond the period of observation, the effect of dose rate or dose fractionation, and the influence of differences in the natural incidence of specific forms of cancer. In addition, uncertainties are introduced by the characteristics of the human experience drawn on for the basic risk factors, e.g., the effect of age at irradiation, the influence of any disease for which the radiation was given therapeutically, and the influence of length of follow-up (NAS/NRC 1980).

As noted above, one of the largest sources of uncertainty involves the choice of the mathematical function used to express the dose-response relationship. An earlier BEIR report (BEIR 1972) used a linear function for this purpose, justifying its use in part by the desirability of conservatism for radiation protection purposes. The BEIR III report (NAS/NRC 1980), however, deviates from this approach by providing an envelope of estimates based on linear, linear-quadratic, and quadratic functions. BEIR III indicates that the linear-quadratic, which results in lower risks than the linear model at low doses and dose rates, is to be regarded as the most realistic. The use of the linear-quadratic function as the most realistic estimate may be justified based on experimental evidence summarized in a report of the NCRP (1980), which suggests that effects at doses rates of less than 5 rad per year would be reduced by a factor between 2 and 10. Questions remain regarding the appropriateness of this reduction, because data on breast and thyroid cancer suggest a response that is linear. The BEIR III linear-quadratic function, which is based on analyses of data on the Japanese atomic-bomb survivors, reduces risks by a factor of 2.3 for leukemia and bone cancer, and of 2.5 for other types of cancer.

A second major source of uncertainty in estimating lifetime risks results because no populations on which estimates of health effects are based have yet been followed to the end of their lifespans. For leukemia and bone cancer, it appears that rates have returned to spontaneous levels 25 to 30 years after exposure. For other cancers, however, a model in which risks are assumed to persist over an exposed individual's lifetime seems more appropriate. The BEIR III estimates (NAS/NRC 1980) are based on the assumption that risks of leukemia and bone cancer persist 2 to 27 years following exposure, while risks of other effects persist for a lifetime after a minimal latent period of 10 years.

Two approaches were used in BEIR III (NAS/NRC 1980) to extend risk estimates beyond the period represented by follow-up data. With the absolute risk projection model, it is assumed that the number of excess cases per unit of population per unit of time expressed as a function of radiation dose remains constant over a specified period. With the relative risk projection model, it is assumed that the ratio of the excess cancer risk to the spontaneous age-specific risk remains constant over the specified period. After early childhood, spontaneous cancer incidence and mortality rates generally increase with age, and because of this the relative risk model yields larger numbers for the years beyond the follow-up period.

The calculations provided by BEIR III require several assumptions that are not discussed here. In particular, sex and age at exposure are treated in a more rigorous fashion than by the earlier BEIR report (1972) or other groups that have attempted risk estimation.

The lifetime risk estimates for mortality from all forms of cancer based on the linear-quadratic model given in BEIR III (NAS/NRC 1980) are summarized in Table N.1 for two exposure situations. BEIR III also provides estimates for continuous exposure to one rad per year from ages 20 to 65, 35 to 65, and 50 to 65 (intended to represent occupational exposures), but these are not reproduced here. BEIR III chose not to provide estimates for exposures lower than one rad per year since it was believed this involved too much uncertainty. Also the BEIR III report was primarily concerned with estimating overall cancer risks. No lifetime risks for specific cancer types (except leukemia and bone cancer) are provided, although evidence regarding many individual cancer types is extensively reviewed.

TABLE N.1. BEIR III Risk Projection Models

	<u>Absolute-Risk Projection Model</u>	<u>Relative-Risk Projection Model</u>
Single exposure to 10 rads:		
Number of excess cases per million persons	766	2,255
% increase over normal risk	0.47	1.4
Continuous exposure to 1 rad/yr, lifetime:		
Number of excess cases per million persons	4,751	11,970
% increase over normal risk	2.8	7.2

The recent NRC 1985 report does provide estimates for specific cancer types and also takes into account epidemiological data and analyses that have become available since the publication of BEIR III. NRC 1985 provides central estimates as well as upper and lower bounds^(a) for the number of deaths and cases, and for the years of life lost and years of life lived after the occurrence of cancer. Except for breast and thyroid cancer, the central estimates are based on a linear-quadratic function that reduces risks at low doses and dose

(a) The meaning of the terms "upper and lower bounds" is not the same as that found in other parts of this report. In NRC 1985, the central estimates and bounds are defined as follows: "The central estimates are intended to reflect the most realistic assessment of radiation risks . . . while the upper and lower bounds are intended to reflect alternative assumptions that are also reasonably consistent with available evidence." (NRC 1985, p. II-94.) Unlike bounds in other parts of this report, they cannot be interpreted as confidence limits.

rates by a factor of 3.3, slightly more than the BEIR III linear-quadratic model. The lower-bound estimates are based on a reduction factor of 10, while the upper-bound estimates are based on a linear model.

Since publication of BEIR III (NAS/NRC 1980), additional support for the assumption that risks persist for a lifetime, and for the use of the relative risk model, has become available. The most recent data on the Japanese atomic bomb survivors (Kato and Schull 1982), extending the follow-up from 30 to 34 years, indicates no tapering off of risks. In a parallel analysis of data both from Japanese survivors and British ankylosing spondylitis patients, Darby (1984) investigated the fit of the relative and absolute models. These recent data and the more rigorous statistical treatment of Darby provide added support for the use of the relative risk model. However, there is still considerable uncertainty for risks beyond the period for which follow-up data are available. Thus the relative risk model may overestimate lifetime cancer risks.

For the reasons noted above, the NRC 1985 report used the relative lifetime risk model for central estimates and upper bounds for breast cancer, lung cancer, gastrointestinal cancers, and for the residual group of all other cancers. The absolute lifetime risk model was used for central and upper bounds for leukemia, bone cancer, skin cancer and thyroid cancer, and was used for the lower bound for all cancer types. Like the BEIR III model (NAS/NRC 1980), risks for leukemia and bone cancer were assumed to persist from 2 to 27 years following exposure, while risks for other cancer types were assumed to have minimal latent periods of 10 years, except for thyroid cancer for which a 5-year minimal latent period was assumed.

In NRC 1985, the updated analyses of the Japanese data were taken into account in obtaining the numerical risk coefficients needed to calculate lifetime risks. For lung cancer, a larger relative coefficient was used for the upper bound than for the central estimate, a procedure intended to reflect the uncertainty in extrapolating to the U.S. population an estimate based on Japanese data. The NRC 1985 report did not treat age at exposure and sex in as detailed a manner as did BEIR III. Age at exposure was considered only in estimates for thyroid effects and the upper-bound estimate for breast cancer; separate estimates were provided for cancers resulting from exposure received in utero.

The central estimates and upper and lower bounds for cancer mortality resulting from one rem of exposure, based on the NRC 1985 model, are summarized in Table N.2. These estimates are applicable to populations with age structure and mortality rates similar to those of the United States. For comparison, BEIR III (NAS/NRC 1980) estimates for such exposure, obtained by dividing the risks for a single 10-rem exposure by 10, are also presented in this table. It should be noted that both the BEIR III and NRC 1985 estimates are based on dose to the relevant organ, or in the case of all cancers, on an appropriate average organ dose.

In addition to estimates of cancer mortality, the NRC 1985 report also provides estimates of cancer incidence, including non-fatal cancers. For all cancers other than leukemia and bone, the total of cancer cases is about 2.5 times the number of fatal cancers. This incidence-mortality ratio varies considerably by cancer site, from a factor of 1.1 for lung cancer to a factor of 10 for thyroid cancer.

TABLE N.2. Comparison of Various Estimates of Cancer Deaths per Million per Rem

Type of Cancer	BEIR III Report (NAS/NRC 1980) (a)				Health Effects Model (NRC 1985)			UNSCEAR Report	ICRP-26		
	Absolute-Risk Model		Relative-Risk Model		Upper Bound	Central Estimate (b)	Lower Bound (b)				
	Linear Model	Linear-Quadratic (b)	Linear Model	Linear-Quadratic (b)							
Leukemia	46(c)	22(c)			48	14	5	15 to 25	20		
Nonleukemic	120	54	454	203	519	174	24	(f)	(f)		
Lung					138	20	5	25 to 50	20		
Bone	1.0(c)	0.5(c)			2	1	0.2	2 to 5	5		
Thyroid	(f)	(f)			7	7	0.7	5 to 15	5		
Cancers resulting from <u>in utero</u> exposure (d)	5.8				6	2.4	2.4	2 to 2.5			
Total	173	77	501(e)	226(e)	573	190	31	100	100		

(a) The BEIR III estimates are the average of sex-specific estimates.

(b) Calculated on the assumption that no individual dose will exceed 10 rem.

(c) BEIR III gives a combined estimate for leukemia and bone cancer. This has been allocated to the two cancer types in proportion to the annual risk coefficients for the two types.

(d) These lifetime risks apply to the entire population and are about 1% of the risk restricted to the in utero population.

(e) Including leukemia and bone cancer deaths based on absolute risk model.

(f) Blanks indicate no data.

Recently, inadequacies in the dose estimates used in the studies of Japanese atomic bomb survivors have been identified by Loewe and Mendelsohn (1981) and Kerr (1981). Studies have been conducted to determine new dose estimates, but revised risk estimates are not yet available. Since risk estimates obtained from the Japanese studies play a major role in determining risk estimates presented in BEIR III (NAS/NRC 1980), NRC 1985, and other reports, this could mean that these estimates will eventually need to be modified as a result of the dose revision. Jablon (1984) has noted, on the basis of preliminary analysis, that the likely effect of the dose revision will be to increase risk estimates based on the earlier dosimetry by less than a factor of two. One of the arguments in support of the quadratic model (one of the models considered in BEIR III) has been based on differences in the dose-response curves between Hiroshima and Nagasaki. This argument has been weakened by the expected dosimetry revisions. It is possible that revised dosimetry will also modify inferences regarding the choice between linear and linear-quadratic functions.

Lifetime risk estimates are also provided in the 1977 UNSCEAR report and in the 1977 Recommendations of the International Commission of Radiological Protection (ICRP 1977), and are also summarized in Table N.2. These latter reports, however, have not given the detailed attention to developing models that clearly indicate the assumptions underlying the estimates provided.

The Radioepidemiological Tables have been recently published (NIH 1985). These tables provide estimates of the probability that certain cancers could result from prior exposure to radiation. Although the tables do not provide the lifetime risk estimates needed in this report, they do provide models for estimating the risks of several cancer types resulting from a range of exposure situations. The model used in the Radioepidemiological Tables is very similar to that used for the NRC 1985 central estimates. In particular, the estimates for cancers other than breast and thyroid were based on a linear-quadratic function that reduces risks at low doses and dose rates by a factor of 2.5, compared with the factor of 3.3 used in NRC 1985. Furthermore, both reports based risk estimates for cancers other than leukemia and bone cancer on the relative risk model. The risk coefficients used in the two reports are reasonably comparable, although the Radioepidemiological Tables have allowed risks to depend upon age at exposure (this was not done for the NRC 1985 central estimates).

N.2 GENETIC EFFECTS

It is known that genetic effects result from alterations within genes, called mutations, or from rearrangements of genes within chromosomes. There is no radiation-dose threshold for the production of mutations, but repair of damage to genetic material can occur during exposure at low dose rates. This information is reviewed and discussed at length in the 1982, and earlier, UNSCEAR reports and in the BEIR I (BEIR 1972) and BEIR III (NAS/NRC 1980) reports.

In the absence of quantitative data relating genetic effects in humans to radiation exposure, estimates of the genetic risk to humans have been based largely on data from animal studies. Two approaches commonly have been employed. In the so-called "direct method,"

estimates of specific types of genetic damage, as measured in experimental animals, are applied, with suitable interspecies correction factors, directly to man. Where animal data suitable for use in the "direct method" are unavailable, an "indirect method," or "doubling dose method," has been employed. This method relies on animal data to establish the amount of radiation required to double the spontaneous incidence of a genetic effect in the test species; it then assumes that this same doubling dose is applicable to humans, and from estimates of the spontaneous occurrence of genetic diseases in humans, calculates the risk of genetic effect per unit dose of radiation. These methods involve the uncertainties of extrapolation from animals to humans, plus very considerable uncertainties as to the normally occurring incidence of genetic diseases in humans.

Genetic disorders have been commonly grouped into four categories, as considered below:

1. Autosomal dominant and X-linked disorders are those caused by the presence of a single defective gene. More than a thousand such disorders are recognized. Examples include polydactyly (extra fingers and toes), achondroplasia (short-limbed dwarfism), Huntington's chorea (progressive involuntary movements and mental deterioration), two types of muscular dystrophy, several kinds of anemia, and retinoblastoma (an eye cancer). Well known X-linked disorders include hemophilia (failure of blood clotting), color blindness, and a severe form of muscular dystrophy. About 1% of all liveborn humans are appreciably handicapped by a disorder of this type. It is generally agreed that these disorders will double in frequency if the mutation rate is doubled.
2. Recessive disorders are those that require mutated genes on both members of a pair of homologous chromosomes. The potential for induction of such disorders by low-level low-LET irradiation has generally been considered negligible.
3. Chromosomal disorders are those characterized by changes in the number of chromosomes, or in the structural sequence within chromosomes. Such disorders are apt to result in early, spontaneous abortion, which is not considered here as a quantifiable effect. It is generally agreed that the increase in these disorders among liveborn humans as a result of low-level low-LET irradiation will be relatively small compared to other types of disorders.
4. Irregularly inherited (multifactorial) disorders have a more complex and ill-defined pattern of inheritance. These disorders include a wide variety of congenital malformations and constitutional and degenerative diseases. About 9% of liveborn humans will be seriously handicapped by such disorders. Because of their poorly understood mechanisms of inheritance, which may in many cases be unaffected by mutations, estimates of radiation risk factors are more uncertain than for other types of disorders.

Table N.3 summarizes recent genetic risk estimates of the BEIR and UNSCEAR committees. These estimates are for effects over all subsequent generations. They were derived by the "indirect method," but are, in several instances, supported by "direct" derivations.

TABLE N.3. Estimates of Genetic Effects of Radiation Over All Generations
 (effects per million liveborn in an average population exposed
 to 1 rem per generation)

Effect	1972 BEIR I	1980 BEIR III	1977 UNSCEAR	1982 UNSCEAR
Dominant and X-linked	50 to 500	40 to 200	100	100
Chromosomal			40	4
Multifactorial	10 to 1000	20 to 900	45	45
Total	60 to 1500	60 to 1100	185	149

It is important to note that the BEIR and UNSCEAR genetic risk estimates are expressed in terms of effects per million liveborn offspring of an average uniformly irradiated population. For comparison with somatic risk estimates, it is necessary to express the genetic risk in terms of the irradiated population rather than in terms of the resulting offspring. The number of offspring produced in the United States per generation is about one-half the number in the total population. Thus the 1982 UNSCEAR risk estimate of 150 effects per million offspring of an average population irradiated at a level of 1 rem, is equivalent to about 75 effects per million rem delivered to the irradiated population. Similarly the BEIR III range of total genetic effects reduces to 30 to 550 effects per million rem delivered to the irradiated population.

To the BEIR and UNSCEAR estimates considered above may be added a very recent analysis, prepared for the Nuclear Regulatory Commission, which proposes a "central estimate" for genetic risk for all generations of 185 effects per million rem delivered to the irradiated population (NRC 1985). This estimate, derived by methods similar to those employed by BEIR and UNSCEAR but with the benefit of some newer information, is not appreciably different from the earlier estimates.

N.3 CONCLUSIONS

For this EIS a range encompassing commonly used cancer risk factors has been employed, as indicated in Table N.4. The possibility of zero risk at very low exposure levels is not excluded by the available data. Values in the lower to middle range of risk estimates of Table N.4 may be more appropriate for comparison with the estimated risks of other energy technologies; values in the upper range may be more appropriate for radiation protection considerations.

A range of 50 to 500 specific genetic effects to all generations per million man-rem was employed in this EIS. This essentially encompasses the range recommended in the BEIR III report (NAS/NRC 1980), and encompasses the central estimates of the 1977 and 1982 UNSCEAR reports, and of the 1985 Improved Radiological Health Effects Model of the NRC. As in the

TABLE N.4. Health Effects Risk Factors Employed in this EIS

Type of Risk	Predicted Incidence per 10^6 man-rem
Fatal cancers from:	
Total body exposure	50 to 500
Lung exposure	10 to 100
Bone exposure	1 to 5
Thyroid exposure	1 to 15
Specific genetic effects to all generations from total body exposure	<u>50 to 500</u>
Total (Total body exposure)	100 to 1000

case of the somatic risk estimates, values in the lower range of this estimate may be more appropriate for comparative risk evaluations, while values in the upper range may be more appropriate for radiation protection considerations.

All estimates of health effects, as quoted elsewhere in this EIS, employ the risk factors summarized in Table N.4. No special risks are considered to be associated with any specific radionuclide except as reflected in the calculation of their dose equivalent (in rems) in the various tissues of concern.

N.4 REFERENCES

- BEIR Report. 1972. The Effects on Populations of Exposure to Low Levels of Ionizing Radiation. National Academy of Sciences/National Research Council, Washington, D.C.
- Darby, S. C. 1984. "Modeling Age- and Time-Dependent Changes in the Rates of Radiation-Induced Cancers." In Atomic Bomb Survivor Data: Utilization and Analysis, ed. R. L. Prentice and D. J. Thompson. Society for Industrial and Applied Mathematics, Philadelphia, Pennsylvania, pp. 67-80.
- International Commission on Radiological Protection (ICRP). 1977. "Recommendations of the International Commission on Radiological Protection." ICRP Publication 26, Annals of the ICRP, 1, No. 3.
- Jablon, S. 1984. "Characteristics of Current and Expected Dosimetry." In Atomic Bomb Survivor Data: Utilization and Analysis, ed. R. L. Prentice and D. J. Thompson. Society for Industrial and Applied Mathematics, Philadelphia, Pennsylvania, pp. 143-152.
- Kato, H., and W. J. Schull. 1982. "Studies of the Mortality of A-Bomb Survivors, 7. Mortality, 1950-1978: Part I. Cancer Mortality." Radiation Research 90:395-432.
- Kerr, G. D. 1981. Findings of a Recent ORNL Review of Dosimetry for the Japanese Atomic-Bomb Survivors. ORNL-TM-8078, Oak Ridge National Laboratory, Oak Ridge, Tennessee.
- Loewe, W. E., and E. Mendelsohn. 1981. "Revised Dose Estimates at Hiroshima and Nagasaki." Health Physics 41:663-666.

- National Academy of Sciences/National Research Council (NAS/NRC). 1980. The Effects on Populations of Exposure to Low Levels of Ionizing Radiation. "BEIR III." Washington, D.C.
- National Council on Radiation Protection and Measurements (NCRP). 1975. Review of the Current State of Radiation Protection Philosophy. NCRP Report No. 43, Washington, D.C.
- National Council on Radiation Protection and Measurements (NCRP). 1980. Influence of Dose and Its Distribution in Time on Dose-Response Relationships for Low-LET Radiations. NCRP Report No. 64, Washington, D.C.
- National Institutes of Health (NIH). 1985. Report of the National Institutes of Health Ad Hoc Working Group to Develop Radioepidemiological Tables. NIH Publication No. 85-2748. Department of Health and Human Services, Washington, D.C., pp. i-viii.
- Nuclear Regulatory Commission (NRC). 1975. Reactor Safety Study: An Assessment of Accident Risks in the U.S. Commercial Nuclear Power Plants. Appendix VI, WASH-1400. NUREG-75/014, Washington, D.C.
- Nuclear Regulatory Commission (NRC). 1985. Health Effects Model for Nuclear Power Plant Accident Consequence Analysis. Vol. 2, NUREG/CR-4214, Nuclear Regulatory Commission, Washington, D.C., Chapter 2.
- United Nations Scientific Committee on Atomic Radiation (UNSCEAR). 1977. Sources and Effects of Ionizing Radiation. United Nations, New York.
- United Nations Scientific Committee on Atomic Radiation (UNSCEAR). 1982. Ionizing Radiation: Sources and Biological Effects. United Nations, New York.

**THIS PAGE INTENTIONALLY
LEFT BLANK**

APPENDIX O

**STATUS OF HYDROLOGIC AND GEOCHEMICAL MODELS USED TO SIMULATE
CONTAMINANT MIGRATION FROM HANFORD DEFENSE WASTES**

**THIS PAGE INTENTIONALLY
LEFT BLANK**

APPENDIX O

STATUS OF HYDROLOGIC AND GEOCHEMICAL MODELS USED TO SIMULATE CONTAMINANT MIGRATION FROM HANFORD DEFENSE WASTES

This appendix presents information concerning the current suite of models used in this EIS to simulate the subsurface migration of contaminants from waste forms that might be disposed of under the Hanford 200 Area Plateau. The models used in this EIS are believed sufficient to support meaningful decisions in the context of the National Environmental Policy Act of 1969 (NEPA). Where uncertainties exist, every attempt has been made to select input values for model parameters so that bottom-line calculations produce conservative estimates of impacts. A conservative value of a parameter tends to produce an overestimation of consequences rather than an underestimation. Where reliable data provide realistic values of parameters, the realistic values are used. Where appropriate, the degree of conservatism in the analytical results is addressed. Also, indication is made where data or analysis tools are technically limited and where assumptions have been made. Every effort has been made to select conservative parameter values and to make assumptions that are conservative but reasonable.

This appendix discusses the status of hydrologic and geochemical models and codes used to predict potential radionuclide and chemical movement away from the various facilities (i.e., ponds, tanks, cribs, and grout vaults) that are covered in this EIS. It is included as background information to use in interpreting radionuclide transport projections made or referenced in Appendix Q and in Volume 1 of this EIS. The modeling is explained by describing the physical, geochemical and stratigraphic setting of the environmental system and discussing conceptual, mathematical and numerical models applied to the Hanford Site. The bulk of this appendix focuses on the aquifer system components (i.e., unsaturated zone and the underlying unconfined saturated zone). In addition to the discussion on the status of models used for this EIS, some advanced aspects of modeling radionuclide and chemical transport are presented. Available tools and data did not support the use of more advanced modeling approaches. However, the more simplistic approach chosen for this EIS has a heavy reliance on conservative data values and modeling assumptions.

The following information is presented in several subsections: 1) a general description of the stratigraphy underlying the 200 Areas at Hanford, 2) a conceptual model and associated mathematical and computational description of hydrologic and solute transport codes used for the unsaturated zone, and 3) a similar description for the underlying saturated aquifer. The controlling physical and chemical phenomena depend strongly on whether or not a protective barrier is placed over a given waste site.

The dominant transport mechanism in the unsaturated zone will be slow diffusion of contaminants through the small amount of relatively immobile soil water where a functional, undisturbed protective barrier is in place over any given waste site. Such diffusion may move radionuclides and chemicals to the edge of the barrier where downward infiltrating water

adverts the material downward to the unconfined aquifer. A conservative 10-m barrier overhang has been employed in all calculations to reduce potential for advective movement. A design option exists to optimize this overhang to ensure that diffusion paths are sufficiently long and performance standards are met. In addition to horizontal diffusion, vertical movement via diffusion alone beneath the barrier was also estimated.

Analyses also were done for cases of "disturbed" or "less-than-perfect" barrier performance. In these cases, it was assumed that water leaks through the protective barrier, leaches the wastes, and advects vertically to the unconfined groundwater aquifer. The appendix is designed to inform the reader of what data, assumptions and models were used for analyzing the thick, unsaturated zone underlying the 200 Areas and the unconfined aquifer between the 200 Areas and the Columbia River.

When contaminated water reaches the unconfined aquifer, it is diluted and hydrodynamically dispersed by the flowing groundwater. Reactive solute carried by the water is chemically retarded as it migrates in a generally horizontal direction from the 200 Areas toward the Columbia River. Although the travel time in the aquifer is relatively short compared to the residence time in the unsaturated zone, the concentrations of radionuclides and chemicals are significantly reduced by various natural physical and chemical mechanisms. Over forty years' experience in monitoring this unconfined aquifer with hundreds of wells has resulted in a relatively good understanding of the behavior of groundwater and nonsorbed contaminants in this zone. Monitoring data have been used to develop conceptual models of the aquifer's physical and chemical characteristics and to calibrate the variable thickness transient (VTT) code used to simulate groundwater movement in the unconfined aquifer. The impact of Hanford operations (e.g., artificial recharge of cooling water, liquid discharge to cribs, etc.) and offsite activities (e.g., irrigation of farmland) on the future behavior of the water table of the unconfined aquifer are analyzed. The impacts of radionuclides and chemicals released from low-level waste disposal sites are not modeled. However, the potential cumulative effects of past and current waste disposal operations are addressed in Section 5.1.4 of this EIS.

0.1 STRATIGRAPHY BEHNEATH THE HANFORD 200 AREAS

A detailed description of the stratigraphic units underlying the Hanford Site can be found in the Environment Assessment of the BWIP (DOE 1984a). The following summary of the stratigraphy is taken from that material. The Columbia River Basalt Group (see Figure 0.1) underlying the Pasco Basin and vicinity consists of three formations; Grande Ronde, Wanapum, and Saddle Mountain Basalts (Swanson et al. 1979).

"...Sedimentary rocks of Miocene age interbedded with the basalts in the basin are designated the Ellensburg Formation (Brown 1959; Newcomb et al. 1972)."

"...Overlying the basalts and interbedded sediments in topographic and structural lows of the central Columbia Plateau are semiconsolidated sediments of the Mio-Pliocene Ringold Formation (Merriam and Buwalda 1917). The thickest sequence of Ringold Formation sediments occurs in the Pasco Basin where coarse-to-fine-grained clastic sediments were deposited by ancestral rivers. These sediments outcrop all along the White Bluffs east of the Site. Erosion since

Period	Epoch	Group	Subgroup	Formation	K-Ar Age Years $\times 10^6$	Member or Sequence	Sediment Stratigraphy or Basalt Flows
QUATERNARY	Pleistocene/ Holocene					Surficial Units	Loess Sand Dunes Alluvium and Alluvial Fans Landslides Talus Colluvium
	Pliocene					Touchet Beds/ Pasco Gravels	
							Plio-Pleistocene Unit Upper Ringold Middle Ringold Lower Ringold Basal Ringold
							Fanglomerate
							Goose Island Flow Martindale Flow Basin City Flow Levee Interbed
					8.5	Ice Harbor Member	Upper Elephant Mountain Flow Lower Elephant Mountain Flow Rattlesnake Ridge Interbed
					10.5	Elephant Mountain Member	Upper Pomona Flow Lower Pomona Flow Selah Interbed
					12.0	Pomona Member	Upper Gable Mountain Flow Gable Mountain Interbed Gable Mountain Interbed Cold Creek Interbed
						Esquatzel Member	Huntzinger Flow Wahluke Flow Sillusi Flow Umatilla Flow Mabton Interbed
						Asotin Member	Lolo Flow Rosalia Flows Quincy Interbed
						Wilbur Creek Member	Upper Roza Flow Lower Roza Flow Squaw Creek Interbed
						Umatilla Member	Aphyric Flows Phryic Flows Vantage Interbed
						Priest Rapids Member	Undifferentiated Flows Rocky Coulee Flow Unnamed Flow Cohassett Flow
						Roza Member	Undifferentiated Flows McCoy Canyon Flow Intermediate-Mg Flow
						Frenchman Springs Member	Low-Mg Flow Above Umtanum Umtanum Flow High-Mg Flows Below Umtanum Very High-Mg Flow At Least 30 Low-Mg Flows
						Sentinel Bluffs Sequence	
						Schwana Sequence	
					16.1		

Ellensburg Formation Teil

FIGURE 0.1. Stratigraphic Units Present in the Pasco Basin (DOE 1984a)

their deposition has reduced their thickness to a range from zero to 450 feet beneath the 200 Areas Plateau. In the central Pasco Basin the Ringold Formation is informally subdivided into four fluvial facies; basal, lower, middle, and upper Ringold units (Tallman et al. 1981; Bjornstad 1984)."

"The Quaternary Period in the central Columbia Plateau is dominated by Pleistocene catastrophic floods that scoured the Channeled Scablands and deposited glaciofluvial sediments in topographic lows. In the Pasco Basin, the glaciofluvial sediments are designated the Hanford Formation."

"Loess, dune sand, alluvium, as well as landslide debris, colluvium and talus veneer the flanks of the basaltic ridges bounding the Pasco Basin. These deposits range from Pleistocene-to-present in age (Myers et al. 1979; Price et al. 1979)."

"The major stratigraphic units present ... [beneath the Hanford Site] ... are the Grande Ronde, Wanapum, and Saddle Mountains Basalts of the Columbia River Basalt Group; and the Ellensburg, Ringold, and Hanford Formations, which are major fluvial units. A thin veneer of surficial sediments is present over much of the area...."

More detailed descriptions of stratigraphic units will be limited to the semiconsolidated and unconsolidated deposits associated with the unconfined aquifer underlying the Hanford Site.

The Ringold Formation

"The Ringold Formation overlies the Columbia River Basalt Group within most of the Pasco Basin, except where 1) basalt outcrops, 2) the glaciofluvial Hanford formation onlaps ridges above the margin of the Ringold Formation, or 3) the Ringold Formation has been eroded and Hanford Formation sediments have been deposited directly on basalt. Based on fossils and paleomagnetic data in the Pasco Basin, the Ringold Formation is interpreted to range from 8.5 million years (post-Ice Harbor Member) to 3.7 million years in age (Tallman et al. 1981, pp. 2-25). Ringold Formation sediments were deposited in a fluvial environment with some lacustrine and fanglomerate facies."

"...The basal Ringold unit represents a complete fining-upward, fluvial cycle consisting of three subunits. These are from oldest to youngest: 1) a coarse facies, 2) a fine facies, and 3) a paleosol. The coarse facies is composed of an angular medium-to-coarse sand and well rounded, polished, cobble gravel...."

"Overlying the basal Ringold unit coarse facies is a conformable sequence of cross-laminated and micaceous, light-colored mud (e.g., mixture of silt and clay) and sand that marks the transition to a lower-energy fluvial environment. This facies grades upward into and is capped by a well-developed laterally extensive paleosol. The paleosol is composed of two relic soil horizons: a laminac to massive, white caliche representative of a "C" horizon overlain by a massive, olive-colored, alluvial "B" soil horizon."

"Laminated silt and clay comprise the lower Ringold unit overlying the basal unit.... It...is distinguished by: 1) the presence of primary sedimentary structures, 2) a distinct gray versus olive color, and 3) a significantly higher natural gamma response in the geophysical logs."

"The middle Ringold unit is texturally and mineralogically similar to sandy gravel of the basalt Ringold facies (Tallman et al. 1981, pp. 2-13 through 2-19) except for a higher proportion of quartzite-to-volcanic porphyry lithologies for the middle Ringold unit. Locally, the middle Ringold unit-sequence is intercalated with thin zones of current-laminated sand and mud."

"The upper Ringold unit...consists of alternatively bedded and laminated sand and mud representative of a low-energy fluvial environment. The maximum

elevation of the upper Ringold unit was probably much higher at one time as indicated by the present elevation of the upper Ringold unit preserved in the White Bluffs to the east.... Large variations in the thickness of the upper Ringold unit...are primarily due to erosion by more recent local streams...."

The Plio-Pleistocene Unit

"Overlying the Ringold Formation...is the Plio-Pleistocene unit that consists of two subunits: a fanglomerate and a paleosol. The fanglomerate facies is generally composed of angular, poorly sorted, gravel derived from the mass wastage off the ridges surrounding the Cold Creek syncline (Bjornstad 1984). The basaltic gravel is often intercalated with zones of loess and caliche, which represent intermittent periods of alluvial fan stabilization.... The Plio-Pleistocene unit appears to correlate with fanglomerate sequences present near the base of the basaltic ridges that bound the Pasco Basin on the north, west and south."

The Hanford Formation

"Catastrophic flood deposits of the Hanford Formation were deposited when ice dams in western Montana and northern Idaho were breached, allowing large volumes of water to spill across eastern and central Washington (Bretz 1923, pp. 51 through 55). Evidence exists for multiple floods; however, the exact timing and frequency of these floods is undetermined (Baker 1973, pp. 123 and 124). Most of the sediments are late Pleistocene, with the last major flood sequence dated at approximately 13,000 years before present (Mullineaux et al. 1977, p. 1105). These deposits (referred to as the Hanford Formation in the Pasco Basin) are composed of two facies; a flood facies (Pasco Gravel) and slackwater facies (Touchet Beds)."

"Pasco Gravels are composed of coarse sand and gravel. They are restricted mainly to the late Pleistocene flood bars that developed along high-energy flood channelways.... Touchet Beds are a rhythmically bedded and fine-grained, slack-water flood facies deposited away from the flood bars and generally coeval with the Pasco Gravels...."

0.2 PHYSICS AND CHEMISTRY OF THE AQUIFER SYSTEM

The aquifer system at Hanford of central importance to this EIS is composed of a single unconfined saturated zone covered by a single unsaturated zone. The term "saturated" refers to the water-filled voids in the porous medium. In a saturated zone, such void space is typically filled with water. In a partially saturated or unsaturated zone, the void space contains both water and air. The upper portion of the saturated zone is referred to as the phreatic zone or the unconfined aquifer, and the partially saturated zone is referred to as the zone of aeration or the vadose zone. They are separated by the water table, that location in the aquifer system where the pressure is atmospheric. Both the unsaturated zone and the upper unconfined saturated zone support a significant level of structural complexity, especially over large lateral dimensions.

The sediments of central importance to this EIS are 1) semiconsolidated sediments of the Mio-Pliocene Ringold Formation, 2) glaciofluvial sediments known as the Hanford Formation deposited by the Pleistocene catastrophic floods, and 3) loess, dune sand, and alluvium that veneer the flanks of the basaltic ridges. These sediments comprise the vadose zone and unconfined aquifer that underlie the Hanford Site. The unconfined aquifer is most strongly influenced by local phenomena such as drainage from Dry Creek and Cold Creek Valleys, stage

of the Columbia River, infiltration of precipitation, and infiltration of waste and/or relatively clean process water from the current operation of the facilities at Hanford. For this EIS, it was assumed that the regional groundwater system of the Pasco Basin and, hence, the deeper basalt formations have a negligible effect on the near-surface unconfined aquifer. Therefore, modeling activities emphasized the upper semiconsolidated and unconsolidated deposits and the soil moisture and groundwater they contain. This assumption of isolation between the unconfined aquifer and underlying upper unit of the confined system may not be totally valid (Dove et al. 1982). There is some evidence of erosional windows where the uppermost basalt confining layer may be missing. However, there must also exist a driving force due to head differences above and below the confining layer. The aquifer intercommunication effect, if any, seems negligible from the standpoint of contaminant transport (Graham 1983). Iodine-129 has been found in monitoring wells in both confined and unconfined aquifers on and off the Hanford Site. The significance of this finding relative to aquifer intercommunication has not been shown (WHC 1987).

Fluid flow and solute transport differ significantly in the vadose zone compared to the unconfined aquifer. Because the void space in the vadose zone is occupied by water and air, fluid flow can occur in either phase. The ability of any porous medium to conduct water relates directly to its hydraulic conductivity, and this parameter can be several orders of magnitude smaller in a vadose zone than in a saturated zone. Water has a greater affinity than air for the smaller voids. Therefore, the less water there is in the system, the more difficult it is for water to pass through the porous material. Hydraulic conductivity in the vadose zone is a highly nonlinear function of the suction pressure and the water content (i.e., percent saturation) of the soil moisture in the porous medium. Transport of a solubilized contaminant through a porous medium correlates with pore-water velocity. This velocity is directly related to the volumetric discharge and inversely related to the water content of the porous medium. In other words, it can take an incredibly long time for a small amount of water to pass through relatively dry sediments compared to the length of time required to transect wetter, but still unsaturated, sediments. Transport may be further affected by geochemical interactions between the contaminants and the porous material.

The spatial and temporal variability in geohydrologic properties and microclimate play an important role in determining the hydrologic response of the system. Spatial variability in the thickness of both the vadose zone and the unconfined aquifer depends on the spatial variability of the geologic deposits, the elevation of the land surface, the elevation of the low-permeability porous or fractured media that form the hydrologic bottom of the unconfined aquifer, and the elevation of the water table. The elevation of the water table is, in turn, affected by spatial and temporal variability in natural events (e.g., precipitation) and man-caused factors (e.g., infiltration from ponds, ditches, irrigation). Spatial variability occurs also in key water flow parameters, including hydraulic conductivity, porosity, and storativity. To lend perspective on the spatial variability of subsurface hydrologic flow parameters, one only need look at today's land surface and the variations in material types (e.g., clay, silt, sand, gravel) being deposited or eroded by wind, rivers and lakes.

Solute contaminant transport in the subsurface is controlled by advection (hydrodynamic dispersion), molecular diffusion, and geochemical interactions. Advection and hydrodynamic dispersion refer to movement of solute at a rate dependent on the various water pathways and velocities. Molecular diffusion refers to the gradual mixing of molecules of two or more substances as a result of random motion and/or a chemical concentration gradient. Diffusive flux spreads solute via the concentration gradient (i.e., Fick's Law). Diffusion is a dominant transport mechanism when advection is insignificant and is usually a negligible transport mechanism when water is being advected in response to various forces. Variability in the advection process gives rise to a third transport process called hydrodynamic dispersion. Hydrodynamic dispersion is a result of variability in travel paths, i.e., velocities, taken by advected solute.

Groundwater systems subjected to the release of contaminants undergo a geochemical evolution. In other words, the contaminants interact geochemically with the water in the sediments and the sediments themselves. Two key reactions are dissolution/precipitation and adsorption/desorption. We assume the system is originally in a state of geochemical equilibrium between the solid particles and the ambient waters. The aqueous and solid phases are then altered by the introduction of contaminants, and there is a tendency to approach a new equilibrium. This is a kinetic (i.e., dynamic) process requiring a finite time for completion. However, it may occur rapidly relative to long time periods (i.e., thousands of years) of interest in this EIS. Therefore, we have assumed an instantaneous equilibrium reaction for EIS level assessments. Geochemical processes may also be irreversible or at least directionally dependent (e.g., adsorption and desorption may be represented by different model parameters) and yet a reversible assumption and single-valued model parameters may often be employed. Given the tremendous increase in complexity introduced by adding chemical kinetics and considerations of irreversibility, the assumptions of instantaneous equilibrium and reversibility seem justified for this EIS assessment. Equilibrium reactions can be modeled with equilibrium thermodynamic relations. Whether viewed as kinetic or equilibrium reactions, there are spatial and temporal distributions of chemical speciation (variations in chemical form), adsorption/desorption reactions and precipitation/dissolution reactions occurring in the aquifer system. These reactions lead to the radionuclide retardation mechanisms of 1) chemical precipitation/dissolution of bulk solid phases, 2) chemical substitution of one element for another in a solid phase, 3) exchange of a stable isotope of an element with a radioactive isotope in solution, 4) cation and anion exchange, and 5) adsorption (Muller, Langmuir and Duda 1983). Typically, all these mechanisms are folded into a single empirical distribution coefficient that implicitly assumes the reactions go to equilibrium and are reversible, and the chemical environment along a solute flow path does not vary in either space or time. The limitations associated with this assumption are well known to the authors, but the paucity of Hanford geochemical data precludes a more rigorous analysis at this time. Furthermore, every attempt has been made to use conservative estimates, assumptions and judgments when data are limited.

Microbiological reactions are not considered in the retardation or acceleration of radionuclide transport. In addition to possible effects of microbiological degradation on waste

form leach rates, there is some indication that radionuclide migration rates could also be influenced by a microbial presence (West et al. 1982; West and McKinley 1984; West et al. 1985). Mobile microbes may transport, either internally or externally, sorbed ionic- or particle-bound radionuclides while micro-organisms may cover the surfaces of rocks, thus decreasing their retardation of groundwater-transported species. In addition, the presence of microorganisms can affect groundwater chemistry by altering pH and Eh, thus catalyzing specific REDOX reactions and chemically altering mineral surfaces, and by introducing labile organic byproducts. Such changes in groundwater chemistry would alter radionuclide solubility, speciation and sorption in a complex manner. However, too little quantitative data have been derived to incorporate microbiological effects in transport equations. Once again, every attempt was made to be conservative in the amount of safety credit assumed for radionuclide retardation (geochemical interactions) in the geomedia.

0.3 THE CONCEPTUAL MODEL

The formulation of the conceptual model(s) is by far the most important and difficult step in any risk or safety assessment. The conceptual model or models of a geohydrologic system (i.e., unsaturated zone and upper unconfined saturated zone) are the simplified description of geological strata and the physical and chemical phenomena important to water movement and solute transport within the system. Existing Hanford information on well logs, water levels in wells, and water quality (chemistry) data are interpreted by hydrogeologists and geochemists to yield one or more conceptual models in concert with all observations. The conceptual model(s) is the analyst's evaluation of how the complex natural system works. To remain current and defensible, the conceptual model must be continually reviewed and updated as new field and laboratory data are collected and greater insight is gained regarding the complex subsurface environment and its response to human activities. Another important factor in conceptualization is keeping track of changes in irrigation and water disposal practices at or near Hanford since such activities can significantly affect the conceptual model(s). The review process ensures that continuing data collection programs are responsive to the unresolved physical and chemical issues in the conceptual model, and that inconsistencies do not develop between the conceptual model (formulated and used for continuing performance assessment predictions) and more recent field observations and interpretations. In other words, the models used for predicting the future must be shown to adequately reflect the past and the present data.

Due to a limitation of data, the conceptual model(s) of the unsaturated (vadose) zone demonstrates a rather high degree of uncertainty; however, every attempt has been made to be conservative. The conceptual model of the Hanford unconfined aquifer system is quite reliable in that it is based on the extensive surveillance data collected over the last forty years at Hanford. These data were also used to calibrate the computer codes. Certainly, because only a finite number of points are sampled to define the continuum of the entire site, the conceptual model is to some extent subjective. The following discussion first describes models of water movement in the vadose (unsaturated) zone in the underlying unconfined aquifer and then describes models of geochemical interaction and transport in both

zones. The current conceptual model (below) represents DOE's understanding of the present geohydrologic system beneath the Hanford Site. In many instances hypothetical release scenarios described elsewhere in this EIS include changes in the climate and water management practices, and the emplacement of protective barriers. Predictive modeling and expert judgment have been used in the incorporation of such changes into the conceptual model(s) of future conditions beneath the Hanford Site.

0.3.1 Water Movement in the Vadose Zone

0.3.1.1 Functioning Protective Barrier In Place

With a protective barrier in place over the waste sites and operating as designed, it is assumed that no water infiltrates the wastes and the underlying vadose (unsaturated) zone. This is the anticipated condition which results in insignificant water movement in the vadose zone. In the absence of advecting water, the movement of contaminants is restricted to the very slow process of diffusion through the static water column in response to a concentration gradient. Such diffusion is only important because of the very long EIS assessment times (e.g., thousands of years).

Soil moisture already present in the porous medium beneath a protective barrier will seek a new equilibrium after placement of the barrier. With the barrier in place and after the soil moisture has reached a new equilibrium, vertical redistribution of soil moisture near the waste form will be greatly reduced and become negligible as a contaminant transport mechanism in comparison to diffusion of contaminants through the relatively immobile soil water. Greater isolation of the waste is achieved when the waste form (e.g., tank waste, grout, etc.) is stored further from the edge and closer to the center of the barrier, thus being free from the small degree of lateral movement of water from zones beyond the edge of the barrier to zones slightly beneath the barrier. Water travel times associated with pathlines labeled (b), (c), (d), etc., in Figure 0.2 increase compared to that of the essentially vertical one labeled (a), and the travel times become greater as the pathline origins become more distant from that of (a). We assume, based on preliminary performance assessment modeling and field experience at other sites, that wastes at Hanford can be effectively isolated with a properly engineered and undisturbed protective barrier. Performance assessment of the

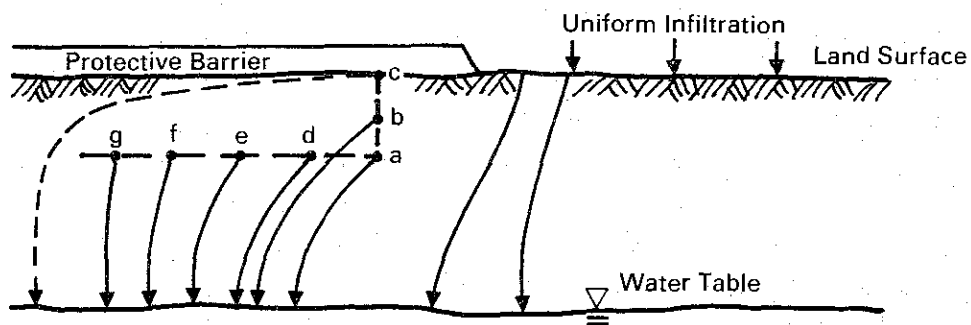


FIGURE 0.2. Depiction of Pathlines from Points Originating at Various Candidate Waste Source Locations

protective barrier will require an accurate model of water balance within the barrier and source release and migration through the vadose zone to the water table. Model analysis should consider the emplacement of wastes and construction of the protective barrier. Simulations presented in this EIS are based on the assumption that the soil profile is currently in an equilibrium state of drainage and that the travel time of moisture to the water table can be estimated. Once the protective barrier is placed over the waste, existing soil moisture will drain from the soil profile more slowly as the new cover moisture equilibrium is approached. Travel times from the waste deposit will increase. Pore water velocities may initially be very similar to those of the current equilibrium state. However, as the barrier takes effect, the velocity will drop and travel times will increase. As equilibrium is approached in the soil moisture profile beneath the protective barrier, the waste form will be increasingly isolated from the deep unconfined groundwater system.

0.3.1.2 No Barrier or Less-Than-Optimal Barrier Performance

If any water does get to the various waste sites, due either to the absence of a protective barrier or less-than-optimal barrier performance (Appendix M), then this new water would be introduced into the relatively thick and dry unsaturated (vadose) zone underlying the Hanford Site. Flow of water in the vadose zone occurs in response to the gradient of the total potential and is strongly influenced by soil texture (i.e., sand, silt, clay). Under conditions of significant infiltration in a given geologic medium due to uniform rainfall/precipitation and evapotranspiration, water movement in the vadose zone, if any, can be visualized as occurring in a vertical column and being limited to the vertical direction. Under these conditions, with sufficient precipitation, the major driving force is the gravity potential. In the vadose zone, under conditions of pond or tank leakage (i.e., point source infiltration), moisture movement could occur in a horizontal direction. Furthermore, horizontal layering of tight (low permeability) materials can lead to some lateral spreading which would result in a delay in arrival times calculated for a more porous average soil. However, such layers are rarely continuous over significant horizontal distances, and the water will normally resume a vertical flow direction. One reason to retain the assumption of vertical water movement in this EIS is the paucity of soil water characteristic data for Hanford soils within the three-dimensional soil system. Furthermore, this is the conservative approach. A knowledge of the spatial and vertical variations in hydrologic information would be necessary to define the existence and extent of one or more sediment layers that could spread the water horizontally and somewhat reduce the transport times and concentrations of radionuclides and chemicals to the unconfined saturated aquifer.

Soil moisture in the porous medium beneath a protective barrier may be subjected to direct infiltration if the barrier is disrupted (see Appendix M). To demonstrate the potential impact of such a disruption, a barrier removal event was arbitrarily assumed to coincide with a future (wetter) climate change which is assumed to occur 500 years after the loss of Site institutional control; i.e., in the year 2650. Barrier removal implies the removal of the upper-layer sands, silts and cobbles, leaving exposed basalt riprap with some silt and sand in the interstices. A soil removal scenario is assumed such that 50% of incipient precipitation would infiltrate the basalt riprap and that this infiltrating water would directly

contact 10% of the waste stored beneath the barrier. Thus surficial barrier removal is not estimated; rather, barrier removal is assumed to be sufficient to expose 10% of the waste inventory to direct leaching. It is important to recognize these waste leaching factors as assumptions, not calculated predictions. However, the water movement predictions in the vadose (unsaturated) zone were based on the aforementioned modeling.

0.3.2 Water Movement in the Saturated Unconfined Aquifer

In the current conceptual model of the unconfined aquifer underlying Hanford, the aquifer is assumed to be a porous medium vertically homogeneous and horizontally heterogeneous. At any given point in space, just the opposite (i.e., vertically heterogeneous and horizontally homogeneous) is the proper assumption. However, at Hanford the various layers, when tracked over any lateral extent, are undulating and/or discontinuous; a certain lithological layer may be 100 ft deep in one borehole and 150 ft deep in another. Therefore, a conceptual model of the system is assumed horizontally. The water table is the upper extent of the unconfined aquifer, and, in the existing calibrated model of the Hanford Site (Reisenauer 1979a,b,c) local infiltration through the vadose zone has been assumed negligible with respect to fluctuating levels of the water table. Onsite waste water discharge practices and offsite irrigation have, however, been taken into consideration with respect to changing water table elevations in the future. The lower limit of the unconfined aquifer is the upper basalt surface or, in some areas, the clay zones of the lower unit of the Ringold formation. These formations are believed to form a low-permeability boundary and supply a negligible quantity of water to the aquifer. Therefore, it is assumed that the bottom of the unconfined aquifer is impermeable. Although this assumption may not be totally valid, the consequences of making it, from the contaminant transport standpoint, are deemed insignificant.

Although the Ringold formation exhibits distinct layering, aquifer parameters are assumed to be vertically homogeneous. Spatial or horizontal variability within the Ringold formation has also been observed, and there are basalt outcrops that completely interrupt the formation continuity. These outcrops, notably Gable Butte and Gable Mountain, are composed of less permeable material than the surrounding Ringold formation; therefore they are assumed to be impermeable islands within the aquifer. Variability in the conductance of the unconfined aquifer is related to both the hydraulic conductivity of the medium and the thickness of the aquifer, both of which vary significantly over the Hanford area. This overall horizontal variability in conductivity is modeled with a spatially varying (i.e., heterogeneous) transmissivity distribution.

Water is introduced to the aquifer as run-off from the higher elevations; as infiltration from ponds, trenches, and cribs currently operated by the Department of Energy; as recharge from the Yakima River; and possibly as natural recharge through Hanford area sediments. Groundwater from the unconfined aquifer discharges to the Columbia River. Basalt formations of the Yakima Ridge, Umtanum Ridge, and Rattlesnake Hills form low-permeability boundaries to the south and southwest that are assumed to be essentially impermeable (see Figure Q.1 in Appendix Q). Run-off and any infiltration from these formations, Cold Creek and Dry Creek Valleys, and the basalt outcrops are assumed to enter the aquifer at the

associated section of the model boundary. To the north and east, the unconfined aquifer is bounded by the Columbia River, and to the southeast the aquifer is bounded by the Yakima River. On these boundaries the elevation of the water table is specified by the elevation of the river. The currently calibrated model of the unconfined aquifer includes the release of water from ponds, trenches, and cribs associated with the operation of the Hanford Site. Most simulations conducted under this study begin in the year 2150, 100 years after Site closure. Therefore releases of water associated with present Site operation have been discontinued.

As discussed in Volume 1 of this EIS, scenario analyses use water infiltration and recharge rates of 0.5 and 5 cm/yr to represent current and wetter conditions. This water is applied uniformly over the Site. These values are applied as average values over all time and do not represent minimum or maximum infiltrations for any given year over a 10,000-year analysis period. Furthermore, for sites with a protective barrier, no such finite levels of infiltration are expected as long as the barrier is undisturbed.

Field studies conducted at Hanford under the National Low-Level Waste Management Program have shown that when the major part of the annual precipitation occurs during months with low average potential evapotranspiration and where soils are vegetated but coarse-textured and well-drained, significant drainage can occur from the root zone (Kirkham and Gee 1984). While not a general statement for the entire Hanford Site, this finding suggests that in those areas of the Site having coarse-textured soils and sparse or no vegetation, one could expect infiltration to supply water to the unconfined aquifer in measurable quantities during wet years. A previously conducted study, using lysimeters near the 200 East Area, concluded that unsaturated sediments retain little or no additional water under existing arid climate conditions (Isaacson and Brown 1978; Last, Easley and Brown 1976). From an analysis of water storage for one of these lysimeters for over a 14-year period (Fayer, Gee and Jones 1986), the evidence suggests that deep-rooted plants have been successful in cycling meteoric water which has infiltrated into coarse-textured soil. These differing results underscore the important contributions of soil and vegetation to the variability in the distribution of infiltration over the entire Hanford Site. A range of values of 0.5 to 5 cm/yr was used to represent current and wetter conditions which may vary with time.

The range of annual recharge at a given location depends upon soil texture, plant cover, and topography as well as precipitation intensity and frequency. Recharge at Hanford may vary from zero to values in excess of the annual precipitation (Fayer, Gee, and Jones 1986; Walter et al. 1986). For this reason, it is unacceptable to arbitrarily select a fraction of the annual precipitation or evaporation (as proposed by Narasimhan, White, and Tokunaga 1986), as an estimate of the annual recharge. The recharge at an unprotected site (i.e., where there is no protective barrier) may vary considerably from year to year; hence, a range of recharge values is possible. Given the present understanding of recharge at the Hanford Site, a lower limit of 0.5 cm/yr was selected to represent a possible non-zero value for unprotected sites (see Appendix M.5.2.4 for a discussion of evidence suggesting an even lower limit of recharge than 0.5 cm/yr; see also page xxix). Wetter conditions (due to wetter climate, bare or coarse soils, topographic effects or combinations of these factors) at

unprotected sites are reflected in the 5 cm/yr recharge value. At 5 cm/yr, and at typical water contents (5 to 10% by volume) and travel lengths (50 to 65 m), water-soluble contaminants will move through the unsaturated zone in less than 100 years, so that long-term isolation of soluble contaminants is not possible. Therefore, the rate of 5 cm/yr is used in this EIS to reflect any condition where the site is unusually wet due to a wetter climate or unusual surface characteristics, i.e., coarse gravel surface, void of vegetation.

0.3.3 Contaminant Transport in the Total System (Vadose Zone and the Unconfined Aquifer)

The previous discussions focused on the essentially vertical movement, or lack thereof, of water in the unsaturated (vadose) zone and essentially horizontal flow of water in the unconfined saturated aquifer that ultimately discharges to the Columbia River. The following discussion concerns contaminant transport away from the waste sites, down through the unsaturated zone and then horizontally through the unconfined aquifer to the river. It is significant that many natural physical and chemical mechanisms act along these flow paths to radically delay the travel time and decrease the concentration of many radionuclides and chemicals. In simple terms, contaminants can be removed from the water via precipitation as solids or adsorption (plating out) on the natural sediments through which the water flows. Precipitation may occur because a solubility limit for a specific radionuclide or chemical is exceeded, or a mechanism similar to crystallization may occur.

The conceptual model of the Hanford Site employed in this EIS considers radionuclide transport as occurring in streamtubes originating at the contaminant source and traversing first the vadose zone in predominantly a vertical direction and then the unconfined aquifer in predominantly a horizontal direction (see Figure 0.3). These streamtubes are assumed to

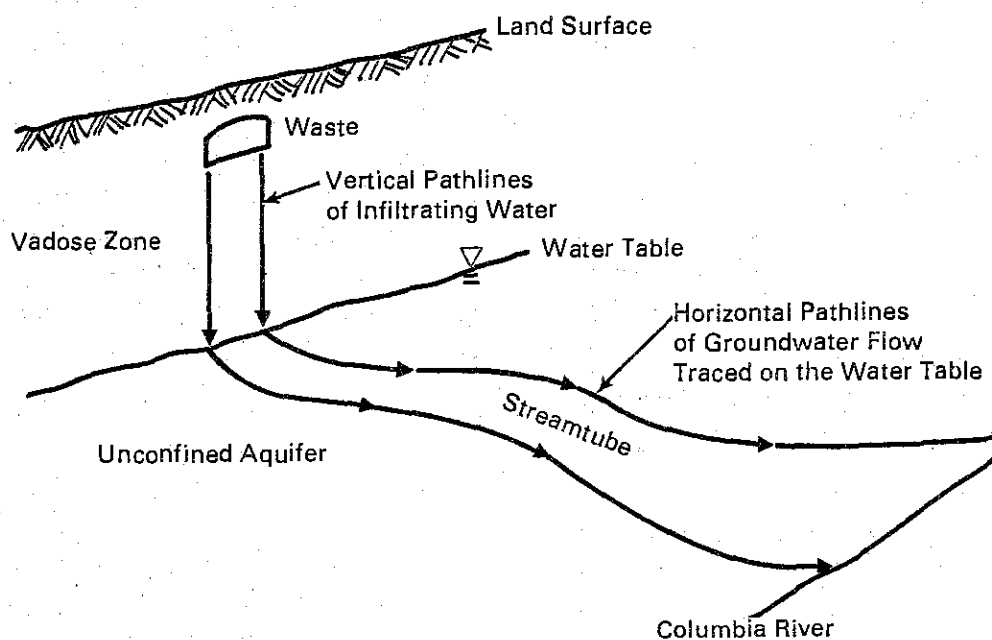


FIGURE 0.3. Depiction of the Streamtube Approach to Transport in the Vadose Zone and the Unconfined Aquifer

be vertical in the vadose zone. Any lateral movement due to layering would only add to the tortuosity and travel time and decrease the concentration. Streamtubes in the unconfined aquifer are defined by the aforementioned groundwater model pathlines. The width of any streamtube in the unconfined aquifer is simply defined by the projection of the cross-sectional area of the associated source (waste site) width to the water table. Thus streamtubes arising from different sources will have different widths. No dilution is being assumed for hydrodynamic dispersion, laterally, within any given streamtube, but the original plume is spread, and thus concentrations reduced somewhat, by dividing the contaminant plume among the various streamtubes in the transport model. Stratigraphic and spatial detail in the vadose zone sediments are not sufficient to suggest the existence of a continuous and significant horizontal short cut in the transport pathway, especially since the 200 Areas are so far from the Columbia River. Soil moisture characteristic curves, relative conductivity curves, and saturated hydraulic conductivity values have not been obtained for the spatial variation of vadose zone sediments at depth.

Radionuclide transport is influenced by the processes of advection, hydrodynamic dispersion, dilution, chemical retardation, and decay. The same is true for chemicals except that they do not decay. Advection, if any, is defined by the pore-water velocity (speed and direction), which varies in each streamtube. When a distinct advection transport pathway is modeled within the vadose zone (i.e., for the less-than-optimal barrier performance scenarios), dispersion phenomena are characterized by a diffusion-type dispersion coefficient that is a function of the travel time (i.e., the time required for moisture to traverse the vadose zone). Within the unconfined aquifer, longitudinal dispersion is introduced through the variation in travel times among the various streamtubes that conduct radionuclides and chemicals away from the source. There is no defined dispersion coefficient within a given streamtube, but the water travel time varies from streamtube to streamtube and thus hydrodynamic dispersion, or plume spreading, is introduced via averaging over all the different streamtube velocities. The dispersion model considers longitudinal dispersion but neglects transverse dispersion. By neglecting transverse dispersion within a given streamtube, solute mass that would actually migrate to adjacent streamtubes is retained in the originating streamtube. Thus the concentration and its spatial gradient will be higher in predictions than in reality. This means that conservative peak concentration and travel times will be predicted in the analyses. Radioactive decay is modeled with the standard half-life model. The use of the linear sorption isotherm model and its limitations in representing retardation are described in the geochemistry subsections.

0.3.4 Geochemical Interactions--Retardation

Retardation encompasses all processes that hinder solute migration in solution, including ideal ion exchange, isotopic exchange, mineral precipitation, co-precipitation in amorphous coatings, chemisorption or specific adsorption onto surface sites of solid adsorbents, redox or hydrolysis-mediated precipitation/sorption, and physical filtration of small particles. Of most interest are adsorption processes, defined as the surface processes by which radionuclides or chemicals in solution become incorporated onto the solid phase surfaces. The term "adsorption" is more general and includes more processes than ideal ion exchange but

excludes precipitation of identifiable mineral or amorphous solids and physical filtration of particles. It is important to separate and distinguish precipitation, physical filtration, and adsorption processes. This separation is not always easy because of limited data on solubility limits and speciation (complexation) of some radionuclides and chemicals. It is important also to note that radionuclides and/or chemicals may exist as one or more species (chemical forms or complexes) and that speciation can change in the subsurface environment because of natural changes in Eh, pH and pore-water chemistry.

Measurement of the ratio of adsorbate between the solid phase of interest (i.e., rock, sediment, or soil) and the solution phase (i.e., soil water or groundwater) is commonly used to quantify adsorption tendencies. Several somewhat standardized laboratory techniques (Serne and Relyea 1983) are commonly used to determine the ratio. The ratio or distribution coefficient is often called K_d , D, or R_d . Confusion arises because the term "distribution coefficient" has been used by scientists from diverse disciplines much more selectively, and these same symbols have been used to represent other parameters.

Most laboratory experiments performed to measure distribution coefficients for radionuclides and chemicals are not designed to systematically investigate the effect of important parameters and do not attempt to identify the processes causing the observed adsorption. Because the studies are empirical in nature, the symbol R_d is used for these types of values. R_d values are easily measured in the laboratory, especially by batch experimentation. Being an empirical measurement, the R_d value does not necessarily represent an equilibrium value or require some of the other assumptions inherent in the more rigorous use of the term K_d . R_d is thought of simply as the observed distribution ratio of nuclide or chemical between the solid and solution phases. K_d is reserved for equilibrium reactions that show reversibility and reactions that do not yield a distribution ratio that is dependent on tracer concentration in solution.

The conceptual model of geochemical interactions used in the transport equation to assess radionuclide or chemical retardation at Hanford is limited to the linear distribution coefficient or K_d approach. The simplicity of this approach is recognized as a potential technical limitation in such modeling efforts. Because K_d data do not exist for the spectrum of soils underlying Hanford, single conservative values of K_d have been adopted to represent individual radionuclides in all media. Thus the influence of spatial variability in media is not addressed in the model of adsorption applied here. Conservative values of K_d have been selected whenever a range exists. In other words, within the constraints imposed by the K_d approach and the available data, every attempt has been made to be conservative. However, for a variety of reasons, this total K_d approach in handling geochemical interactions of the contaminant source and subsequent interactions between mobilized contaminants and the subsurface geochemical environment cannot be stated as necessarily conservative. More desirable approaches are required to conduct equilibrium geochemical modeling and coupled solute transport and geochemical modeling. Such approaches are the subject of ongoing research. It will be several years, however, before modeling the chemically complex defense waste system (radionuclides and chemicals) on the scale of the Hanford Site can be addressed by this more rigorous coupled solute transport and geochemistry methodology.

0.4 MATHEMATICAL AND NUMERICAL MODELS

Computer-based numerical models are the result of applying a numerical technique to a mathematical model and developing a computational analogue (code) to the mathematical model. Numerical techniques reduce the partial differential equations to an algebraic system of equations that can be solved by iterative or matrix computer methods. Numerical techniques commonly applied to mathematical models of geohydrologic systems include finite-difference methods, finite-element methods, boundary-integral methods, and random-walk methods.

The numerical models that have been applied in this EIS to determine radionuclide migration from the 200 Areas plateau and the 300 Area disposal sites range from simple to moderately complex. At the complex extreme, the computer-based Variable Thickness Transient (VTT) code (Reisenauer 1979a,b,c) is used to compute hydraulic head, pathlines, and travel times in the unconfined aquifer. Even more complex, three-dimensional models, or more appropriately stochastic modeling techniques could be applied if such accuracy and resolution were required and the data available. At the simple extreme, a unit hydraulic gradient assumption gives rise to a relatively straightforward hand calculation for the vertical movement of moisture in the vadose zone. Use of these two methods in the same analysis is appropriate since each model uses the available data from its respective domain (i.e., unconfined aquifer, vadose zone).

The model of a specific site, for example the unconfined aquifer underlying Hanford (referred to as the "Hanford model"), is the computer-based analogue to the true physical system. Input files containing the data for the conceptual model are used to execute the computer-based numerical models for the Hanford Site. An iterative procedure is followed to calibrate the site-specific numerical model. This iterative calibration procedure establishes consistency between the computer-based Hanford model and the observations that have been made at the Hanford Site in the past four decades, and results in improved numerical models. An inverse method to automate the calibration process is proposed as a future activity under the project providing modeling support for liquid waste management of the 200 Areas.

0.4.1 Moisture Movement and Diffusive Contaminant Release in the Vadose Zone

A variety of computer-based numerical models are available for predicting the movement of moisture in the vadose zone. However, the general lack of site-specific Hanford data on soil characteristic curves for the major soil horizons of the vadose zone precludes application of these deterministic models and codes. The modeling approach employed is to assume that unit hydraulic gradient conditions apply and define the hydraulic conductivity and moisture content indicative of the steady-state solution to the Richards' equation (Richards 1931). The unit hydraulic gradient model of moisture movement assumes that, in a given soil layer, water will drain at a rate equal to the unsaturated conductivity of the soil. This model enables one to approximate travel time and utilize all available data on vadose-zone sediments.

0.4.1.1 Unit Hydraulic Gradient Model

Darcy or discharge velocity in a one-dimensional and vertically aligned unsaturated soil column is defined by:

$$q = K(\theta) \left(1 + \frac{\partial \psi(\theta)}{\partial z}\right) \quad (0.1)$$

where q = Darcy velocity

$K(\theta)$ = hydraulic conductivity as a function of moisture content

θ = moisture content

ψ = suction head

z = vertical cartesian coordinate

and the soil moisture characteristic curve and hydraulic conductivity curve are defined by the two following relationships:

Soil moisture characteristic curve:

$$\psi = \psi_e \left(\frac{\theta_s}{\theta}\right)^b \quad (0.2)$$

where ψ_e = suction head at air entry

θ_s = moisture content at saturation

b = curve fit parameter

Hydraulic conductivity curve:

$$K = K_s \left(\frac{\psi_e}{\psi}\right)^n \quad (0.3)$$

where K_s = hydraulic conductivity at saturation

$n = 2 + 3/b$.

Of interest is the case in which infiltration rate is less than the saturated hydraulic conductivity and, consequently, unsaturated flow occurs throughout the profile. In this case, the hydraulic gradient of the steady-state solution becomes one; i.e.,

$$1 + \frac{\partial \psi(\theta)}{\partial z} \approx 1 \quad (0.4)$$

and the hydraulic conductivity has a value corresponding to the given infiltration rate (Hanks and Ashcroft 1980, pp. 62-69, 78-82). Thus Equation (0.1) becomes

$$q \approx K(\theta) \quad (0.5)$$

Substituting the soil characteristic and conductivity curves (Equations 0.2 and 0.3) into Equation (0.5) yields:

$$q = K_s \left(\frac{\theta}{\theta_s}\right)^{2b+3} \quad (0.6)$$

Solving for moisture content one obtains:

$$\theta = \theta_s \left(\frac{q}{K_s} \right)^{1/(2b+3)} \quad (0.7)$$

The pore water velocity, v , within the soil column is defined as Darcy velocity divided by moisture content; i.e.,

$$v = q/\theta \quad (0.8)$$

and finally the travel time is given by the distance traveled divided by the pore-water velocity,

$$T = L/v = L\theta/q \quad (0.9)$$

where L is column length. Equation (0.7) can be substituted into Equation (0.9) to obtain a direct relationship between travel time and infiltration rate:

$$T = \frac{L\theta_s}{q} \left(\frac{q}{K_s} \right)^{1/(2b+3)} \quad (0.10)$$

Travel times based on the equation above are used in both the source and transport models. Application of soils data to this theory is described in Appendix Q.

The unit hydraulic gradient model of moisture movement is used only to approximate travel time from beneath the source to the water table. This is a conservative model in that it neglects the potential for lateral spreading of the available water.

0.4.1.2 Description of the Simplified Approach to Release Beneath a Protective Barrier

For those wastes placed beneath protective barriers, one must examine the two-dimensional flow system that will exist adjacent to and beneath the barrier. Placement of a protective barrier over waste is an attempt to isolate it from intrusion and from infiltrating water that will carry source releases of radionuclides and chemicals to the water table. This is done to improve upon the good natural isolation afforded waste by an unsaturated soil environment and a semi-arid climate.

The simplified approach shown in Figure 0.4 essentially breaks the vadose zone into two distinct regions: 1) a diffusion-controlled zone directly beneath the barrier and extending to the water table and 2) an advection-controlled zone adjacent to the barrier. Use of such a model implies that the barrier is completely effective immediately after placement. It is assumed that as the soil moisture profile drains to its new equilibrium (i.e., in response to barrier placement), the soil moisture initially in contact with waste remains near the waste while in effect it drains to a new, lower equilibrium moisture content.

The simplified approach or model also assumes times of initial release from the waste forms. Two examples of interest are single-shell tanks and grout vaults. With the

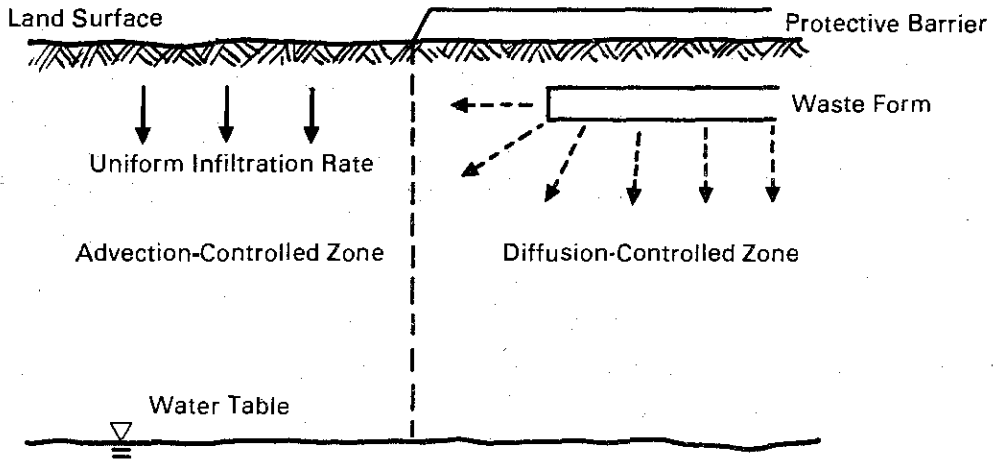


FIGURE 0.4. Diffusion- and Advection-Controlled Regions of the Simplified Model for Release of Waste with Barrier Emplaced

single-shell tanks, release is predicated on hygroscopic forces causing water vapor to diffuse into a tank, dissolve the salt cake waste form, and leak from the tank. This scenario is based also on the assumption that a significant portion of the steel and concrete tank shell has corroded away and no longer isolates waste from soil. This conservative approach is used because of the long performance assessment time (e.g., thousands of years) needed in this EIS. While leaks have occurred during the last few decades (Routson et al. 1979) at Hanford, they have resulted from very small surface area disruptions (e.g., weld failure). Leach of the remaining solid waste in these tanks by the vapor diffusion mechanism through these relatively small surface areas is assumed to be virtually insignificant. Because time is necessary before surface area corrosion and vapor diffusion can provide significant releases, it is illogical to begin such a release immediately. One can also assume that although leaks, implying structural failure, may occur for virtually all single-shell tanks in the next two centuries, in the arid climate and dry soils of the Hanford Site the tanks will retain some measure of containment integrity for salt cake (i.e., a solid waste form) for several centuries. The release model for single-shell tanks is based on the assumption that moisture can freely enter and leave every tank in the year 2150, 100 years after Site closure. The date was arbitrarily selected; however, a measure of conservatism is included by not limiting the flux of moisture to that of the hygroscopic-related transport process. Essentially, the assumption is that all contamination that can be transported by the vadose zone soil is available for transport from the single-shell tank sources beginning in the year 2150. In the case of the grout waste form, the hygroscopic forces will again cause moisture to be drawn to the grout initially. However, the duration of such a phenomenon has not been studied. Consequently, releases from grout are assumed to begin immediately upon placement of the grout waste in vaults.

0.4.1.3 Diffusion-Controlled Release Model

Transport in the diffusion-controlled zone beneath the protective barrier is modeled as occurring through one-dimensional streamtubes that conduct the radionuclides to either the advection-controlled zone or directly to the water table (see Figure 0.5). Contamination delivered to the advection-controlled zone is subsequently moved to the water table after the

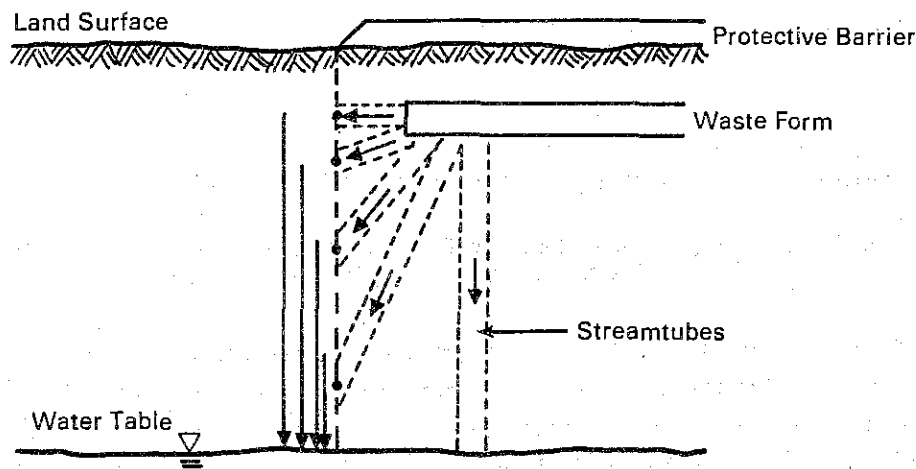


FIGURE 0.5. Streamtubes Conducting Contamination to the Water Table

travel time associated with the distance to the water table has elapsed. A fraction of the waste inventory is associated with each pathway to the water table.

Contaminant transport through each streamtube is governed by the diffusive mass or activity flux equation:

$$J = -\theta DA \frac{\partial C}{\partial X} \quad (0.11)$$

where J = activity or mass flux (Ci/t or M/t)

θ = moisture content (-)

D = modified molecular diffusion coefficient (L^2/t)

A = streamtube cross section (L^2)

C = activity or mass concentration (Ci/L^3 or M/L^3)

X = longitudinal streamtube coordinate (L)

and satisfies influent and effluent Dirichlet boundary conditions of C_0 and 0, respectively. The influent condition of $C = C_0$ is based on an assumption that contamination concentration at the source/soil interface is at an equilibrium solution concentration value. The effluent condition of $C = 0$ is based on an assumption that moisture movement in the advective-controlled zone dilutes and removes the contamination upon its arrival at the diffusion/advection zone interface. The treatment of the diffusive release is further simplified by assuming a linear concentration profile within the streamtube. First release from the

diffusion pathway is estimated by applying a sequence of quasi-steady-state linear concentration profiles. Flux defined by Equation (0.11) is equated to the time rate of change in storage within the concentration profile; i.e.,

$$J = A \frac{\partial}{\partial t} (R \theta \int_0^x C dx) \quad (0.12)$$

where R is the retardation factor. Substituting Equation (0.11) into (0.12), substituting a linear concentration profile for concentration everywhere, and performing the indicated integration one obtains:

$$x^2 = 4 Dt/R \quad (0.13)$$

for all times, t , that precede first arrival. The time of first release, T , is obtained by substituting L , the length of the streamtube, for x :

$$T = RL^2/4D \quad (0.14)$$

Once first release has occurred, a period of steady-state release, with flux defined by the linear profile, continues until the source is depleted. The source will be depleted after a period of time, t_0 , defined as:

$$t_0 = T + \frac{M_0 - AR\theta C_0 L/2}{\theta D A C_0 / L} \quad (0.15)$$

where: $M_0 = \rho_0 Ah$ = total mass of contamination in pathway source, ρ_0 = initial source density and h = thickness of source deposit.

Once the source is depleted, release of the contaminant stored in the soil profile (i.e., streamtube) is given by the diffusive flux associated with the linear concentration profile. One equates flux leaving the streamtube with the change in storage:

$$\theta D C^*/L = - \frac{\partial}{\partial t} (R \theta \frac{C^* L}{2}) \quad (0.16)$$

where C^* is the concentration at the source, less than C_0 . Initially the concentration is C_0 ; finally it goes to zero. The solution for C^* is:

$$C^* = C_0 e^{-\beta(t-t_0)} \quad (0.17)$$

where $\beta = 2D/RL^2 = 1/2T$.

The flux leaving the streamtube, J_L , is given by:

$$J_L = \frac{\theta A D C_0}{L} e^{-\beta(t-t_0)} \quad (0.18)$$

One can visualize the release to the water table as occurring in three stages: 1) zero release, 2) constant release, and 3) exponentially decreasing release. These steps are portrayed on a time line in Figure 0.6. Results are shown for a second case in Figure 0.7 representing a source that is depleted before first arrival at the end of the streamtube.

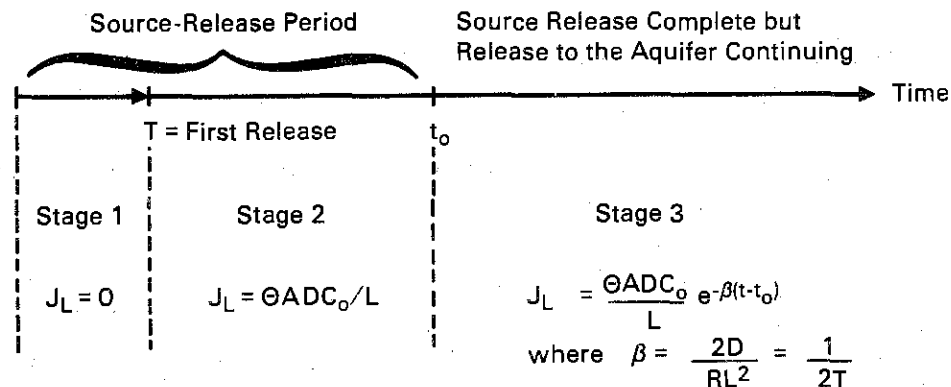


FIGURE 0.6. Time Line of Release Through a Diffusion-Controlled Streamtube When Source Release Period Exceeds First Release Time

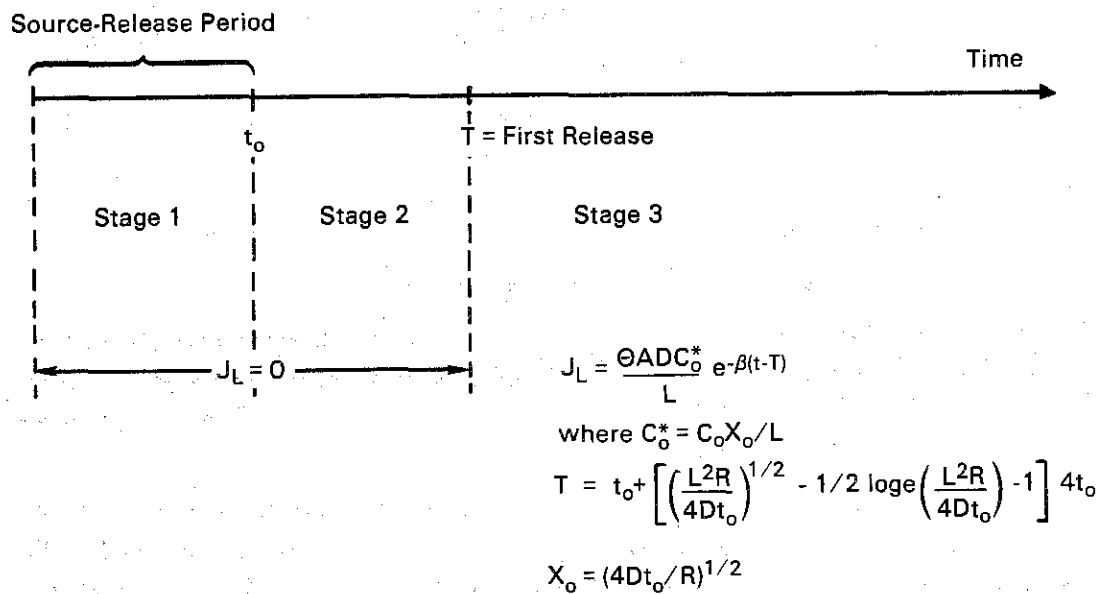


FIGURE 0.7. Time Line of Release Through a Diffusion-Controlled Streamtube When First Release Time Exceeds Source Release Period

Note that the complete definition of the diffusion coefficient for molecular diffusion in the vadose zone is as follows:

$$D_p = \Theta \left(\frac{L}{L_e} \right)^2 \alpha \gamma D_0 \quad (0.19)$$

where diffusive flux is given by:

$$J = -D_p A \frac{\partial c}{\partial x} \quad (0.20)$$

and θ = volumetric moisture content

$(\frac{L}{L_e})^2$ = tortuosity factor

α = viscosity factor

γ = anion exclusion coefficient

D_0 = molecular diffusion coefficient

D_p = effective diffusion coefficient.

Bresler, McNeal and Carter (1982, pp. 85-86) provide the following estimate of the effective diffusion coefficient in a sandy loam medium:

$$D_p = D_0 a \exp(b\theta) \quad (0.21)$$

where $a = 0.005$ and $b = 10$. The range over which this empirical equation is valid has not been tested for Hanford soils but preliminary calculations indicate that it probably does not hold for water contents less than 5%. An expression for the combined correction factor is obtained by equating the equations for D_p . One obtains:

$$(\frac{L}{L_e})^2 \alpha \gamma = \frac{D_0 \exp(10\theta)}{\theta} \quad (0.22)$$

$$\text{therefore, } D = \frac{0.005 \exp(10\theta)}{\theta} D_0, \text{ for } \theta > 0.05 \quad (0.22a)$$

For consistency, when applying the effective diffusion coefficient in the preceding equations, the θD product is replaced by D_p .

0.4.1.4 Moisture Movement Beneath a Protective Barrier

Preliminary analyses based on steady-state flow beneath the barrier indicate that isolation of waste is increased when it is placed further away from the barrier edge or closer to the barrier center. Thus, one could expect to be able to tailor the barrier design to ensure adequate isolation of each waste site and type.

Attempts with state-of-the-art models failed to define conclusively the movement of moisture beneath a protective barrier. New modeling techniques are being developed within the scientific community that hold promise of resolving these very difficult physical and mathematical problems involving flow of water in soils of low moisture content in large-scale systems containing coarse-grained soils. Efforts to achieve steady-state and transient solutions to the moisture movement problem are continuing under the Barrier Development Program (Adams and Wing 1987). Two significant efforts may be necessary to fully understand moisture movement in the vicinity of wastes: the development and/or application of an efficient, fully three-dimensional moisture movement code, and the acquisition of soil characteristic data in sufficient spatial resolution to reveal the three-dimensional character of the soils surrounding and underlying the waste.

0.4.2 Water Movement in the Unconfined Aquifer

The mathematical model applied to the unconfined aquifer is a vertically integrated form of the groundwater flow equation. This model assumes the vertical column of water-saturated sediments can be modeled by a vertically homogeneous, isotropic value of the hydraulic conductivity. This means that variability in the properties of these layered sediments can be adequately represented by a vertically averaged value. Horizontal variability in hydraulic conductivity is accounted for by a heterogeneous model that admits a suite of deterministic, spatially varying, hydraulic conductivity coefficients. The mathematical formulation expects external and internal boundaries to be well defined. This is achieved by specifying the hydraulic head along river boundaries, the water flux at aquifer boundaries, and a zero water flux at impermeable boundaries. Operations that currently dispose of water in ponds, trenches, and cribs on the Hanford Site will be discontinued when the long-term modeling period of interest in this study begins. The thickness of the saturated aquifer formation is allowed to vary spatially and is defined by the topography of the aquifer bottom; i.e., low-permeability basalt flows and thick clay sequences, in conjunction with the water table elevation of the unconfined aquifer which forms the upper boundary of the unconfined aquifer system. Heterogeneity of physical properties of the aquifer (i.e., hydraulic conductivity) is incorporated in the model by a piece-wise constant representation of the properties. Thus, conductivity is assumed to be constant over a finite area associated with a node. At the next node the conductivity may, if appropriate, take on a new value.

The VTT model of water movement in a confined or unconfined aquifer is based on the vertically averaged groundwater flow equation. Originally designed and implemented to model the Hanford Site (Kipp et al. 1976), this code has been updated twice (Reisenauer 1979a,b,c; Bond, Newbill, and Gutknecht 1981) and applied to a variety of aquifer systems. Standards of code documentation, e.g., NUREG-0856 (Silling 1983), adopted since publication of the series of documents by Reisenauer (1979a,b,c) are not specifically addressed in more recent documentation. However, the code itself is well documented and its application to the unconfined aquifer underlying the Hanford Site is a matter of record.

Cearlock (1971) described the application of the VTT code as a tool for management of the Hanford groundwater system. Kipp et al. (1976) used data on the aquifer bottom, water table surface and aquifer properties to calibrate the groundwater flow model. Cearlock et al. (1975) later applied the transmissivity iterative calculation (TIC) routine to recalibrate the groundwater flow model of the Hanford unconfined aquifer based on the VTT code. Recalibration of the VTT model is undertaken when a sufficient amount of new water level or transmissivity data have been collected from Hanford wells. Figure 0.8 shows the hydraulic conductivity distribution on the Hanford Site as currently used in the two-dimensional, finite-difference groundwater model. An effort to improve detailed understanding of and modeling capability for the unconfined aquifer is currently under way as part of a project providing modeling support for liquid waste management of the 200 Areas.

The VTT model of the unconfined aquifer underlying Hanford has been calibrated to a water table perturbed by water disposal practices followed in the operation of the Hanford Site. One key assumption is that after site closure the aquifer reverts to pre-1940

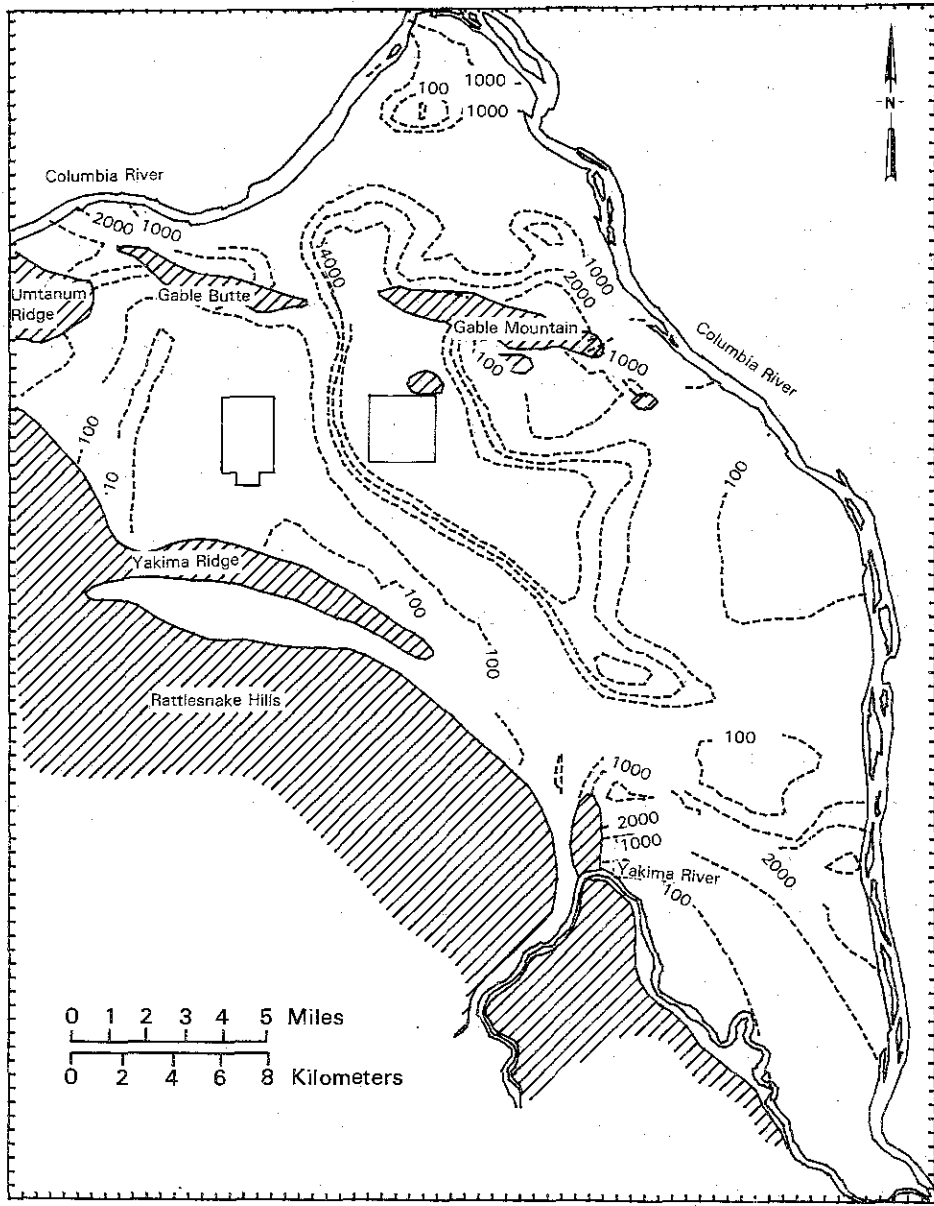


FIGURE 0.8. Patterns of Hydraulic Conductivity on the Hanford Site

conditions; i.e., negligible withdrawal by pumping and no infiltration from major water disposal activities at the land surface. However, the simulations conducted for this EIS rely upon the transmissivity values arrived at in the calibration to current water table elevations. Changes in the saturated thickness of the unconfined aquifer (i.e., the water table elevation) due to applying the infiltration rates of 0.5 and 5 cm/yr were found to be relatively small. Certainly, the groundwater mounds underlying current disposal ponds vanish, but aside from these isolated areas changes in water levels are small. Thus, use of

the transmissivity and hydraulic conductivity values calibrated to current water elevations should not introduce significant error in the post-site-closure VTT model of the unconfined aquifer.

VTT is capable of simulating constant-head and specified-flux boundary conditions in a multi-aquifer system. Its multi-aquifer capability is achieved by modeling a set of vertically integrated groundwater flow equations (i.e., one for each aquifer) and coupling the aquifers through interaquifer transfer or leakance terms. Transient simulations of the hydraulic head can be made using constant or time varying boundary conditions. Typically, steady-state simulations driven by constant boundary conditions are used to determine the response of the aquifer to long-term scenarios. While the VTT code is capable of multi-aquifer and transient modeling, its application to the unconfined aquifer beneath Hanford utilizes its single-aquifer, steady-state formulation. The VTT model is based on the Boussinesq equation with appropriate initial and boundary conditions (Reisenauer 1979a). The independent spatial variables are in the horizontal plane and the nonlinear free-surface boundary condition is incorporated into the governing differential equation. Initially assuming a zero reference elevation and no source terms, the governing equation is:

$$n \frac{\partial h}{\partial t} - \frac{\partial}{\partial x} \left(K_h \frac{\partial h}{\partial x} \right) - \frac{\partial}{\partial y} \left(K_h \frac{\partial h}{\partial y} \right) = 0 \quad (0.23)$$

To expand this equation to apply to an aquifer with varying bottom elevation, $h_b(x,y)$, and to include sink/source terms (e.g., for infiltration), the following changes are made:

- assume the bottom slope is negligible
- replace h in Equation (0.23) by $h-h_b$ because the lower integration limit is nonzero
- add the sink/source term, Q .

The resulting equation is the Boussinesq equation for unsteady flow:

$$n \frac{\partial h}{\partial t} = \frac{\partial}{\partial x} \left[K(h-h_b) \frac{\partial h}{\partial x} \right] + \frac{\partial}{\partial y} \left[K(h-h_b) \frac{\partial h}{\partial y} \right] + Q \quad (0.24)$$

where: n = vertical average of effective porosity

h = elevation of the free surface above a reference datum

h_b = elevation of the aquifer bottom from the reference datum

Q = sink/source strength

K = vertically averaged isotropic value of hydraulic conductivity

x,y = horizontal spatial coordinates.

Basic assumptions of the Boussinesq flow model for describing saturated unconfined flow in VTT are (Reisenauer 1979a,b,c):

- Flow is by an incompressible fluid that saturates a rigid porous soil matrix.
- Compressibility effects of the fluid and soil matrix can be neglected.

- Hydraulic conductivity and effective porosity are represented by vertically averaged values that are isotropic but heterogeneous.
- Free surface and bottom topography slopes are slight ($<5^\circ$).
- Vertical velocities are small and can be neglected.
- Dependent variables are continuous.
- Flow in the capillary fringe can be neglected.
- Seepage surfaces are not modeled.

The Boussinesq formulation presented above is implemented in the VTT code and applied to predict the elevation of the free surface (i.e., hydraulic head) in the unconfined aquifer.

In addition to supplying a simulation of hydraulic head, the VTT model develops a groundwater velocity distribution from the hydraulic head distribution and uses it to trace pathlines and determine travel times. In addition to being a first approximation to transport, the pathline algorithm establishes the variety of streamtube lengths and travel times experienced by the fluid. These data, discussed in the next subsection, are used in a transport model, which employs the stochastic viewpoint that dispersion is manifest in the variability of travel times experienced by the transported solute or radionuclide.

Finite difference approximations are used in the VTT model for the terms contained in the groundwater flow equation. These difference expressions, when applied to all terms, result in a set of algebraic equations. The solution method applied to these algebraic equations within the VTT code can vary depending on the complexity of the groundwater system and on whether a steady-state or transient simulation is undertaken. Transient simulations utilize the successive line overrelaxation technique. Steady-state simulations that include an unconfined aquifer are achieved with a Newton iteration technique, and those that include only confined aquifers are achieved with the Cholesky decomposition method. The steady-state version of the model was used for the long-term simulations required for the HDW-EIS.

Some important three-dimensional issues of solute transport cannot be analyzed with the VTT code. These issues include the three-dimensional migration of chemical wastes that may move from the top to the bottom of the aquifer because of density gradients, and the effect spatial resolution of the bottom topography and sources can have on flow and transport of these density-influenced flows. Modeling elements that comprise the steps leading to a stochastic analysis of the unconfined aquifer (i.e., inverse analysis, kriged surfaces, etc.) are planned as part of the Interim Hanford Waste Management Technology Plan (DOE 1986).

0.4.3 Transport in the Vadose Zone and the Unconfined Aquifer

Transport analysis entails the prediction of contaminant migration within the vadose zone and the aquifer. When the hydrogeologic and geochemical structure of the aquifer is uncertain, such transport predictions are only approximations of possible environmental dispersal. The simplified analysis approach used in this EIS, as the result of a lack in certainty in the values to be used in the model, falls into a category where uncertainties in the predicted values cannot be quantified to any meaningful degree. Furthermore, current models of transport in the vadose zone and unconfined aquifer have not been validated for the

Hanford aquifer system and thus are subject to some criticism. However, the authors have attempted to err on the side of conservatism with respect to cumulative environmental impacts.

Data do not exist to validate long-term transport predictive models at the Hanford Site. Monitoring of the unconfined groundwater aquifer at Hanford is limited to approximately 40 years. Transport times in the vadose zone will significantly exceed this length of time; therefore, monitoring transport only in the unconfined aquifer is not sufficient from a predictive model validation point of view. Planned releases to the vadose zone (e.g., to cribs and trenches) and accidental tank leaks, are transient in character and have not been studied within the vadose zone with the intent to validate vadose zone transport models. While these experiences reveal the geochemical attenuation properties of the vadose zone (described in Appendix V), sampling and reporting of these planned and accidental release events do not provide an adequate data base for validation of vadose zone transport models. This is especially true since sampling has been generally limited to just the sediments and not the aqueous phases (interstitial water).

As it reflects on transport predictions, the calibration of the VTT model of the unconfined groundwater aquifer contributes to validation of the transport simulation. The transport model uses the travel-time predictions from the groundwater model to estimate advective and dispersive components of transport. Thus, accurate calibration of the groundwater model to establish the hydraulic conductivity distribution is essential to our confidence in transport predictions. Calibration of the VTT model to the Site is a continuing activity as described in the subsection on groundwater modeling. Note, however, that calibration and hence validation of the transport model is limited to our confidence in the travel-time distributions supplied by the unconfined aquifer model. Longitudinal dispersion models applied to the vadose zone and unconfined aquifer, and the travel-time model of transport through the vadose zone, have not been calibrated.

0.4.3.1 Technical Issues in Transport Modeling

The groundwater flow patterns and velocities acting within an aquifer ultimately determine the dispersal and environmental arrival times of dissolved radionuclides released from waste burial sites. In principle, the advection-diffusion equation, which depends on the groundwater velocity at each location within the aquifer, can be solved for the concentration of transported radionuclides. Accurate solution of the equation requires complete knowledge of the release rates from the waste sites, the hydrodynamic dispersivity variation over the entire region, and an understanding of the interaction of chemical adsorption and precipitation processes sufficient to model both. These detailed data usually are not available, and simplifying assumptions are made in model applications. Generally, the classical transport prediction approach, which is founded on a deterministic viewpoint, provides only qualitative transport simulation, unless appropriate effective dispersion parameters have already been established from observations of a pre-existing contaminant distribution. Moreover, the random aspects of aquifer properties bring into question the validity of the classical transport equation when applied to large regions or when used to make predictions over hundreds of

years or more. Although Fickian-type transport can be used in some circumstances; its use at Hanford does not seem appropriate; it is therefore not used in this EIS.

A major current technical issue related to transport modeling is the adequate description of field-scale dispersion. Dispersion is basically the spreading of a solute in a porous medium caused by variations in water movement. Hydrodynamic dispersion as observed in laboratory-scale column experiments is only a minor component of field-scale dispersion. Laboratory column tests contain homogeneous material for the most part, whereas actual field conditions embody a myriad of different water flow paths with very large differences in transport behavior. Therefore, dispersion cannot be expressed in terms of only the mean groundwater velocity, as obtained from a groundwater flow simulation. Dispersion is also caused by local and regional variations in flow velocity (direction and magnitude) caused by the natural heterogeneity in the aquifer. A simulated velocity field that adequately represents water flow in an aquifer is generally inadequate to represent field-scale dispersion. In fact, the dispersive spreading process is associated with the unknown and uncharacterized geological variations in hydraulic conductivity. The unknown variation occurs at a spatial scale smaller than that typically used to represent groundwater flow on an aquifer scale.

There is not a clear consensus among groundwater transport experts as to how present mathematical theory should be modified to account for field-scale dispersion. Researchers do agree, however, that if it were necessary to properly represent dispersion, a considerable statistical characterization of uncertain heterogeneity would be required regardless of the particular mathematical implementation. For instance, the work by Gelhar and Axness (1983) and Jury (1982) provides divergent viewpoints on the description of field-scale dispersion. The approach suggested by Jury is easier to apply here because it calls for less conceptual information. DOE is well aware of the current technological evolution in hydrology and transport, is participating in this research, and has attempted to balance these factors in conducting predictive modeling applications for this EIS. Naturally, past data collection efforts have not been designed to accommodate unknown future technical changes.

0.4.3.2 Transport Model Applied to the Unconfined Aquifer

A conceptually simplified transport approach was devised and employed in this EIS to make maximum use of the available aquifer information and reduce subjective assignment of parameter values. The method, which is based on a stochastic formulation of transport (Simmons 1981, 1982), is incorporated in a new code called TRANSS (Simmons, Kincaid and Reisenauer 1986). The code is based on a conceptualization applied and reported previously (Harwell et al. 1982, Chap. 8), but the present code is computationally more general and efficient. A variety of associated technical issues related to application of a simplified approach are also discussed in the Harwell et al. (1982, Chap. 12) report.

Because contaminant transport primarily occurs as movement along pathlines established by groundwater flow patterns, the transport is approximated and described as a composite of one-dimensional and independent groundwater pathlines. Under steady-state flow conditions appropriate to this EIS analysis, the pathlines reduce to streamlines that are fixed in space. Streamlines determine flow tubes (streamtubes) that conduct contaminant migration away from the source. A simple description of the contaminant fluxes leaving a source and

arriving at a specified environmental entry region is the simulation objective of this code. The assumption made of a 5-m vertical mixing zone in the unconfined aquifer defines the quantity of water transmitting the contaminant.

Travel times along the various pathlines determine the rate of solute mass transfer through a particular hydrologic system. The transport simulation consists of a summation of contaminant mass migration along a sampled subset of all possible streamlines leading from the waste sources to an environmental entry (e.g., a groundwater well or river boundary). Travel times are provided by an advection-only model of transport; longitudinal dispersion is ignored in determining the travel time and transverse mixing is also neglected because water does not cross pathlines. The advection-only model of transport is a deterministic approximation to groundwater transport, and it is frequently used as a first approximation when data are insufficient for the calibration of an advection-diffusion model.

0.4.3.3 Mathematical Model of Transport

The transport model contained in the TRANSS code is based on stochastic-convective theory of transport and relates dispersion directly to the variation observed in travel time from a source. Convective (i.e., advective) transport is governed by the following equation:

$$\frac{\partial \rho}{\partial t} + V_p \frac{\partial \rho}{\partial x} = -\lambda \rho \quad (0.25)$$

where $\rho = R\theta C$ = total concentration per bulk porous medium volume

R = retardation factor = $1 + \beta K_d/\theta_s$

θ_s = saturated moisture content in R

θ = moisture content

C = concentration in solution

β = bulk soil density

K_d = distribution coefficient

V = retarded pore-water velocity

λ = decay constant

x = spatial coordinate

t = time.

Convective flux is defined as:

$$J = qC = V_p \quad (0.26)$$

where q = Darcy velocity and $V = q/\theta R = v/R$ (v = pore-water velocity = q/θ).

Equation (0.25) can be rewritten as:

$$\frac{\partial}{\partial t} U + V \frac{\partial}{\partial x} U = 0 \quad (0.27)$$

where $U(x,t) = e^{\lambda t} J(x,t)$ and the flow field is steady state. The retarded pore-water and other associated velocities are only spatially dependent and not time dependent; i.e., $V = V(x)$. Travel time for any solute is defined by:

$$T(x) = \int_0^x \frac{dx}{V(x)} = R \int_0^x \frac{dx}{v(x)} \quad (0.28)$$

The initial condition is zero everywhere; i.e., $J(x,0) = 0$. The upstream boundary condition is given by:

$$U(0,t) = e^{\lambda t} J_0(t), \quad t \geq 0 \quad (0.29)$$

where the time-dependent behavior of the source is defined by $J_0(t)$.

Solution of Equation (0.27) satisfying the initial and boundary conditions is:

$$\begin{aligned} U(x,t)e^{-\lambda t} &= J(x,t) = e^{-\lambda t} e^{[\lambda t - T(x)]} J_0[\lambda t - T(x)] \\ &= e^{-T(x)\lambda} J_0[t-T(x)] \end{aligned} \quad (0.30)$$

If one parameterizes the source release in terms of a fraction-remaining function, then

$$J_0(t) = -\frac{dr}{dt} n(t) \quad (0.31)$$

where $r(t)$ = fraction-remaining function

$n(t)$ = total inventory remaining at time t = $N e^{-\lambda t}$

N = total original inventory at $t = 0$.

If $f(t) = -dr/dt$, Equation (0.30) can be rewritten as:

$$J(x,t) = N e^{-\lambda t} f[t-T(x)] \quad (0.32)$$

The expectation (i.e., mean) flux is given by:

$$\bar{J}(x,t) = N e^{-\lambda t} \int_0^\infty f(t-\gamma) P(\gamma;x) d\gamma \quad (0.33)$$

where t is the travel time and $P(\gamma;x)$ is the probability density function (pdf) of the retarded travel time for random $T(x)$.

Solutions to the advection-diffusion transport equation; i.e., $A(x,t)$, determine some particular pdf for the stochastic-convective method:

$$P(t;x) = \frac{d}{dt} A(x,t) \quad (0.34)$$

Such a pdf is related to Fickian transport where

$$\bar{C}(x,t) = C_0 [A(x,t) - A(x,t-t^*)] \quad (0.35)$$

is a solution of the advection-diffusion equation

$$R \frac{\partial C}{\partial t} + v \frac{\partial C}{\partial x} = D \frac{\partial^2 C}{\partial x^2} \quad (0.36)$$

The mean pore-water velocity, \bar{v} , and the diffusion-type dispersion coefficient, D , are assumed to be constants. The pdf can be defined for either concentration or mass flux upstream boundary conditions which define C_0 for all time: $0 \leq t \leq t^*$.

0.4.3.4 Limitations of the Transport Model

The component one-dimensional systems or flow tubes are termed independent because contaminant transfer that would occur between or among them in actuality is neglected. Hydrodynamic dispersion, which always occurs naturally in an aquifer, causes the transfer of contaminants between the ideal streamtubes of water flow. That transfer process is called transverse dispersion and ultimately produces spreading and dilution of contaminant concentration. Incorporation of a transverse dispersion description into a transport analysis considerably complicates calculations. Moreover, the use of an inappropriate transverse dispersion coefficient in conjunction with a complex aquifer hydrology can lead to erroneous dispersal projections. On the other hand, neglect of transverse dispersion usually results in higher concentration estimates, which tend toward a conservative evaluation of potential environmental impact. Earliest arrival times may not always be accurate when transverse dispersion is neglected; transverse transfer between streamtubes may in some cases shorten the actual contaminant migration travel time by transferring contamination to a streamtube conducting water at a faster rate or over a shorter path. However, arrival times for the originating streamtube will be conservative because of the retention of contaminant resulting in higher concentration gradients and greater dispersion about the solute front. Note, however, that uncertainty in the saturated aquifer transport pathway may be overshadowed by the time required to release contaminant from a barriered zone by diffusion.

Transverse dispersion effects were not included in the present transport analysis because of lack of aquifer information. However, this does not mean that the influence is permanently excluded from the model. The model could represent field-scale dispersion, provided proper aquifer information was available; a sampled subset of particle pathlines as influenced by local transverse dispersion could be used in place of fixed streamlines. For instance, an ensemble of streamlines associated with various possible arrangements of aquifer hydrology could also be employed to represent field-scale dispersion. Such an ensemble could be generated with repeated simulations of groundwater flow patterns associated with hydraulic conductivity spatial variation. This latter approach would represent dispersion as a collection of uncertain contaminant distributions. Such an approach is being proposed as a future activity under the Hanford Waste Management Plan (DOE 1984b). While present aquifer characterization (i.e., data) does permit such a complicated conceptual model, the necessary computational software is not presently available for application to the Hanford Site.

0.4.3.5 Features of the TRANSS Transport Code

The transport code (TRANSS) (Simmons, Kincaid and Reisenauer 1986) devised for this study includes the following features:

- a probability-weighted summation of fluxes (or concentrations), propagated with constant velocity determined by the travel time and length of the hydrologic streamlines, which represents longitudinal dispersion in the saturated zone
- representation of the one-dimensional transport along each streamline, for each velocity value in the velocity distribution, by an analytical solution of the convective-dispersive equation
- simultaneous exponential radioactive decay of contaminant in both waste source and groundwater system (decay based on radioactive half-life)
- retardation of contaminant migration based on a fixed equilibrium sorption description (K_d) for each nuclide (i.e., constant flow velocity retardation factor)
- a general empirical description of contaminant release or a selection from three optional release models: 1) a constant fractional release rate; 2) a solubility concentration limited release; 3) an adsorption equilibrium limited release.

The various radionuclide source release models and scenarios are described in detail in Appendix P.

0.4.3.6 Application to the Hanford Site

Radionuclide transport simulations were accomplished by summing the fluxes over a continuous distribution of flow tubes. The original sample distribution of streamlines was expressed as an equally weighted probability for each travel time (i.e., equal fractions of released contaminant were distributed to each pathway). Travel times were calculated as the total time required to traverse streamlines passing through both the unsaturated zone and groundwater aquifer. Variation in travel times thus represented aquifer-scale dispersion for an assumed hydrologic description simulated with the VTT model. An analytical solution of the advective-diffusion equation described migration along each streamline. A constant dispersion coefficient based on dispersion through the unsaturated zone was applied to the entire system. The dispersion coefficient for the unsaturated zone was assumed to be a constant $0.82 \text{ m}^2/\text{day}$ based on a 64-m depth. The method used to estimate travel time in the unsaturated zone is presented in the preceding subsection describing the unit hydraulic gradient model.

Retardation factors and half-life for each radionuclide modeled are reported in Appendix P. A constant retardation factor was assumed for transport pathways in the vadose zone and aquifer. That is, the retardation factor, R, rather than the distribution coefficient, K_d , is assumed independent of moisture content. When data are limited to single values, the K_d may also be taken to be single-valued and independent of moisture content; however, the moisture content should be fixed at a conservative value in these cases. In this EIS, an attempt was made to be certain that adsorption data were derived from experiments performed

at concentrations below any known solubility constraints, and the authors' professional judgment is that the K_d values represent the best available data and are not biased high. In addition, every effort has been made in the EIS to employ solubility data applicable to Hanford. For example, the nitrate solubility used in the source models (see Appendix P) is representative of Hanford wastes (Barney 1976). Similarly, the solubilities reported by Delegard and Gallagher (1983) probably overestimate solubility because the solutions neglect long-term effects of organic degradation in the presence of radioactivity and rate-dependent precipitation. While interest lies with equilibrium (soil) solution concentrations of these wastes, the available data often relate to waste solutions stored in tanks. Thus, dilute tank waste characteristics are used to conservatively represent equilibrium solution concentrations.

0.4.4 Geochemical Interactions--Retardation

The geochemical model that is currently incorporated into transport codes used to assess radionuclide movement beneath the Hanford Site is limited to the linear distribution coefficient, K_d , model. The K_d model yields the familiar retardation factor expression:

$$R = 1 + \frac{\rho_b}{\theta_s} K_d \quad \text{or} \quad (0.37)$$

$$R = 1 + \frac{\rho (1 - \theta)}{\theta_s} K_d$$

where ρ_b = bulk density of geologic media (solid + voids)

ρ = particle density of geologic media (solid only)

θ_s = saturated moisture content also known as the effective porosity of media (fractional void volume that transmits water in respect to total volume)

K_d = distribution coefficient, also defined as a distribution ratio, R_d

R = retardation factor = velocity of the groundwater divided by the velocity of the center of mass of the retarded constituent.

Because of a desire to provide a conservative estimate of solute mobility in the vadose zone, an effective porosity value has been selected in calculating the retardation factor applicable to unsaturated sediments. Note that if one were to employ the low moisture contents of Hanford sediments in Equation (0.37), one would obtain large retardation factors relative to the saturated value. By using a single value of distribution coefficient (i.e., independent of moisture content) and by assuming a saturated effective porosity in the definition of retardation factor (Equation 0.37), one obtains a minimal and therefore conservative value of retardation factor to apply to transport in the vadose zone. This modification to the linear sorption isotherm can also be couched in terms of the reduced number of sorption sites available in an unsaturated porous medium.

The distribution coefficient is a function of the solution and the solid among other things. Thus, one expects the K_d to vary as the contaminant moves through the subsurface and

contacts media having different and distinct mineral and surface characteristics. However, data are rarely available on the host of media containing and underlying a waste disposal site. Where data exist for radionuclides and soils at Hanford, the lower and therefore most conservative value has been selected and applied to the transport pathway. One exception to this involves the use of a low K_d based on highly concentrated waste near the source and a higher K_d based on lower waste concentration away from the source. This was done for the cases involving release from waste contained in salt cake and sludge stored in single-shell tanks protected by a barrier. The result should be a more realistic and conservative analysis. All other cases including grout, TRU, and liquid waste forms employ a single-valued linear sorption isotherm model for retardation and represent a higher conservative approach.

The term K_d implies a linear relationship exists between the amount of radionuclide adsorbed per gram of adsorbent and the amount of radionuclide that remains in solution, i.e.,

$$K_d = \frac{A_{\text{solid}}}{A_{\text{solution}}} \quad (0.38)$$

where A_{solid} = amount bound to solid (typically counts/g, moles/g, etc.)

A_{solution} = amount left in solution (typically counts/mL, moles/mL, etc.).

The distribution coefficient thus has units of mL/g or more generally volume per unit mass.

For correct usage of K_d in Equation (0.37), the nuclide must be at equilibrium at all times and places over the region being analyzed. That is, if kinetic hindrances are present, the predictions based on Equation (0.37) can be in error. The retardation processes must be completely reversible so that nuclide release from the solid is not inhibited. The distribution coefficient cannot be dependent upon the radionuclide concentration present (or total mass present between solution and solid phases). This is equivalent to the linear isotherm constraint. Equation (0.37) also relies upon the assumption that the transporting fluid contacts all of the available solid surfaces. Finally, there is no provision in Equation (0.37) that explicitly accounts for variations in K_d caused by changes in groundwater composition. It is assumed that changes in K_d caused by spatial variability in mineralogy would be accounted for by using various strata with individual K_d values for each strata present in the transport model.

The following discussion compares present knowledge of how well Hanford geochemical conditions meet these assumptions and the implications from continued use of Equation (0.37) to predict nuclide retardation.

The assumption that equilibrium conditions are met is probably correct for the retardation mechanisms controlling trace concentrations of radionuclides in the Hanford sediments. Surface reactions such as ion exchange and chemisorption reach equilibrium within a few hours to a few days. Longer-term reactions, such as weathering of the Hanford sediments to produce new minerals or amorphous coatings, could change the adsorption surfaces available, thus affecting nuclide adsorption. Slow changes to the major mineralogy could alter adsorption sites, if large amounts of solution with anomalous characteristics (compared to existing

groundwater), such as tank supernatant solution, percolate through the sediments. If the waste solution volume is small relative to the overall groundwater volume, this potential long-term nonequilibrium condition would be localized and would not significantly affect regional predictive modeling exercises.

Evidence on nuclide retardation shows that most fission products, and most lanthanide and actinide radionuclides, do not desorb in a totally reversible fashion. Barney (1984) shows significant differences in desorption distribution ratios for interbed materials from Columbia River basalts. Wolfsberg et al. (1979, 1981); Vine et al. (1980), and Erdal et al. (1979) report on tuffaceous and argillitic sediments. In all cases there is significant irreversibility in the desorption of most radionuclides. It would be reasonable to expect that in the Hanford sediments all radionuclides, excepting perhaps strontium, cesium, and radium, would exhibit a degree of irreversible adsorption. The use of Equation (0.37) introduces conservatism in that it overestimates the amount of radionuclide that migrates as well as the rate of migration.

When laboratory data are available that differentiate adsorption from desorption, for example $K_{d\text{ads}} = 10 \text{ mL/g}$, $K_{d\text{des}} = 30 \text{ mL/g}$, one can use an algorithm that selects the former value when the leachate plume is contacting fresh sediment (adsorption is occurring) and selects the latter value when clean groundwater is percolating through heavily contaminated sediments (desorption is occurring). This two-valued K_d approach is a potential improvement and would account for the irreversibility often observed in laboratory studies (i.e., would make the analysis more realistic).

The assumption that radionuclide adsorption follows a linear isotherm is also often not met. However, for many systems, the measured K_d decreases as the mass of radionuclide (more correctly, the total mass of the element) in the experimental system increases; provided no solubility limits are exceeded. From a practical standpoint, many laboratory determinations of K_d are performed using higher than expected concentrations to facilitate ease in counting and higher precision. If the radionuclide exhibits a nonlinear isotherm, the K_d observed in the laboratory probably is biased low compared to the distribution coefficient one would observe at the very low concentration expected in the field. Great care must be used to assure that precipitation of an insoluble phase is not occurring, in which case the observed K_d might be biased high.

If the effects of varying the radionuclide (total element) concentration are systematically studied by isotherm experiments, one can ascertain the region of linearity or estimate the amount of nonlinearity by using the Freundlich equation:

$$X = KC^N \quad (0.39)$$

where X = amount of solute adsorbed per unit weight of solid

C = equilibrium solute solution concentration

K, N = constants.

The Freundlich isotherm is easily transformed to a linear equation by taking the logarithms of both sides of Equation (0.39)

$$\log X = \log K + N \log C \quad (0.40)$$

By plotting $\log X$ on the y-axis and $\log C$ on the x-axis, the best-fit straight line yields N as the slope and $\log K$ as the intercept. When N equals one, the Freundlich isotherm (Equation 0.39) reduces to a linear relationship, and since X/C is the ratio of the amount of solute adsorbed to the equilibrium solution concentration (the definition of K_d), the Freundlich K constant becomes equivalent to the value of the K_d . When N is less than one, the measured K_d value decreases as the equilibrium radionuclide concentration increases. The greater the absolute difference in $1-N$ the more nonlinearity in the system. By plotting laboratory nuclide adsorption data as a log-log relationship, one can also look for signs of precipitation. If precipitation starts to occur, $\log X$ will dramatically increase, and $\log C$ will remain fixed. When this occurs the calculated K_d value is biased high because it includes precipitation as well as adsorption processes.

Equation (0.37) assumes a porous medium where the solution can contact all the solid surfaces. This condition is met for the glaciofluvial sediments of the unconfined aquifer overlying the Hanford basalts. In the vadose zone (partially saturated zone), Equation (0.37) must be corrected to reflect those soil sites that may not see liquid if the porosity term in the denominator has been reduced to account for unsaturated pore space. A simple assumption is to multiply the p_b/θ_{unsat} term by the fractional saturation value (i.e., 25% saturation = 0.25 p_b/θ_{unsat}). This is equivalent to leaving the expression p_b/θ_s intact in both unsaturated and saturated zone simulations.

When the solution contacting the sediments changes dramatically with time, as when a tank solution leaks for a short time and mixes with extant groundwater, the K_d value for a given radionuclide and sediment type will also typically change.

Parameters such as the amount and types of ions in the groundwater (especially competing ions and complex-forming ligands), pH, Eh, temperature, and laboratory experimental procedures (e.g., solid/liquid separation techniques and contact times) can effect the distribution coefficient. Systematic empirical laboratory studies have often been performed to investigate the effects of many of these variables on the adsorption of radionuclides on soils, sediments, or rocks. The most common approach is to systematically vary one or more parameter and measure the resultant distribution coefficient; then using available statistical analyses schemes, a predictor relationship is developed. Factorial design strategies are often invoked to define a system for varying the independent variables and to determine their effect upon the dependent variable(s) (typically the distribution coefficient). Commonly used statistical methods to derive quantitative predictor equations include standard linear or nonlinear regression, stepwise regression and adaptive learning networks.

The empirical predictor equations commonly take the form of a nonlinear multinomial expression such as:

$$K_d(Sr) = a(Ca^{2+}) + b(Na^+) + c(K^+) + d(Ca^{2+})(Na^+) + e(Ca^{2+})(K^+) + f(Na^+)(K^+) + g(Ca^{2+})(Na^+)(K^+) + \dots \quad (0.41)$$

where a , b , . . . h are regression coefficients and (Ca^{2+}) , (Na^+) and (K^+) are solution concentrations (M) of competing macro cations or complexing ligands. In this example, the independent variables were (Ca^{2+}) , (Na^+) and (K^+) and the dependent variable was the distribution coefficient for strontium. Squared terms such as $(Ca^{2+})^2$ or $(K^+)^2$ do not significantly increase the predictor equations goodness-of-fit for the data and thus these quadratic terms are often omitted. For other empirical models, other powered terms may be useful.

These techniques have been used successfully to develop empirical relationships that describe the distribution coefficient in terms of other variables. Selected examples relevant to Hanford include Routson et al. (1981), Delegard and Barney (1983), Routson and Serne (1972) and Serne et al. (1973).

Although the empirical relationships generated from these types of statistical analyses are more powerful than knowledge of individual distribution coefficients, they should not be used to predict K_d values for conditions beyond the range studied. Further, the statistical relationships delineate only the apparent effects that the chosen independent variables have on the distribution coefficients but do not identify conclusively the cause or process controlling the adsorption process. That is, statistical analysis may suggest a very strong relationship between one variable, for instance pH, and the distribution coefficient when the actual adsorption process is controlled by hydrous iron oxide scavenging. As iron oxide stability is a function of pH, there could be a statistical relationship calculated that suggests the adsorption is directly caused by pH. Empirical and purely statistical approaches are useful in assessing radionuclide adsorption tendencies, but they do not lead to a general understanding of the physicochemical processes controlling the interactions among rocks, groundwaters, and radionuclides. Several investigators have voiced concern over the use of empirical distribution coefficients and by inference, the statistical procedures (Moody 1981; Reardon 1981; Coles and Ramspott 1982). Therefore, more rigorous mechanistic studies that rely upon thermodynamic constructs have been and currently are being used to increase our knowledge of trace constituent adsorption processes. Systematic studies to determine the effects of competing ions and pH (another way to refer to competing H^+ ions) can be related to thermodynamic models.

Given the complexity of the waste liquors and radionuclide retardation processes, the use of theoretically based adsorption models such as ideal ion exchange or surface complexation (often called triple-layer binding models), (Davis, James and Leckie 1978) was not deemed appropriate for this analysis.

One improvement would be to explicitly separate solubility constraints from adsorption in transport modeling and to consider radionuclide speciation. Currently, thermodynamic codes such as MINTEQ (Felmy et al. 1984), PHREEQUE (Parkhurst et al. 1980), or EQ3/6 (Wolery 1979) are used to predict probable solubility constraints and speciation distributions for the radionuclides. To use such codes one must input details on the chemical makeup of the waste or groundwater such as pH, Eh, and total analytical concentration of major and minor cations and anions. For elements that are present in the data base of the equilibrium geochemistry code, predictions are possible for the controlling solid phases that can fix the

element concentrations for the specified conditions and a speciation distribution of the dissolved portion (for example % of total Pu present as Pu^{4+} , PuOH^{3+} , Pu(OH)_2^{2+} , PuO_2^+ , PuO_2^{2+} , $\text{PuO}_2\text{CO}_3(\text{aq})$, etc.).

At present such solubility constraints for plutonium and americium have been incorporated into Hanford radionuclide migration predictions as a constraint on the mass or concentration leaving the waste form. That is, solubility of plutonium and americium is considered in the source term. No explicit solubility calculations are used in the chemical reaction aspects of the far-field transport analysis. The approach employed in this EIS is adequate as long as the geochemical conditions in the far field do not change in a fashion that would allow a more insoluble compound to precipitate.

There are missing thermodynamic data that directly affect the utility of geochemical codes. For example, the single-shell tank wastes are very high in dissolved solids and may contain significant concentrations of complexing agents. The former condition may exhibit significant activity (thermodynamic) corrections that, at present, no geochemical code can properly model. The complexing agents can drastically change the solubility and species distributions and, thus, K_d values. Thus it is difficult to quantify the effects of chelating agents on the transport rates of radionuclides in sediments.

To overcome problems with theoretical considerations, one can use empirical data such as those reported by Delegard and Gallagher (1983) and Delegard and Barney (1983) for Hanford high-level waste components. The former report addresses solubility of radionuclides in the presence of the range of ionic strength and organic complexants found in Hanford wastes and gives predictor relationships for radionuclide solubilities. The latter addresses adsorption of radionuclides in the presence of the range of ionic strength and organic complexants found in Hanford wastes and gives predictor relationships for radionuclide adsorption.

At present the available data base of radionuclide adsorption onto Hanford soils includes laboratory-derived K_d values for Co, Sr, Np, Pu, Am, Cs, Ru and Sb for high-level tank leak solutions [Knoll 1966, 1969; Delegard and Barney 1983; letter report R. J. Serne 1975(a)] and Sr, Zr, Tc, Ru, I, Cs, Ce, Eu, Co, Np, Pu, Am and Cm for selected sediments and solutions similar to diluted Hanford wastes and groundwaters [Ames and Rai 1978; Rhodes 1957; Benson 1960; Serne and Rai 1976; Routson et al. 1976; Sheppard et al. 1976; Hajek 1966; Routson and Serne 1972; Serne et al. 1973; Routson et al. 1978, 1980, 1981; Gee et al. 1981; R. J. Serne letter report 1979a(b)]. For many other elements, K_d values can be estimated by analogy to other similar elements (see, for example, letter reports R. J. Serne 1979a, 1979b).

Solubility constraints for the elements (and thus radionuclides) As, Cr, Ni, Se, Sr, Ag, Cd, I, Cs, Ba, Pb, U, Am, Pu and Np as well as nonradioactive species are available for

- (a) As documented in a 1975 personal communication from R. J. Serne, Pacific Northwest Laboratory, to Dr. W. H. Price, Rockwell Hanford Operations.
- (b) As documented in a personal communication dated 29 January 1979 from R. J. Serne, Pacific Northwest Laboratory (PNL), to R. Eckerlin, Department of Army, Corps of Engineers, Seattle District; as documented in a personal communication dated 2 May 1979 from R. J. Serne, Pacific Northwest Laboratory, to J. Washburn, PNL.

dilute waste and groundwaters via geochemical codes and laboratory data (Felmy et al. 1984; Rai and Serne 1977, 1978; Rai, Serne and Moore 1980; Rai, Strickert and McVay 1982; Rai et al. 1981).

The solubility data for dilute solutions are adequate for typical groundwaters but may not be representative for dilute solutions arising from Hanford defense wastes. This is because dilute solutions at Hanford may contain organic complexants and inorganic ligands not found in natural groundwater systems. Thermodynamic data for these complexants and ligands are not tabulated and may not be known. For high-level, high-salt waste solutions only empirical solubility data for Co, Sr, Np, Pu and Am exist (Delegard and Gallagher 1983) and the solubility values for Pu, as an example, may be higher than one would find if the precipitate formed in the laboratory were allowed to crystallize for several years (Rai and Ryan 1983). Therefore, when definitive solubility constraint data are not available, credit is not taken for such a retardation mechanism in the EIS.

0.5 REFERENCES

- Adams, M. R., and N. R. Wing. 1987. Protective Barrier and Warning System Development Plan. RHO-RL-PL-35-P, Rockwell Hanford Operations, Richland, Washington.
- Ames, L. L., and D. Rai. 1978. Radionuclide Interactions with Soil and Rock Media. Rep. EPA 520/6-78-007, Vol. 1, Environmental Protection Agency, Office of Radiation Programs, Las Vegas, Nevada.
- Baker, V. R. 1973. "Paleohydrology and Sedimentology of Lake Missoula Flooding in Eastern Washington." Special Paper 144, Geological Society of America, Boulder, Colorado.
- Barney, G. S. 1976. Vapor-Liquid-Solid Phase Equilibria of Radioactive Sodium Salt Wastes at Hanford. ARH-ST-133, Atlantic Richfield Hanford Company, Richland, Washington.
- Barney, G. S. 1984. "Radionuclide Sorption and Desorption Reactions with Interbed Materials from the Columbia River Basalt Formation." Geochemical Behavior of Disposed Radioactive Waste, eds. Barney, Navratil and Schultz. ACS Symposium Series 246, pp. 3-24, American Chemical Society, Washington, D.C.
- Benson, D. W. 1960. Review of Soil Chemistry Research at Hanford. HW-67201, Hanford Atomic Products Operation, Richland, Washington.
- Bjornstad, B. N. 1984. Suprabasalt Stratigraphy Within and Adjacent to the Reference Repository Location. SD-BWI-DP-039, Rockwell Hanford Operations, Richland, Washington.
- Bond, F. W., C. A. Newbill and P. J. Gutknecht. 1981. Variable Thickness Transient Groundwater Flow Model: User's Manual. EPRI-CS-2011, Electric Power Research Institute, Palo Alto, California.
- Bresler, E., B. L. McNeal and D. L. Carter. 1982. Saline and Sodic Soils, Principles-Dynamics-Modeling. Springer-Verlag, New York, pp. 85, 86.
- Bretz, J. H. 1923. "The Channeled Scablands of the Columbia Plateau." Journal of Geology 31(8):617-649.
- Brown, D. J. 1959. Subsurface Geology of the Hanford Separation Areas. HW-61780, Hanford Atomic Products Operation, Richland, Washington.
- Cearlock, D. B. 1971. A Systems Approach to Management of the Hanford Groundwater Basin. BNWL-SA-3860, Pacific Northwest Laboratory, Richland, Washington.

- Cearlock, D. B., K. L. Kipp and D. R. Friedrichs. 1975. The Transmissivity Iterative Calculation Routine--Theory and Numerical Implementation. BNWL-1706, Pacific Northwest Laboratory, Richland, Washington.
- Coles, D. G., and L. D. Ramspott. 1982. "Migration of Ruthenium-106 in a Nevada Test Site Aquifer: Discrepancy Between Field and Laboratory Results." Science 215:1235-1237.
- Davis, J. A., R. O. James and J. O. Leckie. 1978. "Surface Ionization and Complexation of the Oxide/Water Interface I. Computation of Electrical Double Layer Properties in Simple Electrolytes." J. Colloid Interface Sci. 63:480-499.
- Delegard, C. H., and G. S. Barney. 1983. Effects of Hanford High-Level Waste Components on Sorption of Cobalt, Strontium, Neptunium, Plutonium, and Americium on Hanford Sediments. RHO-RE-ST-1 P, Rockwell Hanford Operations, Richland, Washington.
- Delegard, C. H., and S. A. Gallagher. 1983. Effects of Hanford High-Level Waste Components on the Solubility of Cobalt, Strontium, Neptunium, Plutonium, and Americium on Hanford Sediments. RHO-RE-ST-3 P, Rockwell Hanford Operations, Richland, Washington.
- Department of Energy (DOE). 1984a. Draft Environmental Assessment, Reference Repository Location, Hanford Site, Washington. DOE/RW-0017, Washington, D.C.
- Department of Energy (DOE). 1986. Interim Hanford Waste Management Technology Plan. DOE/RL/01030-T4, Richland Operations Office, Richland, Washington.
- Dove, F. H., et al. 1982. AEGIS Technology Demonstration for a Nuclear Waste Repository in Basalt. PNL-3632, Pacific Northwest Laboratory, Richland, Washington, pp. 3.1-3.46.
- Erdal, B. R., R. D. Aguilar, B. P. Bayhurst, P. Q. Oliver and K. Wolfsberg. 1979. Sorption-Desorption Studies on Argillite I. Initial Studies of Strontium, Technetium, Cesium, Barium, Cerium, and Europium. LA-7455-MS, Los Alamos National Laboratory, Los Alamos, New Mexico.
- Fayer, M. J., G. W. Gee, and T. L. Jones. 1986. UNSAT-H Version 1.0: Unsaturated Flow Code Documentation and Application for the Hanford Site. PNL-5899, Pacific Northwest Laboratory, Richland, Washington.
- Felmy, A. R., D. C. Girvin and E. A. Jenne. 1984. MINETQ: A Computer Program for Calculating Aqueous Geochemical Equilibria. EPA-600/3-84-032, available as PB84-157148 from National Technical Information Service, Springfield, Virginia.
- Gee, G. W., and A. C. Campbell. 1980. Monitoring and Physical Characterization of Unsaturated Zone Transport-Laboratory Analysis. PNL-3304, Pacific Northwest Laboratory, Richland, Washington.
- Gee, G. W., A. C. Campbell, P. J. Wierenga and T. L. Jones. 1981. Unsaturated Moisture and Radionuclide Transport: Laboratory Analysis and Modeling. PNL-3616, Pacific Northwest Laboratory, Richland, Washington.
- Gelhar, L. W., and C. L. Axness. 1983. "Three-Dimensional Stochastic Analysis of Macrodispersion in Aquifers." Water Resources Research 19(1):161-180.
- Graham, M. J. 1983. Hydrogeochemical and Mathematical Analyses of Aquifer Intercommunication, Hanford Site, Washington State. Ph. D. Dissertation, Indiana University, Bloomington, Indiana.
- Hajek, B. F. 1966. Plutonium and Americium Mobility in Soils. BNWL-CC-925, Pacific Northwest Laboratory, Richland, Washington.
- Hanks, R. J., and G. L. Ashcroft. 1980. Applied Soil Physics, Soil Water and Temperature Applications. Springer-Verlag, New York, pp. 62-69 and 78-82.
- Harwell, M. A., et al. 1982. Reference Site Initial Assessment for a Salt Dome Repository. (Chapt. 8, pp. 8.1 - 8.26; Chapt. 12, pp. 12.1 - 12.77; Ref. 1-6). Vol. 1, PNL-2955 Pacific Northwest Laboratory, Richland, Washington.

- Isaacson, R. E., and D. J. Brown. 1978. "Environmental Assessment Related to Hanford Radioactive Waste Burial." RHO-SA-36, Rockwell Hanford Operations, Richland, Washington.
- Jury, W. A. 1982. "Simulation of Solute Transport Using a Transfer Function Model." Water Resources Research 18(2):363-368.
- Kipp, K. L., A. E. Reisenauer, C. R. Cole and C. A. Bryan. 1976. Variable Thickness Transient Groundwater Flow Model: Theory and Numerical Implementation. BNWL-1703, Pacific Northwest Laboratory, Richland, Washington.
- Kirkham, R. R., and G. W. Gee. 1984. "Measurements of Unsaturated Flow Below the Root Zone at an Arid Site." In Proceedings of the National Water Well Association Conference on Characterization and Monitoring of the Vadose Zone. National Water Well Association, Las Vegas, Nevada (PNL-SA-11629).
- Knoll, K. C. 1966. Reaction of High-Salt Aqueous Plus Organic Waste With Soil. BNWL-CC-313, Pacific Northwest Laboratory, Richland, Washington.
- Knoll, K. C. 1969. Reactions of Organic Wastes in Soils. BNWL-860, Pacific Northwest Laboratory, Richland, Washington.
- Last, G. V., P. G. Easley and D. J. Brown. 1976. Soil Moisture Transport During the 1974-1975 and 1975-1976 Water Years. ARH-ST-146, Atlantic Richfield Hanford Company, Richland, Washington.
- Merriam, J. C., and J. P. Buwalda. 1917. "Age of Strata Referred to the Ellensburg Formation in the White Bluffs of the Columbia River." University of California Publications, Bulletin of the Department of Geology, 10(15):255.
- Moody, J. B. 1981. Radionuclide Migration/Retardation: Research and Development Technology Status Report. ONWI-321, Office of Nuclear Waste Isolation, Columbus, Ohio.
- Muller, A. B., D. Langmuir and L. E. Duda. 1982. "The Formulation of an Integrated Physiochemical-Hydrologic Model for Predicting Waste Nuclide Retardation in Geologic Media." In Scientific Basis for Nuclear Waste Management VI, Proceedings of Materials Research Society Symposia, D. G. Brookins, ed., pp. 547-564. North Holland, New York.
- Mullineaux, D. R., R. E. Wilcox, W. F. Ebaugh, R. Fryxell and M. Rubin. 1977. "Age of the Last Major Scabland Flood of Eastern Washington as Inferred from Associated Ash Beds of Mount St. Helens Set S." Geological Society of America, Abstracts with Programs, 9(7):1105.
- Myers, C. W., et al. 1979. Geologic Studies of the Columbia Plateau: A Status Report. RHO-BWI-ST-4, Rockwell Hanford Operations, Richland, Washington.
- Narasimhan, T. N., A. F. White, and T. Tokunaga. 1986. "Groundwater Contamination From an Inactive Uranium Tailings Pile 2. Application of a Dynamic Mixing Model." Water Resources Research 22(13):1820-1834.
- Newcomb, R. C., J. R. Strand and F. J. Frank. 1972. Geology and Groundwater Characteristics of the Hanford Reservation of the U.S. Atomic Energy Commission, Washington. U.S. Geological Survey Professional Paper 717, USGS, Reston, Virginia.
- Parkhurst, D. L., D. C. Thorstenson and L. N. Plummer. 1980. PHREEQE - A Computer Program for Geochemical Calculations. Open File Report 80-96, U.S. Geological Survey, Washington, D.C.
- Price, S. M., R. B. Kasper, M. K. Additon, R. M. Smith and G. V. Last. 1979. Distribution of Plutonium and Americium Beneath the 216-Z-1A Crib: A Status Report. RHO-ST-17, Rockwell Hanford Operations, Richland, Washington.
- Rai, D., and R. J. Serne. 1977. "Plutonium Activities in Soil Solutions and the Stability and Formation of Selected Plutonium Minerals." J. Environ. Qual. 6:89-95.

Rai, D., and R. J. Serne. 1978. Solid Phases and Solution Species of Different Elements in Geologic Environments. PNL-2651, Pacific Northwest Laboratory, Richland, Washington.

Rai, D., R. J. Serne and D. A. Moore. 1980. "Solubility of Plutonium Compounds and Their Behavior in Soils." Soil Sci. Soc. Am. J. 44:490-495.

Rai, D., R. G. Strickert, D. A. Moore and R. J. Serne. 1981. "Influence of an Americium Solid Phase on Americium Concentrations in Solutions." Geochim. Cosmochim. Acta. 45:2257-2265.

Rai, D., R. G. Strickert and G. L. McVay. 1982. "Neptunium Concentrations in Solutions Contacting Actinide-Doped Glass." Nucl. Tech. 58:69-76.

Rai, D., and J. L. Ryan. 1983. "Crystallinity and Solubility of Pu(IV) Oxide and Hydrous Oxide in Aged Aqueous Suspensions." Radiochim. Acta. 30:213-216.

Reardon, E. J. 1981. "K_d's--Can They Be Used to Describe Reversible Ion Sorption Reactions in Contaminant Migration?" Ground Water 19:279-286.

Reisenauer, A. E. 1979a. Variable Thickness Transient Groundwater Flow Model: Volume 1. Formulation. PNL-3160-1, Pacific Northwest Laboratory, Richland, Washington.

Reisenauer, A. E. 1979b. Variable Thickness Transient Groundwater Flow Model: Volume 2. User's Manual. PNL-3160-2, Pacific Northwest Laboratory, Richland, Washington.

Reisenauer, A. E. 1979c. Variable Thickness Transient Groundwater Flow Model: Volume 3. Program Listings. PNL-3160-3, Pacific Northwest Laboratory, Richland, Washington.

Reisenauer, A. E., K. T. Key, T. N. Narasimhan and R. W. Nelson. 1982. TRUST: A Computer Program for Variably Saturated Flow in Multidimensional, Deformable Media. NUREG/CR-2360, Nuclear Regulatory Commission, Washington, D.C.

Rhodes, D. W. 1957. "The Effect of pH on the Uptake of Radioactive Isotopes from Solution by a Soil." Soil Sci. Soc. of Am. Proc. 21:389-392.

Richards, L. A. 1931. "Capillary Conduction of Liquids through Porous Mediums." Physics 1:318-333.

Routson, R. C., and R. J. Serne. 1972. One-Dimensional Model of the Movement of Trace Radioactive Solute Through Soil Columns: The PERCOL Model. BNWL-1718, Pacific Northwest Laboratory, Richland, Washington.

Routson, R. C., G. Jansen and A. V. Robinson. 1976. "241Am, 237Np, and 99Tc Sorption on Two United States Subsoils from Differing Weathering Intensity Areas." Health Physics 33:311-317.

Routson, R. C., G. S. Barney and R. O. Seil. 1978. Measurement of Fission Product Sorption Parameters for Hanford 200 Area Sediment Types: Progress Report. RHO-LD-73, Rockwell Hanford Operations, Richland, Washington.

Routson, R. C., W. H. Price, D. J. Brown and K. R. Fecht. 1979. High-Level Waste Leakage from the 241-ST-106 Tank at Hanford. RHO-ST-14, Rockwell Hanford Operations, Richland, Washington.

Routson, R. C., G. S. Barney and R. M. Smith. 1980. Hanford Site Sorption Studies for the Control of Radioactive Wastes: A Review. RHO-SA-155, Rev. 1, Rockwell Hanford Operations, Richland, Washington.

Routson, R. C., G. S. Barney, R. H. Smith, C. H. Delegard and L. Jensen. 1981. Fission Product Sorption Parameters for Hanford 200 Area Sediment Types. RHO-ST-35, Rockwell Hanford Operations, Richland, Washington.

Serne, R. J., R. C. Routson and D. A. Cochran. 1973. Experimental Methods for Obtaining PERCOL Model Input Verification Data. BNWL-1721, Pacific Northwest Laboratory, Richland, Washington.

- Serne, R. J., and D. Rai. 1976. "Adsorption-Precipitation Behavior of Eu in Soils and Standard Clays." Agronomy Abstracts p. 132.
- Serne, R. J., and J. F. Relyea. 1983. "The Status of Radionuclide Sorption-Desorption Studies Performed by the WRIT Program." In the Technology of High-Level Nuclear Waste Disposal, Vol. 1. DOE/TIC-621, pp. 203-254, Technical Information Center, U.S. Department of Energy, Oak Ridge, Tennessee.
- Sheppard, J. C., J. A. Kittrick and T. L. Hardt. 1976. Determination of Distribution Ratios and Diffusion Coefficients of Neptunium, Americium, and Curium in Soil-Aquatic Environments. RLO-2221-T-12-2 (WSU 76/13-33), Washington State University, Pullman, Washington.
- Silling, S. A. 1983. Final Technical Position on Documentation of Computer Codes for High-Level Waste Management. NUREG-0856, Nuclear Regulatory Commission, Washington, D.C.
- Simmons, C. S. 1981. Relationships of Dispersive Mass Transport and Stochastic Convective Flow Through Hydrologic Systems. PNL-3302, Pacific Northwest Laboratory, Richland, Washington.
- Simmons, C. S. 1982. "A Stochastic-Convective Transport Representation of Dispersion in One-Dimensional Porous Media Systems." Water Resources Research 18(4):1193-1214.
- Simmons, C. S., C. T. Kincaid, and A. E. Reisenauer. 1986. A Simplified Model for Radioactive Contaminant Transport: The TRANSS Code. PNL-6029, Pacific Northwest Laboratory, Richland, Washington.
- Swanson, D. A., T. L. Wright, P. R. Hooper and R. D. Bentley. 1979. Revisions in Stratigraphic Nomenclature of the Columbia River Basalt Group. Bulletin 1454-G, U.S. Geological Survey, Washington, D.C.
- Tallman, A. M., J. T. Lillie and D. R. Fecht. 1981. "Suprabasalt Sediments of the Cold Creek Syncline Area." In Subsurface Geology of the Cold Creek Syncline, eds. C. W. Myers and S. M. Price, RHO-BWI-ST-14, Rockwell Hanford Operations, Richland, Washington.
- Vine, E. N., et al. 1980. Sorption-Desorption Studies on Tuff II. A Continuation of Studies with Samples from Jackass Flats, Nevada and Initial Studies with Samples from Yucca Mountain, Nevada. LA-8110-MS, Los Alamos National Laboratory, Los Alamos, New Mexico.
- Walter, M. B., R. J. Serne, T. L. Jones, and S. B. McLaurine. 1986. Chemical Characterization, Leach and Adsorption Studies of Solidified Low-Level Wastes. PNL-6047, Pacific Northwest Laboratory, Richland, Washington.
- West, J. M., I. G. McKinley and N. A. Chapman. 1982. "The Effect of Microbial Activity on the Containment of Radioactive Waste in a Deep Geological Repository." In Scientific Basis for Nuclear Waste Management, Vol. V. Elsevier Press, New York.
- West, J. M., and I. G. McKinley. 1984. "The Geomicrobiology of Nuclear Waste Disposal." Mat. Res. Soc. Symp. Proc. 26.
- West, J. M., N. Christofi and I. G. McKinley. 1985. "An Overview of Recent Microbiological Research Relevant to the Geologic Disposal of Nuclear Waste." Radioactive Waste Management and the Nuclear Fuel Cycle 6(1):79-95.
- Westinghouse Hanford Company (WHC). 1987. Data Compilation: Iodine-129 in Hanford Groundwater. WHC-EP-0037, Richland, Washington.
- Wolery, T. J. 1979. Calculation of Chemical Equilibrium Between Aqueous Solution and Minerals: The EQ3/6 Software Package. UCRL-52658, Lawrence Livermore Laboratory, Livermore, California.
- Wolfsberg, K., et al. 1981. Sorption-Desorption Studies in Tuff III. A Continuation of Studies with Samples from Jackass Flats and Yucca Mountain, Nevada. LA-8747-MS, Los Alamos National Laboratory, Los Alamos, New Mexico.

APPENDIX P

RELEASE MODELS AND RADIONUCLIDE INVENTORIES FOR SUBSURFACE SOURCES

✓ LEFT BLANK
THIS PAGE INTERNATIONALLY

APPENDIX P

RELEASE MODELS AND RADIONUCLIDE INVENTORIES FOR SUBSURFACE SOURCES

This appendix includes information about the models used in this EIS to simulate the release from waste forms that might be disposed of under the Hanford 200 Areas plateau. The models used in this EIS are believed sufficient to support meaningful decisions in the context of the National Environmental Policy Act of 1969 (40 CFR 1500-1517). Where uncertainties exist, input values were chosen for model parameters so that calculations produce conservative estimates of impacts. A conservative value of a parameter tends to overestimate consequences rather than underestimate. Where reliable data provide realistic values of parameters applicable to the Hanford Site, the realistic values are used.

The rate of release from a source is important in determining the mass flux and concentration of radionuclides and chemicals in the subsurface environment. Release models depend on the character of the storage facility, the form of the waste, and the physical processes and chemical reactions that affect the waste. The level of conservatism in the release models is based on knowledge of the processes and reactions that dominate releases under assumed conditions.

In all cases a 10,000-year period of interest is simulated. Analyses are conducted for two average annual groundwater recharge scenarios: the current climate of 0.5 cm/yr and a wetter climate of 5 cm/yr. A zero recharge scenario is not calculated or discussed in any detail because it is an extremely unlikely event. Such a scenario implies that there is no moisture movement. Transport by diffusion alone will not result in release to the water table 64 m below the wastes in the time period of interest.

The range of average annual groundwater recharge from 0.5 to 5 cm/yr is viewed as the range of probable or mean values for the climate (see 0.3.2 and Vol. 2 page xxix). Under future climate conditions, the mean precipitation and hence infiltration rate are projected to lie within the presently observed extremes (Kukla 1979). The 5-cm/yr annual infiltration rate is therefore viewed as a reasonable annual average value of a continuous wetter climate.

P.1 RELEASE MODELS

Release models applied in these analyses are presented as fraction-remaining equations. These curves represent the fraction of radionuclide activity remaining in the source. Initially the fraction remaining is equal to one, and when the source is depleted its value is zero. The following source parameters are defined for each radionuclide:

N = the total initial inventory, Ci

$n(t) = N \exp^{-(\lambda t)}$ = the current total activity, regardless of location within the system,
Ci

t = time, year

λ = 0.693/half-life, year⁻¹

T = release period, year

r(t) = fraction-remaining curve, where $r(0)=1$ and $r(T)=0$

m(t) = activity remaining in source at any time, Ci

$J_0(t)$ = activity flux into the flow system, Ci/yr.

Activity remaining in the source as a function of time is defined as:

$$m(t) = r(t)n(t) \quad (P.1)$$

The rate of source depletion is written as:

$$\frac{dm}{dt} = -\lambda m - J_0 \quad (P.2)$$

The negative sign on the flux term ($-J_0$) indicates the activity flux is leaving the source.

Substitution of Equation (P.1) into Equation (P.2) gives:

$$n \frac{dr}{dt} + \frac{dn}{dt} r = -\lambda rn - J_0 \quad (P.3)$$

The total activity, n, is depleted by decay, i.e.,

$$\frac{dn}{dt} = -\lambda n \exp(-\lambda t) = -\lambda n \quad (P.4)$$

Substituting Equation (P.4) into Equation (P.3) gives:

$$n \frac{dr}{dt} = -J_0 \quad (P.5)$$

Assuming one of the following:

- the activity flux as a function of remaining source activity (i.e., retardation or desorption limit)
- the activity flux due to a constant solution concentration (i.e., solubility limit)
- the mass flux due to a constant solution concentration of a nondecaying chemical or the fraction-remaining curve (e.g., linear release)

the companion relationships that define the release rate can be developed from the above equations.

The release models presented are conceptually simple. More detailed and less conservative models will be possible when events, processes, and reactions that govern radionuclide releases from the facilities (i.e., tanks, cribs, burial sites, and grout disposal vaults) are better understood. The release models do not consider the effects of microbiological degradation of the waste form on leach rates. There have not been enough quantitative data derived to incorporate microbiological effects, although recent information indicates that this may be a factor (West et al. 1985). Technically defensible evidence of the dominant

process or processes controlling radionuclide release is essential for their use as controlling factors in long-term analyses. These conceptual models of source leaching are predicated on the objective of conservatism and technical defensibility.

P.1.1 Adsorption-Controlled Release Model

The model for adsorption-controlled release assumes infiltrating water comes into contact with the waste and then continues to carry solute vertically to the water table. Release is governed by the retardation factor and source strength of individual radionuclides in the solid phase. The flux of activity entering the soil column is given by:

$$J_0 = AqC \quad (P.6)$$

where C is the concentration of radionuclide in solution, A is the land surface area of the waste deposit, and q is the infiltration rate. The solution concentration can be rewritten as a function of total (i.e., solution and solid) concentration, δ , as follows,

$$\delta = \theta C + \beta S \quad (P.7)$$

where θ is volumetric moisture content, β is bulk soil density, and S is the solid concentration that is related to solution concentration by the distribution coefficient, K_d , of the linear sorption isotherm, i.e.,

$$S = CK_d \quad (P.8)$$

Substituting Equation (P.8) into Equation (P.7):

$$\delta = \theta C \left(1 + \frac{\beta K_d}{\theta}\right) = \theta C R_f \quad (P.9)$$

where the bracketed quantity is the retardation factor, R_f . To ensure that retardation is bounded, the moisture content, θ , in the retardation factor is held at a constant value of 0.33. This is denoted θ_r , e.g.,

$$R_f = \left(1 + \frac{\beta K_d}{\theta_r}\right) \quad (P.10)$$

This is also physically realistic because R_f does not approach infinity as θ approaches zero. Even at relatively low moisture content, R_f remains finite because sorption sites exposed to solute remain virtually constant. By employing a relatively high θ_r , one creates a finite and relatively low, hence conservative, value of retardation factor. Note that the dry extreme of the applicability of these equations is commonly taken as 15 bars of suction. Finally, concentration can be rewritten as:

$$C = \frac{\delta}{\theta R_f} \quad (P.11)$$

Substituting Equation (P.11) into Equation (P.6) yields:

$$J_0 = Aq \frac{\delta}{\theta R_f} \quad (P.12)$$

The total concentration, δ , can be rewritten in terms of the source strength, m , and the source volume given here as the product of area, A , and depth of waste deposit, h , i.e.,

$$J_0 = Aq \frac{m}{A h \theta R_f} = \frac{qm}{h \theta R_f} \quad (P.13)$$

If this expression for activity flux is substituted into Equation (P.2):

$$\frac{dm}{dt} = -\lambda m - \frac{qm}{h \theta R_f} \quad (P.14)$$

Using the initial condition that m is equal to the total initial inventory of a radionuclide, N , one obtains the following solution to Equation (P.14),

$$m = N \exp - \left(\lambda + \frac{q}{R_f \theta h} \right) t \quad (P.15)$$

The fraction-remaining equation is then defined by Equation (P.1) as:

$$r = \frac{m}{N} = \exp - \left(qt / R_f \theta h \right) \quad (P.16)$$

P.1.2 Solubility-Controlled Release Model

The model for solubility-controlled release is based on infiltrating water contacting the waste form and carrying radionuclides away from the source at their maximum solution concentration. The flux of activity entering the soil column is given as:

$$J_0 = AqC_0 \quad (P.17)$$

where C_0 is the solution concentration. Substituting this expression into Equation (P.5) and rewriting it slightly, one obtains:

$$N \exp (-\lambda t) \frac{dr}{dt} = -AqC_0 \quad (P.18)$$

Solving Equation (P.18) and using the initial value of one for fraction remaining, i.e., $r(0) = 1$, gives the following fraction-remaining equation:

$$r = 1 + \frac{AqC_0}{N\lambda} (1 - \exp \lambda t) \quad (P.19)$$

By solving for the time associated with $r(t) = 0$, the release period for this model is defined as:

$$T = \frac{1}{\lambda} \log_e \frac{N\lambda + AqC_0}{AqC_0} \quad (P.20)$$

This model of a decaying source can also be applied to simulate cases where the flux, J_0 , is specified by replacing AqC_0 with J_0 in Equations (P.19) and (P.20).

P.1.3 Linear Release or Dissolution-Controlled Release Model

A linear release function can be applied as a piecewise continuous approximation to any release function. In addition to this general utility, the linear release function is a model for a dissolution-controlled release of a nondecaying chemical. Such a dissolution release is assumed to be caused by infiltrating water directly contacting a waste form and becoming saturated with the dissolving chemicals or radionuclides. The dominant chemical component of the solid governing the dissolution process could be nitrate salt. If radionuclides are uniformly mixed in the soluble solid, one can assume that a congruent release of radionuclides occurs as the salt is dissolved and transported away from the source. A simple linear fraction-remaining expression is defined to represent the release of nitrate salt, i.e.,

$$r(t) = (T - t)/T \quad (P.21)$$

where T is the known release period based on the mass of salt to be dissolved, the rate of water infiltration, and the surface area of the waste intercepting infiltration. While the mass flux of salt is constant, the activity flux of a radionuclide is depleted by decay. Thus the activity flux entering the soil column is given by:

$$J_0 = \left(\frac{N}{T}\right) \exp(-\lambda t) \quad (P.22)$$

This model of radionuclide release differs from the solubility model (Equation P.19) because control of the release is assumed to lie in the solution concentration of a nondecaying chemical species.

P.1.4 Diffusion-Controlled Release Beneath a Protective Barrier

The analysis of release from beneath the protective barrier (Appendices M and O) is predicated on the authors' professional judgment that the barrier will eliminate advection as a viable or dominant mechanism for the transport of radionuclides and chemicals in the soils beneath the barrier. A sketch of the conceptual model for release from beneath a barrier is shown in Figure P.1. Principal assumptions are as follows:

- Pathways of release have two segments dominated by two distinctly different transport processes--diffusion beneath the barrier and advection adjacent to the barrier.

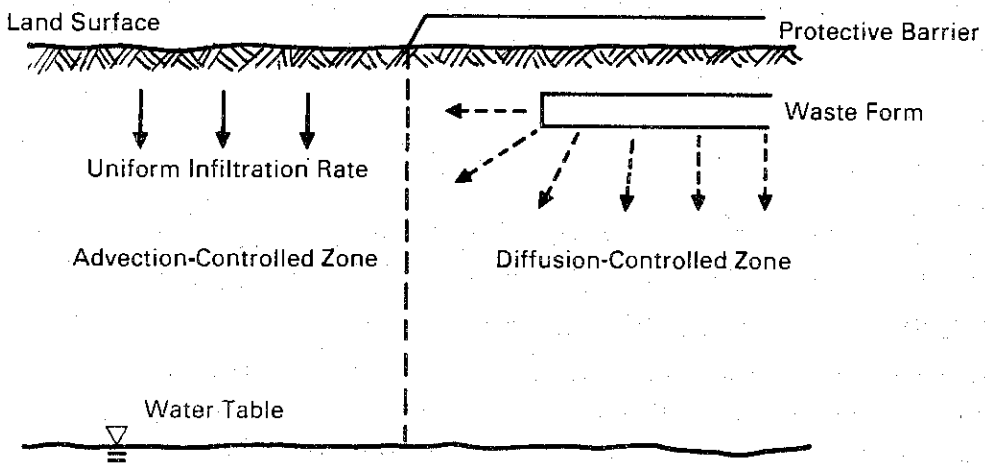


FIGURE P.1. Conceptual Model for Release from Beneath a Barrier

- The waste forms in either vaults or tanks can be idealized as rectangular solids (i.e., containing several vaults or tanks) with a square upper surface and a uniform thickness.
- Minimum distance to a pathway dominated by advective forces (i.e., distance to the edge of the barrier) is 10 m.
- Vertical distance from the bottom of the waste form to the water table is a uniform 64 m.
- Moisture content in the soil column is everywhere constant. For the 0.5- and 5-cm/yr infiltration rates the moisture contents are 6.4 and 7.8%, respectively. These values are based on saturated hydraulic conductivity and the relative permeability versus saturation curve of a soil representing the soil profile beneath the 200 East Area plateau. The relationship between infiltration and moisture content is described in the unit hydraulic gradient model subsection of Appendix 0.
- Transport in the diffusion-controlled zone can be modeled to provide relative solutions for comparison of the various alternatives by employing 1) one-dimensional pathway discretizations and 2) a linear concentration profile over the length of the diffusion-controlled pathway.
- Distribution coefficients for retarded radionuclides and chemicals are different in the two pathways. Solute concentrations in the advective zone will be more dilute than in the diffusion zone; therefore, where data are available for single-shell tank wastes, distinct distribution coefficient values are assigned to the two pathways.

- Transient effects of moisture drainage from groundwater mounds created by the disposal of water during plant operation are neglected. This assumption is based on 1) our knowledge that existing and future waste disposal operations are located away from water disposal operations and 2) an assumption that water disposal does not affect moisture content in soils underlying waste disposal sites.
- Prior releases of contamination (e.g., tank leaks, crib disposals) are not included in these simulations because most are not categorized as high-level or transuranic (TRU) wastes and those that are high-level or TRU wastes are of negligible quantity compared with the inventory studied.

The objective in defining the release from a barrier-covered source is to provide a source term for the transport model. This transport model could simulate transport in the vadose and saturated zones or only in the saturated zone. In the latter case, applied here to barrier-covered waste, the waste and vadose zone are included in the source model. Thus the source model provides a release to the water table of the unconfined aquifer. There are three distinct calculations made to achieve an arrival time and activity flux distribution at the water table. These calculation steps provide an estimate of 1) a period of negligible release, 2) a diffusion-controlled pathway flux, and 3) the advection pathway travel time. The mathematical models for these calculations are given in subsections on the diffusion-controlled release model and the unit hydraulic gradient model found in Appendix O.

Release to the water table from the diffusion-controlled source is cumulative. Each pathway from the waste form has associated with it a fraction of the waste volume and its surface area. For the cases of interest to the Hanford defense waste scenario being considered, each pathway has a diffusion segment between 10 and 64 m long and an advection segment between 64 and 0 m long. The release is given by the release from the diffusion pathway; however, the time of arrival at the water table is the cumulative time of transport through the diffusive and advective pathways. First arrival for each pathway to the water table is the time of diffusive pathway breakthrough plus the advective travel time. Final arrival time is the sum of breakthrough time, release duration, and advective travel time. The flux of solute is integrated for all pathways arriving at the water table to provide a cumulative flux released to the unconfined aquifer. In summary, the source release model takes radionuclides released from the source, transports them through the vadose zone by both diffusive and advective transport pathways, and accumulates the release to provide a fraction-remaining curve for application to the unconfined aquifer.

Release from wastes stored beneath the protective barrier is governed by the solution concentration of nitrate at the waste form and the ability of the diffusion-controlled pathway to conduct mass to advection-controlled pathways (e.g., beyond the barrier edge or in the saturated aquifer). A congruent release of radionuclides and other chemicals is assumed.

Two cases are developed in Appendix O for release via the diffusion-controlled pathway to the water table. Recall that the release is accumulated from all diffusion and advection pathways to provide an overall release model directly interfacing with the streamtube transport model of the unconfined aquifer. In the first case, release from the source continues

after first release to the advection-dominated zone. Thus, contaminant mass in the source exceeds the amount of contaminant that can be stored in the soil profile as a result of steady-state transport. In the second case, the source is exhausted before contamination fills the steady-state profile. In each case, transport in the diffusion-controlled zone is modeled with a linear concentration profile. Once contamination reaches an advection-controlled pathway it is assumed the contamination is swept away and a zero concentration exists indefinitely at the exit from the diffusion-controlled pathway.

Defining M_0 as the mass available for release and M^* as the storage available in the vadose zone soil profile, the first case is based on the assumption that source mass or activity is sufficient to fill the soil profile before it is depleted, i.e.,

$$M_0 > M^* \quad (P.23)$$

where $M_0 = \rho_0 Ah$ = total mass of contamination initially in the pathway source

ρ_0 = initial source density

A = bottom surface area or cross section of the pathway source

h = thickness of the source deposit

and

$M^* = \rho^* Ah = A R_f \theta C_0 L / 2$ = total mass of contamination possible in soil profile
assuming a linear concentration profile

$\rho^* = \text{critical source density} = \frac{R_f \theta C_0}{2} \frac{L}{h}$

R_f = retardation factor

θ = volumetric moisture content

C_0 = solution concentration at source/soil interface

L = length of diffusion-controlled pathway.

For this case the release has three stages characterized by 1) no release, 2) steady-state release, and 3) exponentially decreasing release. These were developed in Appendix 0 as:

$$J_L = \begin{cases} 0 & , t < T_0 \\ \theta A D C_0 / L & , T_0 \leq t < t_0 \\ \frac{\theta A D C_0}{L} \exp [-\beta (t - t_0)] & , t > t_0 \end{cases} \quad (P.24)$$

where D = molecular diffusion coefficient corrected for application to unsaturated media

$$\beta = \frac{2D}{R_f L^2}$$

$$t_0 = \frac{R_f L^2}{4D} + \frac{Lh}{\theta D C_0} (\rho_0 - \rho^*) = \text{time of source depletion}$$

$$T_0 = \frac{R_f L^2}{4D} = \text{time of first release to an advection-controlled pathway.}$$

The fraction-remaining curve for this release at the end of the diffusion-controlled pathway, which is the source equation for the advection-controlled pathway, is given by:

$$r_L(t) = \begin{cases} 1 & , t < T_0 \\ 1 - (t - T_0)/T^* & , T_0 \leq t \leq t_0 \\ 1 - \{\beta^{-1}[1-e^{-\beta(t-t_0)}] + t_0 - T_0\}/T^* & , t > t_0 \end{cases} \quad (P.25)$$

where $T^* = \beta^{-1} + t_0 - T_0$.

A simplified approach utilizing the nondecaying chemical release model has been applied to the radionuclide release problem. The first release and source depletion time relationships are taken from the chemical model. Because of this, releases are predicted to occur earlier and last longer than they actually will occur. The chemical model is applied by specifying the source/soil interface concentration of the radionuclide. Flux of the radionuclide to an advection-controlled pathway is approximated by decaying the release predicted by the chemical release model. Essentially, the chemical release model is used to create a fraction-remaining curve. The fraction-remaining curve is then used to release a radionuclide of the same source/soil interface concentration by simply correcting the release curve for decay.

Release in the second case occurs when the source mass is less than the mass that can be stored in the soil during transport, i.e.,

$$M_0 < M^* \quad (P.26)$$

and first release to an advection-controlled pathway occurs after time T_0 where T_0 satisfies:

$$\frac{L}{x_0} - \log_e \left(\frac{L}{x_0} \right) - 1 = \alpha (T_0 - t_0) \quad (P.27)$$

and

$$x_0 = \sqrt{4Dt_0/R_f}$$

$$\alpha = D/R_f x_0^2 = 1/4t_0$$

$$t_0 = \left(\frac{p_0 h}{\theta C_0} \right)^2 / R_f D = \text{time of source depletion.}$$

Explicitly, T_0 is given by:

$$T_0 = t_0 + 4t_0 \left(\frac{L}{x_0} \right) - \log_e \left(\frac{L}{x_0} \right) - 1 \quad (P.28)$$

The release appears two-staged for the second case; a zero release period and an exponentially decreasing release over all time, i.e.,

$$J_L = \begin{cases} 0 & , t < T_0 \\ \left(\frac{x_0}{L}\right) J_0 \exp [-\beta(t-T_0)] & , t > T_0 \end{cases} \quad (P.29)$$

where $J_0 = \theta A D C_0 / L$. The fraction-remaining curve for release in the second case is given by:

$$r_L(t) = \begin{cases} 1 & , t < T_0 \\ \exp[-\beta(t-T_0)] & , t > T_0 \end{cases} \quad (P.30)$$

As in the case of the three-stage release for radionuclides, the two-stage release for radionuclides is approximated with the chemical release model corrected for decay.

For those diffusion-controlled pathways that are intercepted by advection-controlled pathways in the vadose zone, a time delay is applied to the diffusive mass flux to account for travel time to the water table. Retarded pore-water velocity in the vadose zone is given by:

$$v = q/\theta R_f \quad (P.31)$$

where v = retarded velocity

q = Darcy velocity (infiltration rate)

θ = volumetric moisture content

R_f = retardation factor.

Delay time for travel through the advection pathway is given by:

$$t^* = Z(L)/v \quad (P.32)$$

where $Z(L)$ is the length of the advection pathway. The fraction-remaining curve for either case is now defined by r_L^* , where translation of the time variable relates r_L^* to r_L , i.e.,

$$r_L^*(t) = r_L(t - t^*) \quad (P.33)$$

P.2 RELEASE MODELS FOR SPECIFIC WASTE FORMS

The release models described in the previous section are used to model the release of radionuclides and chemicals from four specific waste forms: salt and sludge, liquid in tanks, grout, and all TRU wastes. In most cases there are two models for the various waste forms according to presence or absence of a protective barrier above the waste site. The model parameters used are described for each waste form and barrier option in the release model descriptions that follow and in summary tables at the conclusion of this appendix. The models applied to specific waste forms under barrier or no-barrier options are summarized in Table P.1. Note that the adsorption, solubility and linear release models apply to the

TABLE P.1. Summary of Release Models Applied to Waste Forms

Barrier	Salt Cake and Sludge in Single-Shell Tanks	Liquid in Double-Shell Tanks	Grout in Vaults	TRU
No barrier or direct leaching under functional or disruptive barrier failure scenarios	Solubility Model for radionuclides and Linear Release Model for chemicals	Adsorption Model	Linear Release Model for nitrate and congruent release of radionuclides	Adsorption and Solubility Models
Barrier intact and 100% effective	Diffusion-Controlled Model with nondecaying source for chemicals and radionuclide release simulated by decaying the flux to advection-controlled zone.	Diffusion-Controlled Model with decaying source	Diffusion-Controlled Model with nondecaying source for nitrate and congruent release of radionuclides	Not analyzed

direct leaching scenarios when a barrier is not present, or when functional or disruptive failures have occurred to an established barrier. The diffusion-controlled model applies to cases where the barrier is intact and virtually 100% effective.

The migration and fate of leachate from the strontium and cesium capsules are not modeled in this EIS because such a release will probably not occur before a significant period of time (i.e., 700 to 1,000 years). Drywells have been selected as the disposal facility for these capsules. The spacing of drywells in the soil environment is a determining factor in the temperature within the drywell and in its surrounding soils. For example, a drywell spacing of 5.2 m (17 ft) for the storage of fuel rods has been shown to yield a peak canister temperature of 335°C (635°F), an encasement wall temperature of 332°C (630°F), and a cladding temperature of 357°C (675°F) (Rockwell Hanford Operations and Kaiser Engineers 1979). For strontium and cesium capsules a somewhat different spacing may be required based on the heat generated by the capsules. An ongoing study into the integrity of CsCl capsules reports that capsule storage at less than 450°C is recommended and that storage at <150°C could provide isolation from the soil environment for long periods of time (Bryan and Divine 1985). Thus spacing can be selected to achieve a capsule storage temperature that permits continued safe storage of the strontium and cesium capsules.

P.2.1 Salt Cake and Sludge in Single-Shell Tanks

At present the single-shell tanks at Hanford contain a minimum of waste in liquid form due to the jet pumping program that has placed liquid wastes in double-shell tanks. Most of the remaining inventory is contained in the salt cake and sludge deposit left in the tanks after pumping is complete (Rockwell 1985). It is known that several tanks have leaked; indeed, the leaks prompted the current policy of storing liquid waste in double-shell tanks. However, once liquid is removed from a leaking tank, direct liquid discharge from the tank becomes negligible as a long-term release mechanism and other mechanisms dominate the source-release phenomenon for the solid waste. The release of chemicals and radionuclides in the

salt cake and sludge will occur as a result of these other mechanisms. The operative mechanisms for future releases from single-shell tanks are assumed to be dissolution and leakage, caused by either infiltrating water or water introduced to tanks via vapor diffusion. The infiltration and vapor diffusion mechanisms provide water for the two cases, i.e., absence or presence of a protective barrier.

Note that when a protective barrier is in place and diffusion is the operative transport mechanism, release from the source can be a result of dissolution and leakage to the soil caused by water supplied by vapor diffusion or be a result of a simple diffusive release from the source to the soil. Vapor diffusion is advanced here only as a mechanism that could yield a greater release than molecular diffusion. Either mechanism would supply contaminant to the diffusion-controlled pathway that transports contaminant from beneath the protective barrier.

Liquid release due to a tank leak can be very rapid after only a minor disruption of the tank surface, e.g., a weld failure only a few feet long. However, both infiltrating water and vapor diffusion differ from liquid release because they depend heavily on a significant surface area of the tank being available for uninhibited moisture movement into the tank. This implies a major disruption or degradation of the outer concrete shell and inner steel liner of each tank. Using the most severe corrosion rate determined by laboratory work to apply to the tanks (6 mil/yr) and the liner thickness (3/8 in.), one can estimate the onset of functional failure of the steel liner in 60 years (DeFigh-Price 1982). The operational life of a single-shell tank to the point at which water could freely enter and leave the tank could be several hundred years. However, in the absence of data demonstrating longer operational life, the single-shell tanks are assumed to offer no resistance to water movement in the year 2150, the same time that institutional control is assumed to be lost. This implies that concrete or steel remaining at that time would no longer present any barrier to movement of moisture. Because of the semiarid climate and soils at Hanford, this is highly unlikely and therefore a conservative assumption.

In the first scenario (i.e., barrier absent), infiltrating water is assumed to contact the radionuclides and chemicals and carry them away at constant solution concentrations. Chemicals are released at their own solution concentrations (see Appendix U). Release depends on the ability of moisture to freely enter and leave the tank. Again, because of the tank structure, the expectation of unimpeded movement of moisture is unlikely for several centuries even though limited leaching associated with a tank surface disruption could occur before the year 2150. The independent release of radionuclides represents a conservative release. Radionuclide concentrations are based on the maximum solution concentrations as reported in Schulz (1980). Use of maximum solution concentrations to model all radionuclide and chemical constituents of the salt cake and sludge results in a preferential leach process that exhausts individual constituents independently of other constituents.

The second scenario assumes negligible moisture movement near the tanks due to the placement of a protective barrier at the land surface. Release is assumed to occur when soil moisture is drawn into the tank by the vapor-diffusion mechanism, vapor condenses, salt cake

dissolves, and a slow release of liquid delivers contaminated liquid to the soil surrounding the tank. The barrier is designed to prevent any net water infiltration and to inhibit intrusion by vegetation, wildlife, or humans (see Appendix M). Thus moisture movement around the tank is assumed negligible. While net downward moisture movement is assumed negligible, soil moisture in the unsaturated soil would provide a pathway for the conduction of solute by the molecular diffusion process resulting from the concentration gradient. Near the barrier edge, annual net moisture infiltration becomes the dominant transport mechanism and slowly conducts contamination through the unsaturated zone to the water table of the unconfined aquifer. Certainly part of the waste is released directly to the water table after traversing the vadose zone via the molecular diffusion mechanism.

P.2.1.1 Direct Leach Scenario--Infiltration

Where no protective barrier is placed above the waste, the direct leach scenario postulates direct contact by infiltrating water, dissolution of the radionuclides and chemicals and movement of the solution downward to the water table. The individual radionuclides and chemicals would be carried away at solution concentrations shown in Table P.2. Pertinent data for the non-barrier cases of salt cake and sludge leaching are summarized in Table P.2 for the 200 East and 200 West Areas. Leach periods for the different infiltration rates are shown in the table for each of the radionuclides and chemicals. The solubility release model is applied to radionuclide releases, and the linear release model is applied to chemical releases.

Direct leaching by infiltrating water assumes that water can freely enter and leave the tank structure and that all infiltration contacting and leaving the tank carries solute at maximum solution concentrations to the water table. Conservatism of this release model lies in the fact that 1) all tanks will not degrade to the same degree at once, 2) failure of existing containment structures would not immediately permit free entry and egress of water, and 3) maximum known concentrations applied to all tanks are known to exist in relatively few tanks and to be associated with specific processes, treatments, and waste streams. A more realistic release model would include individual tank inventories, a time history of individual tank or tank farm failure, and a time history of failure severity. However, data for such an approach are not available.

P.2.1.2 Indirect Leach Scenario--Diffusion

When the protective barrier is in place over a waste site and virtually 100% effective, it is assumed that infiltrating moisture is prevented from contacting the waste (see Appendix M). In such a case, the waste is transported by molecular diffusion through the soil moisture of the unsaturated zone directly to the water table, or to the advection-controlled zone adjacent to the barrier, where infiltrating moisture will transport the waste down to the water table. In the absence of data to the contrary, it is assumed that the diffusion-controlled transport process is the limiting mechanism. This is conservative because if control of the release were governed by the waste form a slower and lower release would occur.

The solution of the diffusion equation, driven by a Dirichlet (i.e., fixed) solute concentration boundary condition, is used to model the release. Derived for a finite domain,

TABLE P.2. Concentrations and Leach Periods for Radionuclides and Chemicals in Single-Shell Tanks (no protective barrier)

Chemical or Radionuclide	Concentration (a,b,c)	Site Location	Leach Periods, yr (d)			
			for Specific Infiltration Rates, cm/yr	0.1	0.5	5
^{14}C	7.6 $\mu\text{Ci/L}$	200 E	5,490	1,400	150	49
		200 W	7,250	2,010	225	73
^{63}Ni	$1.5 \times 10^3 \mu\text{Ci/L}$	(e)	--	--	--	--
			--	--	--	--
^{90}Sr	$1.6 \times 10^5 \mu\text{Ci/L}$	200 E	--	16	1.8	<1
		200 W	--	20	2.4	<1
^{93}Zr	35 $\mu\text{Ci/L}$	--	--	--	--	--
^{99}Tc	$3.4 \times 10^2 \mu\text{Ci/L}$	200 E	1,070	213	21.3	7.1
		200 W	1,470	294	29.4	9.8
^{129}I	0.2 $\mu\text{Ci/L}$	200 E	2,960	593	59.3	20
		200 W	3,680	735	73.5	25
^{137}Cs	$6.7 \times 10^5 \mu\text{Ci/L}$	200 E	10.7	2.2	0.2	<1
		200 W	--	--	0.2	<1
^{151}Sm	$7.2 \times 10^3 \mu\text{Ci/L}$	200 E	--	71	9	<1
		200 W	--	--	9	<1
^{237}Np	0.5 $\mu\text{Ci/L}$	200 E	1,700	341	34	11
		200 W	2,060	412	41	14
^{238}U	$1.2 \times 10^{-3} \mu\text{Ci/L}$	200 E	6.8×10^6	1.4×10^6	1.4×10^5	4.5×10^4
		200 W	6.9×10^6	1.4×10^6	1.4×10^5	4.6×10^4
$^{239-240}\text{Pu}$	1.6 $\mu\text{Ci/L}$	200 E	8.9×10^4	4.2×10^4	7.4×10^3	2,640
		200 W	6.4×10^4	2.5×10^4	3.5×10^3	1,200
^{241}Am	$1.3 \times 10^3 \mu\text{Ci/L}$	200 E	--	75	8	1.5
		200 W	--	66	7	1.4
NO_3^-	0.3 g/mL	200 E	(f)	890	89	*
		200 W	*	1,200	120	*
NO_x^-	0.14 g/mL	200 E	*	95	9.5	*
		200 W	*	126	12.6	*
F^-	$1.9 \times 10^{-6} \text{ g/mL}$	200 E	*	1.2×10^6	1.2×10^5	*
		200 W	*	1.6×10^6	1.6×10^5	*
$\text{Cr}(\text{as } \text{CrO}_4^{2-})$	$1.1 \times 10^{-2} \text{ g/mL}$	200 E	*	24	2.4	*
		200 W	*	33	3.3	*
Cd	$1.1 \times 10^{-8} \text{ g/mL}$	200 E	*	9.5×10^5	9.4×10^4	*
		200 W	*	1.3×10^6	1.3×10^5	*
Hg	$3.2 \times 10^{-4} \text{ g/mL}$	200 E	*	7.7	0.7	*
		200 W	*	10	1	*

(a) All concentrations except that for cadmium and fluoride are from Schulz 1980.

(b) Fluoride concentration is extrapolated from Lindsay 1979.

(c) Cadmium concentration from Rai and Zachara et al. 1984.

(d) Leach periods are based on the inventory, the solution concentration, and the infiltration rate of water passing the waste form. Total land surfaces associated with single-shell tanks in 200 East and 200 West Areas are $2.7 \times 10^8 \text{ cm}^2$ and $3.4 \times 10^8 \text{ cm}^2$, respectively.

(e) Insignificant release due to short half-life and high distribution coefficient; therefore, not calculated.

(f) These cases not calculated; only non-barriered releases calculated for chemicals.

TABLE P.3. Single-Shell Tank Leach by Diffusion

	200 East	200 West
Number of tanks	66	83
Barrier area, ha (10^4 m^2)	12	15
Assume 4 equal subareas		
1/4 mass, g	1.2×10^{10}	2.1×10^{10}
Perimeters, m	690	780
Molecular diffusion coefficient, cm^2/day	1	1
Moisture content, % volume		
0.5 cm/yr	6.4	6.4
5 cm/yr	7.8	7.8

the solution and its gradient are evaluated at finite distances to approximate time period and activity flux of the release. The assumptions and models are completely described in Appendix 0 (Section 0.4.1.3) and are summarized in Section P.1.4. Data for the release of radionuclides and chemicals from the salt cake and sludge are summarized in Table P.3. Maximum solution concentrations for the radionuclides and chemicals are reported in Table P.2.

As part of the 5-cm/yr infiltration rate case, a disruptive failure scenario is hypothesized to occur such that 10% of the waste inventory is exposed to direct leaching by infiltrating water. It is assumed that the infiltration rate will increase because the exposed coarse rock or riprap underlying the soil moisture barrier will inhibit evaporation. Infiltration is assumed to be 50% of the assumed average wetter annual precipitation rate of 30 cm/yr (Kukla 1979); thus infiltration would be 15 cm/yr. The release periods for the disruptive failure scenario are shown in Table P.2. Also, as part of the 5-cm/yr infiltration rate case, a functional failure scenario is hypothesized to occur such that 50% of the waste inventory is exposed to direct leaching by infiltrating water. This scenario assumes that water would infiltrate the underlying waste at a rate of 0.1 cm/yr under precipitation conditions of 30 cm/yr (see Appendix M). Release periods for the functional failure scenario are shown in Table P.2.

P.2.2 Liquid-Release Scenario for Double-Shell Tanks

The 100% liquid-release scenario for double-shell tanks applies only to the no disposal action. Under the liquid-release scenario, all liquids stored in double-shell tanks are assumed to leak out in the year 2150 for an unspecified reason. All other alternatives assume the liquid is removed to within 0.05% volume.

Release of liquid from the tanks would result in displacement of soil moisture with tank liquor. It is assumed that, after a brief transient period during which displacement would

occur, the soil moisture profile would reach equilibrium. It is further assumed that an average moisture content of 7.8% for the 5-cm/yr case exists in the soils surrounding the tanks and would be indicative of moisture content before and after such a release. Similarly, 6.4% moisture content corresponds to the 0.5-cm/yr infiltration case. These moisture contents are based on the relative conductivity curve for a sandy soil indicative of vadose zone deposits at Hanford. It is probable that the tank structure and geologic stratigraphy would act to spread a plume horizontally as it moved to the water table. The cross section of contaminated soil could be viewed as a vertically standing cone; however, the leaching of such a contaminated cross section is not readily modeled. The analyses here assume a cylindrical column of soil, which simplifies the infiltration calculation, i.e., infiltration area is equal to cylindrical cross section.

If a double-shell tank were full (i.e., 3,800 m³), its release would displace all soil moisture (at 7.8%) in the soil column above the water table in a cylindrical section with a radius of 15.6 m. This represents a radius 36% greater than that of a typical tank. It is possible that lateral migration due to silt and clay lenses would be significantly greater. Parameters for the liquid-release model (e.g., the thickness of contaminated deposits and the area of infiltration interception) are given in Table P.4. While the tank liquor and all nonsorbed radionuclides are distributed throughout the soil column, those radionuclides known to sorb are assumed to be held in the upper portion of the soil column. Thickness of the contaminated deposit depends on each radionuclide's K_d.

TABLE P.4. Parameters for the Liquid-Release Model for Double-Shell Tanks

	5 cm/yr, θ = 7.8%		0.5 cm/yr, θ = 6.4%	
	200 East	200 West	200 East	200 West
Number of tanks	25	3	25	3
• 100% Release (3,800 m ³ /tank)				
Height of deposit, m	64	64(a)	64	64(a)
Radius of each cylindrical section, m	15.6	15.6	17.2	17.2
Existing area of interception, m ² (11 tanks in East Area)	8,410	2,290	10,200	2,800
Future area of interception, m ² (14 tanks in East Area)	10,700	0	13,000	0
Total	19,110	2,290	23,200	2,800
• 0.05% release (1.9 m ³ /tank)				
Height of deposit, m	1	1	1	1
Bottom area, m ²	24.4	24.4	29.7	29.7

(a) Due to the existence of U Pond, the depth to the water table beneath the 200 West Area has been ~42 m; however, U Pond has been decommissioned, and the water table will drop to ~64 m.

In the case of the 100% inventory release to a system not covered by a barrier, the body of contaminated soil water is assumed to migrate to the water table at a rate defined by the unit hydraulic gradient, the infiltration rate of the climate (e.g., drier or wetter), and the sorption characteristics of the contamination. While the tank leak rapidly displaces existing soil water, the release of the contaminated water to the water table is believed to be controlled by its slower displacement by meteoric water. Thus the time necessary to flush contamination from the soil will depend upon the travel time defined by the infiltration rate, the unit hydraulic gradient model, and the sorption properties of the radionuclide inventory. Release of radionuclides from the contaminated soil column is modeled with the adsorption-controlled release model.

In the case of the 0.05% inventory release to a barrier-covered system, the body of contaminated soil water is assumed to provide a source to diffusion-controlled pathways (e.g., streamtubes conducting contamination by the molecular diffusion mechanism). Release to the water table is modeled as the cumulative release from the suite of diffusion-controlled pathways leading from the source to the advection-controlled pathways and the water table. The model applied for radionuclide releases from the 0.05% liquid inventory corrects for decay by applying the exponential decay to the fraction-remaining equation of a nondecaying chemical.

P.2.3 Release from Grout in Vaults

All grout disposal vaults are to be covered with protective barriers. The release model in Section P.1.4 is based on the viewpoint that the waste and its surrounding vadose zone are a source region supplying a release to the water table of the unconfined aquifer. In this conceptualization there can be one of two controlling factors for the overall release: release from the waste or transport mechanisms. If release from the waste controls the overall release, then the transport mechanism carrying contamination away from the waste is able to transport contamination as fast as the waste form can deliver it to the waste/soil interface. If the transport mechanism controls release, it is unable to transport contamination away from the waste as rapidly as the waste form can deliver it. The model employed herein is based on the assumption that the transport pathway governs the release. Thus future modeling efforts, which take into account the waste-form release characteristics, could result in slower and lower releases to the water table. Preliminary laboratory experiments show that the rate of diffusion through grout is significantly lower than that through the vadose zone, indicating that the diffusion rate used for grout may be conservative.

P.2.3.1 Release Controlled by Leach Rate of the Grouted Waste

Releases from grout depend on the geometry and chemical composition of the grout and the characteristics of the soil and soil water it contacts. While several models exist for the release of contamination from grout samples from laboratory formulations (Moore, Godbee, and Kibbey 1977; Godbee et al. 1980), no data exist that quantify releases to an unsaturated soil environment from grout containing Hanford wastes. Studies have shown that laboratory results can be scaled to field sites by ratioing the volume-to-surface area ratios of the laboratory sample and the field-scale waste form (Moore, Godbee, and Kibbey 1977). Certainly feed streams from different Hanford facilities contain different concentrations of organics, salt

and solids. The grout formulas for the different waste streams will differ. Relative amounts of grout-forming solids, waste feed stream, and makeup water will differ for each major waste stream. Finally, the soil, soil water, and aqueous geochemistry of the soil environment can influence the performance of grouted wastes. The vadose-zone soils, being more conductive than grout, may channel soil water around the grouted wastes, and the oxidizing environment of the Hanford soil (relative to reducing environments elsewhere) may result in geochemical reactions (e.g., precipitation, adsorption) that act to retard migration of radionuclides and chemicals once they have entered the soil system. Because of the variety of models, chemical compositions, and soil environments, leach testing of Hanford grout is in progress. These tests seek to optimize the grout formula used with each waste feed stream proposed for grout disposal at Hanford.

While these studies are conducted, a uniform leach rate for nitrate ion has been assumed to apply to all grouted wastes at Hanford. From preliminary and limited data, a leach rate of 0.007%/yr is assumed for Hanford wastes placed in a vault with a rectangular upper surface and a trapezoidal cross section. The upper surface edge is 35 m; the lower surface edge is 29 m; thickness is 3 m; and the side slopes are 1:1. Because the rate is assumed to be constant for all radionuclides and chemicals, it is essentially a congruent release model. Laboratory and field-lysimeter studies will be conducted to ensure that performance indicated by results shown in this EIS is achievable for grout placed in vaults in Hanford soils.

Because molecular diffusion in the soil water of the porous medium is assumed to control release beneath a protective barrier that excludes recharge water, the grout leach rate model is only employed to analyze the disruptive and functional failure scenarios where infiltrating water directly contacts the grouted waste. For these special cases, moisture flowing around and past the waste form is assumed to carry all contaminants released from the grout to the water table.

P.2.3.2 Release Controlled by the Transport Pathway

If the transport phenomena cannot conduct contamination away from the waste form as rapidly as it is delivered to the waste form/soil interface, the release mechanism is transport-dominated. Essentially, the concentration of contamination adjacent to the waste in the soil water builds up to the point of shutting down the diffusion-controlled grout release mechanism. The constant leach rate of 0.007%/yr yields a complete release in approximately 14,000 years (i.e., $1/0.007\%/\text{yr} = 14,000 \text{ years}$) if the release mechanism dominates. The diffusion-controlled pathway commonly exhibits release periods in excess of the value dictated by the grout release mechanism. Thus, the diffusion transport mechanism does dominate the release process. Nitrate near the grout interface is assumed to exist at a solution concentration of 0.3 g/mL (Barney 1976; Schulz 1980). The volume, surface area, and edge of the grout waste for the different disposal alternatives are shown in Table P.5. Release of nitrate ion to the water table from the barrier-covered grout waste form is modeled by the diffusion-controlled model for a nondecaying source. Radionuclides are released congruent with the nitrate ion. The assumption and models are described in Appendix O (Section 0.4.1.3) and summarized in Section P.1.4.

TABLE P.5. Volumes, Surface Areas, and Edges of the Grout Waste

Inventory	Geologic Disposal (a)		In-Place Stabilization and Disposal or Reference Alternative	
	Existing	Future	Existing	Future
Volume, m ³	736,000	99,000	173,000	99,000
Barrier Surface Area, ha (10 ³ m ²)	73	9	19	10
Grout Surface Area, ha	24.5	3.3	5.8	3.3
Grout Thickness, m	3	3	3	3
Edge of Continuous Square Grout Slab, m	495	182	240	182
Mass of Nitrate (NO ₃ ⁻), kg	1.1 x 10 ⁸	1.9 x 10 ⁶	1.5 x 10 ⁷	1.9 x 10 ⁶

(a) The preferred alternative is bounded by the geologic and reference alternatives.

P.2.4 TRU-Contaminated Unsaturated Zone Soils in the 200 Areas

Release of radionuclides from contaminated soils is assumed to be controlled by a solution concentration in the cases of plutonium (Rai, Serne, and Moore 1980), americium (Rai et al. 1981), and neptunium (Shultz 1980), and by adsorption (i.e., desorption) in the cases of carbon, strontium, and cesium. The solubility model depends on the solution concentration of the radionuclide, the land surface area of contaminated soils, and the net infiltration rate. The latter is described in Appendix 0, and the former data are presented in the final section of this appendix, which summarizes release model data.

The adsorption model depends on the distribution coefficient and the thickness of the contaminated soil deposits. This thickness will differ for each radionuclide, depending on its sorption characteristics; however, data are incomplete for individual radionuclides disposed to the various burial sites. The TRU-contaminated soil sites provide the shallowest contaminated deposits. All other, i.e., pre-1970 buried, and retrievably stored and newly generated TRU wastes are stored in deposits having a thickness greater than 1 m.

The adsorption, or more appropriately the desorption, model of release is based on an assumed uniform, homogeneous deposit of contaminated soil. However, actual soil deposits are known to be more concentrated near the surface and less concentrated at depth. For example, the maximum localized TRU contamination shows concentrations up to 40,000 nCi/g in small localized volumes within only the first 1/3 m of the distribution structure. TRU concentrations drop to less than 1,000 nCi/g at a depth of 2 m and less than 100 nCi/g at a depth of 15 m (Rockwell 1985). Because the maximum value applies to a localized small volume, and because a single thickness of deposit was selected for all TRU wastes released by the adsorption-controlled model, an assumed thickness of 1/3 m was applied to all TRU wastes.

The sensitivity of the adsorption release model to the product of retardation factor and deposit thickness is of interest because these parameters appear in the adsorption model equations. As thickness increases, while retardation factor is held constant for a fixed initial inventory, a slower release occurs. This is due to the one-to-one relationship between solid- and liquid-phase concentration in the retardation model. As the thickness increases, the solid-phase concentration decreases, causing a decrease in the liquid-phase concentration and a slower release. As retardation factor increases and thickness is held constant for a fixed initial inventory, a slower release occurs. Note that a decreasing retardation implies an increasing thickness if depositions have occurred by an adsorption-controlled process. Radionuclides that are more mobile will have a smaller value of retardation and a greater thickness of contaminated soil. Less-mobile radionuclides will have larger values of retardation and shallower deposits of contaminated soil. The product of retardation and thickness appears in the adsorption release model. While no data exist on a definitive relationship between retardation and thickness of contaminated deposits, the trade-off evident in the model implies that a controlled sensitivity to thickness may exist when the relationship between thickness and retardation is taken into account.

The release models for TRU wastes described above apply to the cases that do not involve barriers. Control of infiltrating water by a protective barrier will result in reduced radionuclide release rates for the adsorption model because of the exclusion of infiltrating water and the dominance of molecular diffusion as the transport mechanism. Because projected releases of radionuclides for the cases without barriers have not resulted in health effects (see Appendices Q and R), it is assumed that the slower and less concentrated releases of the barrier cases would also pose no health effects. Therefore, models of release from beneath a protective barrier have not been developed and applied to the TRU wastes stored on the 200 Areas plateau.

P.2.5 TRU-Contaminated Unsaturated-Zone Soils in the 300 Area

Three TRU sites in the 300 Area are modeled as two distinct subareas in this analysis. The 618-1 and 618-2 sites are combined because of their proximity; both are in or near the 300 Area. The 618-11 site is located adjacent to the Washington Public Power Supply System in the 300 Wye area. These two subareas are modeled for 0.5-cm/yr and 5-cm/yr infiltration rates. Due to the proximity of the burial sites to the Columbia River, a constant 8-m depth to water table is assumed to be independent of location and recharge rate. These analyses are for the no disposal action case. In all disposal alternatives these wastes are to be moved to the 200 Areas plateau [see footnote (b) on Table P.6].

Release of radionuclides from the 618 sites is modeled as a retardation or as a solution concentration, i.e., solubility-controlled, release. As such it is assumed that water can freely contact the TRU wastes. The thickness of the storage deposit at each site is 4.6 m, and the distribution coefficients for radionuclides are the same as those used for TRU wastes in the 200 Areas. Table P.6 summarizes the pertinent release model data for the two subareas.

TABLE P.6. Leach Parameters for Direct Infiltration and Contact of TRU Wastes Stored in the 618 Subareas

Radionuclide	Inventory, Ci C_0 , Ci/L (a)	Waste Volume, m ³	Area, m ²	Distribution Coefficient, K_d , mL/g	Thickness, m	ρ , g/cm ³
Subarea 618-1 & 2(b)		1,180	790		4.6	1.8
⁹⁰ Sr	1.3×10^2			0.64		
¹³⁷ Cs	1.5×10^2			26(c)		
²³⁹⁻²⁴⁰ Pu(d)	1.1×10^2	2.6×10^{-7} (e)		(71)(f)		
²⁴¹ Am	4.1×10^1	1.5×10^{-8} (g)		(76)		
Subarea 618-11		7,900	3,100		4.6	1.8
⁹⁰ Sr	8.8×10^2			0.64		
¹³⁷ Cs	9.6×10^2			26(c)		
²³⁹⁻²⁴⁰ Pu	7.5×10^2	2.6×10^{-7}		(71)		
²⁴¹ Am	2.1×10^2	1.5×10^{-8}		(76)		

- (a) These solution concentrations differ from those used for high-ionic-strength, high complexant concentration wastes in single-shell tanks. The TRU wastes are assumed to be more appropriately modeled after crib discharges.
- (b) A recently completed study (DOE 1986b), which examined records of inactive waste disposal locations on the Hanford Site, showed that two 618 sites (618-1 and 618-2) each contained 1.0 g. of plutonium, rather than the previously listed 1,000 g. (Rockwell 1985). As a result of this lower quantity, both sites are now designated as low-level waste (Rockwell 1982).
- (c) Routson et al. (1981).
- (d) Rai et al. (1981); Table P.13.
- (e) Rai, Serne, and Moore (1980), 1.8×10^{-8} moles/L of ²³⁹Pu.
- (f) Numbers in parentheses are distribution coefficients used in the transport analysis of the radionuclides in both vadose and saturated zones.
- (g) Rai et al. (1981), 1.8×10^{-11} moles/L of ²⁴¹Am.

P.3 INVENTORIES AND LOCATIONS OF RADIONUCLIDES

Radionuclide inventories for the various waste forms and storage facilities are given in Tables P.6 through P.13.(a) A number of variables enter into the selection and application of release models. Most important are the waste form and whether a barrier^(b) will cover the waste. This information and a cross reference to inventory are summarized in Tables P.14 through P.17. The inventories tabulated were developed from Rockwell (1985). Tables P.13 through P.17 also indicate whether the waste is stored in 200 East or 200 West.

- (a) Here and elsewhere in this appendix, inventory values are presented to two and sometimes three figures. This has been done to aid in accounting for radionuclides, and it should not be construed as a true measure of accuracy. Since many values are known only to one figure and conclusions would not be altered whether based on one figure or two, it is suggested that inventories be read as though rounded to one figure, e.g., 9.6×10^1 as 1×10^2 .
- (b) Reference to a barrier denotes the protective barrier and marker system.

TABLE P.7. Radionuclide Inventories for Existing Single-Shell Tanks, (a,b) Ci

Radionuclide	200 East		200 West	
	Salt Cake	Sludge	Salt Cake	Sludge
^{14}C	1.6×10^3		2.7×10^3	
^{79}Se	2.6×10^2		5.4×10^2	
^{90}Sr		1.9×10^7		3.2×10^7
^{99}Tc	9.8×10^3		1.7×10^4	
^{129}I	1.6×10^1		2.5×10^1	
^{137}Cs	8.1×10^6		1.1×10^7	
^{151}Sm	3.0×10^5		3.8×10^5	
^{237}Np	2.3×10^1		3.5×10^1	
^{238}U	2.2×10^2		2.8×10^2	
$^{239-240}\text{Pu}$		1.8×10^4		1.0×10^4
^{241}Am	1.8×10^4		2.0×10^4	

- (a) To be conservative, the total curies shown for individual radionuclides exceed the reported inventory for single-shell tanks; however, they are equal to or less than the total existing waste inventory, some of which is stored in double-shell tanks.
- (b) Taken from Table 2-7 of Rockwell 1985.

Inventories of some of the radionuclides provided in Tables P.7, P.8 and P.9 are doubly accounted for both in the inventories and in the dose calculations reported in Appendix R. This conservatism is necessitated because some of the radionuclides may be in either single-shell or double-shell tanks. An ongoing jet pumping program is reducing the liquid volume in single-shell tanks by placing this liquid in double-shell tanks. It has resulted in uncertainty in the radionuclides retained in salt cake, sludge and liquid in single-shell tanks as opposed to those retained in the pumped liquid. Thus, the radionuclide inventories for these radionuclides are included in both single-shell and double-shell tanks and remain doubly accounted for as these wastes are processed for the various alternatives.

In contrast to the doubly accounted for inventories in Tables P.7, P.8 and P.9, best single estimate inventories as the radionuclides presently exist and as they would exist following processing for the various alternatives are given in Tables P.18 through P.22. These tables are structured as best single estimates to inform the reader as to the change of inventory and location of radionuclides with alternatives.

TABLE P.8. Radionuclide Inventories for Grout from Existing Tank Wastes, ^(a) Ci

Radionuclide	Disposal Alternative ^(b)		
	Geologic Disposal ^(c)	In-Place Stabilization and Disposal ^(d)	Reference ^(d) (Combination Disposal)
^{14}C (e)	5×10^3	4×10^3	4×10^3
^{79}Se	9×10^2	1×10^2	1×10^2
^{90}Sr	3×10^5	2×10^7	2×10^6
^{99}Tc (e)	3×10^2	3×10^4	3×10^4
^{129}I	5×10^1	4×10^1	4×10^1
^{137}Cs	2×10^5	2×10^7	2×10^7
^{151}Sm	5×10^3	3×10^5	3×10^4
^{237}Np	3×10^{-1}	6×10^1	6
^{238}U	2	3	3×10^{-1}
$^{239-240}\text{Pu}$	1×10^2	1×10^2	1×10^1
^{241}Am	2×10^2	3×10^4	3×10^3
TOTAL VOLUME, m ³	736,000	173,000	173,000

(a) Taken from Table 2-13b of Rockwell 1985.

(b) The preferred alternative is bounded by the geologic and reference alternatives.

(c) Made from both single- and double-shell tank wastes.

(d) Made from double-shell tank wastes only.

(e) Since it is uncertain whether the ^{14}C and ^{99}Tc in single-shell tanks are salt cake or sludge, the inventories are included as if they existed in both; i.e., these nuclides are doubly accounted for.

P.4 SUMMARY OF SOURCE RELEASE-RATE DATA

The four release models (adsorption, solubility, dissolution, and diffusion) require a variety of data. Data for radionuclide release from salt cake and sludge are summarized in Table P.23. Radionuclide data for liquid release, grout, and TRU wastes are summarized in Tables P.24, P.25, and P.26, respectively.

The transport code used in the simulations accepts a distribution coefficient, K_d , for each radionuclide. Chosen values of K_d , shown in Table P.27, are a conservative representation of values germane to the Hanford Site given in the literature (Delegard and Barney 1983). The distribution coefficient values reported by Delegard and Barney are based on laboratory studies that used synthetic solutions. Their findings are believed to be conservative because the organic complexants used in the experiments were not exposed to radioactivity over any significant period of time. Such exposure is believed to result in the breakdown of organic compounds and, therefore, an increase in retardation. Thus, the distribution coefficients are probably biased low and result in greater mobility. Specifically, K_d

TABLE P.9. Radionuclide Inventories for Existing Double-Shell Tank Wastes, Ci^(a,b,c)

Radionuclide	200 East	200 West
¹⁴ C	3.3×10^3	6.7×10^2
⁷⁹ Se	8.3×10^1	1.7×10^1
⁹⁰ Sr	1.5×10^7	3.0×10^6
⁹⁹ Tc	2.5×10^4	5.0×10^3
¹²⁹ I	3.3×10^1	6.8
¹³⁷ Cs	1.5×10^7	3.0×10^6
¹⁵¹ Sm	2.4×10^5	4.9×10^4
²³⁷ Np	5.0×10^1	1.0×10^1
²³⁸ U	2.5	5.1×10^{-1}
²³⁹⁻²⁴⁰ Pu	8.3×10^1	1.7×10^1
²⁴¹ Am	2.5×10^4	5.1×10^3
TOTAL VOLUME, m ³	37,600	7,600

- (a) The split between 200 East and 200 West has been based on waste volume in the respective areas. The actual split between 200 East and 200 West double-shell inventories may be different. Management of newly generated wastes may alter the configuration. Values shown are representative of one possible split.
- (b) The total curies shown for each radionuclide represent the conservative estimate of inventory in double-shell tanks.
- (c) Taken from Table 2-8 of Rockwell 1985.

values for strontium, neptunium, plutonium, and americium are conservative interpretations of values found in Delegard and Barney. Values for carbon, iodine, and technetium are taken to be zero. Samarium behavior is analogous to americium under oxidizing conditions. Finally, the K_d of cesium is taken as a constant 26 mL/g for all waste forms. Such a value is on the low end of the cesium values reported by Delegard and Barney for various sediment/waste solution combinations.

Values of distribution coefficients (K_d) applied to TRU wastes (i.e., soil sites, pre-1970 solid waste, retrievably stored, and newly generated) also are based on experiments performed by Delegard and Barney. Distribution coefficient values based on experiments with dilute, uncomplexed tank wastes were selected for application to the TRU wastes, as these wastes, in general, do not contain chemical complexants that are likely to mobilize radionuclides. Pre-1970, retrievably stored and newly generated solid wastes are predominantly contaminated material and equipment with no complexant inventory, while soil sites may have received some chemicals as part of past liquid discharges. However, the liquids discharged at these sites should be no more concentrated or complexed than the solutions studied by

TABLE P.10. Radionuclide Inventory of Future Double-Shell Tank Wastes, (a) Ci

<u>Radionuclide</u>	<u>Inventory</u>
^{14}C	2.8×10^2
^{79}Se	2.3×10^2
^{90}Sr	4.2×10^7
^{99}Tc	4.8×10^3
^{129}I	1.2×10^1
^{137}Cs	5.1×10^7
^{151}Sm	4.0×10^5
$^{239-240}\text{Pu}$	6.3×10^3
^{241}Am	3.3×10^5
TOTAL VOLUME, m ³	46,600

(a) Taken from Table 2-42 of Rockwell 1985.

TABLE P.11. Radionuclide Inventories of Grout from Future Tank Waste, (a) Ci

<u>Radionuclide</u>	<u>Geologic Disposal</u>	<u>In-Place Stabilization and Disposal</u>	<u>Reference and Preferred (Combination Disposal)</u>
^{14}C	2.8×10^2	2.8×10^2	2.8×10^2
^{79}Se	2.3×10^2	2.3×10^2	2.3×10^2
^{90}Sr	2.4×10^5	4.2×10^7	1.4×10^6
^{99}Tc	1.6×10^2	4.8×10^3	4.8×10^3
^{129}I	1.2×10^1	1.2×10^1	1.2×10^1
^{137}Cs	1.5×10^6	5.0×10^6	4.1×10^6
^{151}Sm	2.3×10^3	4.0×10^5	1.3×10^4
$^{239-240}\text{Pu}$	2.9×10^2	6.3×10^3	6.3×10^2
^{241}Am	3.0×10^3	3.3×10^5	1.4×10^4

(a) Data for the geologic, in-place, and reference alternatives are taken from Tables 2-45, 2-44, and 2-46, respectively, of Rockwell 1985.

Delegard and Barney. The absence of complexants is an assumption; studies have not been conducted to determine presence or absence of complexants. The presence of these chemical constituents could result in more rapid migration as evidenced from the dilute complexed values of K_d .

TABLE P.12. Radionuclide Inventories for Sr/Cs Capsules in the Drywell Storage Facility, Ci (decayed to 1990)

<u>Radionuclide</u>	<u>In-Place Stabilization and Disposal</u>	<u>No Disposal Action</u>
^{90}Sr	3.1×10^7	3.1×10^7
^{137}Cs	1.0×10^8	5.3×10^7

While conservative compared to available distribution coefficient values, the distribution coefficient model itself is not the most complete attenuation model. Tests run to determine K_d values do not in general consider:

- all competing ions
- the influence of various species of an element and of the implicit average K_d obtained
- the variety of soils contacted by solution.

Trace quantities of various chemicals have been shown to be particularly important in determining appropriate K_d values for radionuclides.

Values of K_d determined from batch experiments on wastes stored in tanks have been applied in this EIS to analyses of wastes stored in tanks, grout, and burial grounds. Studies to determine more appropriate source-term models and adsorption models are planned as part of the Transportable Grout Facility Project and the Hanford Waste Management Plan (DOE 1986b). Attenuation models more sophisticated than the distribution coefficient model used in this EIS are under development. Although these newer models will result in different transport predictions, it is likely that the conservatism in the distribution coefficients used in this EIS analysis ensures that any change will be for better, hence lower, releases.

TABLE P.13. Radionuclide Inventories for TRU, (a) Ci

Radionuclide	Soil Sites		Pre-1970 Buried			Retrievable		Newly Generated 200 West
	200 East	200 West	200 East	200 West	618 Sites	200 East	200 West	
^{14}C	--(b)	--	--	1.0	--	--	2.0	2.0
^{90}Sr	1.9×10^2	3.2×10^3	2.0×10^2	2.0×10^4	1×10^3	5	2×10^4	4.4×10^4
^{137}Cs	9.6×10^1	1.7×10^3	2.0×10^2	2.0×10^4	1×10^3	5	2×10^4	4.6×10^4
$^{239-240}\text{Pu}$	7.7×10^2	1.3×10^4	2.5×10^2	2.4×10^4	9×10^2 (c)	8	2×10^4	2.7×10^4
^{241}Am	2.1×10^2	3.7×10^3	7.2×10^1	7.0×10^3	3×10^2	3	1×10^3	5.4×10^3
^{237}Np	--	--	--	--	--	--	8×10^{-2}	--
^{238}U	--	--	--	--	4×10^{-2}	--	--	--

(a) Data for the soil sites, pre-1970 buried, 200 East and 200 West, pre-1970 buried 618 sites, retrievable, and newly generated wastes are taken from Tables 4-51, 4-60, 2-27, 2-26, and 2-27 of Rockwell 1985. The east/west split is taken from Tables 2-15 and 2-20 for the soil sites and pre-1970 buried TRU.

(b) Dashes indicate no inventory for the specific radionuclide and waste form.

(c) A recently completed study (DOE 1986a), which examined records of inactive waste disposal locations on the Hanford Site, showed that two 618 sites (618-1 and 618-2) each contained 1.0 g of plutonium, rather than the previously listed 1000 g (Rockwell 1985). As a result of this lower quantity, both sites are now designated as low-level waste sites (Rockwell 1987).

TABLE P.14. Inventory and Location Details for Wastes to be Disposed of Near Surface in the Geologic Disposal Alternative (with barrier)

<u>Facility (a)</u>	<u>Waste Form</u>	<u>Inventory (b)</u>	<u>200 Area Location</u>
SST	Combined Salt and Sludge	5%, P.7	East and West
DST and SST	Grout (existing)	Column 1, P.8	East
DST	Waste Slurry (existing)	0.05%, P.9	East and West
DST	Waste Slurry (future)	0.05%, P.10	East and West
DST	Grout (future)	Column 1, P.11	East

(a) SST = single-shell tanks

DST = double-shell tanks

Existing = waste inventory currently stored

Future = waste inventory to be produced.

(b) Inventory cross-referenced to preceding Tables P.7 through P.11.

TABLE P.15. Inventory and Location Details for the In-Place Stabilization and Disposal Alternative (with barrier)

<u>Facility(a)</u>	<u>Waste Form</u>	<u>Inventory(b)</u>	<u>200 Area Location</u>
SST	Combined Salt and Sludge	P.7	East and West
DST (existing)	Liquid	0.05%, P.9	East and West
DST (existing)	Grout	Column 2, P.8	East
DST (future)	Liquid	0.05%, P.10	East
DST (future)	Grout	Column 2, P.11	East
DWSF	Capsules	Column 1, P.12	East
TRU	Contaminated Soils	Columns 1 & 2, P.13	East and West
TRU	Pre-1970 Buried	Columns 3, 4 & 5, P.13	East and West (and 618 sites)(c)
TRU	Retrievably Stored	Columns 6 & 7, P.13	East and West
TRU	Newly Generated	Column 8, P.13	West

(a) SST = single-shell tank.
DST = double-shell tank.

Existing = waste inventory currently stored.

Future = waste inventory to be produced.

DWSF = drywell storage facility.

TRU = transuranic waste.

(b) Inventory cross-referenced to preceding Tables P.7 through P.13.

(c) A recently completed study (DOE 1986a), which examined records of inactive waste disposal locations on the Hanford Site, showed that two 618 sites (618-1 and 618-2) each contained 1.0 g of plutonium, rather than the previously listed 1000 g (Rockwell 1985). As a result of this lower quantity, both sites are now designated as low-level waste sites (Rockwell 1987).

TABLE P.16. Inventory and Location Details for the Reference Alternative (with barrier)

Facility ^(a)	Waste Form	Inventory ^(b)	200 Area Location
SST	Combined Salt and Sludge	P.7	East and West
DST (existing)	Liquid	0.05%, P.9	East and West
DST (existing)	Grout	Column 3, P.8	East
DST (future)	Liquid	0.05%, P.10	East
DST (future)	Grout	Column 3, P.11	East
TRU	Contaminated Soils	Columns 1 & 2, P.13	East and West
TRU	Pre-1970 Buried	Columns 3 & 4, P.13	East and West

(a) SST = single-shell tank
 DST = double-shell tank
 Existing = waste inventory currently stored
 Future = waste inventory to be produced
 TRU = transuranic waste.
(b) Inventory cross-referenced to preceding Tables P.7 through P.13.

TABLE P.17. Inventory and Location Details for No Disposal Action (no barrier)

<u>Facility</u> ^(a)	<u>Waste Form</u>	<u>Inventory</u> ^(b)	<u>200 Area Location</u>
SST	Combined Salt and Sludge	P.7	East and West
DST (existing)	Liquid	P.9	East and West
DST (future)	Liquid	P.10	East and West
DWSF	Capsules	Column 2, P.12	East
TRU	Contaminated Soils	Columns 1 & 2, P.13	East and West
TRU	Pre-1970 Buried	Columns 3, 4, & 5, P.13	East and West (and 618 sites) ^(c)
TRU	Retrievably Stored	Columns 6 & 7, P.13	East
TRU	Newly Generated	Column 8, P.13	West

(a) SST = single-shell tank
DST = double-shell tank

Existing = waste inventory currently stored

Future = waste inventory to be produced

DWSF = drywell storage facility

TRU = transuranic waste.

(b) Inventory cross-referenced to preceding Tables P.7 through P.13.

(c) A recently completed study (DOE 1986a), which examined records of inactive waste disposal locations on the Hanford Site, showed that two 618 sites (618-1 and 618-2) each contained 1.0 g of plutonium, rather than the previously listed 1000 g (Rockwell 1985). As a result of this lower quantity, both sites are now designated as low-level waste sites (Rockwell 1987).

TABLE P.18. Inventory (Ci) and Location of Selected Radionuclides^(a)

	Existing Tank Waste ^(b)			Future Double-Shell Tank Waste	Sr/Cs Capsules in WESF	TRU-Contaminated Soil Sites	Pre-1970 Buried TRU	Retrievably Stored TRU Waste	Newly Generated TRU Waste	Total Inventory (rounded)
	Single-Shell Tank Waste	Double-Shell Tank Waste	Total							
¹⁴ C	3,000	2,000	5,000	280	--(c)	--	1	2	2	5,300
⁷⁹ Se	800	100	900	230	--	--	--	--	--	1,100
⁹⁰ Sr	42,000,000	8,200,000	50,000,000	42,000,000	31,000,000	3,400	20,000	22,000	44,000	120,000,000
⁹⁹ Tc	16,000	14,000	30,000	4,800	--	--	--	--	--	35,000
¹²⁹ I	24	22	46	12	--	--	--	--	--	58
¹³⁷ Cs	11,000,000	11,000,000	22,000,000	51,000,000	53,000,000	1,800	21,000	23,000	46,000	130,000,000
¹⁵¹ Sm	650,000	170,000	820,000	400,000	--	--	--	--	--	1,200,000
²³⁸ U	470	2	470	47	--	2	49	4	5	580
^{239,240} Pu	27,000	110	27,000	6,200	--	14,000	25,000(d)	24,000	27,000	120,000
²⁴¹ Am	28,000	16,000	44,000	330,000	--	3,900	7,200	1,400	5,400	390,000

(a) Radionuclides (with half-lives greater than 20 years) were selected for presentation based on an expectation of significant contribution to population dose or the fact that they might otherwise be of interest. Quantities are decayed to end of 1995.

(b) Based on a 50:50 distribution of soluble radionuclides in solution between single-shell and double-shell tanks; constitutes a best estimate of inventory split between tank classes. (See Tables P.7 through P.11 for a more conservative treatment used in dose calculations.)

(c) Dashes indicate no value reported in Rockwell 1985.

(d) A recently completed study (DOE 1986a), which examined records of inactive waste disposal locations on the Hanford Site, showed that two 618 sites (618-1 and 618-2) each contained 1.0 g of plutonium, rather than the previously listed 1000 g (Rockwell 1985). As a result of this lower quantity, both sites are now designated as low-level waste sites (Rockwell 1987).

TABLE P.19. Inventory (Ci) and Location of Selected Radionuclides^(a) for the Geologic Disposal Alternative^(b)

	To Near-Surface Burial with Barrier and Marker System								
	Single-Shell Tanks ^(c)	Existing Double-Shell Tanks ^(d)	Future Double-Shell Tanks ^(e)	Total In Tanks	Existing Single & Double Shell-Tank Grout	Future Double-Shell Tank Grout	Total In Grout	Total IPSD	
¹⁴ C	150	1	<1	150	4,800	280	5,100	5,300	
⁷⁵ Se	40	<1	<1	40	860	230	1,100	1,100	
⁹⁰ Sr	2,100,000	4,100	21,000	2,100,000	250,000	240,000	490,000	2,600,000	
⁹⁹ Tc	800	7	2	810	300	160	460	1,300	
¹²⁹ I	1	<1	<1	1	45	12	57	58	
¹³⁷ Cs	530,000	5,300	25,000	560,000	210,000	1,500,000	1,700,000	2,300,000	
¹⁵¹ Sm	33,000	87	200	33,000	4,100	2,300	6,400	39,000	
²³⁸ U	24	<1	<1	24	2	39	41	65	
^{239,240} Pu	1,400	<1	3	1,400	140	290	430	1,800	
²⁴¹ Am	1,400	8	160	1,600	220	3,000	3,200	4,800	

	To Geologic Repository								
	Existing Single & Double Shell Glass ^(f)	Future Double-Shell Glass	Sr/Cs Capsules	TRU-Contaminated Soil Site Waste	Pre-1970 TRU Buried Solids Waste	Retrievably Stored TRU Waste	Newly Generated TRU Waste	Total Repository	Total Inventory (rounded)
¹⁴ C	0	0	(e)	--	1	2	2	5	5,300
⁷⁵ Se	0	4	--	--	--	--	--	4	1,100
⁹⁰ Sr	47,000,000	42,000,000	31,000,000	3,400	21,000	22,000	44,000	120,000,000	120,000,000
⁹⁹ Tc	28,900	4,700	--	--	--	--	--	34,000	35,000
¹²⁹ I	0	0	--	--	--	--	--	--	58
¹³⁷ Cs	21,000,000	49,000,000	53,000,000	1,800	21,000	23,000	46,000	120,000,000	130,000,000
¹⁵¹ Sm	780,000	390,000	--	--	--	--	--	1,200,000	1,200,000
²³⁸ U	440	8	--	2	49	4	5	510	580
²³⁹⁻²⁴⁰ Pu	27,000	5,900	--	14,000	25,000 ^(g)	24,000	27,000	120,000	120,000
²⁴¹ Am	44,000	320,000	--	3,900	7,200	1,400	5,400	390,000	390,000

- (a) Radionuclides (with half-lives greater than 20 years) were selected for presentation based on an expectation of significant contribution to population dose or the fact that they might otherwise be of interest. Quantities decayed to end of 1995.
- (b) The geologic alternative represents a bounding case for the preferred alternative.
- (c) 5% of inventory.
- (d) 0.05% of inventory.
- (e) Dashes indicate no value reported in Rockwell 1985.
- (f) Based on a 50:50 distribution of soluble radionuclides in solution between single-shell and double-shell tanks; constitutes a best estimate of inventory split between tank classes. (See Tables P.7 through P.11 for a more conservative treatment used in dose calculations.)
- (g) A recently completed study (DOE 1986a), which examined records of inactive waste disposal locations on the Hanford Site, showed that two 618 sites (618-1 and 618-2) each contained 1.0 g of plutonium, rather than the previously listed 1000 g (Rockwell 1985). As a result of this lower quantity, both sites are now designated as low-level waste sites (Rockwell 1987).

TABLE P.20. Inventory (Ci) and Location of Selected Radionuclides^(a) for the In-Place Stabilization and Disposal Alternative

	Existing Tank Waste ^(b)			Future Double-Shell Tanks Residuals	Future Double-Shell Tank Grout	Encapsulated Waste in DWDF	TRU-Contaminated Soil Sites	Pre-1970 Buried TRU	Retrievably Stored TRU Waste	Newly Generated TRU Waste	Total Inventory (rounded)	
	Single-Shell Tanks	Double-Shell Tanks	Double-Shell Tank Grout									
^{P-34}	¹⁴ C	3,000	1	2,000	<1	280	--(c)	--	1	2	2	5,300
	⁷⁵ Se	800	<1	100	<1	230	--	--	--	--	--	1,100
	⁹⁰ Sr	42,000,000	4,100	8,200,000	21,000	42,000,000	31,000,000	3,400	20,000	22,000	44,000	120,000,000
	⁹⁹ Tc	16,000	7	14,000	2	4,800	--	--	--	--	--	35,000
	¹²⁹ I	24	<1	22	<1	12	--	--	--	--	--	58
	¹³⁷ Cs	11,000,000	5,300	11,000,000	25,000	3,900,000	100,000,000	1,800	21,000	23,000	46,000	130,000,000
	¹⁵¹ Sm	650,000	87	170,000	200	400,000	--	--	--	--	--	1,200,000
	²³⁸ U	470	2	2	<1	47	--	2	49	4	5	58
	^{239,240} Pu	27,000	<1	110	3	6,200	--	14,000	25,000(d)	24,000	27,000	120,000
	²⁴¹ Am	28,000	8	16,000	160	330,000	--	3,900	7,200	1,400	5,400	390,000

(a) Radionuclides (with half-lives greater than 20 years) were selected for presentation based on an expectation of significant contribution to population dose or the fact that they might otherwise be of interest. Quantities are decayed to end of 1995.

(b) Based on a 50:50 distribution of soluble radionuclides in solution between single-shell and double-shell tanks; constitutes a best estimate of inventory split between tank classes. (See Tables P.7 through P.11 for a more conservative treatment used in dose calculations.)

(c) Dashes indicate no value reported in Rockwell 1985.

(d) A recently completed study (DOE 1986a), which examined records of inactive waste disposal locations on the Hanford Site, showed that two 618 sites (618-1 and 618-2) each contained 1.0 g of plutonium, rather than the previously listed 1000 g (Rockwell 1985). As a result of this lower quantity, both sites are now designated as low-level waste sites (Rockwell 1987).

TABLE P.21. Inventory (Ci) and Location of Selected Radionuclides^(a) for the Reference Disposal Alternative^(b)

	To Near-Surface Disposal with Barrier and Marker System										
	Existing Tank Waste ^(c)		Future			Existing		Future		TRU	Total
	Single-Shell Tank Waste	Double-Shell Tank Waste	Double-Shell Tanks	Total Remaining In Tanks	Double-Shell Tank Grout	Double-Shell Tank Grout	Total In Grout	Contaminated Soil Site	Pre-1970 Burial	Disposed of Near Surface	
¹⁴ C	3,000	1	<1	3,000	2,000	280	2,300	--(d)	1	5,300	
⁷⁵ Se	800	<1	<1	800	100	230	330	--	--	1,100	
⁹⁰ Sr	42,000,000	4,100	21,000	42,000,000	820,000	1,400,000	2,200,000	3,400	19,000	44,000,000	
⁹⁹ Tc	16,000	7	2	16,000	14,000	4,800	19,000	--	--	35,000	
¹²⁹ I	24	<1	<1	24	22	12	34	--	--	58	
¹³⁷ Cs	11,000,000	5,300	25,000	11,000,000	11,000,000	4,100,000	15,000,000	1,800	19,000	26,000,000	
¹⁵¹ Sm	650,000	85	200	650,000	170,000	12,000	29,000	--	--	680,000	
²³⁸ U	470	2	<1	470	<1	39	39	2	49	560	
^{239,240} Pu	27,000	<1	3	27,000	11	650	660	14,000	24,000(e)	66,000	
²⁴¹ Am	28,000	8	165	28,000	1,600	16,000	17,000	3,900	6,900	56,000	
To Geologic Repository											
	Retrievably Stored TRU	Newly Generated TRU	Existing Double-Shell Tank Glass	Future Double-Shell Tank Glass	Total In Glass	Sr/Cs Capsules	Total in Repository	Total Inventory (rounded)			
¹⁴ C	2	2	0	0	0	--	0	5,300			
⁷⁵ Se	--	--	0	4	4	--	4	1,100			
⁹⁰ Sr	22,000	45,000	7,400,000	41,000,000	48,000,000	31,000,000	79,000,000	120,000,000			
⁹⁹ Tc	--	--	0	0	0	--	0	35,000			
¹²⁹ I	--	--	0	0	0	--	0	58			
¹³⁷ Cs	23,000	47,000	0	46,000,000	46,000,000	53,000,000	99,000,000	130,000,000			
¹⁵¹ Sm	--	--	150,000	380,000	380,000	--	530,000	1,200,000			
²³⁸ U	4	5	2	8	10	--	19	580			
^{239,240} Pu	24,000	28,000	90	5,600	6,000	--	58,000	120,000			
²⁴¹ Am	1,400	5,600	14,000	320,000	330,000	--	340,000	390,000			

(a) Radionuclides (with half-lives greater than 20 years) were selected for presentation based on an expectation of significant contribution to population dose or the fact that they might otherwise be of interest. Quantities decayed to end of 1995.

(b) The reference alternative represents a bounding case for the preferred alternative.

(c) Based on a 50:50 distribution of soluble radionuclides in solution between single-shell and double-shell tanks; constitutes a best estimate of inventory split between tank classes. (See Tables P.17 through P.11 for a more conservative treatment used in dose calculations.)

(d) Dashes indicate no value reported in Rockwell 1985.

(e) A recently completed study (DOE 1986a), which examined records of inactive waste disposal locations on the Hanford Site, showed that two 618 sites (618-1 and 618-2) each contained 1.0 g of plutonium, rather than the previously listed 1000 g (Rockwell 1985). As a result of this lower quantity, both sites are now designated as low-level waste sites (Rockwell 1987).

**TABLE P.22. Inventory (Ci) and Location of Selected Radionuclides^(a) for the No Disposal Action Alternative
(continued storage)**

	Existing Tank Waste ^(b)			Future Double-Shell Tank Waste	Encapsulated Waste in DWSF	TRU-Contaminated Soil Sites	Pre-1970 Buried TRU	Retrievably Stored TRU Waste	Newly Generated TRU Waste	Total Inventory (rounded)
	Single-Shell Tank Waste	Double-Shell Tank Waste	Total							
14C	3,000	2,000	5,000	280	--(c)	--	1	2	2	5,300
79Se	800	100	900	230	--	--	--	--	--	1,100
90Sr	42,000,000	8,200,000	50,000,000	42,000,000	31,000,000	3,400	20,000	22,000	44,000	120,000,000
99Tc	16,000	14,000	30,000	4,800	--	--	--	--	--	35,000
129I	24	22	46	12	--	--	--	--	--	58
137Cs	11,000,000	11,000,000	22,000,000	51,000,000	53,000,000	1,800	21,000	23,000	46,000	130,000,000
151Sm	650,000	170,000	820,000	400,000	--	--	--	--	--	1,200,000
238U	470	2	470	47	--	2	49	4	5	580
239,240Pu	27,000	110	27,000	6,200	--	14,000	25,000(d)	24,000	27,000	120,000
241Am	28,000	16,000	44,000	330,000	--	3,900	7,200	1,400	5,400	390,000

(a) Radionuclides (with half-lives greater than 20 years) were selected for presentation based on an expectation of significant contribution to population dose or the fact that they might otherwise be of interest. Quantities decayed to end of 1995.

(b) Based on a 50:50 distribution of soluble radionuclides in solution between single-shell and double-shell tanks; constitutes a best estimate of inventory split between tank classes. (See Tables P.7 through P.11 for a more conservative treatment used in dose calculations.)

(c) Dashes indicate no value reported in Rockwell 1985.

(d) A recently completed study (DOE 1986a), which examined records of inactive waste disposal locations on the Hanford Site, showed that two 618 sites (618-1 and 618-2) each contained 1.0 g of plutonium, rather than the previously listed 1000 g (Rockwell 1985). As a result of this lower quantity, both sites are now designated as low-level waste sites (Rockwell 1987).

TABLE P.23. Summary of Release Model Data: Salt Cake and Sludge in Single-Shell Tanks

Disposal Alternative (a)	Area	Radionuclide	Infiltration Rate, cm/yr	Area, m ²	Inventory (c)
<u>Direct Leaching</u>					
NDA	200E	A11	0.5, 5	2.7×10^4	P.7
	200W	A11	0.5, 5	3.4×10^4	P.7
IPSD, RD	200E	A11	0.1, 15	50%, 10% of 2.7×10^4	50%, 10% of P.7
	200W	A11	0.1, 15	50%, 10% of 3.4×10^4	50%, 10% of P.7
GD	200E	A11	0.1, 15	50%, 10% of 2.7×10^4	2.5%, 0.5% of P.7
	200W	A11	0.1, 15	50%, 10% of 3.4×10^4	2.5%, 0.5% of P.7
<u>Indirect or Diffusion-Controlled Leaching (b)</u>					
IPSD, RD	200E	A11	0.5	--	P.7
	200E	A11	5	--	P.7, 50% of P.7
	200W	A11	0.5	--	P.7
	200W	A11	5	--	P.7, 50% of P.7
GD	200E	A11	0.5	--	5%, P.7
	200E	A11	5	--	5%, 2.5% of P.7
	200W	A11	0.5	--	5%, P.7
	200W	A11	5	--	5%, 25% of P.7

(a) NDA = no disposal action

IPSD = in-place stabilization and disposal alternative

GD = geologic disposal alternative

RD = reference disposal alternative.

(b) The bulk of the PSD and GD inventories leach by diffusion from beneath a protective barrier. Data relevant to the diffusion-controlled pathway are given in Table P.3.

(c) Inventory cross-referenced to Table P.7.

TABLE P.24. Summary of Release Model Data: Liquid

<u>Disposal Alternative(a)</u>	<u>Area</u>	<u>Radionuclide</u>	<u>Infiltration Rate, cm/yr</u>	<u>Thickness, m</u>	<u>Area, m²</u>	<u>Inventory(b)</u>
Existing DST for All Disposal Alternatives	200E	A11	0.5 5, 15, (c) 0.1(c)	1 1	29.7 24.4	0.05%, P.9
	200W	A11	0.5 5, 15, 0.1	1 1	29.7 24.4	
Future DST for All Disposal Alternatives	200E	A11	0.5 5, 15, 0.1	1 1	29.7 24.4	0.05%, P.10
	200W	A11	0.5 5	64 64	10,200 8,410	
No Disposal Action (existing)	200E	A11	0.5 5	64 64	2,800 2,290	
	200W	A11	0.5 5	64 64	13,000 10,700	P.10
No Disposal Action (future)	200E	A11	0.5 5	64 64	13,000 10,700	P.10

(a) DST = double-shell tanks.

(b) Inventory cross-referenced to Tables P.9 and P.10.

(c) 10% of the applicable inventory and area are leached in the disruptive failure scenario, and 50% of the applicable inventory and area are leached in the functional failure scenario.

TABLE P.25. Summary of Release Model Data: Grout

Disposal (a) Alternative	Area	Radionuclide	Infiltration Rate, cm/yr	Release Model		Inventory (b)
				Leach Rate Controlled	Diffusion Pathway Controlled	
GD	200E	A11	0.5, 5 15 0.1	X X	X	Column 1, P.8 10% Column 1, P.8 50% Column 1, P.8
GD	200E	A11	0.5, 5 15 0.1	X X	X	Column 1, P.11 10% Column 1, P.11 50% Column 1, P.11
IPSD	200E	A11	0.5, 5 15 0.1	X X	X	Column 2, P.8 10% Column 2, P.8 50% Column 2, P.8
IPSD	200E	A11	0.5, 5 15 0.1	X X	X	Column 2, P.11 10% Column 2, P.11 50% Column 2, P.11
RD	200E	A11	0.5, 5 15 0.1	X X	X	Column 3, P.8 10% Column 3, P.8 50% Column 3, P.8
RD	200E	A11	0.5, 5 15 0.1	X X	X	Column 3, P.11 10% Column 3, P.11 50% Column 3, P.11

- (a) GD = geologic disposal alternative
 IPSD = in-place stabilization and disposal alternative
 RD = reference disposal alternative.
 (b) Inventory cross-referenced to Tables P.8 and P.11.

TABLE P.26. Summary of Release Model Data of TRU Waste for No Disposal Action

Waste Form	Area	Radionuclide	C ₀ , Ci/L	Area, m ²	h, m	β , g/cm ³	K _d , mL/g	Inventory (a)
Soil Sites	200E	90Sr			1/3	1.8	0.64	Column 1,
		137Cs			1/3	1.8	26	P.13
	200W	239Pu	2.6×10^{-7}	1.7×10^3				
		241Am	1.5×10^{-8}	1.7×10^3				
Pre-1970 Burial	200E	90Sr			1/3	1.8	0.64	Column 2,
		137Cs			1/3	1.8	26	P.13
	200W	239Pu	2.6×10^{-7}	2.5×10^4				
		241Am	1.5×10^{-8}	2.5×10^4				
Retrievably Stored	200E	90Sr			1/3	1.8	0.64	Column 3,
		137Cs			1/3	1.8	26	P.13
	200W	239Pu	2.6×10^{-7}	6.3×10^3				
		241Am	1.5×10^{-8}	6.3×10^3				
Newly Generated	200W	90Sr			1/3	1.8	0.64	Column 6,
		137Cs			1/3	1.8	26	P.13
		237Np			1/3	1.8	26	
		239Pu	2.6×10^{-7}	2.3×10^4				
		241Am	1.5×10^{-8}	2.3×10^4				
	200W	14C			1/3	1.8	0	Column 7,
		90Sr			1/3	1.8	0.64	P.13
		237Np			1/3	1.8	16	

(a) Inventory cross-referenced to Table P.13.

TABLE P.27. Distribution Coefficients (mL/g) and Decay Half-Lives (yr) Used in the Leach and Transport Models

Radionuclide	Half-Life, yr ^(a)	Grout (dilute, noncomplexed)	Grout (dilute, complexed)	TRU (dilute, noncomplexed)	Salt Cake and Sludge (complexed) Diffusion Zone (concentrated)	Advection Zone (dilute)
¹⁴ C	5.73×10^3	0	0	0	0	0
⁷⁵ Se	6.5×10^4	3.3	3.3	--	3.3	3.3
⁹⁰ Sr ^(b)	29	0.64	0.39	0.64	0.022	0.39
⁹⁹ Tc	2.13×10^5	0	0	--	0	0
¹²⁹ I	1.6×10^7	0	0	--	0	0
¹³⁷ Cs	30.17	26	26	26	26	26
¹⁵¹ Sm	90	76	5.6	--	5.6	5.6
²³⁷ Np ^(b)	2.14×10^6	16	8.7	16	3.9	8.7
²³⁹ Pu ^(b)	2.411×10^4	71	21	71	0.63	21
²⁴¹ Am ^(b)	432	76	5.6	76	5.6	5.6

(a) From Walker, Miller, and Feiner 1983.

(b) From Delegard and Barney 1983.

P.5 REFERENCES

- Barney, G. S. 1976. Vapor-Liquid-Solid Phase Equilibria of Radioactive Sodium Salt Wastes at Hanford. ARH-ST-133, Atlantic Richfield Hanford Company, Richland, Washington.
- Bryan, G. H., and J. R. Divine. 1985. Cesium Chloride Compatibility Testing Program Annual Report-Fiscal Year 1984. PNL-5341, Pacific Northwest Laboratory, Richland, Washington.
- Council on Environmental Quality. 1981. Memorandum 46 FR 18026. Washington, D.C.
- DeFigh-Price, C. 1982. Status of Tank-Assessment Studies for Continued In-Tank Storage of Hanford Defense Waste. RHO-RE-ST-4 P, Rockwell Hanford Operations, Richland, Washington.
- Delegard, C. H., and G. S. Barney. 1983. Effect of Hanford High-Level Waste Components on Sorption of Cobalt, Strontium, Neptunium, Plutonium, and Americium on Hanford Sediments. RHO-RE-ST-1 P, Rockwell Hanford Operations, Richland, Washington.
- Department of Energy (DOE). 1986a. Draft Phase I Installation Assessment of Inactive Waste-Disposal Sites at Hanford. Washington, D.C.
- Department of Energy (DOE). 1986b. Interim Hanford Waste Management Plan. DOE/RL/0103D-T5, Richland Operations Office, Richland, Washington.
- Gardner, W. R. 1965. "Movement of Nitrogen in Soil." In Soil Nitrogen, ed. W. V. Bartholomew, and F. E. Clark. American Society of Agronomy, pp. 551-572.
- Gee, G. W., and R. R. Kirkham. 1984. Arid Site Water Balance: Evapotranspiration Modeling and Measurements. PNL-5177, Pacific Northwest Laboratory, Richland, Washington.
- Godbee, H. W., E. L. Compere, D. S. Joy, A. H. Kibbey, J. G. Moore, C. W. Nestor, Jr., O. U. Anders and R. M. Neilson, Jr. 1980. "Application of Mass Transport Theory to the Leaching of Radionuclides from Waste Solids." Nuclear and Chemical Waste Management 1:29-35.
- Kukla, G. K. 1979. "Probability of Expected Climate Stresses in North America in the Next One Million Years." In Summary of FY-1978 Consultant Input for Scenario Methodology Development, eds. B. L. Scott et al. PNL-2851, Pacific Northwest Laboratory, Richland, Washington.
- Lindsay, W. L. 1979. Chemical Equilibria in Soils. John Wiley and Sons, New York.
- Moore, J. G., H. W. Godbee and A. H. Kibbey. 1977. "Leach Behavior of Hydrofracture Grout Incorporating Radioactive Wastes." Nuclear Technology 32:39-52.
- Rai, D., R. J. Serne and D. A. Moore. 1980. "Solubility of Plutonium Compounds and Their Behavior in Soils." Soil Science Soc. Am. J. 44(3):490-495.
- Rai, D., R. G. Strickert, D. A. Moore and R. J. Serne. 1981. "Influence of an Americium Solid Phase on Americium Concentrations in Solutions." Geochim. Cosmochim. Acta 45(11):2257-2265.
- Rai, D., J. M. Zachara, A. P. Schwab, R. L. Schmidt, D. C. Girvin and J. E. Rogers. 1984. Chemical Attenuation Rates, Coefficients, and Constants in Leachate Migration, Volume 1: A Critical Review. EPRI-EA-3356, Vol. 1, Electric Power Research Institute, Palo Alto, California.
- Rockwell Hanford Operations. 1985. Hanford Defense Waste Disposal Alternatives: Engineering Support Data for the HDW-EIS. RHO-RE-ST-30 P, Richland, Washington.
- Rockwell Hanford Operations. 1987. Engineering Support Data Update for the Hanford Defense Waste-Environmental Impact Statement. RHO-RE-ST-30 ADD P, Richland, Washington.
- Rockwell Hanford Operations and Kaiser Engineers. 1979. Dry Well Storage Facility Conceptual Design Study. RHO-C-25, Vol. 1, Rockwell Hanford Operations, Richland, Washington.

Routson, R. C., G. S. Barney, R. M. Smith, C. H. Delegard and L. Jensen. 1981. Fission Product Sorption Parameters for Hanford 200 Area Sediment Types. RHO-ST-35, Rockwell Hanford Operations, Richland, Washington.

Schulz, W. W. 1980. Removal of Radionuclides from Hanford Defense Waste Solutions. RHO-SA-51, Rockwell Hanford Operations, Richland, Washington.

U.S. Code of Federal Regulations (CFR), Title 40, Part 1500-1517. Council on Environmental Quality. 1985. "Regulations for Implementing the Procedural Provisions of the National Environmental Policy Act." U.S. Government Printing Office, Washington, D.C.

Walker, F. W., D. G. Miller and F. Feiner. Revised 1983. Chart of the Nuclides. General Electric Company, San Jose, California.

West, J. M., N. Christofi and I. G. McKinley. 1985. "An Overview of Recent Microbiological Research Relevant to the Geologic Disposal of Nuclear Waste." Radioactive Waste Management and the Nuclear Fuel Cycle: 6(1)79-95.

**THIS PAGE INTENTIONALLY
LEFT BLANK**

APPENDIX Q

APPLICATION OF GEOHYDROLOGIC MODELS TO POSTULATED RELEASE
SCENARIOS FOR THE HANFORD SITE

**THIS PAGE INTENTIONALLY
LEFT BLANK**

APPENDIX Q

APPLICATION OF GEOHYDROLOGIC MODELS TO POSTULATED RELEASE SCENARIOS FOR THE HANFORD SITE

Q.1 INTRODUCTION

A series of groundwater pathway analyses for each of the alternatives was made using a combination of hydrologic and transport models. The source terms and their releases for the various alternatives are contained in Appendix P, where the inventories and each individual case involving a groundwater pathway are described.

The two-dimensional groundwater computer model (VTT) (Reisenauer 1979) and the one-dimensional transport model (TRANSS), used in these analyses, are described in Appendix O. Their application to the Hanford waste disposal sites is described here. The scenarios investigated cover a 10,000-year period beginning in the year 2150. Two climatic conditions were assumed: 1) the current climate, in which the upper bound of average annual groundwater recharge beneath the 200 Areas plateau with no protective barrier, is represented by 0.5 cm/yr (the lower bound is zero; see discussion in Appendix M); and 2) a wetter climate with an average annual recharge of 5 cm/yr assuming no protective barrier. Two types of environmental contact with the contaminant plume were studied: 1) a hypothetical domestic well located 5 km from the 200 Areas fence and 2) groundwater entering the Columbia River. The radionuclide concentrations (in curies per liter) and discharge flux (curies per year) were calculated for these locations and are reported in this appendix. These data were used to calculate long-term doses to individuals on site and to downstream Columbia River populations (see Appendix R and Chapter 5 of Volume 1). Hazardous chemicals are discussed in Appendix U. Integrated flux for each alternative was calculated, and the results are found in Appendix R.

The variety of disposal options requires that several different modeling techniques be used to study the transport of radionuclides through the groundwater pathway. Each of the following applies in various combinations, depending upon whether or not there is a protective barrier: 1) a diffusion model in the unsaturated soil beneath the barrier, 2) an advection model in the unsaturated soil for the no-barrier case and barrier failure scenarios, and 3) an advection model in the unconfined aquifer. These are discussed in detail in Appendix O.

Q.2 SCENARIOS AND ASSUMPTIONS

Scenarios of climate conditions considered as part of this study include assumed cases of 0.5- and 5-cm/yr infiltration applied uniformly over the Site. For studying postdisposal impacts, it was assumed that the Hanford Site would be abandoned after the year 2150 (see

Volume 1). In the future, as facilities are shut down, the disposal of large volumes of cooling and waste waters at Hanford will stop. These artificial recharges have, over the life of the Hanford Project, raised the water table more than 9 m near the 200 East Area and 26 m in the 200 West Area (Graham et al. 1981).

The postulated scenarios for the migration of radionuclides contain the following assumptions:

- The current water disposal ponds have been decommissioned by the year 2100, and a new water table is established.
- Scenario 1. A 0.5-cm/yr maximum infiltration rate is assumed and modeled as typical of the current climate.
- Scenario 2. A climatic change occurs for the Columbia Plateau which increases the annual precipitation to 30.1 cm/yr and the annual average infiltration and groundwater recharge on the 200 Areas plateau and the Hanford Site in general to 5 cm/yr. This is modeled as indicative of a wetter climate.

Disruptive Barrier Failure: In this climate scenario, protective barriers over waste are assumed partially to fail. Soil is removed by a hypothetical unspecified mechanism, exposing a percentage of the rock riprap to the weather, which leads to 10% of the underlying waste inventory being contacted by 15 cm/yr infiltration. This amounts to 50% of the incident precipitation being trapped by the riprap catchment (see Appendix P). The enhanced infiltration results from spring and fall precipitation penetrating the bare rock barrier where it is inaccessible to plant roots and direct solar radiation for evapotranspiration and evaporation. The assumption was made that as much as 50% of the future climate precipitation would infiltrate beneath the bare rock portion of the barrier. This is referred to as a "disruptive barrier failure," and is assumed to occur 500 years after barrier placement.

Functional Barrier Failure: A second barrier failure mode is analyzed in which it is assumed that, for whatever reason, 50% of the barriers over the waste forms partially fail (leak) in such a way that 50% of the waste inventories are exposed to 0.1 cm/yr infiltration beneath the barrier.

Q.3 VADOSE-ZONE MODELING

Few site-specific data on soils were available from which to estimate travel time for water passing through the unsaturated zone on the 200 Areas plateau for various infiltration rates. To avoid gross error, the following approach was used. A 5-gallon sample was taken from each of six major soil horizons visible in the 15-m-deep Hanford 241-AP tank farm excavation. Laboratory analyses provided particle-size distributions, saturated hydraulic conductivity, and water-retention characteristics. Replicate measurements were made on each

sample. These data were matched according to particle size and geologic soil type with a generalized stratigraphic column of the soils extending to the water table beneath the nearby 216-A-8 and 216-A-37 200 East Area cribs (Fecht et al. 1979). Actual data on soils deeper than 15 m were not available. Travel-time calculations were made on this postulated column with several soil variations.

Travel times for water to move through a soil profile can be estimated for a given flux, q , when assuming a unit hydraulic gradient and steady-state infiltration. For layered soils the travel time is a summation of travel times through each layer. The equation used for determining total time, T , is discussed in Appendices M and O and can be written as:

$$T = \sum_i^j (\theta_i t_i / q) \quad (Q.1)$$

where q = the assumed steady-state flux

i = the index of the soil layer

j = the number of layers

θ_i = the water content of soil layer i for flux q

t_i = thickness of each soil layer.

The rate at which water can travel through an unsaturated (vadose) zone is extremely sensitive to the moisture content of the sediment. A one or two percent increase in moisture content can affect water travel times by an order of magnitude. Under future climates the nominal depth to the water table from the bottom of waste storage tanks and proposed grout disposal vaults is estimated at between 60 and 68 m. An average of 64 m was assumed for these analyses. Travel time for water to move this distance through the layered, unsaturated soil system varies from 99 to 149 years for the 5-cm/yr recharge case, depending on the choice of the soil layer combinations and thicknesses. Travel times also were calculated for the 0.5-cm/yr recharge indicative of current climatic conditions. Water travel times for these conditions ranged from 800 to 1,200 years and averaged 970 years. Because of the lack of detailed soil data, the travel times in the vadose zone are assumed to be 100 years for the 5-cm/yr flux and 925 years for 0.5-cm/yr flux through the vadose zone under drier conditions. For the barrier failures, travel times of the water from the waste forms to the water table were estimated to be 76 years for the 15-cm/yr infiltration and 4,200 years for the 0.1-cm/yr infiltration. The listing on page Q.4 summarizes the travel time data for the unsaturated zone from the waste form to the water table.

The analysis is based on the infiltration characteristics and travel times of water for the soil stratigraphy of the region east of 200 East Area. The 200 West Area is known to have different soils and exhibits greater stratigraphic heterogeneity than does the 200 East Area. Since soils data for 200 West Area are not available for a significant portion of the soil profile, we assumed that the above data on travel times applied to both areas for these analyses. The presence of significant thicknesses of wind-deposited silts and sands and the

<u>Assumed Infiltration, cm/yr</u>	<u>Thickness of Vadose Zone Used, m</u>	<u>Water Travel Time Through Vadose Zone, yr</u>
0.0	68-75	Infinite
0.1(a)	64	4,200
0.5	64	925
5.0	64	100
15.0(a)	64	76

(a) Water table height still established by 5-cm/yr recharge (64 m).

presence of caliche layers (Tallman et al. 1979) suggests longer travel times in a strictly one-dimensional unsaturated zone underlying the 200 West Area. However, due to a lack of data, we elected to assume no credit for the potentially longer travel times under the 200 West Area.

Q.4 AQUIFER MODELING

The central portion of the Hanford Site is bounded on the north and east by the Columbia River and on the western part of the southern boundary by the Yakima River. The Rattlesnake Hills lie along the remainder of the southern boundary. At the western boundary lie the terminus of the Yakima and Umtanum Ridges and their inner valley. These ridges, hills, and valleys constitute a sizable recharge area that supplies groundwater flow to the aquifer system beneath the Site. On occasion, under extreme snow-melt conditions, some limited overland flow occurs and quickly infiltrates. Chapter 4 of Volume 1 of this EIS discusses the Hanford Site geology and hydrology. The conceptual model of the unconfined aquifer used for the contaminant pathways analysis is a modification of the present Hanford conceptual model discussed in Appendix O.

The quantity of recharge changes the water volume and flow rate through the vadose (unsaturated) zone and then laterally in the unconfined Hanford aquifer system leading to the river. In areas where an increase in precipitation would cause intermittent surface water run-off and enhanced localized recharge (e.g., basalt outcroppings), the cumulative water flow was assumed to enter the groundwater system at the edges of the Hanford aquifer. The quantity of water corresponding to the 0.5-cm/yr and the 5-cm/yr infiltration scenarios was accumulated from the north slope of Rattlesnake Hills and Ory Creek Valley (an area of about 260 km²). These water volumes were distributed to the southwest boundary of the respective hydrological conceptual models. On the west side of the aquifer the increase accumulated from about 140 km² of watershed from Yakima Ridge and Cold Creek Valley and was applied as supplementary flow to that continually crossing the present flow boundary. The flanks of Gable Mountain and Gable Butte and the terminus of Umtanum Ridge also accumulated water that was applied to the aquifer at these boundaries.

Under the uniform 0.5-cm/yr infiltration, relatively dry climate scenario, the water table drops to near a pre-Hanford (1945) level condition. The largest influence on the water

table will occur from underground flows originating in the offsite irrigated area in the Cold Creek Valley. Flow in the unconfined aquifer moves from the Cold Creek area across the Hanford Site in an easterly direction toward the Columbia River. Because of the lowered water table, the thickness of the unconfined aquifer decreases and the basalt outcrops extending above the water table become larger. One of these outcrops, just north of 200 East Area, extends beneath TRU solid waste burial grounds and some tank farms. To account for disposal directly above this feature, it was assumed any infiltrating water or leachate would drain off the basalt and enter the aquifer at its nearest contact edge. Groundwater streamlines and travel times were generated from these locations in this scenario, as presented in Figure Q.1.

Modeling the 5-cm/yr infiltration case produces a higher water table. Comparing the water table of the 5-cm/yr annual average recharge scenario with a recent water table map of the unconfined aquifer shows that the water table contours are generally higher with the wetter climate. Under the 200 East Area the increase is about 3 m over a 1983 water table; under 200 West Area the increase ranges from zero under 216-U-10 Pond to 6 m in the northwest corner. The rise of the water table due to the future climate scenario was not enough to intercept the topographic surface and form permanent streams or lakes in the low areas around Gable Mountain or in Cold Creek Valley. For a point of comparison the contours and streamlines indicating direction of flow paths for a 1983 simulated water table are shown in Figure Q.2.

The significant feature of the water table resulting from a 5-cm/yr annual average recharge is that a groundwater flow divide develops under the broad plain southeast of the 200 Areas plateau. This divide causes a major shift in the streamlines from the 200 Areas disposal sites (contours shown in Figure Q.3). Under the postulated future climate change scenario (5-cm/yr recharge), those streamlines originating at the disposal sites indicate that the direction of flow is through the gap between Gable Mountain and Gable Butte before entering the river. For the 0.5-cm/yr case, water beneath both the 200 East and 200 West Areas follows streamlines, shown in Figure Q.1, to the southeast, entering the Columbia River along the eastern edge of the Site, similar to the present groundwater flow pattern (see Figure Q.2).

Solute or contaminant transport modeling was of two fundamentally different types: 1) diffusion only, no advection from the waste to the water table for a site with a properly functioning protective barrier, and 2) advection from the waste to the water table for cases with either no barrier or an improperly functioning barrier. The following discussion on solute transport modeling is focused on the advection case(s).

To calculate contaminant transport vertically through the unsaturated (vadose) zone and then laterally in the aquifer to the river, a streamtube approach was used. The lateral spread of contaminants in the aquifer was determined by calculating streamlines from the edges of the waste site. This assumes little lateral spreading as the leachate travels

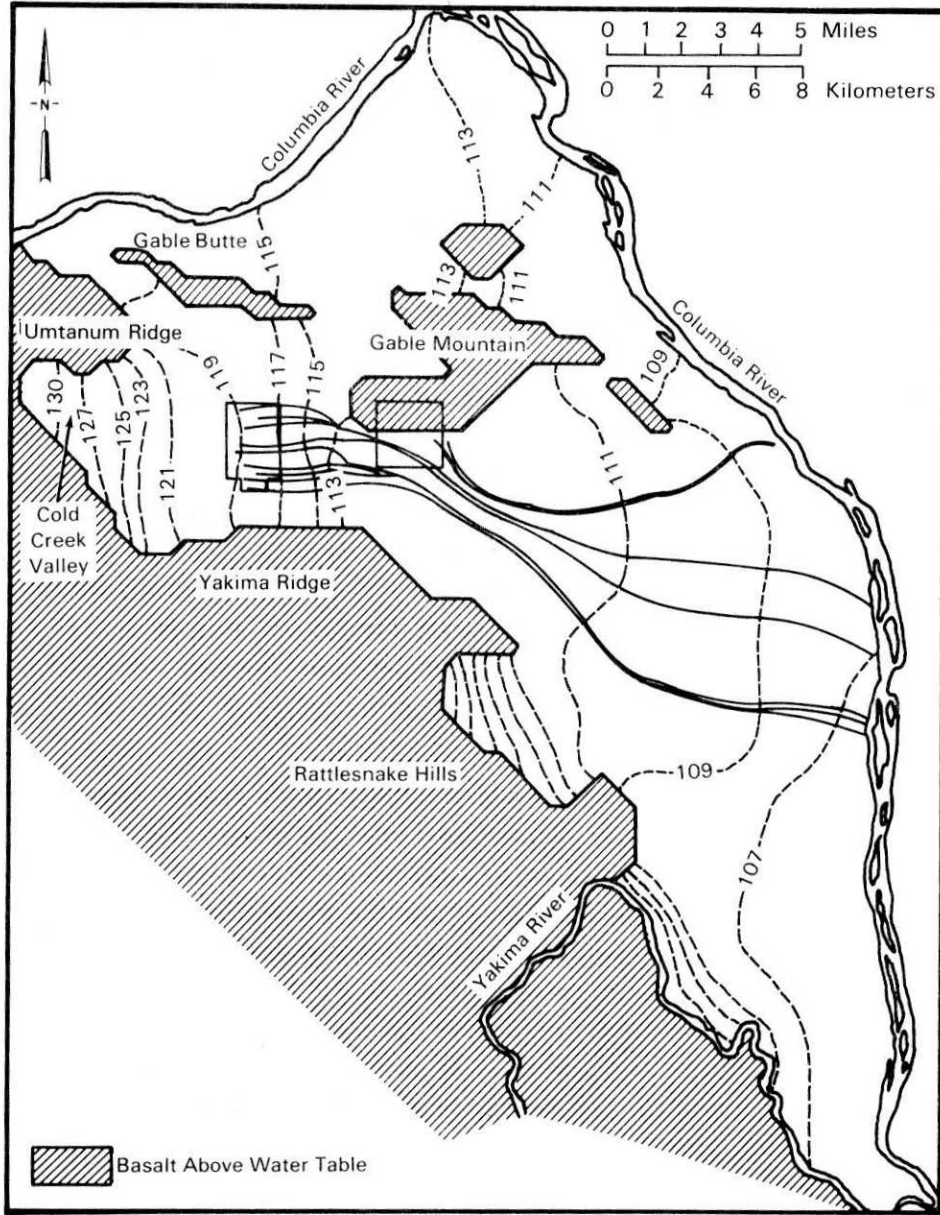


FIGURE Q.1. Groundwater Contours (in meters above MSL) and Streamlines from the 200 Areas Waste Sites to the River, Assuming Steady-State Conditions, 0.5-cm/yr Recharge, and No Pond Disposals (artificial recharge)

downward from the waste sites to the water table. A number of streamlines were calculated in the aquifer inside each streamtube from the source to the accessible environment (e.g., 5-km well and/or river).

The aquifer model calculates the groundwater velocities along the streamlines. Along any flow path, the velocity variation is related to the hydraulic gradient, the hydraulic conductivity and the effective porosity encountered. Thus, each streamline or each sector of

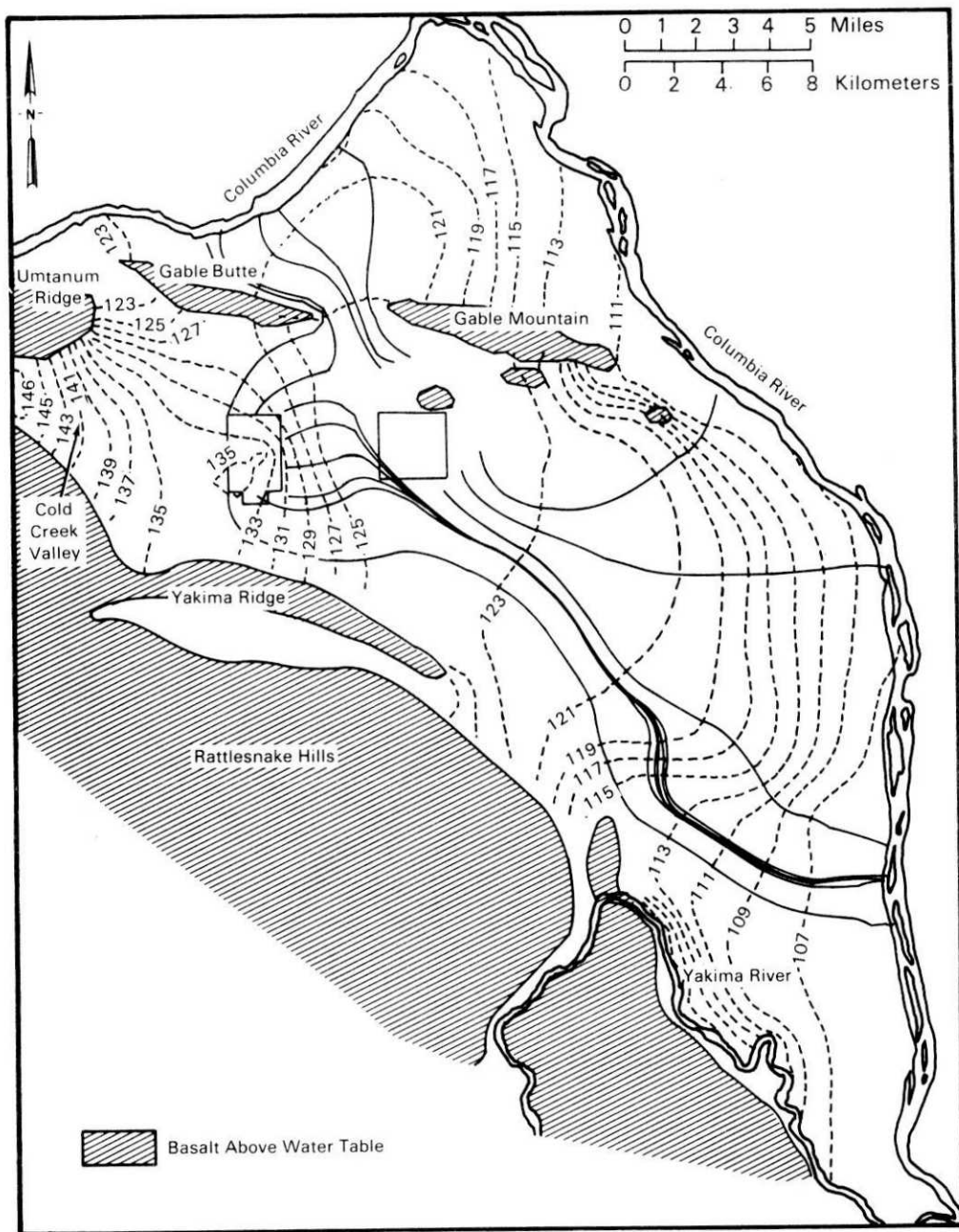


FIGURE Q.2. Water-Table Contour Map of the Hanford Unconfined Aquifer with Streamlines Indicating Direction of Flow from the 200 Areas Plateau (simulated 1983 conditions). Contours in meters above MSL.

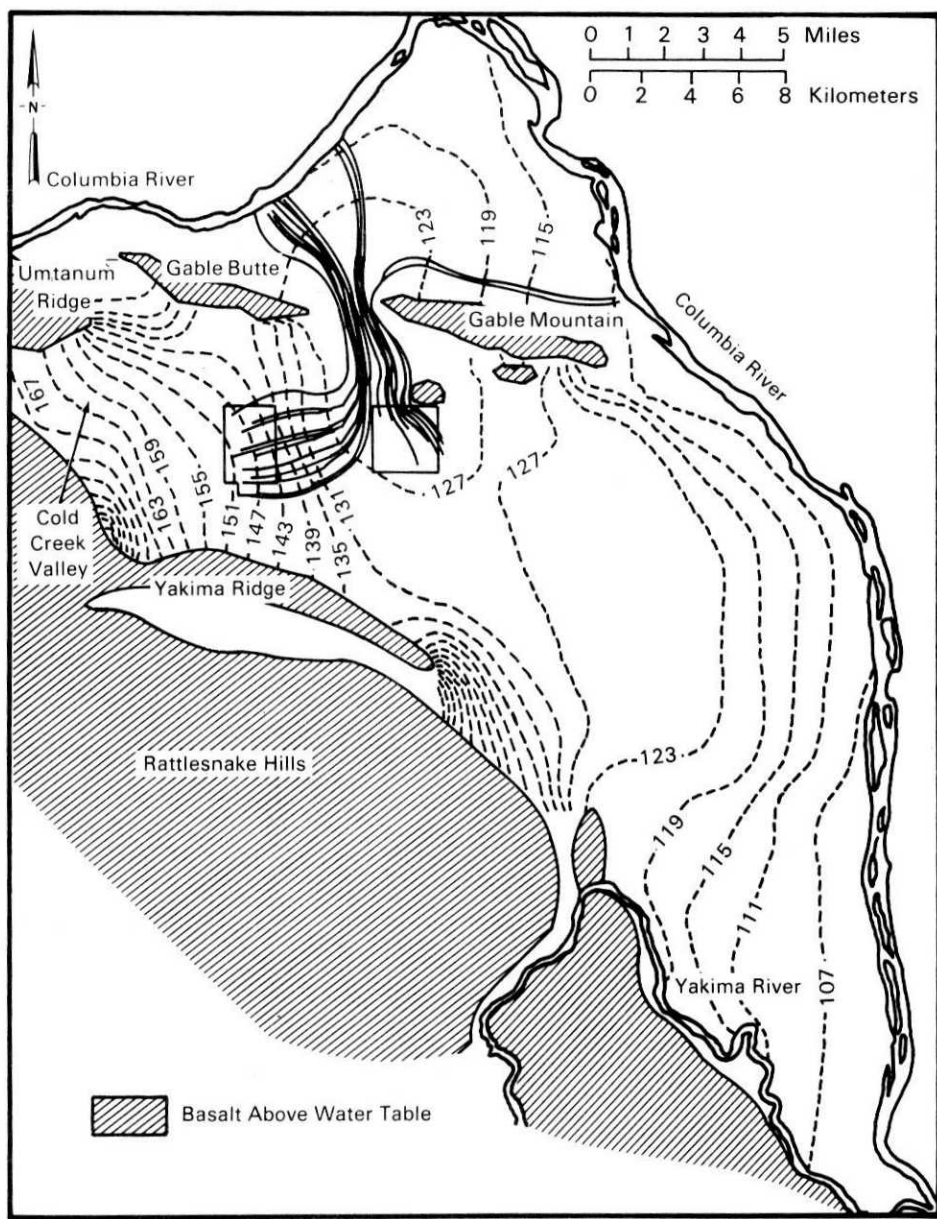


FIGURE Q.3. Groundwater Contours (meters above MSL) and Streamlines Showing Flow from Waste Sites in 200 East and 200 West Areas with 5-cm/yr Annual Average Recharge Scenario

a given streamline is likely to have a different velocity. The transport model uses a suite of travel times and streamlines in a given flow path to arrive at an average groundwater velocity. Typical groundwater velocities are shown in the table below for a variety of starting locations:

	Typical Average Groundwater Velocities, m/yr	
	Wetter Climate (5 cm/yr)	Current Climate (0.5 cm/yr)
200 West (tank farm average) to the 5-km well	760	104
200 West (tank farm average) to the Columbia River	235	31
200 East (tank farm average) to the 5-km well	1200	145
200 East (tank farm average) to the Columbia River	790	66

This is but a subset of velocities calculated for the 200 Area disposal sites. In an aquifer system as large and complex as the one under the Hanford Site, velocities are highly variable.

The distance and travel time in the unsaturated zone are included in the transport modeling from a given site. Additionally, for the radionuclides that are retarded by adsorption, the time of travel is multiplied by the retardation factor for each nuclide shown in the results tables. This results in the retarded velocity value of the radionuclide. Radioactive decay is accounted for in both the source term and in the flow system during the time of transport.

In analyzing the potential for contamination of the environment through release of radionuclides, it is useful to compare predicted results to the release limits specified in Section 40 CFR 191.13 of the EPA standards, which relates to radioactive materials released into the accessible environment. Although this EPA standard is designed for deep geologic disposal sites, it is still instructive to apply it to the Hanford Defense Waste EIS analysis. The EPA standard 40 CFR 191 addresses cumulative releases over a 10,000-year period across a hypothetical boundary 5 km from the waste. This 5-km boundary causes some confusion when we consider the size of the 200 Areas plateau, the number of waste sites buried there, and whether or not the site marker boundary should be used in this determination.

Therefore, for the purposes of analysis, a well in the unconfined aquifer, from 3 to 5 km from the cumulative waste sites area, is assumed to be the accessible environment. This eliminates the perception of drilling through a neighboring waste form to a site well 5 km from a given waste site. Since the radionuclides of interest have long half-lives, this assumption is considered reasonable. Travel times for flow in the unsaturated zone and the flow to 5 km in the aquifer for the various release models show that the delay time in the unsaturated zone above the water table dominates the system. Time of travel to the 5-km well in the aquifer itself is relatively unimportant as indicated by the following comparison of travel times.

Scenario	Travel Time in Vadose, yr	Travel Time in Aquifer, yr
0.5-cm/yr Infiltration	~925	~2 to 25
5-cm/yr Infiltration	~100	~1 to 5
Barrier Functioning	$\sim 5 \times 10^3$ to 3×10^6	~1 to 15
Disruptive Barrier Failure	76	~1 to 5
Functional Barrier Failure	~4,200	~1 to 5

Q.5 SOLUTE TRANSPORT ANALYSES

The method of groundwater pathway analysis for migrating contaminants from each waste form follows a pattern. Radionuclides are released from each waste form to the surrounding soil water. The release mechanisms that move contaminants from a waste form to a groundwater pathway are described in Appendix P for each waste form and the various disposal alternatives. The two fundamentally different transport mechanisms in the unsaturated zone are diffusion of contaminants through an essentially immobile soil moisture column (barrier case) and advection of contaminants through the unsaturated zone (no barrier or disturbed case). In either situation, transport in the aquifer is via advection due to the influence of off-site water recharge and discharge conditions.

For the case with a properly functioning protective barrier, contaminants released to the soil water immediately adjacent to a tank or grout vaults beneath a protective barrier are transported through the soil water only by a diffusive mechanism (i.e., response to a chemical concentration gradient) either until it reaches infiltrating water flowing downward past the edge of the barrier or until it reaches the groundwater aquifer. With no protective barrier, downward-advection unsaturated flow is assumed to be the dominant transport mechanism to the groundwater.

Regardless of the dominant transport mechanism, there will be geochemical interactions between the contaminants and the sediments along the path(s). For this EIS analysis, no safety credit was assumed for chemical precipitation. However, for radionuclides that display adsorption on Hanford sediments, a retarded velocity was computed based on the use of a linear distribution coefficient (K_d) model. The advantages and disadvantages of this approach are discussed in Appendix O. The distribution coefficients were applied as single values determined by the geochemistry of the waste form. Chemical speciation was not considered, nor were variations in geochemical conditions along the transport pathways. The K_d values are delineated in Appendix P and their variations are discussed. As a given contaminant enters the aquifer from the vadose zone, it also is dispersed (spread) longitudinally in the groundwater as it is transported down gradient within a streamtube. Such dispersion is due to the considerable variations in travel paths and thus travel times within any given streamtube and varies from one streamtube to another.

Two points of groundwater release to the accessible environment were analyzed: 1) the groundwater flow into the Columbia River and 2) a domestic well assumed to penetrate the aquifer approximately 5 km from the 200 Area fence line. The well is assumed to pump water

containing radionuclides diluted only in the top 5 m of the aquifer. There may be more dilution in reality, but no credit was assumed for this potentially greater mixing depth.

Concentrations (curies per liter) entering the wells are estimated by diluting nuclide flux with a quantity of flow captured in the flow tube defined by the streamlines. The flow-tube size was based on the distance between two streamlines started at opposite edges of the waste form and an assumed 5-m-deep contaminant plume. Such concentration estimates are expected to be greater than those taking into account transverse dispersion with the subsequent additional dilution. Thus the analysis is in this regard conservative. Total radionuclide flux (curies per year) is calculated at the river boundary.

Q.6 RESULTS OF FLOW AND SOLUTE TRANSPORT MODELING

Inventories of the radionuclides assumed for the various disposal alternatives are listed in Tables P.6 through P.15 in Appendix P. The parameters for the various release models that input to the transport simulations are also described in Appendix P. Table Q.1 shows which waste forms apply under the various disposal alternatives. The transport is calculated separately for each case. The analysis results in a curve of concentration versus time for the domestic well or radionuclide flux versus time entering the river. These data are used in calculation of the dose in Appendix R and are finally summarized in Chapter 5 of Volume 1.

TABLE Q.1. Waste Forms for the Various Disposal Alternatives

Disposal Alternative	Waste Form										
	Single-Shell Tanks		Existing Double-Shell Tanks		Future Double-Shell Tanks		Sr/Cs Capsules	Soil	Pre-1970 TRU	Retrievable	New
	Salt and Sludge	Grout	Liquid	Grout	Liquid	Grout					
Geologic Repository	X (c)		X	X	X	X	(a)	(a)	(a)	(a)	(a)
In-Place Stabilization and Disposal	X	(b)	X	X	X	X	X	X	X	X	X
Reference (combination disposal)	X	(b)	X	X	X	X	(a)	X	X	(a)	(a)
No Disposal Action (continued storage)	X	(b)	X	(b)	X	(b)	X	X	X	X	X

(a) Waste sent to repository.

(b) Waste form does not apply to this situation.

(c) X means waste form applies to this alternative.

Because of the number of analyses made, the results are summarized here only by reporting the peak concentration and the time of arrival of this peak concentration at the domestic well. Similarly, the peak flux and its arrival time at the river are shown in summary form. Two generic curves are also shown in Figure Q.4 to clarify the following tables and to lend perspective on the typical shape of the curves of concentration and/or flux as a function of time. The typical curve has a first arrival of very low concentration, then increases to a peak, and then finally decreases as the contaminant plume passes. In some cases the peaks are sharp, and in others (with long release times) the peaks are smaller and the curve shows a long, gradual decline. The entire curve, and not just the peak, is used for calculating dose (Appendix R).

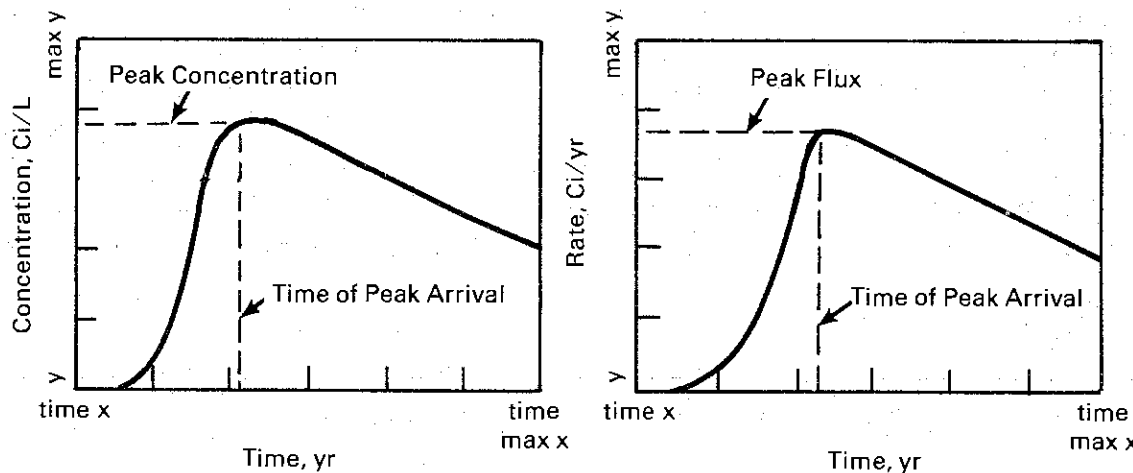


FIGURE Q.4. Generic Curves for Peak Concentration and Peak Flux at Accessible Environment

Q.6.1 Results of the "Current Climate" Simulations

The results of the 0.5-cm/yr recharge scenario (current climate) are presented before those for the 5 cm/yr recharge scenario (wetter climate). The barrier failure results are in separate tables following the wetter climate results for each alternative.

Results of the Geologic Disposal Alternative for the 0.5-cm/yr Recharge

The geologic disposal alternative assumes that most of the defense wastes are disposed off site in a deep geologic repository. Only the residuals of the final processing and packaging remain on site and are placed in near-surface disposal sites. (See Volume 1, Chapter 3 for details.) A description of the waste forms included in the geologic disposal alternative is provided as follows:

Waste Form	Description
Single-Shell Tanks Residual	The bulk of the wastes is shipped off site, but 5% of the salt and sludge remains in the tanks in 200 East and 200 West Areas and the tanks are covered with a barrier.
Single-Shell and Double-Shell Tanks Grout	The liquid containing salts from processing and packaging waste from the tanks is disposed of as low-level grout in the 200 East Area.
Existing Double-Shell Tanks Residual	The liquid residual remaining in the tanks is assumed to contain 0.05% of their original inventory.
Future Double-Shell Tanks Residual	The liquid residual remaining in the tanks of future-generated tank wastes is assumed to contain 0.05% of the original inventory.
Future Double-Shell Tanks Grout	The liquid resulting from processing and packaging future-generated HLW for offsite disposal is disposed of as low-level grout in the 200 East Area.

Table Q.2 summarizes the results by waste form for the geologic disposal alternative.

Results of the In-Place Stabilization and Disposal Alternative for 0.5-cm/yr Recharge

Under the in-place stabilization and disposal alternative, the HLW and TRU would be stabilized in place and isolated from ecosystems by use of protective barriers. Any sites covered with a properly functioning protective barrier are not exposed to recharge, and thus diffusion is the dominant transport mechanism. Processing of wastes would be minimized. This alternative results in eight additional cases, as listed below.

Waste Form	Description
Single-Shell Tanks	Salt and sludge in the tanks in both 200 East and 200 West Areas are left in place, stabilized, and covered with barriers.
Existing Double-Shell Tanks Grout	Existing liquids are immobilized and disposed of as grout in vaults in 200 East Area.
Future Double-Shell Tanks Grout	Future HLW liquids are immobilized and disposed of as grout in vaults in 200 East Area.
Existing Double-Shell Tanks Residual	The liquid residual remaining in the tanks is assumed to contain 0.05% of their original inventory.
Future Double-Shell Tanks Residual	The liquid residual remaining in the tanks of future-generated tank wastes is assumed to contain 0.05% of the inventory.
Strontium/Cesium Capsules	Strontium and cesium capsules are placed in drywells near the surface and covered with barriers.
TRU-Contaminated Soil	TRU-contaminated soil sites are left in place and covered with barriers.
Pre-1970 Buried TRU Solid Waste	Pre-1970 TRU buried solid waste sites are left in place and covered with barriers.
RS/NG TRU (Retrievably Stored and Newly Generated)	Retrievably stored TRU wastes are left in place and covered with barriers. Newly generated TRU wastes are disposed of in burial grounds and covered with barriers.

TABLE Q.2. Transport Assessment of the Geologic Repository Alternative (Processing Residuals Only) for the 0.5-cm/yr Annual Average Recharge Scenario^(a)

Radio-nuclide ^(b)	Inventory, Ci	Retardation Factor	Release ^(c) Time, yr	5-km Well		Columbia River Boundary	
				Peak Arrival, yr After Disposal	Peak Nuclide Concentration, Ci/L	Peak Arrival, yr After Disposal	Peak Nuclide Flux Rate, Ci/yr
Single-Shell Tanks Residual: 200 East							
¹⁴ C	8.0×10^1	1.0	2.7×10^6	5,000	4.1×10^{-12}	5,500	1.7×10^{-4}
⁹⁹ Tc	4.9×10^2	1.0	2.5×10^6	5,000	2.0×10^{-11}	5,500	2.0×10^{-3}
¹²⁹ I	8.0×10^{-1}	1.0	2.5×10^6	5,000	3.3×10^{-14}	5,500	3.3×10^{-6}
²³⁸ U	1.1×10^1	1.0	8.7×10^9	5,000	$<1 \times 10^{-14}$	5,500	$<1 \times 10^{-6}$
⁷⁹ Se	1.3×10^1	19.0	2.7×10^6	7,000	3.3×10^{-13}	65,000	3.7×10^{-7}
Single-Shell Tanks Residual: 200 West							
¹⁴ C	1.5×10^2	1.0	1.5×10^6	5,100	7.6×10^{-12}	5,300	2.6×10^{-4}
⁹⁹ Tc	8.5×10^2	1.0	2.6×10^6	5,100	5.1×10^{-11}	5,300	3.1×10^{-3}
¹²⁹ I	1.3	1.0	2.6×10^6	5,100	1.3×10^{-13}	5,300	4.7×10^{-6}
²³⁸ U	1.4×10^1	1.0	9.0×10^9	5,100	$<1 \times 10^{-14}$	5,300	$<1 \times 10^{-6}$
⁷⁹ Se	2.7×10^1	19.0	1.5×10^6	8,200	1.6×10^{-12}	68,000	6.0×10^{-7}
Existing Double- and Single-Shell Tanks Grout: 200 East							
¹⁴ C	5.0×10^3	1.0	3×10^6	4,920	9.1×10^{-11}	5,200	3.6×10^{-3}
⁹⁹ Tc	3.0×10^2	1.0	3×10^6	4,920	9.8×10^{-12}	5,200	4.0×10^{-4}
¹²⁹ I	5.0×10^1	1.0	3×10^6	4,920	1.7×10^{-12}	5,200	6.7×10^{-5}
²³⁸ U	2.0	1.0	3×10^6	4,920	6.7×10^{-14}	5,200	2.7×10^{-6}
⁷⁹ Se	9.0×10^2	19.0	3×10^6	5,400	2.0×10^{-11}	75,000	6.6×10^{-6}
Existing Double-Shell Tanks Residual: 200 East							
¹⁴ C	1.7	1.0	2.6×10^6	4,950	8.5×10^{-13}	5,000	$<1 \times 10^{-6}$
⁹⁹ Tc	1.3×10^1	1.0	2.6×10^6	4,950	3.6×10^{-12}	5,000	1.9×10^{-5}
⁷⁹ Se	4.2×10^{-2}	19.0	2.6×10^6	5,900	1.1×10^{-4}	67,000	1.0×10^{-9}
Existing Double-Shell Tanks Residual: 200 West							
¹⁴ C	3.4×10^{-1}	1.0	2.3×10^6	5,000	2.2×10^{-13}	5,400	$<1 \times 10^{-6}$
⁹⁹ Tc	2.5	1.0	2.3×10^6	5,000	9.8×10^{-12}	5,400	5.3×10^{-6}
¹²⁹ I	3.4×10^{-3}	1.0	2.3×10^6	5,000	1.4×10^{-14}	5,400	$<1 \times 10^{-6}$
⁷⁹ Se	8.5×10^{-3}	19.0	2.3×10^6	8,200	1.2×10^{-14}	59,000	$<1 \times 10^{-6}$
Future Double-Shell Tanks Residual: 200 East							
⁹⁹ Tc	2.4	1.0	2.2×10^6	4,950	4.5×10^{-14}	5,200	5.9×10^{-6}
Future Double-Shell Tanks Grout: 200 East							
¹⁴ C	2.8×10^2	1.0	3×10^6	4,920	1.2×10^{-11}	5,200	4.6×10^{-4}
⁹⁹ Tc	1.6×10^2	1.0	3×10^6	4,920	1.2×10^{-11}	5,200	4.9×10^{-4}
¹²⁹ I	1.2×10^1	1.0	3×10^6	4,920	9.1×10^{-13}	5,200	3.7×10^{-5}
⁷⁹ Se	2.3×10^2	19.0	3×10^6	5,500	1.2×10^{-11}	68,000	4.8×10^{-6}

(a) The geologic alternative represents a bounding case for the preferred alternative.

(b) Sr, Cs, Sm, Np, Pu, and Am included in the analysis; where not listed, either arrived below the concentration limit of 1×10^{-14} Ci/L or at a rate of less than 1×10^{-6} Ci/yr, or were delayed beyond 20,000 years.

(c) The time required to release the total inventory into an advective pathway.

The overall impact of the groundwater pathway for the in-place stabilization and disposal alternative must also contain the impacts from residual slurry remaining in both the existing double-shell and future double-shell tank wastes; these were calculated for the geologic disposal alternative and can be found in Table Q.2. There were no releases to the water table from the strontium/cesium capsules since no probable release mechanisms in the 600 years of concern were found. With a barrier placed over the TRU-contaminated soil sites, the pre-1970 TRU burial grounds and the retrievably stored/newly generated (RS/NG) TRU sites, only small to no impacts were determined by analogy to the results in Table Q.5 where no barrier was used. Results from the first three items are found in Table Q.3.

Results of Reference Alternative (combination disposal) for the 0.5-cm/yr Recharge

The reference alternative includes in-place stabilization of single-shell tanks and retrieval and immobilization of HLW/TRU from double-shell and future double-shell tank wastes, which will be sent to a repository. The remainder will be processed into grout.

Under the reference alternative only two new waste forms were defined that needed groundwater pathway analysis. These result from immobilizing the reprocessed existing and future double-shell tank wastes and disposing of them as grout in vaults in the 200 East Area. For details of these disposal options see Volume 1, Section 3.3.

Waste Form	Description
Existing Double-Shell Tanks Grout	Non-HLW residual tank liquid disposed of as grout in vaults and cover with barriers.
Future Double-Shell Tanks Grout	Non-HLW residual future tank liquid disposed of as grout in vaults and cover with barriers.
Existing Double-Shell Tanks Residual	The liquid residual remaining in the tanks is assumed to contain 0.05% of their original inventory.
Future Double-Shell Tanks Residual	The liquid residual remaining in the tanks of future-generated tank wastes is assumed to contain 0.05% of the inventory.
Single-Shell Tanks	Salt and sludge in the tanks in both 200 East and 200 West Areas are left in place, stabilized, and covered with barriers.
TRU-Contaminated Soil	TRU-contaminated soil sites are left in place and covered with barriers, except for 618-11, which would be removed for geologic repository disposal under the preferred alternative.
Pre-1970 Buried TRU	Pre-1970 buried TRU solid waste sites are left in place and covered with barriers.

The results of these cases are detailed in Table Q.4.

The impacts of the groundwater pathway analysis for the reference alternative should include the results of the loss of the 0.05% residual liquid from the existing double-shell tanks and future double-shell tank cases from Table Q.2 and the salt and sludge from stabilized single-shell tanks from Table Q.3.

**TABLE Q.3. Transport Assessment of the In-Place Stabilization and Disposal Alternative
for the 0.5-cm/yr Annual Average Recharge Scenario**

Radio-nuclide(a)	Inventory, Ci	Retardation Factor	Release Time, yr	5-km Well		Columbia River Boundary	
				Peak Arrival, yr After Disposal	Peak Nuclide Concentration, Ci/L	Peak Arrival, yr After Disposal	Peak Nuclide Flux Rate, Ci/yr
<u>Single-Shell Tanks: 200 East</u>							
^{14}C	1.6×10^3	1.0	3.3×10^6	4,980	4.7×10^{-12}	5,500	4.7×10^{-4}
^{99}Tc	9.8×10^3	1.0	2.5×10^6	4,980	2.1×10^{-10}	5,500	2.3×10^{-2}
^{129}I	1.6×10^1	1.0	2.6×10^6	4,980	1.8×10^{-13}	5,500	1.9×10^{-5}
^{238}U	2.2×10^2	1.0	1.7×10^9	4,980	$<1 \times 10^{-14}$	5,500	$<1 \times 10^{-6}$
^{79}Se	2.6×10^2	19.0	3.3×10^6	7,000	3.2×10^{-12}	66,000	8.8×10^{-6}
<u>Single-Shell Tanks: 200 West</u>							
^{14}C	3.0×10^3	1.0	4.2×10^6	5,100	1.7×10^{-11}	5,300	6.2×10^{-4}
^{99}Tc	1.7×10^4	1.0	2.6×10^6	5,100	7.8×10^{-10}	5,300	3.0×10^{-2}
^{129}I	2.5×10^1	1.0	2.5×10^6	5,100	6.1×10^{-13}	5,300	2.3×10^{-5}
^{238}U	2.8×10^2	1.0	1.8×10^9	5,100	$<1 \times 10^{-14}$	5,300	$<1 \times 10^{-6}$
^{79}Se	5.4×10^2	19.0	4.2×10^6	8,800	1.2×10^{-11}	67,000	1.2×10^{-5}
<u>Existing Double-Shell Tanks Grout: 200 East</u>							
^{14}C	4.0×10^3	1.0	3×10^6	4,920	1.4×10^{-10}	5,200	5.5×10^{-3}
^{99}Tc	3.0×10^4	1.0	3×10^6	4,920	1.9×10^{-9}	5,200	7.6×10^{-2}
^{129}I	4.0×10^1	1.0	3×10^6	4,920	2.5×10^{-12}	5,200	1.0×10^{-4}
^{238}U	3.0	1.0	3×10^6	4,980	1.9×10^{-13}	5,200	7.7×10^{-6}
^{79}Se	1.0×10^2	19.0	3×10^6	5,400	4.3×10^{-12}	71,000	1.1×10^{-6}
<u>Future Double-Shell Tanks Grout: 200 East</u>							
^{14}C	2.8×10^2	1.0	3×10^6	4,920	7.2×10^{-12}	5,100	4.6×10^{-4}
^{99}Tc	4.8×10^3	1.0	3×10^6	4,920	2.2×10^{-10}	5,100	1.5×10^{-3}
^{129}I	1.2×10^1	1.0	3×10^6	4,920	5.6×10^{-13}	5,100	3.7×10^{-5}
^{79}Se	2.3×10^2	19.0	3×10^6	5,400	7.4×10^{-12}	68,000	4.8×10^{-6}

(a) Sr, Cs, Sm, Np, Pu, and Am included in the analysis; where not listed, either arrived below the concentration limit of 1×10^{-14} Ci/L or at a rate of less than 1×10^{-6} Ci/yr, or were delayed beyond 20,000 years.

Results of No Disposal Action (continued storage) for the 0.5-cm/yr Recharge

No disposal action (continued storage) requires that tanked wastes be maintained in tanks and retanked about every 50 years. The strontium/cesium capsules would be stored in caissons, and the TRU soil sites would be left as disposed. Under this option the following cases are defined and analyzed.

TABLE Q.4. Transport Assessment of the Reference Alternative for the 0.5-cm/yr Annual Average Recharge Scenario^(a)

Radio-nuclide ^(b)	Inventory, Ci	Retardation Factor	Release Time, yr	5-km Well		Columbia River Boundary	
				Peak Arrival, yr After Disposal	Peak Nuclide Concentration, Ci/L	Peak Arrival, yr After Disposal	Peak Nuclide Flux Rate, Ci/yr
<u>Existing Double-Shell Tanks Grout: 200 East</u>							
¹⁴ C	4.0×10^3	1.0	2.5×10^6	4,920	1.4×10^{-10}	5,200	5.5×10^{-3}
⁹⁹ Tc	3.0×10^4	1.0	2.5×10^6	4,920	1.9×10^{-9}	5,200	7.5×10^{-2}
¹²⁹ I	4.0×10^1	1.0	2.5×10^6	4,920	2.5×10^{-12}	5,200	2.0×10^{-4}
²³⁸ U	3.0×10^{-1}	1.0	2.5×10^6	4,920	1.9×10^{-14}	5,200	$<1 \times 10^{-6}$
⁷⁹ Se	1.0×10^2	19.0	2.5×10^6	6,100	4.1×10^{-12}	71,000	1.1×10^{-6}
<u>Future Double-Shell Tanks Grout: 200 East</u>							
¹⁴ C	2.8×10^2	1.0	3.0×10^6	4,920	1.1×10^{-11}	5,100	4.6×10^{-4}
⁹⁹ Tc	4.8×10^3	1.0	3.0×10^6	4,920	3.6×10^{-10}	5,100	1.5×10^{-2}
¹²⁹ I	1.2×10^1	1.0	3.0×10^6	4,920	9.1×10^{-13}	5,100	3.7×10^{-5}
⁷⁹ Se	2.3×10^2	19.0	3.0×10^6	5,400	1.2×10^{-11}	68,000	4.8×10^{-6}

(a) The reference alternative represents a bounding case for the preferred alternative.

(b) Sr, Cs, Sm, Np, Pu, and Am included in the analysis; where not listed, either arrived below the concentration limit of 1×10^{-14} Ci/L or at a rate of less than 1×10^{-6} Ci/yr, or were delayed beyond 20,000 years.

Waste Form	Description
Single-Shell Tanks	Salt and sludge remain in tanks with no barrier. The tanks are assumed to deteriorate and to release their contents after 160 years.
Existing Double-Shell Tanks	Double-shell slurry (DSS) remains in tanks with no barrier. The tanks are assumed to deteriorate and to release their contents after 160 years.
Future Double-Shell Tanks	Future wastes remains in tanks with no barrier. The tanks are assumed to deteriorate and to release their contents after 160 years.
Strontium/Cesium Capsules	Strontium/cesium capsules are placed in caissons or drywells with no barrier.
TRU-Contaminated Soil	TRU-contaminated soil sites are left as disposed.
Pre-1970 Buried TRU	Pre-1970 buried TRU solid waste sites are left as disposed.
RS/NG TRU	Retrievably stored TRU sites are left as stored, but for these analyses are assumed available for leaching. Newly generated TRU wastes are placed in the ground, but for these analyses are assumed available for leaching.

TABLE Q.5. Transport Assessment for No Disposal Action (continued storage) for the 0.5-cm/yr Annual Average Recharge Scenario

Radio-nuclide(a)	Inventory, Ci	Retardation Factor	Release Time, yr	Peak Arrival, yr After Disposal	Peak Nuclide Concentration, Ci/L	5-km Well		Columbia River Boundary	
						Single-Shell Tanks: 200 East	Peak Arrival, yr After Disposal	Peak Nuclide Flux Rate, Ci/yr	
<u>Single-Shell Tanks: 200 East</u>									
^{14}C	1.6×10^3	1.0	1,400	1,190	9.7×10^{-9}	1,690	9.3×10^{-1}		
^{99}Tc	9.8×10^3	1.0	210	1,190	4.5×10^{-7}	1,690	2.6×10^1		
^{129}I	1.6×10^1	1.0	590	1,190	2.7×10^{-10}	1,690	2.7×10^{-2}		
^{239}Pu	1.8×10^4	4.4	4.2×10^4	5,000	2.0×10^{-9}	7,200	1.9×10^{-1}		
^{238}U	2.2×10^2	1.0	1.4×10^6	1,190	1.6×10^{-12}	1,690	1.6×10^{-4}		
^{79}Se	2.6×10^2	19.0	5,000	18,300	6.8×10^{-10}	23,000	6.0×10^{-2}		
<u>Single-Shell Tanks: 200 West</u>									
^{14}C	3.0×10^3	1.0	2,000	1,290	3.4×10^{-8}	1,500	1.2		
^{99}Tc	1.7×10^4	1.0	290	1,290	1.6×10^{-6}	1,500	5.8×10^1		
^{129}I	2.5×10^1	1.0	740	1,290	9.6×10^{-10}	1,500	3.4×10^{-2}		
^{239}Pu	1.0×10^4	4.4	2.5×10^4	5,500	7.2×10^{-9}	5,800	2.5×10^{-1}		
^{238}U	2.8×10^2	1.0	1.4×10^6	1,290	5.8×10^{-12}	1,500	2.0×10^{-4}		
^{79}Se	5.4×10^2	19.0	6,000	19,800	2.8×10^{-9}	24,000	6.5×10^{-2}		
<u>Existing Double-Shell Tanks: 200 East</u>									
^{14}C	3.3×10^3	1.0	3,710	270	6.8×10^{-7}	500	5.0		
^{99}Tc	2.5×10^4	1.0	3,710	270	5.3×10^{-6}	500	3.0×10^1		
^{129}I	3.3×10^1	1.0	3,710	270	7.1×10^{-9}	500	4.0×10^{-2}		
^{239}Pu	8.3×10^1	4.4	3,920	3,540	1.5×10^{-8}	4,600	8.2×10^{-2}		
^{238}U	2.5	1.0	3,710	270	5.3×10^{-10}	500	3.0×10^{-3}		
^{90}Sr	1.5×10^7	1.1	1,560	850	8.0×10^{-12}	1,110	$<1 \times 10^{-6}$		
^{79}Se	8.3×10^1	19.0	4,600	2,200	8.7×10^{-9}	6,600	3.6×10^{-2}		
<u>Existing Double-Shell Tanks: 200 West</u>									
^{14}C	6.7×10^2	1.0	3,710	320	6.6×10^{-7}	550	6.8×10^{-1}		
^{99}Tc	5.0×10^3	1.0	3,710	320	5.0×10^{-6}	550	5.4		
^{129}I	6.8	1.0	3,710	320	6.9×10^{-9}	550	7.4×10^{-3}		
^{239}Pu	1.7×10^1	4.4	3,920	3,850	2.0×10^{-8}	4,730	1.4×10^{-2}		
^{90}Sr	3.0×10^6	1.1	1,560	910	2.5×10^{-12}	1,080	1.5×10^{-8}		
^{238}U	5.1×10^{-1}	1.0	3,710	320	5.2×10^{-10}	550	5.5×10^{-4}		
^{79}Se	1.7×10^1	19.0	4,600	3,200	3.6×10^{-9}	7,600	2.8×10^{-3}		
<u>Future Double-Shell Tanks: 200 East</u>									
^{14}C	2.8×10^2	1.0	3,710	260	2.6×10^{-9}	500	3.2×10^{-1}		
^{99}Tc	4.8×10^3	1.0	3,710	260	4.7×10^{-8}	500	5.8		
^{129}I	1.2×10^1	1.0	3,710	260	1.2×10^{-10}	500	1.5×10^{-2}		
^{239}Pu	6.3×10^3	4.4	3,920	3,500	5.3×10^{-8}	4,500	6.2		
^{79}Se	2.3×10^2	19.0	4,600	2,200	1.0×10^{-10}	6,600	9.3×10^{-3}		
<u>Pre-1970 Burial Sites: 200 West</u>									
^{14}C	1.0	1.0	5	1,300	1.3×10^{-9}	1,430	2.6×10^{-2}		
<u>Retrievably Stored TRU: 200 West</u>									
^{14}C	2.0	1.0	10	1,300	3.0×10^{-9}	1,430	1.2×10^{-2}		
<u>Newly Generated TRU: 200 West</u>									
^{14}C	2.0	1.0	30	1,200	1.7×10^{-9}	1,500	1.7×10^{-2}		

(a) Sr, Cs, Sm, Np, Pu, and Am included in the analysis; where not listed, either arrived below the concentration limit of 1×10^{-14} Ci/L or at a rate of less than 1×10^{-6} Ci/yr, or were delayed beyond 20,000 years.

Analysis of TRU-contaminated soil sites, pre-1970 buried TRU solid waste sites, and newly generated TRU wastes showed no concentrations of radionuclides at the 5-km well exceeding 10^{-14} Ci/L and no flux greater than 10^{-6} Ci/yr entering the river. For the strontium/cesium capsules, the canisters in their handling containers were expected to last beyond the decay period necessary to render the strontium and cesium harmless. The radionuclide releases to the environment from the groundwater pathway for the remaining cases are summarized in Table Q.5.

Q.6.2 Results of the Wetter Climate Scenario (5 cm/yr recharge)

The wetter climate scenario has been analyzed for each case defined above. A recharge rate of 5 cm/yr is assumed to represent wetter climate. Two-dimensional modeling of the groundwater aquifer for this recharge rate showed a higher water table with generally shorter travel times to the well and the river. The analyses made for this scenario parallel those in Section Q.6.1.

A protective barrier is placed over a number of the waste sites, as indicated in Appendix P. This protective barrier essentially eliminates water recharge. However, to lend perspective, an analysis of two barrier failures is provided. These analyses include a disruptive barrier failure and a functional barrier failure. As indicated in Appendix P, water infiltration beneath the exposed (soil layer removed) riprap is assumed to increase to 15 cm/yr or essentially 50% of the incident 30.1 cm/yr of precipitation.

Results of the Geologic Disposal Alternative for 5-cm/yr Recharge

The results summarized here are for the same cases as discussed for the continued drier climate except that the cases for recharge of 5 cm/yr include barrier-failure cases described under Scenario 2, Section Q.2, and in Appendix P.

Waste Form	Description
Single-Shell Tanks Residual	The bulk of the wastes is shipped off site, but 5% of the salt and sludge remains in the tanks in 200 East and 200 West Areas and the tanks are covered with barriers.
Single-Shell and Double-Shell Tanks Grout	The liquid containing salts from processing and packaging waste from the tanks is disposed of as low-level grout in the 200 East Area.
Existing Double-Shell Tanks Residual	The liquid residual remaining in the tanks is assumed to contain 0.05% of their original inventory.
Future Double-Shell Tanks Residual	The liquid residual remaining in the tanks of future-generated tank wastes is assumed to contain 0.05% of the inventory.
Future Double-Shell Tanks Grout	The liquid resulting from processing and packaging future-generated HLW for offsite disposal is disposed of as low-level grout in the 200 East Area.

Table Q.6 shows these results with the barriers intact. Table Q.7 includes the results for the disruptive barrier failure, and Table Q.8 includes the results for the functional barrier failure.

Results of the In-Place Stabilization and Disposal Alternative for 5-cm/yr Recharge

The results of the in-place stabilization and disposal alternative for the 5-cm/yr recharge can be compared to the similar cases for the 0.5-cm/yr recharge. This alternative calls for stabilizing in place the single-shell tanks and grouting the double-shell tanks. The waste forms are described below for this alternative.

Waste Form	Description
Single-Shell Tanks	Salt and sludge in the tanks in both 200 East and 200 West Areas are left in place, stabilized, and covered with barriers.
Existing Double-Shell Tank Grout	Existing liquids are immobilized and disposed of as grout in vaults in 200 East Area.
Future Double-Shell Tank Grout	Future liquids are immobilized and disposed of as grout in vaults in 200 East Area.
Existing Double-Shell Tanks Residual	The liquid residual remaining in the tanks is assumed to contain 0.05% of the original inventory.
Future Double-Shell Tanks Residual	The liquid residual remaining in the tanks of future-generated tank wastes is assumed to contain 0.05% of the original inventory.
Strontium/Cesium Capsules	Strontium and cesium capsules are placed in drywells near the surface and covered with barriers.
TRU-Contaminated Soil	TRU-contaminated soil sites are left in place and covered with barriers.
Pre-1970 TRU	Pre-1970 buried TRU solid waste sites are left in place and covered with barriers.
RS/NG TRU (Retrievably Stored and Newly Generated)	Retrievably stored TRU wastes are left in place and covered with barriers. Newly generated TRU wastes are disposed of in burial grounds and covered with barriers.

Again, no impact was found from the TRU-contaminated soil, pre-1970 TRU, and RS/NG TRU sites since under this alternative there are barriers placed over these facilities. The no-impact conclusion for these four cases is made by analogy to results of similar cases in the no disposal action alternative, which uses no barrier. Table Q.9 shows the results for the in-place stabilization and disposal alternative with the barriers intact. Table Q.10 includes the results for the disruptive barrier failure, and Table Q.11 includes the results for the functional barrier failure.

Reference Alternative (combination disposal) for the 5-cm/yr Recharge

Under the reference alternative for the 5-cm/yr recharge, only two new waste forms were defined, as described below, which require additional groundwater pathway analysis. These cases result from disposing of the existing and future double-shell tank wastes as grout.

TABLE Q.6. Transport Assessment of the Geologic Repository Alternative for the 5-cm/yr Annual Average Recharge^(a)

Radio-nuclide ^(b)	Inventory, Ci	Retardation Factor	Release Time, yr	5-km Well		Columbia River Boundary	
				Peak Arrival, yr After Disposal	Peak Nuclide Concentration, Ci/L	Peak Arrival, yr After Disposal	Peak Nuclide Flux Rate, Ci/yr
<u>Single-Shell Tanks Residual: 200 East</u>							
¹⁴ C	8.0×10^1	1.0	2.5×10^6	4,900	2.1×10^{-13}	4,920	1.8×10^{-4}
⁹⁹ Tc	4.9×10^2	1.0	2.5×10^6	4,900	2.3×10^{-12}	4,920	2.0×10^{-3}
¹²⁹ I	8.0×10^{-1}	1.0	2.5×10^6	4,900	$<1 \times 10^{-14}$	4,920	3.3×10^{-6}
²³⁸ U	1.1×10^1	1.0	7.2×10^7	4,900	$<1 \times 10^{-14}$	4,920	$<1 \times 10^{-6}$
⁷⁹ Se	1.3×10^1	19.0	2.5×10^6	5,000	4.0×10^{-14}	5,200	3.8×10^{-5}
<u>Single-Shell Tanks Residual: 200 West</u>							
¹⁴ C	1.5×10^2	1.0	2.6×10^6	4,970	3.5×10^{-12}	5,000	2.9×10^{-4}
⁹⁹ Tc	8.5×10^2	1.0	2.6×10^6	4,970	3.7×10^{-11}	5,000	3.1×10^{-3}
¹²⁹ I	1.3	1.0	2.6×10^6	4,970	5.5×10^{-14}	5,000	4.8×10^{-6}
²³⁸ U	1.4×10^1	1.0	5.2×10^7	4,970	$<1 \times 10^{-14}$	5,000	$<1 \times 10^{-6}$
⁷⁹ Se	2.7×10^1	19.0	2.6×10^6	6,200	7.7×10^{-13}	6,500	6.4×10^{-5}
<u>Single-Shell and Existing Double-Shell Tanks Grout: 200 East</u>							
¹⁴ C	5.0×10^3	1.0	3×10^6	4,900	2.5×10^{-11}	4,930	3.7×10^{-3}
⁹⁹ Tc	3.0×10^2	1.0	3×10^6	4,900	2.7×10^{-12}	4,930	4.0×10^{-4}
¹²⁹ I	5.0×10^1	1.0	3×10^6	4,900	4.5×10^{-13}	4,930	6.7×10^{-5}
²³⁸ U	2.0	1.0	3×10^6	4,900	1.8×10^{-14}	4,930	$<1 \times 10^{-6}$
⁷⁹ Se	9.0×10^2	19.0	3×10^6	5,100	5.7×10^{-12}	5,400	8.4×10^{-4}
<u>Double-Shell Tanks Residual: 200 East</u>							
⁹⁹ Tc	1.3×10^1	1.0	2.2×10^6	4,900	2.5×10^{-14}	4,920	2.1×10^{-5}
<u>Double-Shell Tanks Residual: 200 West</u>							
¹⁴ C	3.4×10^{-1}	1.0	2.3×10^6	4,950	7.3×10^{-14}	4,980	$<1 \times 10^{-6}$
⁹⁹ Tc	2.5	1.0	2.3×10^6	4,950	2.3×10^{-12}	4,980	5.9×10^{-5}
<u>Future Double-Shell Tanks Residual: 200 East</u>							
⁹⁹ Tc	2.4	1.0	2.3×10^6	4,900	6.3×10^{-15}	4,920	5.9×10^{-6}
<u>Future Double-Shell Tanks Grout: 200 East</u>							
¹⁴ C	2.8×10^2	1.0	3.0×10^6	4,900	3.1×10^{-12}	4,920	4.8×10^{-4}
⁹⁹ Tc	1.6×10^2	1.0	3.0×10^6	4,900	3.2×10^{-12}	4,920	4.9×10^{-4}
¹²⁹ I	1.2×10^1	1.0	3.0×10^6	4,900	2.4×10^{-13}	4,920	3.7×10^{-5}
⁷⁹ Se	2.3×10^2	19.0	3.0×10^6	5,100	3.3×10^{-12}	5,400	4.9×10^{-4}

(a) The geologic alternative represents a bounding case for the preferred alternative.

(b) Sr, Cs, Sm, Np, Pu, and Am included in the analysis; where not listed, either arrived below the concentration limit of 1×10^{-14} Ci/L or at a rate of less than 1×10^{-6} Ci/yr, or were delayed beyond 20,000 years.

TABLE Q.7. Transport Assessment of the Geologic Repository Alternative for the 5-cm/yr Annual Average Recharge Scenario--Disruptive Barrier Failure^(a)

Radio-nuclide ^(b)	Inventory, Ci	Retardation Factor	Release Time, yr	5-km Well		Columbia River Boundary	
				Peak Arrival, yr After Disposal	Peak Nuclide Concentration, Ci/L	Peak Arrival, yr After Disposal	Peak Nuclide Flux Rate, Ci/yr
<u>Single-Shell Tanks Residual: 200 East--Disruptive Barrier Failure</u>							
¹⁴ C	8.0	1.0	2.5	580	1.9×10^{-9}	590	1.5
⁹⁰ Sr	9.5×10^4	3.1	<1	740	2.8×10^{-13}	790	1.2×10^{-4}
⁹⁹ Tc	4.9×10^1	1.0	<1	580	2.8×10^{-8}	590	3.0×10^1
¹²⁹ I	8.0×10^{-2}	1.0	<1	580	3.8×10^{-11}	590	3.0×10^{-2}
²³⁷ Np	1.2×10^{-1}	48.0	<1	4,200	1.4×10^{-12}	4,900	1.5×10^{-3}
²³⁸ U	1.1	1.0	2,300	580	5.6×10^{-13}	590	4.9×10^{-4}
²³⁹ Pu	9.0×10^1	115.0	410	9,800	1.6×10^{-10}	1,100	1.8×10^{-1}
²⁴¹ Am	9.0×10^1	31.5	<1	2,900	1.4×10^{-11}	3,400	7.1×10^{-3}
⁷⁹ Se	1.3	19.0	<1	2,000	3.4×10^{-11}	2,300	3.6×10^{-2}
<u>Single-Shell Tanks Residual: 200 West--Disruptive Barrier Failure</u>							
¹⁴ C	1.5×10^1	1.0	3.6	620	2.0×10^{-8}	650	1.4
⁹⁰ Sr	1.6×10^5	3.1	<1	860	6.2×10^{-14}	940	1.5×10^{-6}
⁹⁹ Tc	8.5×10^1	1.0	<1	620	1.3×10^{-7}	650	2.0×10^1
¹²⁹ I	1.3×10^{-1}	1.0	<1	620	1.9×10^{-10}	650	2.5×10^{-2}
²³⁷ Np	1.8×10^{-1}	48.0	<1	6,000	3.5×10^{-12}	7,500	8.2×10^{-4}
²³⁸ U	1.4	1.0	290	620	5.7×10^{-11}	650	6.1×10^{-4}
²³⁹ Pu	1.0×10^1	115.0	7	14,000	1.5×10^{-10}	15,000	3.6×10^{-2}
²⁴¹ Am	1.0×10^2	31.5	<1	4,500	3.3×10^{-12}	5,100	2.0×10^{-4}
⁷⁹ Se	2.7	19.0	<1	2,900	1.8×10^{-10}	3,200	2.5×10^{-2}
<u>Double-Shell and Single-Shell Tanks Grout: 200 East--Disruptive Barrier Failure</u>							
¹⁴ C	5.0×10^2	1.0	1.4×10^4	880	2.4×10^{-9}	900	3.2×10^{-2}
⁹⁹ Tc	3.0×10^1	1.0	1.4×10^4	880	1.6×10^{-10}	900	2.1×10^{-3}
¹²⁹ I	5.0	1.0	1.4×10^4	880	2.6×10^{-11}	900	3.6×10^{-4}
²³⁷ Np	3.0×10^{-2}	48.0	1.4×10^4	4,700	1.6×10^{-13}	5,450	2.1×10^{-6}
²³⁹ Pu	1.0×10^1	115.0	1.4×10^4	10,500	3.8×10^{-11}	41,000	2.2×10^{-6}
⁷⁹ Se	9.0×10^1	19.0	1.4×10^4	2,200	4.0×10^{-10}	2,500	5.4×10^{-3}
<u>Future Double-Shell Tanks Grout: 200 East--Disruptive Barrier Failure</u>							
¹⁴ C	2.8×10^1	1.0	1.4×10^4	880	1.3×10^{-11}	900	1.8×10^{-3}
⁹⁹ Tc	1.6×10^1	1.0	1.4×10^4	880	8.3×10^{-12}	900	1.1×10^{-3}
¹²⁹ I	1.2	1.0	1.4×10^4	880	7.5×10^{-13}	900	8.6×10^{-5}
²³⁹ Pu	2.9×10^1	115.0	1.4×10^4	10,500	5.6×10^{-11}	12,000	1.4×10^{-2}
⁷⁹ Se	2.3×10^1	19.0	1.4×10^4	2,200	9.2×10^{-12}	2,500	1.4×10^{-3}

TABLE Q.7. (contd)

Radio-nuclide ^(b)	Inventory, Ci	Retardation Factor	Release Time, yr	5-km Well		Columbia River Boundary	
				Peak Arrival, yr After Disposal	Peak Nuclide Concentration, Ci/L	Peak Arrival, yr After Disposal	Peak Nuclide Flux Rate, Ci/yr
<u>Double-Shell Tanks Residuals: 200 West--Disruptive Barrier Failure</u>							
¹⁴ C	3.4×10^{-2}	1.0	1.0	620	2.2×10^{-9}	640	6.9×10^{-3}
⁹⁹ Tc	2.5×10^{-1}	1.0	<1	620	1.8×10^{-8}	640	3.0×10^{-2}
¹²⁹ I	3.4×10^{-4}	1.0	<1	620	2.3×10^{-11}	640	1.2×10^{-4}
²³⁸ U	2.6×10^{-4}	1.0	49	620	2.1×10^{-12}	640	5.3×10^{-6}
⁷⁹ Se	4.2×10^{-2}	19.0	<1	3,000	2.7×10^{-12}	3,300	1.0×10^{-5}
<u>Double-Shell Tanks Residuals: 200 East--Disruptive Barrier Failure</u>							
¹⁴ C	1.6×10^{-1}	1.0	<1	575	2.1×10^{-9}	590	9.8×10^{-2}
⁹⁹ Tc	1.3	1.0	<1	575	1.7×10^{-8}	590	8.0×10^{-1}
¹²⁹ I	1.7×10^{-3}	1.0	<1	575	2.3×10^{-11}	590	1.0×10^{-3}
²³⁸ U	1.3×10^{-4}	1.0	24	575	3.1×10^{-12}	590	1.5×10^{-3}
²⁴¹ Am	1.3	31.0	<1	3,000	5.0×10^{-12}	3,400	1.0×10^{-4}
⁷⁹ Se	8.5×10^{-4}	19.0	<1	2,000	2.6×10^{-12}	2,300	1.1×10^{-4}
<u>Future Double-Shell Tanks Residual: 200 East--Disruptive Barrier Failure</u>							
¹⁴ C	1.4×10^{-2}	1.0	5	580	3.5×10^{-12}	600	3.0×10^{-3}
⁹⁹ Tc	2.4×10^{-1}	1.0	5	580	6.5×10^{-11}	600	5.5×10^{-2}
¹²⁹ I	6.0×10^{-4}	1.0	5	580	1.6×10^{-13}	600	1.4×10^{-4}
²³⁹ Pu	3.2×10^{-1}	115.0	600	9,500	5.8×10^{-13}	11,000	4.7×10^{-4}
⁷⁹ Se	1.2×10^{-1}	19.0	100	2,000	1.4×10^{-13}	2,300	1.2×10^{-4}

(a) The geologic alternative represents a bounding case for the preferred alternative.

(b) Sr, Cs, Sm, Np, Pu, and Am included in the analysis; where not listed, either arrived below the concentration limit of 1×10^{-14} Ci/L or at a rate of less than 1×10^{-6} Ci/yr, or were delayed beyond 20,000 years.

TABLE Q.8. Transport Assessment of the Geologic Repository Alternative for the 5-cm/yr Annual Average Recharge Scenario--Functional Barrier Failure^(a)

Radio nuclide ^(b)	Inventory, Ci	Retardation Factor	Release Time, yr	5-km Well		Columbia River Boundary	
				Peak Arrival, yr After Disposal	Peak Nuclide Concentration, Ci/L	Peak Arrival, yr After Disposal	Peak Nuclide Flux Rate, Ci/yr
<u>Single-Shell Tanks Residual: 200 West--Functional Barrier Failure</u>							
¹⁴ C	7.5×10^1	1.0	7.0×10^2	4,340	9.1×10^{-10}	4,360	7.9×10^{-2}
⁹⁹ Tc	4.3×10^2	1.0	9.3×10^1	4,340	2.1×10^{-8}	4,360	5.0
¹²⁹ I	7.0×10^{-1}	1.0	2.6×10^2	4,340	3.0×10^{-11}	4,360	3.4×10^{-3}
²³⁸ U	7.0×10^{-1}	1.0	3.1×10^5	4,340	2.4×10^{-13}	4,360	2.0×10^{-5}
<u>Single-Shell Tanks Residual: 200 East--Functional Barrier Failure</u>							
¹⁴ C	4.0×10^1	1.0	3.8×10^2	4,220	6.8×10^{-10}	4,280	6.2×10^{-2}
⁹⁹ Tc	2.5×10^2	1.0	5.4×10^1	4,220	1.9×10^{-9}	4,280	3.3
¹²⁹ I	4.0×10^{-1}	1.0	1.5×10^2	4,220	1.7×10^{-12}	4,280	2.7×10^{-3}
²³⁸ U	5.5	1.0	3.4×10^5	4,220	4.6×10^{-13}	4,280	1.6×10^{-5}
<u>Existing Single- and Double-Shell Tanks Grout: 200 East--Functional Barrier Failure</u>							
¹⁴ C	2.5×10^3	1.0	1.4×10^4	4,400	3.9×10^{-7}	4,450	9.7×10^{-2}
⁹⁹ Tc	1.5×10^2	1.0	1.4×10^4	4,400	3.9×10^{-8}	4,450	1.1×10^{-2}
¹²⁹ I	2.5×10^1	1.0	1.4×10^4	4,400	6.6×10^{-9}	4,450	1.8×10^{-3}
²³⁸ U	1.0	1.0	1.4×10^4	4,400	2.6×10^{-10}	4,450	7.1×10^{-5}
<u>Future Double-Shell Tanks Grout: 200 East--Functional Barrier Failure</u>							
¹⁴ C	1.4×10^2	1.0	1.4×10^4	4,400	3.8×10^{-10}	4,450	5.6×10^{-3}
⁹⁹ Tc	8.0×10^1	1.0	1.4×10^4	4,400	3.7×10^{-10}	4,450	5.6×10^{-3}
¹²⁹ I	6.0	1.0	1.4×10^4	4,400	2.8×10^{-13}	4,450	4.3×10^{-5}
<u>Double-Shell Tanks Residual: 200 West--Functional Barrier Failure</u>							
¹⁴ C	1.7×10^{-1}	1.0	72	4,300	5.2×10^{-11}	4,330	1.4×10^{-4}
⁹⁹ Tc	1.3	1.0	180	4,300	1.8×10^{-9}	4,330	7.0×10^{-3}
¹²⁹ I	1.7×10^{-3}	1.0	290	4,300	2.0×10^{-12}	4,330	5.9×10^{-6}
²³⁸ U	2.6×10^{-1}	1.0	49	4,300	1.4×10^{-14}	4,330	3.5×10^{-8}
<u>Double-Shell Tanks Residual: 200 East--Functional Barrier Failure</u>							
¹⁴ C	8.5×10^{-1}	1.0	6.5	4,300	2.4×10^{-12}	4,320	8.5×10^{-3}
⁹⁹ Tc	6.5	1.0	1.1	4,300	3.1×10^{-11}	4,320	1.1×10^{-1}
¹²⁹ I	8.5×10^{-3}	1.0	2.5	4,300	4.1×10^{-14}	4,320	1.4×10^{-4}
²³⁸ U	6.5×10^{-4}	1.0	64	4,300	$<1 \times 10^{-14}$	4,320	1.6×10^{-5}
<u>Future Double-Shell Tanks Residual: 200 East--Functional Barrier Failure</u>							
¹⁴ C	7.0×10^{-2}	1.0	286	4,400	1.6×10^{-13}	4,420	3.4×10^{-4}
⁹⁹ Tc	1.2	1.0	286	4,400	4.7×10^{-12}	4,420	9.9×10^{-3}
¹²⁹ I	3.0×10^{-3}	1.0	286	4,400	1.2×10^{-14}	4,420	2.5×10^{-5}

- (a) The geologic alternative represents a bounding case for the preferred alternative.
 (b) Se, Sr, Cs, Sm, Np, Pu, and Am included in the analysis; where not listed, either arrived below the concentration limit of 1×10^{-14} Ci/L or at a rate of less than 1×10^{-6} Ci/yr, or were delayed beyond 20,000 years.

TABLE Q.9. Transport Assessment of the In-Place Stabilization and Disposal Alternative for the 5-cm/yr Annual Average Recharge

Radio-nuclide(a)	Inventory, Ci	Retardation Factor	Release Time, yr	5-km Well		Columbia River Boundary	
				Peak Arrival, yr After Disposal	Peak Nuclide Concentration, Ci/L	Peak Arrival, yr After Disposal	Peak Nuclide Flux Rate, Ci/yr
<u>Single-Shell Tanks: 200 East</u>							
^{14}C	1.6×10^3	1.0	2.9×10^6	4,900	5.7×10^{-13}	4,920	5.9×10^{-4}
^{99}Tc	9.8×10^3	1.0	2.3×10^6	4,900	2.5×10^{-11}	4,920	2.5×10^{-2}
^{129}I	1.6×10^1	1.0	2.4×10^6	4,900	2.0×10^{-14}	4,920	2.1×10^{-6}
^{238}U	2.2×10^2	1.0	1.4×10^9	4,900	$<1 \times 10^{-14}$	4,920	$<1 \times 10^{-6}$
^{79}Se	2.6×10^2	19.0	3.0×10^6	5,100	5.5×10^{-13}	5,300	4.3×10^{-4}
<u>Single-Shell Tanks: 200 West</u>							
^{14}C	3.0×10^3	1.0	3.5×10^6	4,970	9.1×10^{-12}	4,980	7.5×10^{-4}
^{99}Tc	1.7×10^4	1.0	2.4×10^6	4,970	7.5×10^{-10}	4,980	3.4×10^{-2}
^{129}I	2.5×10^1	1.0	2.5×10^6	4,970	2.3×10^{-13}	4,980	2.7×10^{-5}
^{238}U	2.8×10^2	1.0	1.4×10^9	4,970	$<1 \times 10^{-14}$	4,980	$<1 \times 10^{-6}$
^{79}Se	5.4×10^2	19.0	3.0×10^6	6,200	1.3×10^{-11}	6,500	5.6×10^{-4}
<u>Existing Double-Shell Tanks Grout: 200 East</u>							
^{14}C	4.0×10^3	1.0	2.8×10^6	4,900	3.7×10^{-11}	4,920	5.6×10^{-3}
^{99}Tc	3.0×10^4	1.0	2.8×10^6	4,900	5.0×10^{-10}	4,920	7.6×10^{-2}
^{129}I	4.0×10^1	1.0	2.8×10^6	4,900	6.7×10^{-13}	4,920	1.0×10^{-4}
^{238}U	3.0	1.0	2.8×10^6	4,900	5.1×10^{-13}	4,920	7.7×10^{-6}
^{79}Se	1.0×10^2	19.0	2.8×10^6	5,100	1.2×10^{-12}	5,400	1.8×10^{-4}
<u>Future Double-Shell Tanks Grout: 200 East</u>							
^{14}C	2.8×10^2	1.0	2.7×10^6	4,900	3.1×10^{-12}	4,920	4.8×10^{-4}
^{99}Tc	4.8×10^3	1.0	2.7×10^6	4,900	9.5×10^{-11}	4,920	1.5×10^{-2}
^{129}I	1.2×10^1	1.0	2.7×10^6	4,900	2.4×10^{-13}	4,920	3.7×10^{-5}
^{79}Se	2.3×10^2	19.0	2.7×10^6	5,100	3.3×10^{-12}	5,400	4.9×10^{-4}

(a) Sr, Cs, Sm, Np, Pu, and Am included in the analysis; where not listed, either arrived below the concentration limit of 1×10^{-14} Ci/L or at a rate of less than 1×10^{-6} Ci/yr, or were delayed beyond 20,000 years.

TABLE Q.10. Transport Assessment of the In-Place Stabilization and Disposal Alternative for the 5-cm/yr Annual Average Recharge Scenario--Disruptive Barrier Failure

Radio-nuclide(a)	Inventory, Ci	Retardation Factor	Release Time, yr	5-km Well		Columbia River Boundary	
				Peak Arrival, yr After Disposal	Peak Nuclide Concentration, Ci/L	Peak Arrival, yr After Disposal	Peak Nuclide Flux Rate, Ci/yr
<u>Single-Shell Tanks: 200 East--Disruptive Barrier Failure</u>							
^{14}C	1.6×10^2	1.0	49	570	3.5×10^{-9}	600	3.1
^{90}Sr	1.9×10^6	2.6	<1	740	5.5×10^{-12}	800	1.9×10^{-3}
^{99}Tc	9.8×10^2	1.0	7	570	1.6×10^{-7}	600	1.4×10^2
^{129}I	1.6	1.0	20	570	9.3×10^{-11}	600	8.1×10^{-2}
^{237}Np	2.3	48.0	11	4,000	2.7×10^{-11}	5,000	3.0×10^{-2}
^{239}Pu	1.8×10^3	4.4	2.7×10^3	9,800	5.9×10^{-10}	12,000	4.9×10^{-1}
^{241}Am	1.8×10^3	31.5	1.5	3,000	3.2×10^{-10}	3,500	8.7×10^{-2}
^{238}U	2.2×10^1	1.0	4.5×10^4	570	5.6×10^{-13}	600	4.9×10^{-4}
^{79}Se	2.6×10^1	19.0	50	2,000	6.0×10^{-10}	2,300	5.2×10^{-1}
<u>Single-Shell Tanks: 200 West--Disruptive Barrier Failure</u>							
^{14}C	3.0×10^2	1.0	73	630	4.5×10^{-8}	680	3.8
^{90}Sr	3.2×10^6	3.1	<1	860	9.3×10^{-13}	1,000	5.7×10^{-6}
^{99}Tc	1.7×10^3	1.0	10	630	1.0×10^{-6}	680	1.0×10^2
^{129}I	2.5	1.0	24	630	1.1×10^{-9}	680	9.3×10^{-2}
^{237}Np	3.5	48.0	14	6,700	1.1×10^{-10}	7,500	1.7×10^{-2}
^{239}Pu	1.0×10^3	115.0	1.2×10^3	16,000	3.2×10^{-9}	19,000	1.5×10^{-1}
^{241}Am	2.0×10^3	31.5	14	3,720	8.0×10^{-11}	>20,000	--
^{238}U	2.8×10^1	1.0	4.6×10^4	630	7.2×10^{-12}	680	6.1×10^{-4}
^{79}Se	5.4×10^1	19.0	80	3,000	2.5×10^{-9}	3,300	5.5×10^{-1}
<u>Existing Double-Shell Tanks Grout: 200 East--Disruptive Barrier Failure</u>							
^{14}C	4.0×10^2	1.0	1.4×10^4	880	1.8×10^{-9}	900	2.5×10^{-2}
^{99}Tc	3.0×10^3	1.0	1.4×10^4	880	1.6×10^{-8}	900	2.1×10^{-1}
^{129}I	4.0	1.0	1.4×10^4	880	2.1×10^{-11}	900	2.9×10^{-4}
^{237}Np	6.0	48.4	1.4×10^4	4,770	3.1×10^{-11}	5,400	4.3×10^{-4}
^{239}Pu	1.0×10^1	115.0	1.4×10^4	10,500	3.9×10^{-11}	12,000	5.0×10^{-4}
^{238}U	3.0×10^{-1}	1.0	1.4×10^4	880	1.6×10^{-12}	900	2.1×10^{-4}
^{79}Se	1.0×10^1	19.0	1.4×10^4	2,200	4.5×10^{-11}	2,500	6.0×10^{-4}
<u>Future Double-Shell Tanks Grout: 200 East--Disruptive Barrier Failure</u>							
^{14}C	2.8×10^1	1.0	1.4×10^4	880	1.3×10^{-10}	900	1.8×10^{-3}
^{99}Tc	4.8×10^2	1.0	1.4×10^4	880	2.5×10^{-9}	900	3.4×10^{-2}
^{129}I	1.2	1.0	1.4×10^4	880	6.3×10^{-12}	900	8.6×10^{-5}
^{239}Pu	6.3×10^2	115.0	1.4×10^4	10,500	2.4×10^{-9}	12,000	3.2×10^{-2}
^{241}Am	3.3×10^4	31.5	1.4×10^4	3,200	1.1×10^{-9}	3,600	4.8×10^{-3}
^{79}Se	2.3×10^1	19.0	1.4×10^4	2,200	1.0×10^{-10}	2,500	1.4×10^{-3}

(a) Sr, Cs, Sm, Np, Pu, and Am included in the analysis; where not listed, either arrived below the concentration limit of 1×10^{-14} Ci/L or at a rate of less than 1×10^{-6} Ci/yr, or were delayed beyond 20,000 years.

TABLE Q.11. Transport Assessment of the In-Place Stabilization and Disposal Alternative for the 5-cm/yr Annual Average Recharge Scenario--Functional Barrier Failure

Radio-nuclide ^(a)	Inventory, Ci	Retardation Factor	Release Time, yr	5-km Well		Columbia River Boundary	
				Peak Arrival, yr After Disposal	Peak Nuclide Concentration, Ci/L	Peak Arrival, yr After Disposal	Peak Nuclide Flux Rate, Ci/yr
Single-Shell Tanks: 200 West--Functional Barrier Failure							
¹⁴ C	1.5×10^3	1.0	7.3×10^3	4,340	9.2×10^{-10}	4,360	7.1×10^{-2}
⁹⁹ Tc	8.5×10^3	1.0	1.5×10^3	4,340	6.7×10^{-8}	4,360	5.0
¹²⁹ I	1.3×10^1	1.0	3.7×10^3	4,340	4.0×10^{-11}	4,360	3.0×10^{-3}
²³⁸ U	1.4×10^2	1.0	6.9×10^6	4,340	2.4×10^{-13}	4,360	1.8×10^{-5}
Single-Shell Tanks: 200 East--Functional Barrier Failure							
¹⁴ C	8.0×10^2	1.0	5.5×10^3	4,400	7.4×10^{-11}	4,450	6.6×10^{-2}
⁹⁹ Tc	4.9×10^3	1.0	1.1×10^3	4,400	5.2×10^{-9}	4,450	4.5
¹²⁹ I	8.0	1.0	3.0×10^3	4,400	3.1×10^{-12}	4,450	2.7×10^{-3}
²³⁸ U	1.1×10^2	1.0	6.8×10^6	4,400	1.9×10^{-14}	4,450	1.6×10^{-5}
Existing Double-Shell Tanks Grout: 200 East--Functional Barrier Failure							
¹⁴ C	2.0×10^3	1.0	1.4×10^4	4,400	5.5×10^{-10}	4,450	8.4×10^{-2}
⁹⁹ Tc	1.5×10^4	1.0	1.4×10^4	4,400	6.9×10^{-9}	4,450	1.1
¹²⁹ I	2.0×10^1	1.0	1.4×10^4	4,400	9.3×10^{-12}	4,450	1.4×10^{-3}
²³⁸ U	1.5	1.0	1.4×10^4	4,400	7.0×10^{-13}	4,450	1.1×10^{-5}
Future Double-Shell Tanks Grout: 200 East--Functional Barrier Failure							
¹⁴ C	1.4×10^2	1.0	1.4×10^4	4,400	3.8×10^{-11}	4,450	5.8×10^{-3}
⁹⁹ Tc	2.4×10^3	1.0	1.4×10^4	4,400	1.1×10^{-9}	4,450	1.7×10^{-1}
¹²⁹ I	6.0	1.0	1.4×10^4	4,400	2.8×10^{-11}	4,450	4.3×10^{-4}

(a) Se, Sr, Cs, Sm, Np, Pu, and Am included in the analysis; where not listed, either arrived below the concentration limit of 1×10^{-14} Ci/L or at a rate of less than 1×10^{-6} Ci/yr, or were delayed beyond 20,000 years.

For details of these disposal options see Volume 1, Section 3.3. Table Q.12 shows the results for these two cases with the barriers intact.

Waste Form	Description
Existing Double-Shell Tanks Grout	Low-activity residual tank liquid disposed of as grout in vaults and cover with barriers.
Future Double-Shell Tanks Grout	Low-activity residual future tank liquid disposed of as grout in vaults and cover with barriers.
Existing Double-Shell Tanks Residual	The liquid residual remaining in the tanks is assumed to contain 0.05% of the original inventory.
Future Double-Shell Tanks Residual	The liquid residual remaining in the tanks of future-generated tank wastes is assumed to contain 0.05% of the original inventory.
Single-Shell Tanks	Salt and sludge in the tanks in both 200 East and 200 West Areas are left in place, stabilized, and covered with barriers.
TRU-Contaminated Soil	TRU-contaminated soil sites are left in place and covered with barriers.
Pre-1970 TRU	Pre-1970 TRU buried solid waste sites are left in place and covered with barriers.

TABLE Q.12. Transport Assessment of the Reference Alternative (combination disposal) for the 5-cm/yr Annual Average Recharge^(a)

Radio-nuclide ^(b)	Inventory, Ci	Retardation Factor	Release Time, yr	5-km Well		Columbia River Boundary	
				Peak Arrival, yr After Disposal	Peak Nuclide Concentration, Ci/L	Peak Arrival, yr After Disposal	Peak Nuclide Flux Rate, Ci/yr
<u>Existing Double-Shell Tanks Grout: 200 East</u>							
¹⁴ C	4.0×10^3	1.0	3.0×10^6	4,900	3.7×10^{-11}	4,930	5.6×10^{-3}
⁹⁹ Tc	3.0×10^4	1.0	3.0×10^6	4,900	5.0×10^{-10}	4,930	7.6×10^{-2}
¹²⁹ I	4.0×10^1	1.0	3.0×10^6	4,900	6.7×10^{-13}	4,930	1.0×10^{-4}
⁷⁹ Se	1.0×10^2	19.0	3.0×10^6	5,100	1.2×10^{-12}	5,400	1.8×10^{-4}
<u>Future Double-Shell Tanks Grout: 200 East</u>							
¹⁴ C	2.8×10^2	1.0	3×10^6	4,900	3.1×10^{-12}	4,920	4.8×10^{-4}
⁹⁹ Tc	4.8×10^3	1.0	3×10^6	4,900	9.5×10^{-11}	4,920	1.5×10^{-2}
¹²⁹ I	1.2×10^1	1.0	3×10^6	4,900	2.4×10^{-13}	4,920	3.7×10^{-5}
⁷⁹ Se	2.3×10^2	19.0	3×10^6	5,100	3.3×10^{-12}	5,400	4.9×10^{-4}

(a) The reference alternative represents a bounding case for the preferred alternative.

(b) Sr, Cs, Sm, Np, Pu, and Am included in the analysis; where not listed, either arrived below the concentration limit of 1×10^{-14} Ci/L or at a rate of less than 1×10^{-6} Ci/yr, or were delayed beyond 20,000 years.

The impacts of the groundwater pathway analysis for the reference alternative should include the results of existing and future double-shell tank residuals from Table Q.6, and salt and sludge stabilized in single-shell tanks from Table Q.9, discussed under the in-place stabilization and disposal alternative. Table Q.13 includes the results of the disruptive barrier failure for this alternative; Table Q.14 contains the results of the functional barrier failure.

TABLE Q.13. Transport Assessment of the Reference (combination disposal) Alternative for the 5-cm/yr Annual Average Recharge Scenario--Disruptive Barrier Failure^(a)

Radio-nuclide ^(b)	Inventory, Ci	Retardation Factor	Release Time, yr	5-km Well		Columbia River Boundary	
				Peak Arrival, yr After Disposal	Peak Nuclide Concentration, Ci/L	Peak Arrival, yr After Disposal	Peak Nuclide Flux Rate, Ci/yr
<u>Existing Double-Shell Tanks Grout: 200 East--Disruptive Barrier Failure</u>							
¹⁴ C	4.0×10^2	1.0	1.4×10^4	880	1.7×10^{-10}	900	2.5×10^{-2}
⁹⁹ Tc	3.0×10^3	1.0	1.4×10^4	880	1.4×10^{-9}	900	2.1×10^{-1}
¹²⁹ I	4.0	1.0	1.4×10^4	880	1.9×10^{-12}	900	2.9×10^{-4}
²³⁷ Np	6.0×10^{-1}	48.0	1.4×10^4	4,770	2.8×10^{-13}	5,400	5.0×10^{-5}
²³⁹ Pu	1.0	115.0	1.4×10^4	10,700	3.4×10^{-13}	12,000	5.0×10^{-5}
²³⁸ U	3.0×10^{-2}	1.0	1.4×10^4	880	1.4×10^{-14}	900	2.5×10^{-5}
⁷⁹ Se	1.0×10^1	19.0	1.4×10^4	2,200	4.0×10^{-12}	2,500	6.0×10^{-4}
<u>Future Double-Shell Tanks Grout: 200 East--Disruptive Barrier Failure</u>							
¹⁴ C	2.8×10^1	1.0	1.4×10^4	880	1.2×10^{-11}	900	1.8×10^{-3}
⁹⁹ Tc	4.8×10^2	1.0	1.4×10^4	880	2.2×10^{-10}	900	3.4×10^{-2}
¹²⁹ I	1.2	1.0	1.4×10^4	880	5.6×10^{-13}	900	8.6×10^{-5}
²³⁹ Pu	6.3×10^1	115.0	1.4×10^4	10,500	1.1×10^{-11}	12,000	1.4×10^{-4}
⁷⁹ Se	2.3×10^1	19.0	1.4×10^4	2,200	9.2×10^{-12}	2,500	1.4×10^{-3}

(a) The reference alternative represents a bounding case for the preferred alternative.

(b) Sr, Cs, Sm, Np, Pu, and Am included in the analysis; where not listed, either arrived below the concentration limit of 1×10^{-14} Ci/L or at a rate of less than 1×10^{-6} Ci/yr, or were delayed beyond 20,000 years.

No Disposal Action (continued storage) for 5-cm/yr Recharge

The no disposal action alternative requires that the tanked wastes be maintained in tanks and retanked periodically. Assuming loss of institutional control, the tanks eventually leak. The strontium/cesium capsules would be stored in caissons, and the TRU soil sites

TABLE Q.14. Transport Assessment of the Reference (combination disposal) Alternative for the 5-cm/yr Annual Average Recharge Scenario--Functional Barrier Failure^(a)

Radio-nuclide ^(b)	Inventory, Ci	Retardation Factor	Release Time, yr	5-km Well		Columbia River Boundary	
				Peak Arrival, yr After Disposal	Peak Nuclide Concentration, Ci/L	Peak Arrival, yr After Disposal	Peak Nuclide Flux Rate, Ci/yr
<u>Existing Double-Shell Tanks Grout: 200 East--Functional Barrier Failure</u>							
¹⁴ C	2.0×10^3	1.0	1.4×10^4	4,400	3.8×10^{-11}	4,450	8.4×10^{-2}
⁹⁹ Tc	1.5×10^4	1.0	1.4×10^4	4,400	1.1×10^{-9}	4,450	1.1
¹²⁹ I	2.0×10^1	1.0	1.4×10^4	4,400	2.8×10^{-12}	4,450	1.4×10^{-5}
²³⁸ U	1.5×10^{-1}	1.0	1.4×10^4	4,400	7.0×10^{-14}	4,450	1.1×10^{-5}
<u>Future Double-Shell Tanks Grout: 200 East--Functional Barrier Failure</u>							
¹⁴ C	1.4×10^2	1.0	1.4×10^4	4,400	5.5×10^{-10}	4,450	5.8×10^{-3}
⁹⁹ Tc	2.4×10^3	1.0	1.4×10^4	4,400	6.9×10^{-9}	4,450	1.7×10^{-1}
¹²⁹ I	6.0	1.0	1.4×10^4	4,400	9.3×10^{-12}	4,450	4.3×10^{-4}

(a) The reference alternative represents a bounding case for the preferred alternative.

(b) Se, Sr, Cs, Sm, Np, Pu, and Am included in the analysis; where not listed, either arrived below the concentration limit of 1×10^{-14} Ci/L or at a rate of less than 1×10^{-6} Ci/yr, or were delayed beyond 20,000 years.

would be left as disposed. No barriers would be constructed over the waste sites, permitting direct infiltration of water to the wastes. This option (see Table Q.15) includes the following:

Waste Form	Description
Single-Shell Tanks	Salt and sludge remain in tanks with no barrier. The tanks are assumed to deteriorate and to release their contents after 160 years.
Double-Shell Tanks	Liquid remains in tanks with no barrier. The tanks are assumed to deteriorate and to release their contents after 160 years.
Future Double-Shell Tanks	Future liquids remain in tanks with no barrier. The tanks are assumed to deteriorate and to release their contents after 160 years.
Strontium/Cesium Capsules	Strontium/cesium capsules are placed in caissons or drywells with no barrier.
TRU-Contaminated Soil	TRU-contaminated soil sites are left as disposed.
Pre-1970 TRU	Pre-1970 buried TRU solid waste sites are left as disposed.
RS/NG TRU	Retrievably stored TRU sites are left as stored, but for these analyses are assumed available for leaching and newly generated TRU wastes are left as stored, but for these analyses are assumed available for leaching.

**TABLE Q.15. Transport Assessment for No Disposal Action (continued storage)
for the 5-cm/yr Annual Average Recharge Scenario**

Radio-nuclide(a)	Inventory, Ci	Retardation Factor	Release Time, yr	5-km Well		Columbia River Boundary	
				Peak Arrival, yr After Disposal	Peak Nuclide Concentration, Ci/L	Peak Arrival, yr After Disposal	Peak Nuclide Flux Rate, Ci/yr
<u>Single-Shell Tanks: 200 West</u>							
¹⁴ C	3.0×10^3	1.0	220	330	1.5×10^{-7}	340	1.3×10^1
⁹⁰ Sr	3.2×10^7	1.1	3	330	1.1×10^{-5}	350	9.7×10^2
⁹⁹ Tc	1.7×10^4	1.0	29	330	6.6×10^{-6}	340	5.6×10^2
¹²⁹ I	2.5×10^1	1.0	74	330	4.0×10^{-9}	340	3.4×10^{-1}
²³⁷ Np	3.5×10^1	22.3	41	3,600	1.8×10^{-9}	4,000	2.7×10^{-1}
²³⁹ Pu	1.0×10^4	4.4	3.5×10^3	880	3.3×10^{-8}	960	2.8
²⁴¹ Am	2.0×10^4	31.5	7	4,700	4.2×10^{-10}	5,200	2.8×10^{-2}
²³⁸ U	2.8×10^2	1.0	1.4×10^5	330	2.4×10^{-11}	340	2.0×10^{-3}
⁷⁹ Se	5.4×10^2	19.0	200	3,000	7.5×10^{-9}	3,400	2.8
<u>Single-Shell Tanks: 200 East</u>							
¹⁴ C	1.6×10^3	1.0	150	270	1.2×10^{-8}	280	1.0×10^1
⁹⁰ Sr	1.9×10^7	1.1	2	270	5.6×10^{-6}	295	4.0×10^3
⁹⁹ Tc	9.8×10^3	1.0	21	270	5.2×10^{-7}	280	4.5×10^2
¹²⁹ I	1.6×10^1	1.0	59	270	3.1×10^{-10}	280	2.7×10^{-1}
²³⁷ Np	2.3×10^1	22.3	34	2,400	2.8×10^{-10}	2,800	2.6×10^{-1}
²³⁹ Pu	1.8×10^4	4.4	7.4×10^3	650	2.7×10^{-10}	700	2.2
²⁴¹ Am	1.8×10^4	31.5	8	3,300	1.1×10^{-9}	3,800	4.0×10^{-1}
²³⁸ U	2.2×10^2	1.0	1.4×10^5	270	1.9×10^{-12}	280	1.6×10^{-3}
⁷⁹ Se	2.6×10^2	19.0	150	2,100	4.5×10^{-9}	2,400	3.5
<u>Existing Double-Shell Tanks: 200 East</u>							
¹⁴ C	3.3×10^3	1.0	450	170	3.5×10^{-8}	190	3.1×10^1
⁹⁰ Sr	1.5×10^7	1.1	190	240	1.2×10^{-6}	250	7.7×10^2
⁹⁹ Tc	2.5×10^4	1.0	450	170	2.7×10^{-7}	190	2.4×10^2
¹²⁹ I	3.3×10^1	1.0	450	170	3.6×10^{-10}	190	3.2×10^{-1}
²³⁷ Np	5.0×10^1	22.3	960	2,300	2.2×10^{-10}	2,600	1.8×10^{-1}
²³⁹ Pu	8.3×10^1	4.4	480	524	7.9×10^{-10}	600	7.1×10^{-1}
²⁴¹ Am	2.5×10^4	31.5	1,360	3,100	5.1×10^{-10}	3,600	1.8×10^{-1}
²³⁸ U	2.5	1.0	450	170	2.7×10^{-11}	190	2.4×10^{-2}
⁷⁹ Se	8.3×10^1	19.0	8,500	390	4.6×10^{-11}	650	2.6×10^{-2}
<u>Existing Double-Shell Tanks: 200 West</u>							
¹⁴ C	6.7×10^2	1.0	450	220	2.4×10^{-6}	240	5.8
⁹⁰ Sr	3.0×10^6	1.1	190	470	2.1×10^{-5}	310	3.6×10^1
⁹⁹ Tc	5.0×10^3	1.0	450	220	1.7×10^{-5}	240	4.4×10^1
¹²⁹ I	6.8	1.0	450	220	2.3×10^{-8}	240	6.1×10^{-2}
²³⁷ Np	1.0×10^1	22.3	960	3,400	1.0×10^{-8}	3,740	2.4×10^{-2}
²³⁹ Pu	1.7×10^1	4.4	480	750	4.6×10^{-8}	830	1.1×10^{-1}
²⁴¹ Am	5.1×10^3	31.5	1,360	4,700	1.8×10^{-9}	4,980	2.2×10^{-3}
²³⁸ U	5.1×10^{-1}	1.0	450	220	1.7×10^{-9}	240	4.5×10^{-3}
⁷⁹ Se	1.7×10^1	19.0	8,500	940	1.3×10^{-8}	1,600	3.5×10^{-2}

TABLE Q.15. (contd)

Radio-nuclide(a)	Inventory, Ci	Retardation Factor	Release Time, yr	5-km Well		Columbia River Boundary	
				Peak Arrival, yr After Disposal	Peak Nuclide Concentration, Ci/L	Peak Arrival, yr After Disposal	Peak Nuclide Flux Rate, Ci/yr
<u>Future Double-Shell Tanks: 200 East</u>							
^{14}C	2.8×10^2	1.0	450	170	3.0×10^{-9}	190	2.6
^{90}Sr	4.2×10^7	1.1	190	240	3.4×10^{-6}	250	2.2×10^3
^{99}Tc	4.8×10^3	1.0	450	170	4.8×10^{-8}	190	4.6×10^1
^{129}I	1.2×10^1	1.0	450	170	1.3×10^{-10}	190	1.2×10^{-1}
^{239}Pu	6.3×10^3	4.4	480	520	6.2×10^{-8}	600	5.4×10^1
^{241}Am	3.3×10^5	31.5	1,360	3,140	6.5×10^{-9}	3,500	3.7
^{79}Se	2.3×10^2	19.0	8,500	2,900	1.3×10^{-10}	650	1.1×10^{-1}
<u>Pre-1970 Burial Sites: 200 West</u>							
^{14}C	1.0	1.0	4	260	9.0×10^{-10}	300	2.6×10^{-2}
<u>Newly Generated TRU: 200 West</u>							
^{14}C	2.0	1.0	4	260	9.2×10^{-10}	300	5.8×10^{-1}
^{90}Sr	4.4×10^4	4.5	16	660	6.5×10^{-12}	680	1.1×10^{-4}
<u>Retrievably Stored TRU: 200 West</u>							
^{14}C	2.0	1.0	4	260	9.2×10^{-10}	300	5.8×10^{-1}
^{90}Sr	2.0×10^4	4.5	16	620	7.5×10^{-3}	1,000	$<1 \times 10^{-6}$

(a) Sr, Cs, Sm, Np, Pu, and Am included in the analysis; where not listed, either arrived below the concentration limit of 1×10^{-14} Ci/L or at a rate of less than 1×10^{-6} Ci/yr, or were delayed beyond 20,000 years.

Q.7 300 AREA TRU BURIAL GROUNDS

Three TRU burial sites exist away from the 200 Areas plateau. These are the 618-11 site, formerly known as the 300 Wye burial ground, and the 618-1 and 2 sites near the 300 Area (see footnote b in Table Q.16). The 618-1 and 2 sites are adjacent and are treated here as a single source.

The hydrologic and transport modeling of these sites paralleled that of the 200 Areas sites. The distance between the bottom of the burial trenches and the climate-changed water table at both locations is 9 m. Without a protective barrier, the travel time for water in the vadose zone was estimated at 14 years for the 5-cm/yr recharge (wetter climate) and 114 years for the 0.5-cm/yr (current climate) recharge since the soils are much drier.

Water streamlines and cumulative travel times from the 618-11 site to the Columbia River were calculated to be 16 to 17 years for the 5-cm/yr infiltration and 117 to 160 years for 0.5-cm/yr infiltration using the same aquifer modeling approach as used in the 200 Areas cases. For the 618-11 site a domestic well was placed 2 km down gradient and the concentration of radionuclides was calculated. Because the 618-1 and 618-2 sites are near the

TABLE Q.16. Transport Assessment of the 618 Burial Ground Sites for 5-cm/yr Recharge

Radio-nuclide	Inventory, Ci	Retardation Factor	Release Time, yr	5-km Well		Columbia River Boundary	
				Peak Arrival, yr After Disposal	Peak Nuclide Concentration, Ci/L	Peak Arrival, yr After Disposal	Peak Nuclide Flux Rate, Ci/yr
<u>No Barrier over 618-1 and 2 Sites</u>							
⁹⁰ Sr	130	4.5	150	(a)		240	1.3×10^{-2}
²³⁹ Pu	110	390.0	10	(a)	(b)	7,000	6.7×10^{-1}
²⁴¹ Am	41	415.0	51	(a)		7,200	2.6×10^{-6}
<u>No Barrier over 618-11 Site</u>							
⁹⁰ Sr	880	4.5	16	310	2.1×10^{-9}	400	1.2×10^{-3}
²³⁹ Pu	750	390.0	19	13,000	6.2×10^{-8}	<20,000	--

(a) Due to proximity to the Columbia River, release is only calculated to the river.

(b) A recently completed study (DOE 1986a), which examined records of inactive waste disposal locations on the Hanford Site, showed that two 618 sites (618-1 and 618-2) each contained 1.0 g of plutonium, rather than the previously listed 1000 g (Rockwell 1985). As a result of this lower quantity, both sites are now designated as low-level waste sites (Rockwell 1987).

Columbia River, the travel times in the groundwater aquifer were taken from a detailed study of the 300 Area aquifer (Lindberg and Bond 1979) which showed 0.8 to 0.14 years for the 0.5-cm/yr and 5-cm/yr infiltration cases. The short distance to the river precluded a 2- or 5-km well scenario. Although the inventory contained ¹³⁷Cs, ⁹⁰Sr, ²³⁹Pu, and ²⁴¹Am, the results indicate that only ⁹⁰Sr and ²³⁹Pu were detected at the domestic well and only ⁹⁰Sr in the river for the 618-11 site. For the 618-1 and 2 sites, ⁹⁰Sr, ²⁴¹Am and ²³⁹Pu all entered the river. Results are shown in Table Q.16.

Q.8 WATER TABLE CHANGES RESULTING FROM POTENTIAL IRRIGATION SCENARIOS

After site closure or loss of institutional control, the possibility of irrigation on Hanford land becomes real. The most likely areas to be farmed because of their suitability for agriculture are those irrigated in the past in the area of White Bluffs and the old Hanford town site. Another possible area for irrigation is the extension of horticulture farming through Cold Creek Valley and the north slopes of the Rattlesnake Hills. Because of the limited volume of groundwater available from the unconfined groundwater aquifer, the irrigation water will need to be pumped from deep inter-basalt aquifers or from the Columbia River.

For the irrigation scenarios we assumed the water application pattern discussed above. Thus, none of the water would be actually applied directly to the waste sites of the 200 and 300 Areas. However, there would still be some influence on the water table beneath the waste sites. This concern was addressed by using the variable thickness transient (VTT)

groundwater model (Reisenauer 1979) to simulate the steady-state conditions beneath the Hanford Site for two scenarios. The several possible areas of irrigation are identified in Figure Q.5. For comparison, a 1983 water table was simulated using real 1983 water-disposal records as input. This was done because the model results differ slightly from maps drawn from measured water table elevations. The resulting contours are shown in Figure Q.2.

Four parcels of arable lands were included in the scenarios. The first two areas of offsite land would contribute to recharge along the edge of the aquifer model. These amounted to 9,000 ha on the north slope of the Rattlesnake Hills and 26,700 ha to the west in Cold Creek Valley, shown on Figure Q.5 with arrows indicating the general direction of

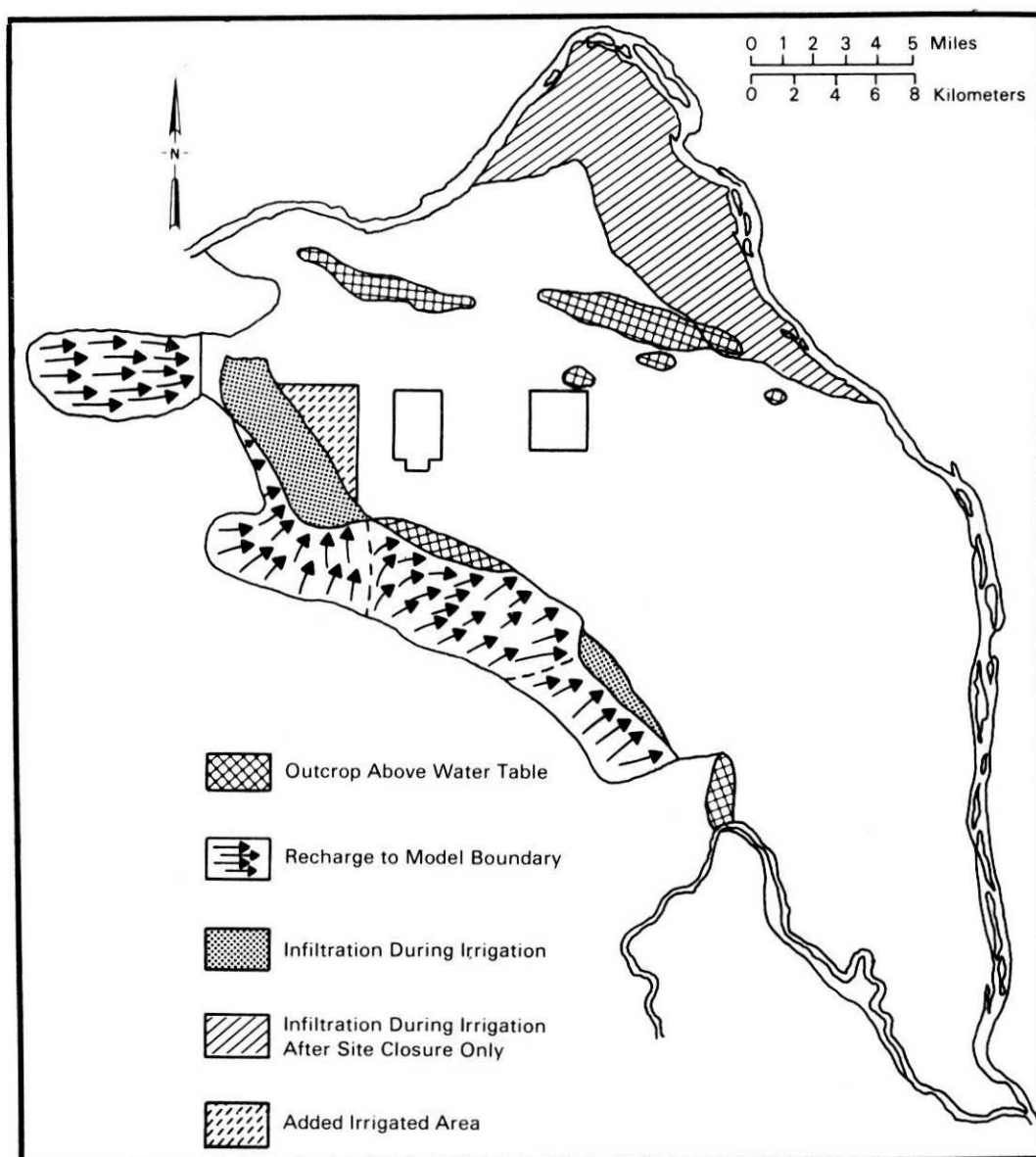


FIGURE Q.5. Location of Irrigated Hanford Site Regions for Simulations

drainage. Another parcel included land (west of Highway 240) adjacent to those areas but located over the aquifer. These are indicated by a small dot pattern in the figure. An additional 760-ha parcel of land lies between the 200 West Area and the highway. Finally, land formerly farmed between the old Hanford Canal and the river was assumed to be irrigated as indicated on Figure Q.5 by diagonal slashes.

Irrigation methods have improved with time to increase the efficiency of the water applied so that plant transpiration utilizes the water and thus infiltration below the root zone is decreased. Therefore, losses to the groundwater table were simulated at two rates; 10% and 20% of the applied irrigation water was assumed to be lost to groundwater recharge. These two values were chosen to bracket low and high water application rates. The first involved irrigation over all the indicated irrigation lands except the added irrigated area next to the 200 West Area. Using an application rate of 1.5 m/yr of water and a loss to recharge of 10% of the water applied, we obtained a 15.2-cm/yr recharge. Irrigation loss to groundwater on land outside the model boundary was integrated and applied to the appropriate boundary as constant recharge. The simulated steady-state water table elevations for this scenario are shown in Figure Q.6.

The second scenario included all the irrigated areas shown on Figure Q.4 except the land north of Gable Mountain along the old Hanford Canal. The irrigation loss to groundwater was assumed to be 20% of the water applied, resulting in 30.5-cm/yr recharge. The resulting water table elevations were checked with land surfaces where streams might form to ensure that proper boundary conditions were used. Although some wetlands occurred along Cold Creek Valley, no permanent surface streams were formed due to a rising groundwater table. The simulated steady-state water table elevations for this scenario are shown in Figure Q.7.

The simulated water tables were compared to existing tank farm bottoms (the deepest-buried wastes in the 200 Areas). The simulated water table elevations were subtracted from the elevations of the tank farm bottoms (obtained from Brown 1960). Table Q.17 lists the unsaturated (vadose) zone thicknesses remaining beneath specific tank farms in the 200 Areas for both water tables. The depths to the 1983 water table also are included for comparison.

Q.9 CONCLUSIONS FROM IRRIGATION MODELING

The principal conclusion of this irrigation study is that the elevation of the 200 Areas plateau precludes the inundation of waste disposal sites by groundwater from offsite irrigation even if more irrigation water were applied than is assumed in this study. This is because surface streams would form around the edges of the higher plateau and thus present a short-circuit avenue for water table drainage. These streams would be at the plateau boundaries and far removed from the proposed waste disposal sites. Thus, regardless of the source of water contributing to a higher water table, wastes stored beneath the plateau would remain in an unsaturated soil profile. The thickness of this vadose zone would change, however. This would affect water and contaminant travel times in this zone.

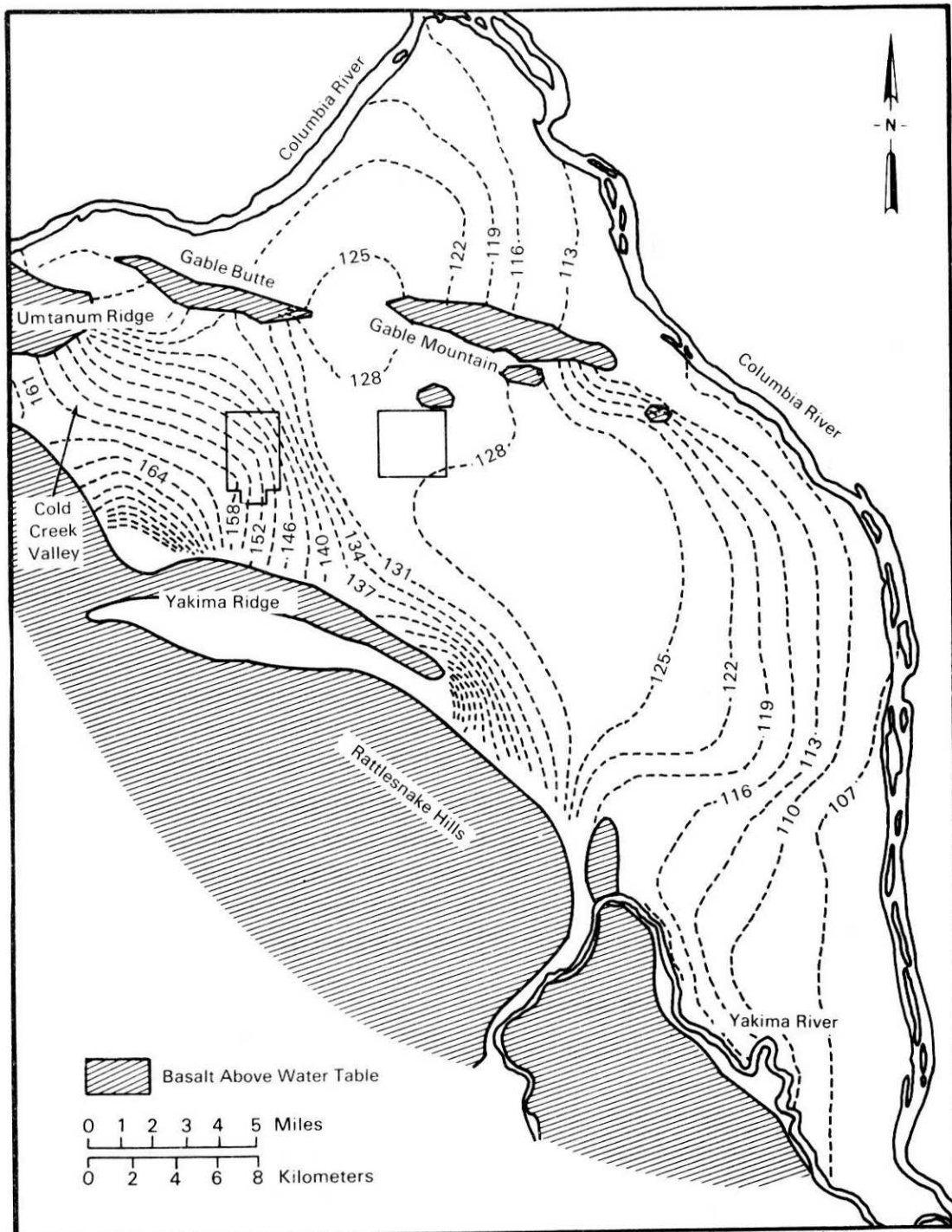


FIGURE Q.6. Estimated Steady-State Water Table Contours at Hanford Site Resulting from 15.2-cm/yr Irrigation Infiltration on the North Slope of Rattlesnake Hills, to the West of the Cold Creek Drainage Boundary, and North of Gable Mountain

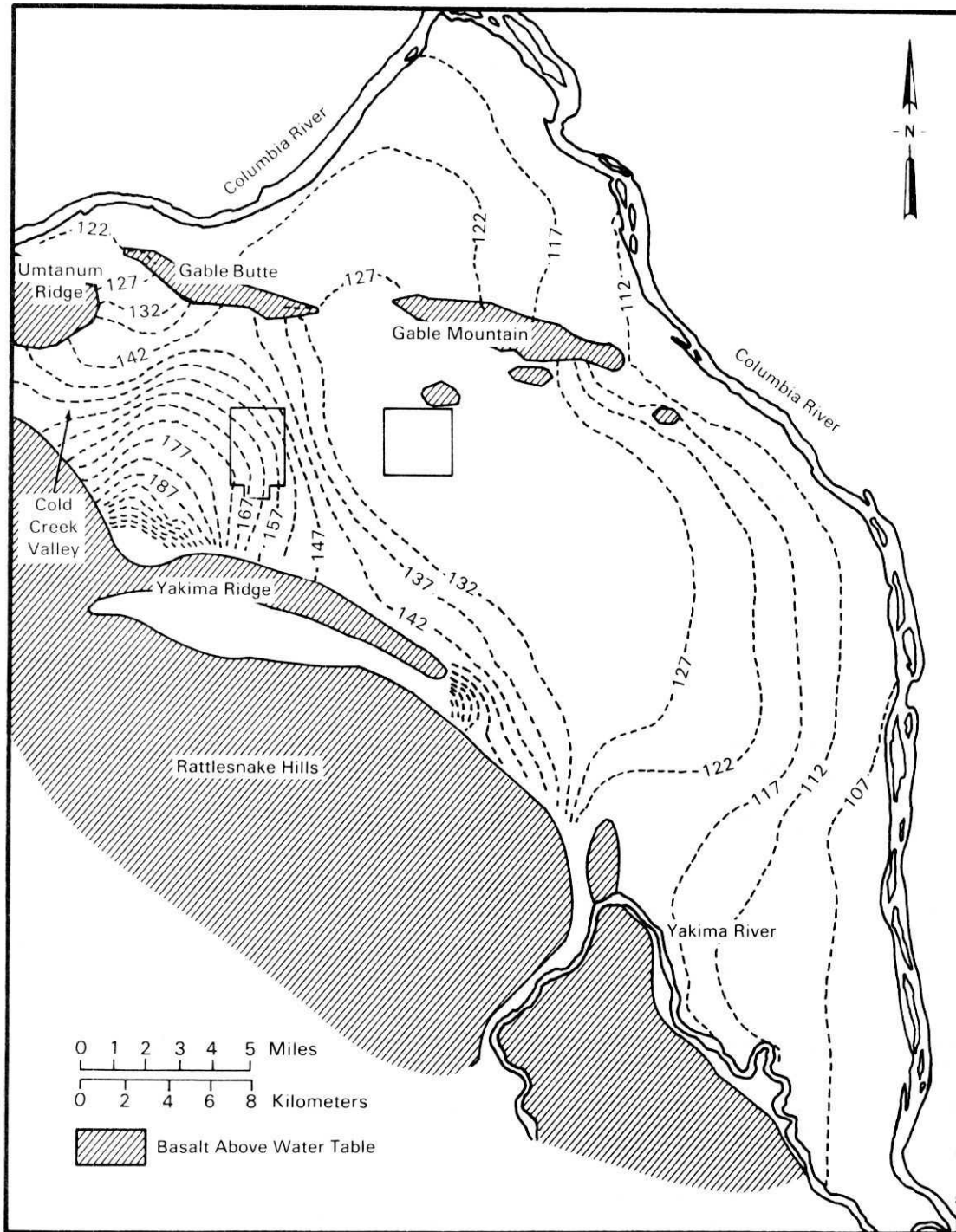


FIGURE Q.7. Estimated Steady-State Water Table (meters above MSL) at Hanford Site After Site Closure Resulting from 30.5-cm/yr Irrigation Infiltration on the North Slope of Rattlesnake Hills, to the West of the Cold Creek Drainage Boundary, and the Added Irrigated Area Between 200 West Area and Highway 240

TABLE Q.17. Unsaturated (vadose) Zone Thickness Between the 200 Area Tank Farms and the Simulated Water Tables

Tank Farm ^(a)	Tank Bottom Elevation, m	1983 Water Table, m	15-cm/yr Water Table, m	30-cm/yr Water Table, m
T	194	61	48	27
TY	191	58	48	27
TX	190	56	42	20
U	191	56	42	20
S	189	54	38	15
SX	185	51	38	16
BY, B	187	63	59	55
C	186	62	66	55
A	193	70	73	63

(a) Tank farms T, TY, TX, U, S, and SX are in the 200 West Area; and BY, B, C, and the A series of tank farms are in 200 East.

Q.10 REFERENCES

- Adams, M. R., L. Jensen and W. W. Schulz. 1986. Preliminary Assessment of the TRAC Model as a Predictor of Key Radionuclide Inventories. RH0-RE-EV-89 P, Rockwell Hanford Operations, Richland, Washington.
- Aldrich, B. C. 1984. Radionuclide Liquid Waste Discharged to Ground in the 200 Areas During 1983. RH0-HS-SR-83-3, Rockwell Hanford Operations, Richland, Washington.
- Brown, D. J. 1960. Geology Underlying 200 Area Tank Farms. HW-67729, General Electric Hanford Atomic Products Operation, Richland, Washington.
- Department of Energy (DOE). 1986. Draft Phase I Installation Assessment of Inactive Waste-Disposal Sites at Hanford. Washington, D.C.
- Fecht, K. R., G. V. Last and M. C. Marratt. 1979. Stratigraphy of the Late Cenozoic Sediments Beneath the 216-A Crib Facilities. RH0-LD-71, Rockwell Hanford Operations, Richland, Washington.
- Graham, M. J., M. D. Hall, S. R. Strait and W. R. Brown. 1981. Hydrology of the Separations Area. RH0-ST-42, Rockwell Hanford Operations, Richland, Washington.
- Lindberg, J. W., and F. W. Bond. 1979. Geohydrology and Ground-Water Quality Beneath the 300 Area, Hanford Site, Washington. PNL-2949, Pacific Northwest Laboratory, Richland, Washington.
- Reisenauer, A. E. 1979. Variable Thickness Transient Groundwater Flow Model, Vol 1. PNL-3160-1, Pacific Northwest Laboratory, Richland, Washington.
- Rockwell Hanford Operations. 1985. Hanford Defense Waste Disposal Alternatives: Engineering Support Data for the Hanford Defense Waste-Environmental Impact Statement. RH0-RE-ST-30 P, Richland, Washington.

Rockwell Hanford Operations. 1987. Engineering Support Data Update for the Hanford Defense Waste-Environmental Impact Statement. RHO-RE-ST-30 ADD P, Richland, Washington.

Tallman, A. M., et al. 1979. Geology of the Separation Areas, Hanford Site, South-Central Washington. RHO-ST-23, Rockwell Hanford Operations, Richland, Washington.